THE UNIVERSITY OF QUEENSLAND

AUSTRALIA

Understanding immunobiology of chikungunya virus disease using mouse models

Yee Suan Poo

BSc (Hons)

A thesis submitted for the degree of Doctor of Philosophy at

The University of Queensland in 2014

School of Medicine

Abstract

Chikungunya virus (CHIKV) is a mosquito borne alphavirus, whose primary disease manifestation in humans is acute and chronic, often debilitating polyarthritis/polyathralgia. Current treatments are often inadequate. This thesis aims to elucidate the roles of several immune components in CHIKV disease, using a mouse model of CHIKV infection and disease, which recapitulates many aspects of human disease. An improved understanding of the immunobiology of CHIKV is required for future development of new interventions for this recently re-emergent virus.

CHIKV polyarthritis/polyathralgia is associated with a prolific monocytes/macrophage infiltration of musculoskeletal tissue in humans, monkeys and mice. The infection in all species is associated with high levels of chemokine (C-C motif) ligand 2 (CCL2), a chemokine that binds chemokine (C-C motif) receptor 2 (CCR2) and is involved in recruitment of monocytes to the sites of infection. Targeting CCL2 or CCR2 signalling has thus been proposed as a potential treatment option for CHIKV disease. Results herein show that CHIKV infection of mice deficient in CCR2 led to a significantly more pronounced and prolonged arthritis that was associated with cartilage damage. The prominent monocytes/macrophages infiltrate seen in wild-type mice was replaced by a prolific neutrophil infiltrate in $CCR2^{-/-}$ mice. The switch in the arthritic infiltrate was associated with changes in the expression of multiple inflammatory mediators, with the loss of anti-inflammatory macrophages and their activities (e.g. efferocytosis) also implicated in the exacerbated inflammatory response. These results illustrated that the recruited monocytes/macrophages in wild-type mice (although associated with acute disease) also have a protective role in CHIKV arthritis. These results suggest caution may be warranted when considering therapeutic targeting of CCR2 for treatment of CHIKV arthritis (Chapter 3).

To study the role of different components of the immune system in CHIKV viraemia and disease, mice deficient in B cells, T cells, CD4+ T cells, natural killer cells and IFN-γ were infected with CHIKV. Results herein confirmed that B cells are crucial for controlling CHIKV viraemia, but showed that T cells also play a role, albeit secondary to antibodies. B cell deficient mice experienced a life long viraemia with little overt pathology evident, supporting the view that CHIKV disease is largely an immunopathology. In T and B cell deficient mice, viraemia was likely controlled by chronic up-regulation of tumour necrosis factor and interferon gamma, but not interferon alpha/beta. Importantly, CD4+ T cells and interferon gamma were shown to play

important roles in acute CHIKV arthritis, with T cells previously thought not to play a significant role (Chapter 4).

CHIKV disease in humans is often associated with chronic arthritic symptoms that persist for months, occasionally over a year, after CHIKV infection. Persistence of CHIKV has been postulated to be responsible for the chronic arthritis. To further investigate this issue, chronic infection and disease parameters were analysed in the established wild-type mouse model of acute CHIKV arthritis. Viraemia is cleared day 4-5 post-infection and neutralising antibodies are detected as early as day 4 post-infection, and rose significantly thereafter. Despite the high levels of neutralising antibodies, replication competent CHIKV could be recovered from feet of infected mice up to day 14 post-infection. Importantly, significant levels of CHIKV RNA (including negative strand RNA) could be detected by quantitative real-time polymerase chain reaction in feet up to day 100 post-infection. Interferon stimulated gene 54, a factor that is up-regulated in response to viral infection and double stranded RNA, was found also to be persistently up-regulated in these feet, suggesting ongoing replication of viral RNA. Microarray analysis of these feet revealed that (i) many of the pathways up-regulated during acute arthritis were maintained during chronic infection, (ii) on-going local inflammatory responses were dominated by type I IFN responses, and (iii) many of the inflammatory pathways identified in chronically infected mouse feet were also found in chronic CHIKV patients. These observations suggest that chronic disease is due to ongoing inflammation stimulated by persistently replicating viral RNA and viral proteins encoded by that RNA (Chapter 5).

In conclusion, this thesis has shown, that inflammatory CCR2+ monocyte can be critical for preventing excessive pathology and resolving inflammation, that distinct immune factors control CHIKV viraemia and arthritis, and that long-term persistence of replicating CHIKV RNA might be the cause of protracted arthritic manifestations in CHIKV patients. These studies will hopefully inform future development of intervention for CHIKV.

Declaration by author

This thesis *is composed of my original work, and contains* no material previously published or written by another person except where due reference has been made in the text. I have clearly stated the contribution by others to jointly-authored works that I have included in my thesis.

I have clearly stated the contribution of others to my thesis as a whole, including statistical assistance, survey design, data analysis, significant technical procedures, professional editorial advice, and any other original research work used or reported in my thesis. The content of my thesis is the result of work I have carried out since the commencement of my research higher degree candidature and does not include a substantial part of work that has been submitted *to qualify for the award of any* other degree or diploma in any university or other tertiary institution. I have clearly stated which parts of my thesis, if any, have been submitted to qualify for another award.

I acknowledge that an electronic copy of my thesis must be lodged with the University Library and, subject to the General Award Rules of The University of Queensland, immediately made available for research and study in accordance with the *Copyright Act 1968*.

I acknowledge that copyright of all material contained in my thesis resides with the copyright holder(s) of that material. Where appropriate I have obtained copyright permission from the copyright holder to reproduce material in this thesis.

Publications during candidature

1. Nakaya, H. I., Gardner, J., **Poo, Y. S.**, Major, L., Pulendran, B. & Suhrbier, A. 2012. Gene profiling of chikungunya virus arthritis reveals significant overlap with rheumatoid arthritis. *Arthritis Rheum*. 64, 3553-3563.

2. **Poo, Y.S.**, Nakaya, H. I., Gardner, J., Larcher, T., Schroder, W.A., Le, T.T., Major, L. & Suhrbier, A 2014. CCR2 Deficiency promotes exacerbated chronic erosive neutrophil-dominated chikungunya virus arthritis. *Journal of Virology*, 88, 6862-6872.

3. **Poo, Y.S.**, Rudd, PA, Gardner, J., Wilson, J., Larcher, T., Colle, M.A., Le, T.T., Nakaya, H.I., Warrilow, D., Allcock, R., Bielefeldt-Ohmannm, H., Lopez, A., Suhrbier, A. Immune factors involved in acute and chronic chikungunya virus infection. (submitted)

Conference abstracts

1. **Poo, Y.S.**, Nakaya, H. I., Gardner, J., Larcher, T., Schroder, W.A., Le, T.T., Major, L. & Suhrbier, A. 'CCR2 Deficiency promotes exacerbated chronic erosive neutrophil-dominated chikungunya virus arthritis' QIMR Student Retreat Mount Tambourine, 26-27 September 2013.

2. Rudd, P.A., **Poo, Y.S.**, Gardner, J., Khromykh, A.A., Suhrbier, A. 'Chikungunya virus persistence and chronic disease in an adult mouse model of infection' Keystone Symposia Positive Strand RNA Viruses, 28 April-3 May 2013.

3. **Poo, Y.S.**, Nakaya, H. I., Gardner, J., Larcher, T., Schroder, W.A., Le, T.T., Major, L. & Suhrbier, A. 'The danger of targeting CCR2 for immunotherapy of inflammatory disease' Australasian Society for Immunology 41st Annual Scientific Meeting Adelaide Australia, 11-15 December 2011.

Publications included in this thesis

1. **Poo, Y.S.**, Nakaya, H. I., Gardner, J., Larcher, T., Schroder, W.A., Le, T.T., Major, L. & Suhrbier, A. CCR2 deficiency promotes exacerbated chronic erosive neutrophil-dominated chikungunya virus arthritis. Accepted. – incorporated as Chapter 3.

Contributor	Statement of contribution
Poo, Y.S (candidate)	Designed experiments (30%) Performed experiments (90%) Wrote and edited the article (35%)
Nakaya, H. I.	Assisted bioinformatics analysis
Gardner, J.	Performed experiments (5%)
Larcher, T.	Analysed Figure 3.4
Schroder, W.A	Designed experiments (10%)
Le, T.T.	Performed experiments (5%)
Major, L.	Wrote and edited the article (5%)
Suhrbier, A.	Designed experiments (60%) Wrote and edited the article (60%)

Contributions by others to the thesis

Professor Andreas Suhrbier – supervised and designed the project; involved in interpretation of data; critically revised this thesis.

Dr. Lee Major – provided day to day technical assistance; critically revised this thesis.

Assistant Professor Nakaya Helder – provided bioinformatics support.

Joy Gardner, Dr. Penny Rudd and Thuy Le – contributed to non-routine technical work.

Statement of parts of the thesis submitted to qualify for the award of another degree

None

Acknowledgements

First and for most, I would like to thank my principal supervisor**,** Professor Andreas Suhrbier, for his advice, support and constructive criticism throughout my PhD years in Queensland Institute of Medical Research. I am indebted to my associate supervisor Dr. Lee Major, for his endless technical guidance and critical proofreading of my thesis.

I would like to acknowledge Joy Gardner, Thuy Le, Assistant Professor Helder Nakaya, Dr. Thibaut Larcher, Clay Winterford and Glynn Rees, for their professional assistance in various experiments performed in this PhD project.

I would also like to thank current and former lab members of Suhrbier lab, Jane Wilson, Dr. Wayne Schroder, Dr. Itaru Anraku, Dr. Penny Rudd, for their encouragement, friendship and understandings. Sincere thanks to my PhD committee members, Professor Denise Doolan and Dr. Ashraful Haque, for sharing their wisdom to me.

I'm grateful to officers in graduate school and School of Medicine, especially Maxine Wienert and Marijke Schmidt, for their excellent and prompt support for candidature-related issues. I also owe special thanks to University of Queensland for awarding me two scholarships – University of Queensland Research Scholarship (UQRS) and University of Queensland International Research Tuition Award (UQIRTA) – that allow me to complete my PhD studies.

I'm thankful to all my buddies and friends in QIMR, Dr. Herng Leow, Candy Chuah and Dr. Yi Chieh Lim. I have to give special thanks to my PhD seniors, Dr. Min-Hsuan Lin and Dr. Yee Leow, for giving me consolation and counsel.

To my late father, for giving me a wonderful life. I am very proud to be your son. Last but not least, to my family members, for their unconditional love and for having faith in me.

Keywords

CHIKV, CCR2 macrophage, neutrophil, inflammation, arthritis, virus persistence, cytokine, microarray

Australian and New Zealand Standard Research Classifications (ANZSRC)

ANZSRC code: 320200, Immunology, 55%

ANZSRC code: 060506, Virology, 35%

ANZSRC code: 080301, Bioinformatics Software, 10%

Fields of Research (FoR) Classification

FoR code: 1107, Immunology, 60%

FoR code: 0605, Microbiology, 40%

Table of contents

Chapter 1: Introduction **1**
1.1 Alphaviruses 1
1.2 Chikungunya virus (CHIKV) 2
1.3 Epidemiology 2
1.3.1 Geographic distribution 2
1.3.2 Mode of transmission—urban and sylvatic cycles 3
1.3.3 Vectors 4
1.4 Clinical manifestations 5
1.4.1 Acute symptoms 5
1.4.2 Chronic arthritic symptoms 5
1.4.3 Severe disease manifestations following CHIKV infection 7
1.5 Biology of the CHIKV 7
1.5.1 Genome organisation 7
1.5.2 Viral particle structure of the CHIKV 8
1.5.3 Entry of virus 9
1.5.4 Translation, replication and transcription of viral RNA 10
1.6 Animal models of CHIKV and RRV disease 14
1.6.1 Non-human primate models 14
1.6.2 Mouse models 14
1.7 Immune responses to CHIKV and RRV 15
1.7.1 Type I interferon (IFN) responses 16
1.7.2 Monocytes/macrophages 17
1.7.2.1 Macrophages: role in arthritic manifestations 17
1.7.2.2 Macrophages and viral persistence 18
1.7.3 Natural killer (NK) cells 18
1.7.4 Adaptive immune responses against the CHIKV 19
1.7.4.1 B cell responses 19
1.7.4.2 T cell responses 20
1.8 Alphavirus vaccine vectors and alphavirus vaccines 22
1.8.1 CHIKV and RRV vaccines 22
1.9 Drug treatments for CHIKV patients 23
1.10 Neutralising antibody-based therapeutics 24
1.11 Conclusions and thesis aims 25

Chapter 2: Material and methods **26**
2.1 Propagation of Vero and C6/36 cells 26
2.2 Virus preparation 26
2.3 Virus titration by 50% cell culture infection dose ($CCID_{50}$) 26
2.4 Ethics statement and care of animals 27
2.5 Mouse infection 28
2.6 Serum collection from CHIKV infected mice 28
2.7 Isolation of infectious CHIKV from feet 29
2.7.1 Mortar and pestle method 29
2.7.2 Homogeniser method 29
2.7.3 Collagenase digestion method 29
2.8 Blood smear 30
2.9 Isolation of infectious CHIKV from various mice tissues 30
2.10 Mouse vaccination 31
2.11 Anti-Ly6G antibody treatment 31
2.12 Foot measurement in mice 31
2.13 Neutralisation assay 32
2.14 RNA extraction from virus infected mice's feet 32
2.15 Synthesis of complementary deoxyribonucleic acid (cDNA) from extracted RNA samples 33
2.16 Quantitative real-time PCR (qRT-PCR) 33
2.17 DNA gel electrophoresis 34
2.18 Cytokine and chemokine detection by cytometric bead array assay 35
2.19 Interferon alpha (IFN-α) detection by Mouse IFN-alpha FlowCytomix Simplex Kit 35
2.20 Histology and immunohistochemistry 35
2.20.1 Leder Stain (for neutrophils) 36
2.20.2 Chromotroph 2R staining (for eosinophils) 36
2.20.3 F4/80 immuno-stain (for macrophages) 36
2.20.4 Ly6G staining (for neutrophils) 37
2.20.5 ApopTag staining (for apoptotic cells) 37
2.20.6 Safranin O staining (for proteoglycans) 37
2.21 Quantification of infiltrating cells in the joint by histology image analysis 38
2.22 T cell proliferation assay 40
2.23 Anti-CHIKV enzyme-linked immunosorbent assay (ELISA) 40
2.24 ELISA for detecting anti-nuclear antibody (ANA) 40
2.25 Microarray experiments and analyses 41

2.26 Statistical analyses 41

Chapter 3: CCR2 deficiency promotes exacerbated chronic erosive neutrophil-dominated chikungunya virus arthritis 42

3.1 Introduction 42

3.2 Results 44

3.2.1 CCR2$^{-/-}$ mice had more severe foot swelling than WT mice 44

3.2.2 WT and CCR2$^{-/-}$ mice had a similar level of CHIKV viraemia and CHIKV RNA persistence in feet 44

3.2.3 Histology and immunohistochemistry of the cellular infiltrates in the arthritic feet of WT and CCR2$^{-/-}$ mice 48

3.2.4 Quantitation of histology and immunohistochemistry of the cellular infiltrates in the arthritic feet of WT and CCR2$^{-/-}$ mice. 52

3.2.5 Antibody-based depletion of neutrophils did not ameliorate foot swelling in CCR2$^{-/-}$ mice 58

3.2.6 Cartilage damage in CHIKV infected CCR2$^{-/-}$ mice. 58

3.2.7 ANA levels in CCR2$^{-/-}$ and WT mice 58

3.2.8 Anti-viral Th1/Th2/Th17 responses in CHIKV-infected WT and CCR2$^{-/-}$ mice. 63

3.2.9 Changes in inflammatory mediators in the arthritic feet and sera of CCR2$^{-/-}$ mice 66

3.2.10 CHIKV infection in IL-10$^{-/-}$ mice 66

Figure 3.13: Foot swelling, viraemia and neutrophil staining in CHIKV infected IL-10$^{-/-}$ mice. 70

3.2.11 Global gene expression changes induced by CHIKV infection. 71

3.3 Discussion 75

Chapter 4: The contribution of B, T, NK cells and IFN-g in the control of viraemia and mediation of arthritis during CHIKV infection 78

4.1 Introduction 78

4.2 Results 80

4.2.1 Viraemia in WT and B cell deficient mice (μMT, Rag-1$^{-/-}$ and Rag2/Il2rg$^{-/-}$ mice) infected with CHIKV 80

4.2.2 Vaccination of μMT mice 84

4.2.3 Treatment of Rag-1$^{-/-}$ and μMT mice with anti-CHIKV antibodies 88

4.2.4 CHIKV arthritis in μMT mice 90

4.2.5 CHIKV arthritis in Rag-1$^{-/-}$ mice 90

4.2.6 Investigation of the role of CD4+ T cells in CHIKV viraemia and arthritis using MHC-II $^{\Delta/\Delta}$ mice 96
4.2.7 Vaccination of μMT mice – foot swelling 96
4.2.8 MHC-II$^{\Delta/\Delta}$ mice produce IgG2c antibodies independent of CD4+ T cells 101
4.2.9 CHIKV arthritis and viraemia in IFN-γ$^{-/-}$ mice 101
4.2.10 Histological analysis of persistently infected Rag-1$^{-/-}$ mice 104
4.2.11 Cytokine profile in the sera of persistently infected Rag-1$^{-/-}$ mice 108
4.2.12 Persistent virus recovered from Rag1$^{-/-}$ mice 110
4.3 Discussion 111
4.3.1 Role of T cells in viraemia control 112
4.3.2 Role of T cells in arthritis 112
4.3.3 Role of B cells in viraemia control 113
4.3.4 Viraemia levels are not correlated to arthritis severity 113
4.3.5 Role of IFN-γ in viraemia control and arthritis 114
4.3.6 TNF and IFN-γ (not IFN-α) were associated with persistently viraemic Rag-1$^{-/-}$ mice. 114
4.3.7 Conclusion 115

Chapter 5: Long-term persistence of CHIKV RNA in WT mice is associated with signs of chronic inflammation 116

5.1 Introduction 116
5.2 Results 118
5.2.1 Isolation of infectious CHIKV from feet 118
5.2.2 Quantification of CHIKV RNA levels in the feet of CHIKV-infected mice 119
5.2.3 Curve fit of the decline in CHIKV RNA levels in feet 123
5.2.4 Relative ratio of the levels of total CHIKV RNA to negative strand CHIKV RNA 123
5.2.5 Quantification of CHIKV RNA levels in the spleen of CHIKV-infected mice 126
5.2.6 Neutralising antibody response post CHIKV infection 126
5.2.7 Quantification of ISG-54 expression in CHIKV infected feet 126
5.2.8 Comparison of global gene expression between CHIKV-infected feet on day 0 and day 30 post infection 129
5.2.8.1 Ingenuity's Canonical Pathway Analysis of up-regulated genes 129
5.2.8.2 Ingenuity's Canonical Pathway Analysis of down-regulated genes 130
5.2.8.3 Ingenuity's Upstream Regulator Analysis of up-regulated genes 132
5.2.8.4 Ingenuity's Upstream Regulator Analysis of down-regulated genes 133
5.3 Discussion 136
5.3.1 Evidence of ongoing CHIKV replication *in vivo* 136

5.3.2 Decline in viral RNA 136
5.3.3 Immune responses that control CHIKV persistence 137
5.3.4 CHIKV-induced chronic inflammation in mice versus humans 138
5.3.5 Conclusion 138

Chapter 6: Summary 139

6.1 Summary of Chapter 3: CCR2 deficiency promotes exacerbated chronic erosive neutrophil-dominated chikungunya virus arthritis 139
6.1.1 Major findings 139
6.1.2 Major implications 139
6.1.3 Future directions 142

6.2 Summary of Chapter 4: The contribution of B, T and NK cells and IFN-γ in the control of viraemia and mediation of arthritis during CHIKV infection 143
6.2.1 Major findings 143
6.2.2 Major implication 143
6.2.3 Future directions 144

6.3 Summary of Chapter 5: Long-term persistence of CHIKV RNA in WT mice is associated with signs of chronic inflammation 144
6.3.1 Major findings 144
6.3.2 Major implications 145
6.3.3 Future directions 145

References 148

Appendices 174

Appendix I 174
Appendix II 175
Appendix III 179
Appendix IV 181
Appendix V 182
Appendix VI 184

List of Figures

Figure 1.1: Distribution of CHIKV cases. 3
Figure 1.2: The genomic organisation of CHIKV. 8
Figure 1.3: CHIKV viral particles. 9
Figure 1.4: Alphavirus replication. 12
Figure 2.1: Foot measurement in mice. 31
Figure 3.1: Foot swelling in CHIKV infected WT and CCR2$^{-/-}$ mice. 45
Figure 3.2: Virus replication in WT and CCR2$^{-/-}$ mice. 46
Figure 3.3: qRT-PCR analyses of CHIKV RNA in CHIKV infected WT and CCR2$^{-/-}$ mice. 47
Figure 3.4: Histology and immunohistochemistry of rheumatic lesions in CHIKV infected WT and CCR2$^{-/-}$ mice. 50
Figure 3.5: Histology quantitation. 54
Figure 3.6: F4/80 staining of cells in foot sections from WT and CCR2$^{-/-}$ mice day 21 post CHIKV infection. 56
Figure 3.7: Anti-Ly6G staining of feet from CCR2$^{-/-}$ and WT mice. 57
Figure 3.8: Foot swelling after neutrophil depletion in CCR2$^{-/-}$ mice. 60
Figure 3.9: Cartilage damage in CCR2$^{-/-}$ feet. 61
Figure 3.10: ELISA for detection of mouse ANA. 62
Figure 3.11: Immune responses in WT and CCR2$^{-/-}$ mice post CHIKV infection. 64
Figure 3.12: qRT-PCR of selected genes in feet and IL-10 in sera of WT and CCR2$^{-/-}$ post CHIKV infection. 68
Figure 3.13: Foot swelling, viraemia and neutrophil staining in CHIKV infected IL-10$^{-/-}$ mice. 70
Figure 3.14: Monocyte/macrophage, M2/resolving macrophages and neutrophils profiles in the feet of CHIKV infected WT and CCR2$^{-/-}$ mice. 72
Figure 3.15: Microarray analysis of arthritic feet from WT and CCR2$^{-/-}$ mice. 74
Figure 4.1: Viraemia in CHIKV infected WT mice and B cell deficient mouse strains (µMT, Rag-1$^{-/-}$ and Rag2/Il2rg$^{-/-}$ mice). 82
Figure 4.2: Viraemia and T cell proliferation assay in vaccinated WT and µMT mice. 86
Figure 4.3: Viraemia in persistently infected Rag-1$^{-/-}$ and µMT mice treated with anti-CHIKV hyperimmune sera. 89
Figure 4.4: Foot swelling in CHIKV infected WT, µMT and Rag-1$^{-/-}$ mice. 92
Figure 4.5: Histological analysis and quantification of feet from CHIKV infected WT, µMT, Rag-1$^{-/-}$ and MHC-II$^{\Delta/\Delta}$ mice. 94
Figure 4.6: Viraemia and foot swelling in CHIKV infected WT and MHC-II$^{\Delta/\Delta}$ mice. 98

Figure 4.7: Foot swelling in vaccinated μMT mice and mock-vaccinated μMT mice following CHIKV infection. 100
Figure 4.8: The presence of anti-CHIKV antibody in CHIKV infected WT and MHC-II$^{\Delta/\Delta}$ mice. 102
Figure 4.9: Viraemia and foot swelling in WT and IFN-γ$^{-/-}$ mice during CHIKV infection. 103
Figure 4.10: Histological analysis of persistently viraemic Rag-1$^{-/-}$ mice. 106
Figure 4.11: Serum cytokine levels in persistently viraemic Rag-1$^{-/-}$ mice..... 109
Figure 5.1: Quantification of CHIKV RNA in CHIKV infected feet and spleens. 120
Figure 5.2: Gel electrophoresis image of the RNA E1 qRT-PCR product..... 122
Figure 5.3: Curve fit of reduction in RNA levels over time and ratio of total CHIKV RNA to negative strand CHIKV RNA. 124
Figure 5.4: Neutralising antibody titres in CHIKV infected mice over time. 127
Figure 5.5: ISG-54 mRNA levels in feet of CHIKV-infected mice over time. 128
Figure 5.6: IPA of canonical pathways active in CHIKV-infected feet on day 30 post infection. . 131
Figure 5.7: Ingenuity's Upstream Regulator Analysis of differentially expressed genes identified in CHIKV-infected feet on day 30 post infection. 134
Figure 6.1: Relationship of monocytes/macrophages and neutrophils in CHIKV arthritis..... 141

List of Tables

Table 1.1 Alphaviruses associated with arthritis and/or arthralgia..... 1
Table 1.2: Frequency of persistent CHIKV arthritic symptoms..... 6
Table 1.3: Vaccines in development for CHIKV and disease..... 24
Table 2.1: List of knock-out mice strains used in various experiments..... 28
Table 2.2: List of primers used for qRT-PCR..... 33
Table 2.3: Parameters for algorithm detecting specific dye..... 39
Table 4.1: Viraemia and arthritis in WT and knock-out mice infected with CHIKV..... 111
Table 5.1: Isolation of infectious CHIKV from the infected feet using 3 different methods..... 118
Table 7.1: Details of the IPA pathways shown in Figure 3.15B..... 174
Table 7.2: Details of the IPA pathways shown in Figure 3.15C..... 175
Table 7.3: Details of the IPA pathways shown in Figure 5.6..... 179
Table 7.4: Details of the IPA pathways for section 5.2.8.2..... 181
Table 7.5: Details of the ingenuity upstream regulator analysis of the 192 more induced in the feet of day 30 post infected mice shown in Figure 5.7..... 182
Table 7.6: Mutations identified in CHIKV recovered from Rag-$1^{-/-}$ mice day 100 post infection. 184

List of Abbreviations

ACS	Ammonium-chloride-Potassium
ANA	Anti-nuclear antibodies
ANOVA	Analysis of variance
BEI	Binary ethylenimine
$CCID_{50}$	50% cell culture infection dose
CCR2	C-C chemokine receptor type 2
cDNA	Complementary deoxyribonucleic acid
CHIKV	Chikungunya virus
CSE	Conserved-sequence element
DAB	Diaminobenzidine
DEG	Differentially expressed gene
DMARDs	Disease-modifying anti-rheumatic drugs
DNA	Deoxyribonucleic acid
dNTPs	Deoxynucleoside triphosphates
DOCK8	Dedicator of cytokinesis 8
dsRNA	Double stranded RNA
ECSA	Eastern, central and southern Africa
EEEV	Eastern equine encephalitis virus
EDTA	Ethylenediaminetetraacetic
EU	Endotoxin unit
FACS	Fluorescence-activated cell sorting
FCS	Foetal calf serum
G-CSF	Granulocyte colony-stimulating factor
H&E	Haematoxylin and eosin
HCl	Hydrochloric acid
HIV	Human deficiency virus
HRP	Horseradish peroxidase
i.p.	Intraperitoneal
i.v.	Intravenously

IFN	Interferon
Ig	Immunoglobulin
IL-6	Interleukin-6
IPA	Ingenuity Pathway Analysis
IPS-1	Interferon promoter stimulator-1
IRGM	Immunity-related GTPase M
ISG	Interferon-stimulated gene
$KHCO_3$	Potassium bicarbonate
M1	Classically activated macrophages
M2	Alternatively activated macrophages
MCP-1	Monocytes chemotactic protein-1
MHC	Major histocompatibility complex
min	Minute
mir-21	MicroRNA 21
mm	Millimetre
mM	Millimolar
NaCl	Sodium chloric
NH_4Cl	Ammonium chloride
NIH	US National Institute of Health
NK	Natural killer
nm	Nanometer
NSAID	Non-steroidal anti-inflammatory drug
NTR	Non-translated region
ORF	Open reading frame
p.i.	Post infection
PARP-1	Activation of Poly(ADP-ribose) polymerase-1
PBS	Phosphate buffered saline
PBST	PBS with Tween 20
PC3	Physical Containment Level 3 (PC3)
PCR	Polymerase chain reaction

qRT-PCR	Quantitative real-time PCR
R2	RPMI 1640 with 2% FCS
R5	RPMI 1640 with 5% FCS
R10	RPMI 1640 with 10% FCS
RA	Rheumatoid arthritis
RC	Replication complex
RIG-I	Retinoic acid-inducible gene 1
RMSP	Rheumatic musculoskeletal pain
RNA	Ribonucleic acid
rpm	Revolutions per minute
RPMI-1640	Roswell Park Memorial Institute-1640 (RPMI 1640)
RRV	Ross River virus
RSE	Repeated-sequence element
RT	Room temperature
sec	Second
SINV	Sindbis virus
STAT3	Signal transducer and activator of transcription 3
TAE	Tris acetate EDTA
TBS	Tris buffered saline
TCR	T cell receptor
Th	T helper
TNE	Tris–HCl, NaCl and EDTA
TNF	Tumour necrosis factor
TRIM	Tripartite motif-containing 24
VEEV	Venezuelan equine encephalitis virus
VLP	Virus-like particle
WEEV	Western equine encephalitis virus
WT	Wild-type
µl	Microliter

You can't connect the dots looking forward; you can only connect them looking backwards. So you have to trust that the dots will somehow connect in your future. You have to trust in something – your gut, destiny, life, karma, whatever. This approach has never let me down, and it has made all the difference in my life.

Steve Jobs 1955-2011

This page intentionally left blank.

Chapter 1: Introduction

1.1 Alphaviruses

Alphaviruses belong to the Togaviridae family of spherical enveloped viruses (60–70 nm in diameter), which have a positive-sense single-stranded ribonucleic acid (RNA) genome (Weaver et al., 2000). The alphavirus genus comprises approximately 30-40 viruses (Kuhn, 2007) that are commonly classified into New World and Old World alphaviruses, based on the location of their discovery (Schwartz and Albert, 2010). New World alphaviruses (found in the Americas), for example, Venezuelan equine encephalitis virus (VEEV), Eastern equine encephalitis virus (EEEV) and Western equine encephalitis virus (WEEV), are generally associated with encephalitis. Old World alphaviruses (found in Europe, Africa and Australasia), for example, Sindbis, Ross River, Barmah Forest, o'nyong-nyong and chikungunya viruses, are generally associated with fever, rash and polyarthritis (Table 1.1).

Table 1.1 Alphaviruses associated with arthritis and/or arthralgia.

Arhtritogenic alphavirus	Geographic distribution	Cases	Comments
Chikungunya	South and East Asia, Africa, West-Pacific	Recurrent epidemics. 2006–2007 >260,000 cases in Reunion Island, >1.4 m in India, 200 in Italy. Travellers and 6,000 in Caribbean.	Polyathritis/arthraligia is the dominant manifestation of symptomatic infection. Often severe at onset and progressively resolving within 3–6 months.
Ross River	Australia	≤8,000 per year in Australia.	
	West-Pacific	Pacific island epidemic 19979/80. Travellers and military.	
Barmah Forest	Australia	500–1,500 per year in Australia.	Rash and arthropathy dominate.
Sindbis Group	Africa, Asia, Australia	Rare.	Probably all the same, or very similar, viruses.
Karelian fever	Russia	Rare.	Arthropathy is the dominant manifestation.
Ockelbo disease	Sweden	≤30 per year	
Pogosta disease	Finland	≤100–200 per year.	
Mayaro	South America	Small sporadic epidemics. Reported in travellers.	Arthropathy is the prominent feature.
O'nyong-nyong	Central & East Africa	Small sporadic epidemics. > 2 million in 1959–62.	
Igbo Ora	Central Africa	Rare.	Probably a strain of chikungunya (Lanciotti et al., 1998).

Adapted from Suhrbier and La Linn (2004) and Suhrbier and Mahalingam (2009).

1.2 hikungunya virus (CHIKV)

CHIKV is an arthritogenic alphavirus that is transmitted by mosquitoes. The word 'chikungunya' is derived from the Makonde (Tanzania) language and can be translated as 'that which bends up', referring to the posture adopted by CHIKV-infected patients with severe joint pain (Charrel et al., 2007). The typical clinical symptoms of CHIKV disease include self-limiting fever, headache, nausea, myalgia (muscle pain), rash, arthritis and persistent arthralgia (joint pain that can last for weeks to months) (Charrel et al., 2007). Recently (2004-2013), a large epidemic swept across Africa and Asia. In Reunion Island the epidemic caused 260,000 cases (one-third of the population), and had a 0.1% fatality rate (Mavalankar et al., 2008, Manimunda et al., 2011, Pialoux et al., 2006). In India, an estimated 1.4–6.5 million cases were believed to have occurred (Schwartz and Albert, 2010). Currently, there is no licensed vaccine for this pathogen, which has been declared a high priority by the US National Institute of Health (NIH) (Ryman and Klimstra, 2008). Patients are normally treated with analgesics, antipyretics and/or non-steroidal anti-inflammatory drugs (NSAIDS) (Jaffar-Bandjee et al., 2010). The understanding of the immunobiology of CHIKV disease is still limited, despite an increasing number of studies in the area.

1.3 Epidemiology

1.3.1 Geographic distribution

CHIKV was first officially isolated and recorded in Tanzania (Ross, 1956). However, the first known CHIKV outbreak has been tracked back to 1779 in Jakarta, where it was mistaken as a dengue outbreak (Carey, 1971). Since the 1956 discovery, laboratory-confirmed autochthonous (local transmission) cases have been reported in approximately 40 countries spanning Africa, Asia, and recently in Europe (Figure 1.1) (Suhrbier et al., 2012, Powers and Logue, 2007). During 1963, India experienced one of the worst CHIKV epidemics, with more than 400,000 individuals infected in Chennai alone (Arankalle et al., 2007). More recent outbreaks have included Congo (50,000 cases in 1999–2000) (Pastorino et al., 2004) and Indonesia (6,000 cases in 2001–2003) (Buonaguro et al., 2013).

In late 2004, the largest-ever recorded CHIKV epidemic began in Kenya and spread to Reunion Island (estimated 300,000 cases in 2005–2006) (Schuffenecker et al., 2006), Malaysia (3,870 reported cases in 2006–2009) (Azami et al., 2013), Thailand (46,069 reported cases in 2008–

2009) (Chusri et al., 2011), Papua New Guinea (1,590 cases in 2012) (Horwood et al., 2013) and the Caribbean (3,700 cases up to February 2014) (Robles, 2014).

This recent outbreak was associated with a new clade of CHIKV that is efficiently transmitted by *Aedes albopictus* (Charrel et al., 2007, Delatte et al., 2008). Three distinct phylogroups of CHIKV are recognised: (i) the eastern, central and southern Africa (ECSA) phylogroup, (ii) the west Africa phylogroup and (iii) the Asian phylogroup (Volk et al., 2010). The new clade of CHIKV emerged from within the ECSA phylogroup (Schuffenecker et al., 2006, Pialoux et al., 2007).

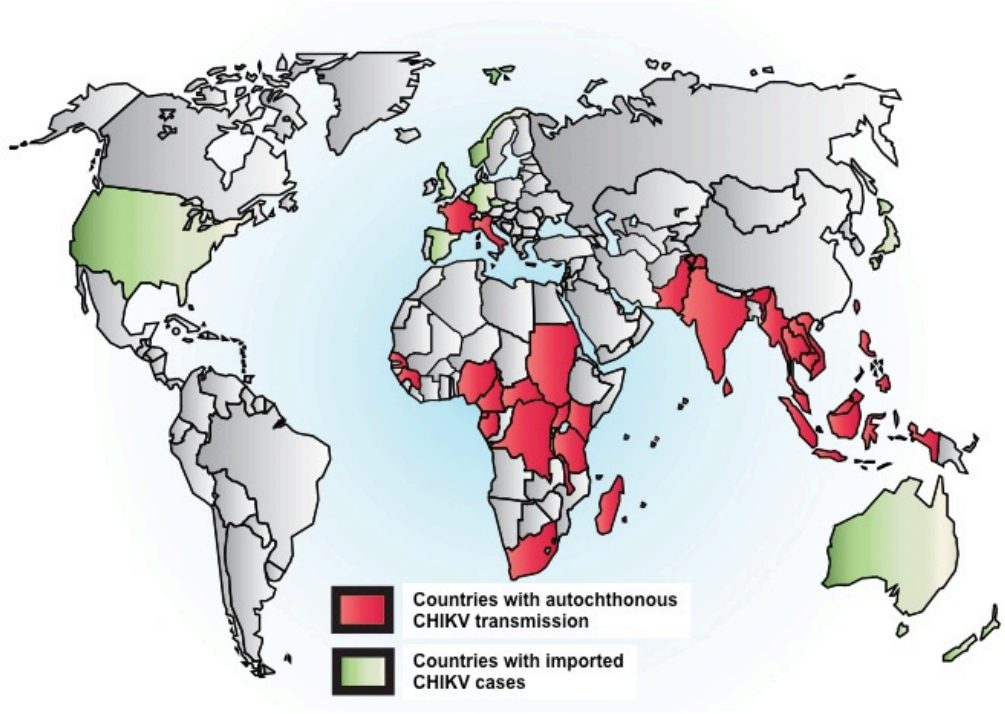

Figure 1.1: Distribution of CHIKV cases.

CHIKV cases have been documented in many parts of the world. In Figure 1.1, the red-coloured countries are those documented with autochthonous CHIKV transmission; green-coloured countries are those documented with imported CHIKV cases. (Adapted from Powers and Logue (2007)).

1.3.2 Mode of transmission—urban and sylvatic cycles

CHIKV can be transmitted via one of two cycles: (i) the urban cycle and/or (ii) the sylvatic cycle. The urban cycle of CHIKV transmission often occurs during epidemics, where CHIKV cycles between a mosquito vector and a human host. The sylvatic cycle usually involves CHIKV

transmission during endemic seasons, where mosquito vector and non-human vertebrate hosts maintain the CHIKV reservoir.

In Africa, CHIKV is thought to be maintained in a sylvatic cycle involving primates (Powers and Logue, 2007). One study reported that in southern Africa (Rhodesia), wildlife including vervets (*Ceropithecus aethiops pygerythrus*) and baboons (*Papio ursius*) were found to be viraemic for three to four days (McIntosh et al., 1964). The level of viraemia was said to be high enough to infect significant numbers of the mosquitoes that feed on infected animals (McIntosh et al., 1964).

Some primates (*Macaca fascicularis* and *Macaca nemestrina leonine*) in Southeast Asia (Philippines, Malaysia and Thailand) were found to have antibodies against CHIKV (Marchette et al., 1978, Nakgoi et al., 2013, McIntosh et al., 1964), suggesting the presence of a sylvatic cycle in places other than Africa. In addition, infectious CHIKV was detected in four macaques (*Macaca fascularis*) during the latest CHIKV epidemic in Malaysia (Apandi et al., 2009). Despite this evidence for the sylvatic cycle in Asia, the urban cycle (human–mosquito) is still believed to be the primary mode of CHIKV transmission outside Africa (Powers and Logue, 2007).

1.3.3 Vectors

CHIKV, like all alphaviruses, is transmitted by invertebrate vectors, mostly mosquitoes (Strauss and Strauss, 1994). *Aedes aegypti* and *Aedes albopictus* are the two main vectors involved in the urban cycle of CHIKV transmission (Singh and Unni, 2011).

Aedes aegypti is prevalent in urban areas where fresh water and warmer temperatures are present (Juliano et al., 2002). *Aedes aegypti* has been the main vector for CHIKV outbreaks in Asia (pre-2004), East Africa (2004–2005) and Comoros (2004–2005) (Powers and Logue, 2007).

Aedes albopictus, commonly known as Asian tiger mosquito, is native to tropical and subtropical latitudes, but has spread into and has adapted to many parts of the world via international trade and travel (Enserink, 2008). *Aedes albopictus* was the primary vector for CHIKV during the most recent major epidemic (Charrel et al., 2007, Delatte et al., 2008, Kumar et al., 2008). Prior to this recent epidemic, *Aedes albopictus* was not a well recognised vector for CHIKV (Tsetsarkin et al., 2009). Two mutations in the structural proteins of CHIKV, namely the A226V mutation on the E1 protein and the I211T mutation on the E2 protein, are believed to have contributed to the adaptation of CHIKV to the *Aedes albopictus* vector (Tsetsarkin et al., 2009,

Vazeille et al., 2007). This adaptation is of some concern, as *Aedes albopictus* can thrive in arid and cold conditions (Benedict et al., 2007) and is spreading to an ever increasing number of countries (Enserink, 2008) including European countries between 1995 to 2012 (Schaffner et al., 2013). Autochthonous transmission of CHIKV may thus also spread to more and more countries worldwide.

1.4 Clinical manifestations

1.4.1 Acute symptoms

CHIKV is able to infect people of any gender and age (Jaffar-Bandjee et al., 2010). CHIKV disease is ordinarily self-limiting and not life threatening, although in the recent epidemic, the disease appeared to be more severe with severe disease manifestations and occasionally mortality (Jaffar-Bandjee et al., 2010). After infection with CHIKV, there is usually a two- to four-day delay before the first disease symptoms appear. In about 5% of 'silent' cases, patients do not experience any disease symptoms (Gerardin et al., 2008). Patients normally experience a sudden onset of fever (39–40ºC), lethargy and rigor for 3 to 12 days (Nargi-Aizenman et al., 2002). In some cases, the fever might resolve in one or two days, but return with the so-called 'saddle-back fever' (Hawman et al., 2013, Carey, 1971). After the onset of fever, nearly all patients develop debilitating polyarthritis (Seymour et al., 2013, White et al., 2001) usually involving peripheral joints (interphalangeal joints, wrists and ankles), proximal joints (knees and elbows) and large joints (shoulders and spine) (Tisserand et al., 2011, Suhrbier et al., 2012). Some patients also experience a maculopapular rash (Peck et al., 1979, Ryman et al., 2000) and oedema (Brighton et al., 1983). Most acute symptoms (aside from polyarthritis/polyarthralgia) usually resolve after seven to 10 days (Ryman et al., 2000, Suhrbier et al., 2012).

1.4.2 Chronic arthritic symptoms

While most of the acute symptoms of CHIKV infection are resolved within one to two weeks, recent studies show that a high percentage of CHIKV-infected patients (ranging from 4.7–75.4%), especially the elderly and patients with high viral loads (Sissoko et al., 2009, Das et al., 2010, Chaaitanya et al., 2011), experience protracted (3–36 months) unresolved arthritic symptoms (Table 1.2). These chronic symptoms include arthralgia, myalgia, asthenia, relapsing or lingering rheumatic musculoskeletal pain (RMSP), polyarthritis, chronic arthritic disability and joint stiffness

(Table 1.2). Studies have associated CHIKV disease with the onset of autoimmune arthritides with cartilage erosion (Bouquillard and Combe, 2009, Ganu and Ganu, 2011). However, these studies are not conclusive, as concurrent autoimmune diseases, rather than CHIKV infections, are believed to be the more likely causes of the autoimmune symptoms seen in these CHIKV-infected patients (Suhrbier et al., 2012). This notion is supported by several studies indicating that chronic CHIKV arthritis does not generally trigger erosion of cartilage and bones (Das et al., 2010, Hoarau et al., 2010, Schilte et al., 2013).

Table 1.2: Frequency of persistent CHIKV arthritic symptoms.

Studies conducted to identify the frequency and duration of arthritic symptoms caused by different CHIKV lineages at different geographic locations.

	CHIKV lineages	Frequency of protracted arthritis	Duration (month)	Symptoms	Studies
Reunion Island	ECSA* epidemic	75.4% (261/346)	36	Arthralgia	Gerardin et al. (2013)
		60% (n/a)	36	RMSP^	Schilte et al. (2013)
		57% (84/147)	15	A range of rheumatic symptoms	Sissoko et al. (2009)
		63.6% (56/88)	18	Athralgia	Borgherini et al. (2008)
		53% (56/106)	3–11	Chronic pain	de Andrade et al. (2010)
France & Italy	ECSA* epidemic	52% (118/227) 34% (78/227)	Mean 23.2	Degenerative disc disease Arthritis	Couturier et al. (2012)
		48% (17/29)	24	Arthralgia	Larrieu et al. (2010)
		66.5% (151/227)	12	Arthralgia, myalgia and asthenia	Moro et al. (2012)
India	ECSA* epidemic	4.7% (24/509)	24	Arthralgia	Chopra et al. (2012)
		57% (249/437)	15	Polyarthritis	Mathew et al. (2011)
		6.1% (14/230)	36	Chronic arthritic disability	Kularatne et al. (2012)
Senegal	Western Africa	12.1 %(13/107)	≥36	Joint stiffness and arthralgia	Brighton et al. (1983)

*ECSA: East/Central/South Africa

^RMSP: relapsing or lingering rheumatic musculoskeletal pain

1.4.3 Severe disease manifestations following CHIKV infection

During the recent outbreak in the Indian Ocean (2006–2008), life-threatening symptoms such as encephalitis, meningoencephalitis, Guillain–Barré syndrome, pneumonia, severe acute nephritis, heart failure and myocarditis were found in some patients (Jaffar-Bandjee et al., 2010, Bodenmann and Genton, 2006, Lemant et al., 2008, Solanki et al., 2007, Economopoulou et al., 2009, Lebrun et al., 2009). These severe disease manifestations and occasional fatalities were rare in CHIKV disease prior to this outbreak (Economopoulou et al., 2009). These severe manifestations were present in about 0.3% of total patients (Pierre et al., 2006), and these patients had a relatively high fatality rate (10.6–33%) (Economopoulou et al., 2009, Renault et al., 2007), whereas patients without severe manifestations had a much lower mortality rate (0.1%) (Pialoux et al., 2007, Mavalankar et al., 2008, Manimunda et al., 2011). Studies have also shown that the elderly are more susceptible to these severe manifestations of CHIKV disease (Economopoulou et al., 2009, Renault et al., 2007).

1.5 Biology of the CHIKV

1.5.1 Genome organisation

Several isolates of CHIKV have been fully sequenced, and these include the S27 African prototype (Khan et al., 2002), isolates from the 1983 Senegal outbreak (Vanlandingham et al., 2005), and six isolates from the Reunion Island and the Seychelles (Schuffenecker et al., 2006). CHIKV has approximately 11,805 nucleotides that contain two open reading frames (ORFs), ORF1 and ORF2, which encode viral proteins (Figure 1.2) (Solignat et al., 2009). The whole genomic 49s RNA is organised as 5' cap-nsP1-nsP2-nsP3-nsP4-(junction region)-C-E3-E2-6K-E1-poly(A)-3' (Figure 1.2). The 5' end of CHIKV genome has a non-translated region (NTR) comprising 76 nucleotides. ORF1 starts at position 77 and terminates at position 7501, while the ORF2 starts at position 7,567 and terminates at position 11,301 (Solignat et al., 2009). A junction sequence of 68 nucleotides in size is located between ORF1 and ORF2 (Solignat et al., 2009). ORF1 encodes the non-structural proteins that are essential for viral replication (Strauss and Strauss, 1994). ORF2 encodes the structural proteins that form the CHIKV viral particle (Strauss and Strauss, 1994).

The 3' NTR contains several conserved-repeated-sequence elements (RSEs) that are postulated to be involved in controlling RNA synthesis (Ou et al., 1983, Pfeffer et al., 1998). For example, deletion of RSEs in Sindbis virus (SINV) changes the dynamics of viral replication (reduced or delayed virus release) (Kuhn et al., 1991, George and Raju, 2000, Hardy and Rice,

2005). Different alphaviruses have 3' NTRs of different lengths, with different numbers of RSEs. In CHIKV, several RSEs are similar to other alphaviruses (Solignat et al., 2009). For example, two copies of RSE are similar to o'nyong'nyong virus (ONNV), and three copies of RSE are similar to those found in Ross River virus (RRV) (Solignat et al., 2009). The poly (A) tail located at the 3' end of NTR, has a 19-nucleotide conserved-sequence element (CSE) that is conserved across all alphaviruses. This CSE acts as the core promoter for the synthesis of negative-sense RNA (Ou et al., 1981).

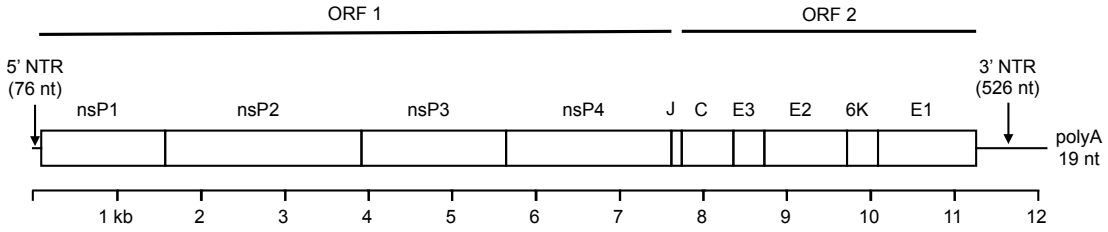

Figure 1.2: The genomic organisation of CHIKV.

The CHIKV genome comprises approximately 11,805 nucleotides that encode for two ORFs. ORF1 encodes the non-structural proteins; ORF2 encodes the structural proteins. ORF: open reading frame; NTR: non-translating region; nsP: non-structural protein; J: junction sequence; C: capsid. (Adapted from (Khan et al., 2002)).

1.5.2 Viral particle structure of the CHIKV

Alphavirus particles are spherical, with a diameter of 60 to 70 nm (Figure 1.3). The alphavirus genome is encapsulated by the capsid protein. This arrangement is called a nucleocapsid. This inner nucleocapsid consists of 240 copies of the capsid protein, which are arranged in a T = 4 icosahedral configuration (a polyhedron with 20 identical triangle surfaces) (Weaver et al., 2012, Caspar and Klug, 1962). The nucleocapsid is enclosed in an outer shell that consists of 80 viral spikes that are also arranged in T = 4 icosahedral configuration. These viral spikes are embedded in, and protruding from, the host-cell-derived lipid bilayer. Each of these viral spikes consists of a trimer of E1-E2 heterodimers (Zhang et al., 2002).

The crystal structure of the E3-E2-E1 mature complex and the pE2-E1 precursor of CHIKV have been solved (Voss et al., 2010). The E1 glycoprotein contains domains I, II and III, and E2 glycoprotein contains domains A, B and C (Voss et al., 2010). The molecular structure of pE2-E1and E3-E2-E1 complex shows that domains A and B of E2 hide the fusion site located in domain II of E1 (Voss et al., 2010). The E2 glycoprotein attaches to the host-cell membrane, then

under acidic conditions in the endosome, the E2-E1 heterodimers disassociate, exposing the E1 fusion site (at the tip of domain II of E1). The fusogenic site of E1 then adheres to the cell membrane to form E1 trimers that drive viral and host-cell membrane fusion, resulting in uncoating and release of the genome from the nucleocapsid (Kielian and Rey, 2006).

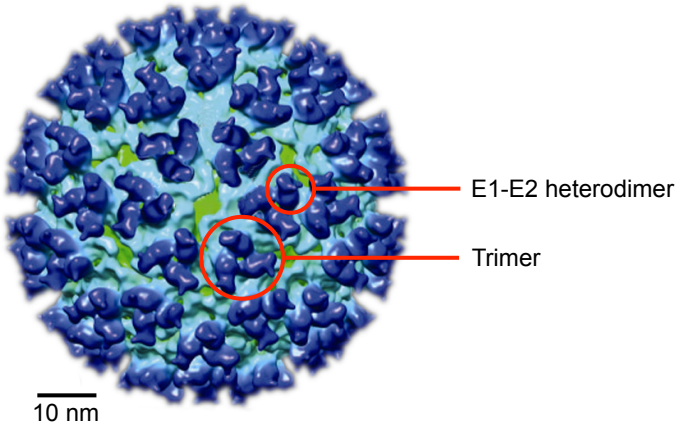

Figure 1.3: CHIKV viral particles.

The viral particle of CHIKV is spherical with a diameter of 60 to 70 nm. The alphavirus genome is encapsulated by the nucleocapsid. The nucleocapsid is enclosed by a viral spike outer shell. The outer shell is comprised of 80 viral spikes. Each viral spike consists of a trimer of E1-E2 heterodimers(Adapted from (Akahata et al., 2010)).

1.5.3 Entry of virus

The entry of alphaviruses into cells is aided by pH-dependent receptor-mediated endocytosis in clathrin-coated vesicles (Sourisseau et al., 2007, Swanson et al., 2010) (Figure 1.4A). Receptors that bind mannose-rich carbohydrates (e.g. dendritic cell-specific ICAM-3-grabbing nonintegrin 1 [DC-SIGN] and liver and lymph node-SIGN [L-SIGN]) are believed to be involved in this process (Guo et al., 2000). The clathrin-coated vesicle delivers viral particles to the endosome. The acidic environment in the endosome triggers an irreversible conformational reorganisation of the viral glycoproteins (Wahlberg et al., 1989) (Figure 1.4B). The E1-E2 heterodimer dissociates, exposing the E1 fusion domain, which leads to the fusion of viral membrane with endosomal membrane (Kielian and Jungerwirth, 1990, Wahlberg et al., 1992) (Figure 1.4B). This fusion leads to the release of 49S RNA genome (encapsulated in nucleocapsid) into the cytoplasm (Powers et al., 2001) (Figure 1.4C).

1.5.4 Translation, replication and transcription of viral RNA

The released 49S RNA genome is translated to non-structural proteins, which are involved in virus replication. The 5' ORF of CHIKV (Figure 1.2) is translated into a large polyprotein (P1234) and in some alphaviruses, into two polyproteins (P123 and P1234) produced by read-through of an opal stop codon located between nsP3 and nsP4 (Figure 1.4D) . These polyproteins are consecutively cleaved by the viral protease found in nsP2 into mature nsP1, nsP2, nsP3 and nsP4. These mature nsPs replicate viral RNA (see below). The nsP2 protein also promotes viral replication by shutting down host-cell transcription (Garmashova et al., 2006) and inhibiting IFNα/β responses (Fros et al., 2010). The P1234 is first cleaved into nsP4 and P123, and then the P123 is subsequently cleaved into nsP1 and P23. The nsP4, nsP1 and P23 then form a replication complex (Figure 1.4; RC-) that synthesises negative strand RNA (Figure 1.4E1). The P23 is eventually cleaved into nsP2 and nsP3 (Lulla et al. 2012). Mature nsP1, nsP2, nsP3 and nsP4 form a replication complex (Figure 1.4; RC+) that synthesises two species of positive strand RNA: 26S subgenomic mRNA (Figure 1.4E2) and the 49S genomic RNA (Figure 1.4E3) (Fayzulin and Frolov, 2004, Frolov et al., 2001). The promoter, which leads to the transcription of negative strand RNA into 26S mRNA, is found in the junction sequence (Figure 1.2) (Ou et al., 1982).

The 26S mRNA is translated into the polyprotein precursor C-pE2-6K-E1 (Figure 1.4F) The C-terminal portion of the capsid is first cleaved by its own autoprotease (a serine-like protease) and this cleavage results in a new N-terminus for the remaining polyprotein pE2-6K-E1 (Garoff et al., 1990) (Figure 1.4G). This N-terminus has a signal sequence for translocating the polyprotein into the rough endoplasmic reticulum for glycoprotein synthesis (Figure 1.4H), where E1 and pE2 are glycosylated. In the golgi apparatus, E1 and pE2 form heterodimers, and these heterodimers trimerise to form the viral spike (Figure 1.4I). The pE2-E1 heterodimers translocate to cell membranes via the Golgi apparatus (Figure 1.4I and J). The pE2 is then cleaved into E2 and E3 by the host protease furin during transport to the cell surface. Some alphaviruses species retain the E3 in the mature spike. E2 is involved in receptor binding, and E3 helps in initial folding (Lobigs and Garoff, 1990). Earlier studies suggested E3 was cleaved and not present in the CHIKV viral particle (Simizu et al., 1984); however, a recent study has revealed that the E3 is still intact in the X-ray crystal structure of E3-E2-E1 complex (mature complex in cytoplasm) (Voss et al., 2010). The cleaved capsid associates with the newly synthesised 49S genomic RNA to form the nucleocapsid (Figure 1.4K). At the host-cell membrane, the nucleocapsid combines with viral spikes to form the mature structural protein and the host-cell lipid bilayer to form mature viral particles that bud from the cell membrane (Figure 1.4L). This budding process is triggered by interaction of the E2 cytoplasmic domain with the nucleocapsid (Lopez et al., 1994).

This page intentionally left blank.

Figure 1.4: Alphavirus replication.

(A) Alphavirus enters the cell with the aid of receptor mediated endocytosis. **(B)** The endosome's acidic condition causes the E1 fusion domain to be exposed. **(C)** The exposed E1 domain subsequently fuses with endosomal membrane and leads to the release of the 49S RNA genome. **(D)** The genomic RNA, which encodes for the non-structural protein get translated into polyprotein P123 or P1234. The polyprotein is further proteolytically processed to form RC- and RC+. **(E1)** The RC- facilitates the replication of negative strand RNA. **(E2)** The RC+ facilitates the production of the 26S subgenomic RNA and **(E3)** the replication of the 49S RNA genomic RNA. **(F)** The 26S subgenomic RNA is translated into polyprotein precursor C-pE2-6K-E1. The capsid is cleaved off from the polyprotein **(G)** and then the remaining (pE2-6K-E1) is cleaved and translocated into the ER. **(H)** In the ER, E1 and pE2 are glycosylated. **(I)** In the golgi apparatus, glycosylated E1 and pE2 form pE2-E1 heterodimer. **(J)** The trimerised heterodimers (viral spike), are then translocated onto the plasma membrane. **(K)** The cleaved capsid and genomic RNA form the nucleocapsid. **(L)** At the plasma membrane, the nucleocapsid and viral spike combine to form the viral particle. the virus then buds from the host-cell membrane.

(Adapted from Kuhn (2007) and Schwartz and Albert (2010)).

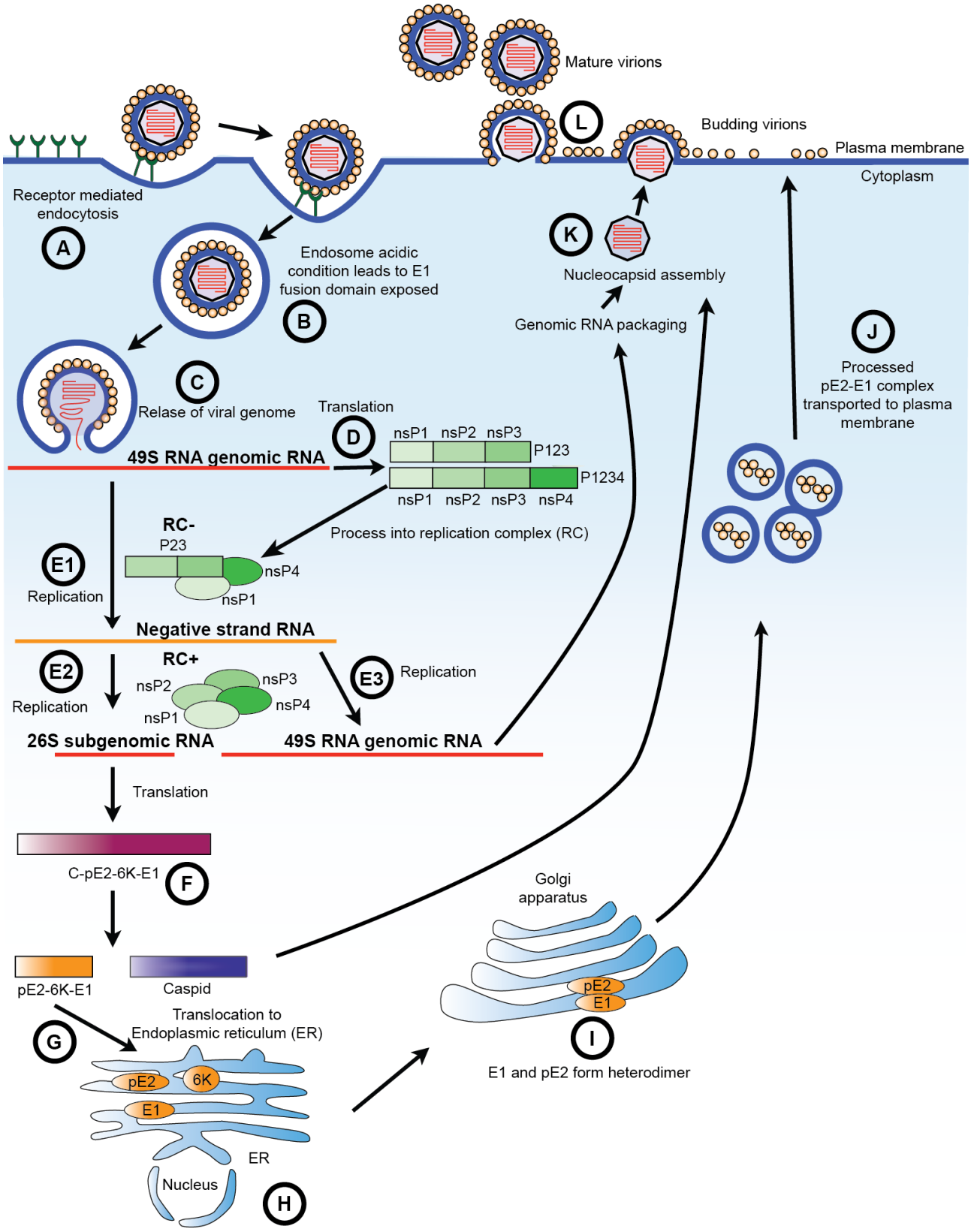
Mature virions
Budding virions
Plasma membrane
Cytoplasm
L
Receptor mediated endocytosis
A
Endosome acidic condition leads to E1 fusion domain exposed
B
K
Nucleocapsid assembly
Genomic RNA packaging
J
Processed pE2-E1 complex transported to plasma membrane
C
Relase of viral genome
Translation
D
nsP1 nsP2 nsP3
P123
P1234
nsP1 nsP2 nsP3 nsP4
49S RNA genomic RNA
Process into replication complex (RC)
RC-
P23
nsP4
nsP1
E1
Replication
Negative strand RNA
E2
Replication
RC+
nsP2
nsP3
nsP4
nsP1
E3
Replication
26S subgenomic RNA
49S RNA genomic RNA
Translation
C-pE2-6K-E1
F
pE2-6K-E1
Caspid
Golgi apparatus
pE2
E1
I
E1 and pE2 form heterodimer
G
Translocation to Endoplasmic reticulum (ER)
pE2
6K
E1
ER
Nucleus
H

1.6 Animal models of CHIKV and RRV disease

1.6.1 Non-human primate models

Non-human primates are a suitable animal model for CHIKV disease, with studies suggesting that they serve as the natural reservoirs of CHIKV in Africa and perhaps Southeast Asia (section 1.3.2). The most comprehensive non-human primate model to date was reported by Labadie et al. (2010), who used cynomolgus macaques (*Macaca fascicularis*). This model involved intravenous/intradermal inoculation of CHIKV. CHIKV-infected macaques developed viral, clinical and pathological features that were comparable to human CHIKV disease. Importantly, in the same model, the infected adult macaques showed long-term persistence of CHIKV, a feature that may explain the protracted arthritic symptoms in humans. The similarities with human CHIKV disease make this model useful for facilitating the development of new interventions for CHIKV disease. For example, this model has been used to investigate the anti-CHIKV antibody's specificity against 'E2EP3', an epitope that was considered for vaccine target (Kam et al., 2012). In addition, cynomolgus macaques were also used to access the efficacy of a live-attenuated vaccine, with macaques vaccinated and then challenged with CHIKV via subcutaneous inoculation (Roy et al., 2014).

Rhesus macaques (*Macaca mulatta*) have also been used to study CHIKV infection (Binn et al., 1967), immune responses triggered by CHIKV (Messaoudi et al., 2013) and have been used in CHIKV vaccine studies (Levitt et al., 1986, Akahata et al., 2010). *Cercopithecus* monkeys, baboons and bonnet monkeys (*Macaca radiata*) (McIntosh et al., 1963, Paul and Singh, 1968) were also shown to be viraemic upon CHIKV inoculation, but there have been no further studies using these models.

1.6.2 Mouse models

Mice have been used extensively to study CHIKV and RRV pathogenesis and to study the efficacy of new interventions for CHIKV and RRV disease. Mouse age, mouse genetic background and site of inoculation have been key factors that have critically affected the viral and pathology outcomes (especially the rheumatic manifestations) in these mouse models. Several studies have used a lethal CHIKV infection model that involves neonates/young mice (Ziegler et al., 2008) or immune-compromised mice (Couderc et al., 2008, White et al., 2011, Werneke et al., 2011, Gardner et al., 2012). Mouse models for RRV have also used young mice (14-21 days old) (Lidbury et al., 2000; Morrison et al., 2006; Lidbury et al., 2008). Neither lethal CHIKV infection models nor use

of young or neonatal mice is ideal. Lethal infection models are of minimal value in studying arthritis as the mice die before arthritic symptoms manifest. eonates are not immunological mature, thus making them less useful for vaccine studies. Use of young mice also complicates vaccine studies as there is insufficient time for vaccination prior to challenge.

Adult wild-type mouse models represent more realistic models of CHIKV disease, not least because arthritis is the main symptom in adult humans infected with CHIKV. However, while viraemia can be established in most adult mice, CHIKV arthritis symptoms are largely absent in mice, which have inoculated intraperitoneally (i.p.) (Suckling et al., 1978), intradermally (Couderc et al., 2008), intranasally (Wang et al., 2008) or intravenously (i.v.) (Teo et al., 2012a). Gardner et al. (2010) reported the first adult, non-lethal-infection mouse model for CHIKV infection with rheumatic manifestation. The adult mice (>6 weeks old) were subcutaneously inoculated with CHIKV at the ventral side of both hind feet, towards the ankle. Infected adult mice developed self-limiting arthritis (with overt foot-swelling evident), tenosynovitis and myositis; as features observed in human CHIKV disease. Foot swelling in infected mice was characterised by a significant degree of mononuclear lymphocytes infiltration in joint and associated tissues including muscle. This prominent mononuclear lymphocytes infiltrate is also prominent in RRV and CHIKV infected humans (Soden et al., 2000, Hoarau et al., 2010), in CHIKV infected primates (Labadie et al., 2010) and RRV infected mice (Lidbury et al., 2000, Lidbury et al., 2008, Morrison et al., 2006).

In another model that was reported later, young mice, which were infected with CHIKV subcutaneously into the foot, also demonstrated foot swelling, arthritis, tenosynovitis and myositis (Morrison et al., 2011). However, the infected younger mice experienced more severe disease, with clear tendonitis, which was less severe in infected adult mice (Morrison et al., 2011, Gardner et al., 2010), again suggesting that mouse age is a factor that influences disease characteristics. The adult WT mouse model for CHIKV infection (Gardner et al., 2010) has been widely used for vaccine studies (Wang et al., 2011a, Prow et al., 2010, Metz et al., 2013b, Garcia-Arriaza et al., 2014), antibody treatment studies (Kam et al., 2012) and disease studies (Teo et al., 2012b, Rudd et al., 2012, Nakaya et al., 2012).

1.7 Immune responses to CHIKV and RRV

CHIKV and RRV infections are rarely fatal in humans. Immune responses in most healthy adults control the viraemia, with acute symptoms usually resolved in one to two weeks, although chronic rheumatic symptoms can last for months to years (Suhrbier et al., 2012). Individuals with

suboptimal immune systems, such as neonates and the elderly, exhibit higher fatality rates (Burt et al., 2012). Arthritic conditions are more severe and chronic in the elderly but are less common in children (Gerardin et al., 2013, Jaffar-Bandjee et al., 2010). Little is known about how these pathologies arise and resolve, especially the arthritic manifestations. CHIKV and RRV infections in joints can lead to a series of antiviral immune responses, including the induction of inflammatory mediators. It has been proposed that these inflammatory mediators result in tissue damage and excessive inflammation, which ultimately leads to the arthritis (Suhrbier and Mahalingam, 2009, Jaffar-Bandjee et al., 2009). The following sections discuss the roles of different arms of the immune system in controlling CHIKV and RRV infection and in mediating the pathology of CHIKV and RRV disease.

1.7.1 Type I interferon (IFN) responses

IFN was discovered more than 50 years ago by Isaacs and Lindenmann as an antiviral protein for influenza virus (Isaacs and Lindenmann, 1957). Since then, IFN has been shown to inhibit many other viruses including CHIKV. The type I IFN response is also a critical antiviral defence mechanism against CHIKV infections. Gifford and Heller showed that CHIKV could trigger IFN production in chicken fibroblasts three hours after infection (Gifford and Heller, 1963). More recent *in vitro* studies have also shown that type I IFN suppresses CHIKV replication (Sourisseau et al., 2007). In patients, type I IFN is up-regulated in the sera and tissues during the acute phase of CHIKV infection (Wauquier et al., 2011, Chow et al., 2011, Ng et al., 2009, Hoarau et al., 2010), indicating the critical role of type I IFN in controlling infection during the acute phase. Consistent with clinical observation, up-regulation of type I IFN is also seen in acute-phase infection in primates, mice and zebrafish (Labadie et al., 2010, Gardner et al., 2010, Rudd et al., 2012, Messaoudi et al., 2013, Palha et al., 2013). Mice with incomplete type I IFN responses are more susceptible to CHIKV infection (Schilte et al., 2010, Rudd et al., 2012, Couderc et al., 2008, Teng et al., 2012), with mice deficient in the IFN-α/β receptor, or IFN response factors 3 and 7 dying within days of infection (Rudd et al., 2012, Couderc et al., 2008, Gardner et al., 2012).

Animal studies have indicated that the up-regulation of type I IFN is rapid, but transient after CHIKV infection (Gardner et al., 2010, Labadie et al., 2010). CHIKV nsP2 has also been shown to block JAK-STAT signalling (Fros et al., 2010), so IFN treatment *before* CHIKV infection (but not IFN treatment *after* CHIKV infection) reduces the CHIKV viraemia and foot swelling in mice (Gardner et al., 2010). These observations clearly indicate that type I IFN is crucial for controlling CHIKV during the early phase of CHIKV infection.

1.7.2 Monocytes/macrophages

Monocytes are generated by haematopoietic stem cells in bone marrow, and are released into circulation where they differentiate into dendritic cells and macrophages. There are at least two phenotypes of macrophages: classically activated (M1) macrophages and alternatively activated (M2) macrophages (Mosser and Edwards, 2008). M1 macrophages promote inflammation and are involved in antiviral defence (Murray and Wynn, 2011). M2 macrophages suppress inflammation, phagocytosis and promote wound-healing (Mosser and Edwards, 2008, Martinez et al., 2009). Macrophage/monocyte infiltrates are prominent features in CHIKV and RRV infection in mice (Lidbury et al., 2000, Morrison et al., 2006, Lidbury et al., 2008, Gardner et al., 2010), monkeys (Labadie et al., 2010) and humans (Soden et al., 2000, Hoarau et al., 2010). Studies also show that CHIKV can infect patient monocytes/macrophages (Her et al., 2010), with primary monocytes (from humans, mice and macaques) also infected by CHIKV *in vitro* (Labadie et al., 2010, Her et al., 2010, Gardner et al., 2010). These studies collectively suggest the involvement of macrophages/monocytes in CHIKV and RRV immunopathogenesis. The following sections discuss the role of macrophages in CHIKV and RRV infection.

1.7.2.1 Macrophages: role in arthritic manifestations

Prolific monocyte/macrophage infiltration is a prominent feature in the musculoskeletal tissues of CHIKV-infected humans, monkeys and mice (Gardner et al., 2010, Hoarau et al., 2010, Labadie et al., 2010, Morrison et al., 2011, Ozden et al., 2007). Microarray analysis of mice feet during peak arthritis has revealed up-regulation of a series of genes associated with macrophage recruitment and activation (Nakaya et al., 2012), again suggesting that macrophages are key players in CHIKV arthritis. This observation is in line with studies showing that the chemical depletion of macrophages ameliorates RRV triggered muscle damage in mice (Lidbury et al., 2000, Lidbury et al., 2008) and CHIKV arthritis in mice (Gardner et al., 2010). Activated macrophages release a series of inflammatory mediators (including prostaglandins, tumour necrosis factor-α (TNF-α) and interleukin-6 (IL-6)), which result in tissue damage, inflammation and arthritis (Suhrbier and Mahalingam, 2009). Consistent with this notion, TNF-α and IL-6 were also found to be up-regulated during peak arthritis in RRV-infected mice (Stoermer et al., 2012). In addition, anti-TNF-α, anti-IFN-γ, or anti- monocyte chemotactic protein-1 treatment reduced the disease severity in RRV-infected mice (Lidbury et al., 2008). Taken together, these studies show that macrophages mediate arthritis in arthritogenic alphaviruses such as CHIKV and RRV.

1.7.2.2 Macrophages and viral persistence

There is convincing evidence that CHIKV and RRV can persist in macrophages. RRV is able to establish persistent infections in many cell lines including mouse muscle cell (Eaton and Hapel, 1976), human synovial fibroblasts (Journeaux et al., 1987) and macrophages cell lines (Linn et al., 1996, Way et al., 2002, Lidbury et al., 2011). CHIKV was found to have persisted in spleen macrophages in macaques months after CHIKV infection (Labadie et al., 2010, Messaoudi et al., 2013). Similarly, CHIKV was found to have persisted in the synovial fluid macrophages in a patient who had chronic CHIKV symptoms for 18 months (Hoarau et al., 2010); RRV was detected in macrophage infiltrated synovium of patients up to 5 weeks post onset of symptoms (Soden et al., 2000). In line with these studies, fully recovered patients have been shown to have significantly higher levels of a mediator that reduces the recruitment of macrophages/monocytes (Chow et al., 2011). This mediator is eotaxin - a natural antagonist that inhibits monocyte/macrophage recruitment by blocking C-C chemokine receptor type 2 (CCR2) (Chow et al., 2011), where CCR2 is found on monocytes/macrophages). It has been proposed that CHIKV could persist in macrophages via an apoptosis-assisted infection mechanism, in which CHIKV hides in apoptotic blebs that can infect neighbouring cells without triggering an antiviral response (Krejbich-Trotot et al., 2011, Joubert et al., 2012). Another study suggests that M2 macrophages are likely to facilitate CHIKV persistence (Stoermer et al., 2012). Taken together, these studies suggest that macrophages are associated with CHIKV and RRV persistence.

1.7.3 Natural killer (NK) cells

NK cells differentiate from common lymphoid progenitor cells in bone marrow (Sun and Lanier, 2011). NK cells are known to provide protection against viral infection, including human cytomegaloviruses, influenza virus, hepatitis viruses and human deficiency virus-1 (HIV) (Lanier, 2008). NK cells exert their antiviral actions mainly by killing the infected cells with cytolytic mediators (perforin and granzymes) (Sun and Lanier, 2011). NK cells also produce large amounts of IFN-γ (Sun and Lanier, 2011, Gerosa et al., 2002), which facilitates the maturation of other immune cells (including macrophages) and the activation of T helper (Th) cells as well as having direct anti-viral activity (Swain et al., 2012). Cell surface molecules can activate or inhibit NK cells. For example, NK cells are activated when there is up-regulation of NK-activating receptors (such as NKG-D) on NK cells and down-regulation of NK-inhibitory ligand (such as human leucocyte antigen A (HLA-A) and CD94) on targeted cells (Lanier, 2008, Lodoen and Lanier,

2005). NK cells can also be activated by several pro-inflammatory cytokines such as type I IFNs, IL-12 and IL-15 (Lanier, 2008).

The role of NK cells in CHIKV infection is not yet clearly defined. A recent study has shown that the acute phase of CHIKV infection triggers transient expansion of NK cells expressing NKG-C and receptor for HLA-C (Petitdemange et al., 2011). This rapid expansion of NK cells has also been seen in human RRV infection (Aaskov et al., 1981, Aaskov et al., 1987). NK cells have also be found to be one of the infiltrating cells in the arthritic feet of CHIKV-infected mice (Gardner et al., 2010), and this is consistent with the up-regulation of IL-12 in the feet of CHIKV-infected mice (Stoermer et al., 2012). The role of NK in CHIKV arthritis is still not known, although NK cells are suspected to be implicated in rheumatoid arthritis (RA), as NK cells produce a range of pro-inflammatory cytokines (such as IFN-γ, receptor activator of nuclear factor kappa-B ligand, macrophage colony-stimulating factor) that may worsen RA pathology (Ahern and Brennan, 2011).

1.7.4 Adaptive immune responses against the CHIKV

Innate immune responses are vital for the rapid detection of viruses, the first-line defence against viruses, and the stimulation of adaptive immune responses (Takeuchi and Akira, 2009). Adaptive immune responses, which consist of the humoral and cell-mediated responses that are mediated by B and T cells, respectively, are thought to be highly specific and effective responses against viral infection. Elderly patients, who are known to have a weaker adaptive immune system (Dorshkind et al., 2009), have been found to be more susceptible to CHIKV infection and can suffer a severe and protracted pathology (Hoarau et al., 2010, Borgherini et al., 2008, Gerardin et al., 2013, Sissoko et al., 2009). Despite the importance of adaptive immune responses in CHIKV disease being known, the precise roles of different arms of adaptive immune responses on CHIKV disease are not entirely established. The potential roles of T and B cells in CHIKV disease, particularly on viraemia control and rheumatic manifestations, are discussed in the following sections.

1.7.4.1 B cell responses

B cells are known to produce antibodies to control CHIKV infection (Eckels et al., 1970, Lum et al., 2013). These antibodies, dominated in humans by immunoglobulin G3 (IgG3), often

target an epitope within the E2 glycoprotein (Kam et al., 2012). Pregnant women infected by CHIKV in the last month before giving birth have been shown to transmit CHIKV to their children (Jaffar-Bandjee et al., 2010). This transmission occurred due to the inadequate time for the mother to generate sufficient levels of anti-CHIKV antibodies that would ordinarily prevent the mother-to-child infection (Jaffar-Bandjee et al., 2010). In addition, anti-CHIKV antibodies have been shown effectively to prevent CHIKV infection, not only in adult WT mice (Selvarajah et al., 2013), but also in type I IFN-deficient mice and neonates (mice), which are known to be more susceptible to CHIKV infection (Couderc et al., 2009, Pal et al., 2013, Selvarajah et al., 2013). Several animal studies have also shown that antibody-based vaccines elicit protection against CHIKV (Eckels et al., 1970, Akahata et al., 2010, Metz et al., 2013a). While it is clear that antibodies are critical and effective in clearing CHIKV viraemia, the effectiveness of antibodies in clearing CHIKV persisting in tissues is less clear. Lum et al. (2013) reported that antibodies were essential in clearing CHIKV infection; conversely, Hawman et al. (2013) showed that injected antibodies could clear the CHIKV viraemia only, but not CHIKV RNA in tissues, in persistently viraemic mice who were deficient in B cells.

The role of B cells in alphaviral arthritic disease is less clear. Some studies have shown that B cells have no role in RRV disease (Morrison et al., 2007, Morrison et al., 2006), while another study reported that a deficiency in B cells leads to more severe arthritic disease in CHIKV-infected mice (Lum et al., 2013). In addition, studies have shown that patients with high levels of CHIKV-specific IgG were associated with long-term rheumatic manifestation, but the mechanism leading to this pathology was unclear (Gerardin et al., 2013, Moro et al., 2012). Further investigation would be required to determine the precise roles of B cells and antibodies in the rheumatic manifestation of CHIKV disease.

1.7.4.2 T cell responses

T cells with αβ T cell receptor (TCR) are the mediators of adaptive immune responses. αβ+ T cells are divided into two groups, based on the expression of co-receptors CD4 and CD8. CD4+ T cells recognise the peptide antigen that is presented by the major histocompatibility complex-II (MHC-II); CD8+ T cells recognise the peptide antigen that is presented by MHC-I. Both CD4+ and CD8+ T cells are often involved in antiviral immune responses. CD4+ T generally mediate antiviral activity by helping B cells to generate antibodies, CD8+ T cells to develop, as well as production of anti-viral cytokines such as IFN-γ and TNF. CD8+ T cells exert their antiviral activity via cytotoxic activity, a process where the virus-infected cells are killed by perforin and

granzyme B secreted by the CD8+ T cells, and/or secretion of antiviral cytokines (e.g. IFN-γ and TNF) (Swain et al., 2012).

The understanding of how T cells are involved in CHIKV disease is still unclear. Clinical and animal studies have shown that CHIKV infections generate robust CHIKV-specific CD4+ and CD8+ T cell responses (Hoarau et al., 2010, Messaoudi et al., 2013, Gardner et al., 2010, Wauquier et al., 2011). A clinical study showed that CD8+ T cells are activated at the early stages of infection (day 2–3) and CD4+ T cells are activated at later stages (Wauquier et al., 2011). Another study showed that aged macaques mount lower levels of anti-CHIKV CD4+ and CD8+ T cell responses compared with adult macaques (Messaoudi et al., 2013). This study also showed that CHIKV persisted in the spleen of older macaques, and postulated that this CHIKV persistence could be attributed to the reduced T cell responses seen in these animals.

Studies have shown that CHIKV vaccines are able to elicit CD8+ T cells targeting the E1 and E2 portions of CHIKV (Garcia-Arriaza et al., 2014, Chattopadhyay et al., 2013), suggesting the potential involvement of CD8+ T cells in combating CHIKV infections. However, adoptively transferred vaccine-induced CHIKV-specific CD8+ T cells have failed to prevent CHIKV infection (Chu et al., 2013). This observation is consistent with a study showing that a deficiency of CD8+ T cells neither aggravated nor ameliorated the viraemia in CHIKV-infected mice (Teo et al., 2012b). In the same study, Teo et al. (2012b) showed that arthritis level (foot swelling) was unaffected by a deficiency of CD8+ T cells, suggesting that CD8+ T cells are not involved in CHIKV arthritis.

Although CD8+ T cells may have little or no role in viraemia control, CD8+ T cells may be involved in clearance of virus from tissues. For example, CD8+T cells have been shown (i) to facilitate the clearance of SINV from the central nervous system (Binder and Griffin, 2001, Kimura and Griffin, 2000) and (ii) to mediate clearance of RRV from macrophages persistently infected by RRV *in vitro* (Linn et al., 1998). These studies collectively suggest that CD8+ T cells are not essential for the viraemia control of alphaviruses, but may be involved in viral clearance from tissues. Whether CD8+ T cells are required for recovery from chronic disease and clearance of viral RNA persisting in joint macrophages remain unresolved (Hoarau et al., 2010, Labadie et al., 2010).

CHIKV infections have been found to trigger a CD4+ response that is biased to the Th1 response in mice (Gardner et al., 2010). Studies have also indicated that a higher Th1 response is correlated with chronic arthritis (Kelvin et al., 2011, Chaaitanya et al., 2011, Hoarau et al., 2010). CD4+ T cells have been shown effectively to control VEEV and SINV in the central nervous

system via the action of IFN-γ (Brooke et al., 2010) (Burdeinick-Kerr et al., 2007). The role of CD4+ T cells in CHIKV viraemia control and disease thus remains unclear.

1.8 Alphavirus vaccine vectors and alphavirus vaccines

Alphaviruses have been extensively studied as potential vaccine vectors (Lundstrom, 2014). For example, influenza virus genes delivered by recombinant VEE replicon vaccines successfully protected mice and birds from influenza infection (Pushko et al., 1997, Schultz-Cherry et al., 2000).

Considerable effort have been expended in the development of alphavirus vaccines, including live attenuated virus vaccines, inactivated vaccines, virus-like particle (VLP) vaccines, virus-vectored vaccines, DNA vaccines and subunit vaccines (Spurgers and Glass, 2011). Despite these efforts, there are no licensed alphavirus vaccines available for human use. The only available vaccine, formalin-activated WEE, is for veterinary use (Barber et al., 1978). The section below discussed the progress of CHIKV and RRV vaccine development.

1.8.1 CHIKV and RRV vaccines

There have been a range of approaches for CHIKV and RRV vaccine development (Table 1.3); however, so far only 4 vaccines have been tested in humans (Ledgerwood, 2013, Edelman et al., 2000, Harrison et al., 1971, Aichinger et al., 2011). The first clinical trial used CHIKV vaccine prepared from formalin-fixed virus cultured in green monkey kidney cells (Harrison et al., 1971). Vaccination in 16 army recruits with this formalin fixed vaccine resulted in the induction of haemagglutination-inhibiting, complement-fixing and neutralising antibodies (Harrison et al., 1971). Another vaccine trial conducted by the US army, used a live attenuated CHIKV vaccine (Edelman et al., 2000). This vaccine consisted of live-attenuated CHIKV (of Asian origin, isolated in Bangkok in 1962) derived from the MRC5 cell line (human foetal fibroblast) (Edelman et al., 2000). Fifty-seven out of 58 of the vaccinated army recruits developed neutralising antibodies, and these persisted for one year in 85% of the recipients. However, this clinical trial was halted due to the development of arthralgia in five of the recipients. The third vaccine comprised Vero-cell derived formalin-inactivated and ultraviolet-inactivated RRV (Aichinger et al., 2011; Holzer et al., 2011). This RRV vaccine resulted in 92.7-92.9% seroconversion in 382 healthy RRV-naive adults. The vaccine candidate is now undergoing Phase III clinical trial in Australia. The fourth vaccine is

a virus-like particle (VLP) vaccine containing the CHIKV structural protein. VLPs are immunogenic but not infectious (Buonaguro et al., 2013) and are considered safer than attenuated-virus vaccines (Wang and Roden, 2013). Akahata et al. (2010) developed a CHIKV VLP vaccine that protected monkeys against CHIKV infection. This VLP vaccine is currently being developed by Bharat Biotech, India and is the only CHIKV vaccine that is currently in clinical development (Phase I completed, but results not reported) (Ledgerwood, 2013).

In addition to the 4 vaccines described above, there are a number of other vaccines in preclinical development (Table 1.3), including live-attenuated CHIKV vaccine (Levitt et al., 1986), chemical-inactivated CHIKV and RRV vaccines (Tiwari et al., 2009, Gardner et al., 2010, Yu and Aaskov, 1994, Aaskov et al., 1997), other VLP vaccines (Metz et al., 2013a, Metz et al., 2013b), recombinant CHIKV vaccines with an encephalomyocarditis virus internal ribosome entry site (IRES) (Roy et al., 2014, Chu et al., 2013, Partidos et al., 2012, Plante et al., 2011), chimeric alphavirus (VEEV/EEV/CHIKV) vector-based vaccines (Chattopadhyay et al., 2013, Wang et al., 2011b, Wang et al., 2008), other virus vector-based vaccines (Garcia-Arriaza et al., 2014, Brandler et al., 2013, Wang et al., 2011a), DNA vaccines (Mallilankaraman et al., 2011, Muthumani et al., 2008) and recombinant protein-based vaccine (Kumar et al., 2012).

1.9 Drug treatments for CHIKV patients

Treatment for CHIKV disease usually involves the use of analgesics and/or NSAIDs, with aspirin to be avoided because of the risk of haemorrhage (Suhrbier et al., 2012) (Chopra et al., 2014). A clinical study suggested that treatment using NSAIDs plus steroids may also be useful in ameliorating the rheumatic symptoms of CHIKV disease (Padmakumar et al., 2009). Methotrexate has occasionally been administered with reported benefit to patients with protracted chronic CHIKV disease suffering from RA-like diseases (Jaffar-Bandjee, 2010; Ganu, 2011). Recent human trials have shown that chloroquine is ineffective in treating acute and chronic CHIKV arthritis (Delogu and de Lamballerie, 2011, Chopra et al., 2014).

Table 1.3: Vaccines in development for CHIKV and disease.

Type of vaccine	Phase of clinical research	References
Live-attenuated CHIKV	Phase II Preclinical—halted	Levitt et al. (1986) Edelman et al. (2000)
Chemical-inactivated CHIKV	Phase I Preclinical	Harrison et al. (1971) White et al. (1972) Tiwari et al. (2009) Gardner et al. (2010)
Chemical-inactivated RRV	Phase I/II Preclinical	Aichinger et al. (2011) Holzer et al. (2011 Yu and Aaskov (1994) Askov et al. (1997)
VLP	Phase I/Preclinical	Akahata et al. (2010) Ledgerwood (2013) Metz et al. (2013b) Metz et al. (2013a)
Recombinant CHIVK vaccines with an encephalomyocarditis virus internal ribosome entry site (IRES)	Preclinical	Roy et al. (2014) Chu et al. (2013) Partidos et al. (2012) Plante et al. (2011)
Chimeric alphavirus vector-based	Preclinical	Chattopadhyay et al. (2013) Wang et al. (2011b) Wang et al. (2008)
Other virus vectors (adenovirus/modified vaccinia virus Ankara/measles) (targeting genes of structural proteins: E1, E2, E3, 6K and C)	Preclinical	Garcia-Arriaza et al. (2014) Brandler et al. (2013) Wang et al. (2011a)
DNA (targeting envelope proteins E1, E2 and E3)	Preclinical	Mallilankaraman et al. (2011) Muthumani et al. (2008)
Recombinant protein-based (targeting E2)	Preclinical	Kumar et al. (2012)

1.10 Neutralising antibody-based therapeutics

Neutralising antibodies are well recognised as potential therapeutics for several virus infections including hepatitis A, hepatitis B, respiratory syncytial, herpes simplex, rabies, measles and vaccinia (Keller and Stiehm, 2000). For CHIKV disease, anti-CHIKV neutralising antibodies were shown to prevent viraemia and pathology in WT mice, as well as highly susceptible immunocompromised mice that lack IFN-α/β receptor or IFN-α/β/γ receptor (Couderc et al., 2009, Gardner et al., 2010, Fric et al., 2013, Pal et al., 2013). However, Suhrbier et al. postulated that

antibody treatment might not be useful for most patients, as patients would have developed anti-CHIKV antibodies by the time they were diagnosed with CHIKV infection, which is usually undertaken by serological testing (Suhrbier et al., 2012). A recent study revealed that although anti-CHIKV antibody treatment is effective in neutralising CHIKV *in vitro*, anti-CHIKV antibody treatment can drive antibody-evading strategies namely CHIKV cell-to-cell transmission, which might conceivably reduce the efficacy of antibody treatment (Lee et al. 2011). Antibody treatment may, nevertheless, be useful for treating patients with a suppressed immune system, such as newborn babies, pregnant women and the elderly, or be used as a prophylactic measure in epidemic settings (Suhrbier et al., 2012).

1.11 Conclusions and thesis aims

The unprecedented magnitude of the recent CHIKV epidemic, which resulted in CHIKV cases in more than 40 countries, has highlighted the threat posed by CHIKV disease. Additional concerns have arisen in the current epidemic associated with the new vector and the relatively high incidence of severe disease manifestations and occasional fatalities. Currently, there is no licensed human vaccine available for CHIKV. Treatment commonly involves the use of analgesics and/or NSAIDS; however, the relief provided by these drugs is often inadequate. To improve the therapies available for CHIKV disease, a better understanding of how viraemia and pathology are controlled is required. While the role that type I IFN responses play in controlling CHIKV infection is now well recognised, the roles of other immune components such as adaptive immune cells (B and T cells), macrophages, NK cells, neutrophils and cytokines are less well defined – in particularly the roles of these cells in viral arthritis and CHIKV persistence. The overall aim of this thesis is to explore the roles of these cells in CHIKV arthritis, and the mechanisms involved in persistence of CHIKV using an adult mouse model that closely mimics human CHIKV disease (see section 1.6.2).

The specific aims of this project are:

Aim 1: To determine the effect of CCR2 deficiency on the arthritis caused by CHIKV.

Aim 2: To examine if an immune response limited to B cell response may protect against CHIKV disease.

Aim 3: To gain more insights into the long-term persistence of CHIKV RNA and its role in driving chronic arthritic disease.

Chapter 2: Material and methods

2.1 Propagation of Vero and C6/36 cells

Vero cells (ATCC # CCL-1) and C6/36 (ATCC # CRL-1660) were cultured in 5% CO_2 atmosphere at 37°C and 28°C, respectively, with 15 ml of R5 media comprising of Roswell Park Memorial Institute-1640 (RPMI 1640) medium (Invitrogen, Carlsbad, USA) supplemented with: (a) 2 mM L-glutamine (Invitrogen), (b) 5% foetal calf serum (FCS) with <0.05 endotoxin unit (EU)/ml (Invitrogen), (c) 10 mM HEPES buffer (Sigma-Aldrich, USA), (d) 100 U/ml penicillin (Invitrogen), and (e) 100 µg/ml streptomycin (Invitrogen). Cells were passaged every 3-4 days. To passage cells, RPMI 1650 medium was removed, and the cell monolayer washed once with 5 ml of phosphate buffered saline (PBS). The cell monolayer was detached from the tissue culture flask by incubating cells with 3 ml of 0.05% trypsin at 37°C for 10 min and gentle tapping of the flask. Detached cells were then diluted in 10 ml of R5 media before seeding into tissue culture flask.

2.2 Virus preparation

CHIKV was isolated from a patient during 2006 CHIKV outbreak in Reunion Island (Gardner et al., 2010). This isolate (LR2006-OPY1) was passaged twice in C6/36 cells in R5 medium (see section 2.1). After 24 hours of infection, virus preparations were harvested then aliquoted and stored at -70ºC.

2.3 Virus titration by 50% cell culture infection dose ($CCID_{50}$)

Virus samples were collected and kept at row 1 (A to H) at -70ºC at a 96-well flat bottom plates. The samples were thawed at room temperature (RT). R2 media (comprising of supplements as in R5 media but with 2% FCS instead of 5% FCS) were dispensed into a 100 ml media reservoir (Vistalab technologies, NY, USA). R2 media (100 µl) were pipetted into four 96-well-plates simultaneously in a row-by-row fashion i.e. pipetting R2 media into row 12 (A to H) of a maximum of 4 plates then continued on row 11-2 (A to H). For row 1 (A to H), 100 µl R2 media were carefully added without touching the sera. Pipette tips were changed for each plate. The media reservoir was changed after dispensing the R2 media into row 1. This procedure prevents the potential cross contamination that might occur during dispensing of the R2 media into the row 1.

Samples were then serially diluted ten-fold down the plate from row 1-12. The media and sera were gently mixed (pipetted up and down 5 times) but avoiding the inclusion of bubbles. Mixed samples (11 µl) from row 1 were transferred to following row that already contained 100 µl R2 media. The second click of the pipette was not triggered as this causes bubble formation. The first click of the pipette was gently released while the pipette tip was still inside the well. The pipette tips were then discarded and then viral dilution was repeated across the plate, changing tips each time. C6/36 cells ($2x10^4$ cells in 100 µl in R5 media) were then added in each well. C6/36 cells were added simultaneously into 4 plates (maximum) in a row-by-row fashion i.e. pipetting C6/36 cells into highest dilution row (row 12) then continued on lower dilution rows (row 11-2). These plates were then incubated in 5% CO_2 atmosphere at 25°C. The infectivity titre (log_{10} $CCID_{50}$/ml) was calculated as described by Reed and Muench (1938).

2.4 Ethics statement and care of animals

All experiments were approved by the QIMR Berghofer animal ethics committee. All knock-out mouse strains were bred at the QIMR Berghofer animal house facility. C57BL/6 mice were purchased from Animal Resources Center (Canning Vale, WA, Australia). All experiments were performed in QIMR Berghofer Animal House and PC3 facility. All animals were handled in accordance with good animal practice as defined by the National Health and Medical Research Council of Australia. The mice are supplied with filtered air, clean water and nutritious food. The mouse cages are changed every week and limited to 6 mice per cage. Adult mice were eunthanised, via carbon dioxide inhalation, before performing any lethal procedures and when the mice were deemed excessively sick (e.g. severe hind limb weakness or repeated dragging of hind legs). To achieve statistic significance, almost all experiments, consisting of 3-6 mice per group, and were independently performed at least two times; (see section 2.26 for statistical analyses). The number of mice and experimental repeats is indicated in the figure legends of each figure. The total number of wild-type mice used in this project was 150; the total number of the knock-out mice used is shown in Table 2.1.

2.5 Mouse infection

CHIKV viral stocks were diluted in R2 media. C57BL/6 mice and various knockout mice (C57BL/6 background) (Table 2.1) were infected with CHIKV (10^4 $CCID_{50}$ in 40 µl R2 media) via subcutaneous injection into the dorso-lateral metatarsal region of each foot. All mice were 6-10 weeks old.

Table 2.1: List of knock-out mice strains used in various experiments.

All knockout mice were on a C57BL/6 background.

Mice strain	Deficiency	No. of mice used	Reference
$CCR2^{-/-}$	C-C chemokine receptor 2 (CCR2)	80	Boring et al. (1997)
$IL\text{-}10^{-/-}$	Interleukin-10 (IL-10)	10	Kuhn et al. (1993)
µMT	B cells	100	Kitamura and Rajewsky (1992)
$Rag\text{-}1^{-/-}$	B and T cells	100	Mombaerts et al. (1992)
RG	B, T and NK cells	20	Song et al. (2010)
$MHC\text{-}II^{\Delta/\Delta}$	CD4+ T cells	25	Madsen et al. (1999)
$IFN\text{-}\gamma^{-/-}$	Interferon-γ (IFN-γ)	25	Dalton et al. (1993)

2.6 Serum collection from CHIKV infected mice

Blood was collected by tail vein bleed. Mice were restrained in a mouse restrainer with tissue paper at the base to cushion mice while the tail is being pulled against the end of restrainer. There are two veins situated left and right (purple colour) on the tail. One of the veins was gently cut across the tail (as opposed to lengthwise) using a sterile scalpel blade no. 23 (Livingstone, Rosebery, Australia). A new blade was used for each group and between mice the blade was sprayed with 80% ethanol and dried on tissue paper. The blood was collected using labelled MiniCollect 0.5 ml Z serum tubes (Greiner Bio-One GmbH, Kremsmunster, Austria). The tails were massaged to collect sufficient blood (roughly 8 drops of blood = 30-40 µl). Excessive blood on the tail was mopped with tissue paper and pressure was applied to the wound for 30 sec to stop the bleeding. Serum tubes were then placed in a sealed container and transported to another Physical Containment 3 (PC3) lab facility at RT. In the PC3 lab, the collected bloods were centrifuged at 7200 revolutions per minute (rpm) for 2.5 min on an Eppendorf Microcentrifuge

5418 (USA). Sera were removed from above gel plug in MiniCollect tubes with 20 µl pipette. Sera (in duplicate, 10 µl per well) were plated into flat bottom 96-well-plates and stored at -70°C.

2.7 Isolation of infectious CHIKV from feet

2.7.1 Mortar and pestle method

Mice feet were excised, lacerated (with surgical blades), weighed and transferred into microcentrifuge tube with 1 ml R10 media (comprising of supplements as in R5 media but with 10% FCS instead of 5% FCS). The samples were then stored at -80ºC, thawed at RT and ground using a mortar and pestle. The ground samples were transferred into microcentrifuge tubes and centrifuged at 1000 rpm at RT for 1 min in an Eppendorf 5418 microcentrifuge. The supernatant was then transferred to a new microcentrifuge tube and the $CCID_{50}$ calculated as described (see section 2.3 for detailed method).

2.7.2 Homogeniser method

Mice feet were excised, weighed and transferred into 2 ml snap-lock tubes (Eppendorf, US) containing 2 ml R10 media and stored at -80ºC. The frozen feet samples were thawed at RT and, two 5mm stainless steel beads (Qiagen GmbH, Hilden, Germany) were added. Feet samples were then homogenised using TissueLyser II (Qiagen GmbH, Hilden, Germany) at 25 Hertz for 3 min, paused for 3 min on ice and homogenised again at 25 Hertz for 3 min. The mixture was centrifuged at 1000 rpm at RT for 1 min in an Eppendorf 5418 microcentrifuge. The supernatant was then transferred to a new microcentrifuge tube, and the virus concentrations were then determined by $CCID_{50}$ as described (see section 2.3 for detailed method).

2.7.3 Collagenase digestion method

Mice feet were excised and transferred onto a 3 cm diameter Petri dish containing 1.5 ml of R10 media. The Petri dish containing the mice feet were placed on ice. The feet samples were thoroughly lacerated using a surgical blade (skin was not removed), digested with 4% collagenase-dispase (Roche, Dee Why, NSW, Australia) and incubated at 38ºC. After 10 min, the feet samples were lacerated again at RT for 5 min and then incubated at 38ºC again. The previous step (laceration and incubation) was again repeated. After the incubation, the tissue suspension was

transferred into a 10 ml tube and centrifuged at 350 rpm for 1 min in an Eppendorf 5810R centrifuge. The supernatant was transferred into a new 15 ml tube containing 5 ml of R10 media. The tube was placed on ice, 6 ml of Percoll (Sigma-Aldrich, USA) was gently added to the bottom of the tube via a glass pipette and centrifuged at 1600 rpm at 4ºC for 30 min. The cell containing interphase layers were then transferred into a new 15 ml tube. The cells were washed once with 5 ml of 100% FCS and centrifuged at 1000 rpm for 6 min. After the centrifugation, the supernatant was discarded. The cell pellet was gently resuspended in 2 ml of ammonium-chloride-potassium (ACS) lysing buffer (0.15M NH_4Cl, 1mM $KHCO_3$, 0.1 mM Na_2ethylenediaminetetraacetic acid (EDTA)) for 30 sec, 8 ml of R10 media was then added and centrifuged at 1000 rpm at 4ºC for 6 min. After the centrifugation, the cell pellet was resuspended in 800 µl R10 media, filtered through nylon mesh (38 µm pore size) (Seflar Filter Specialist, Blacktown, Australia) and plated into a single well on 24-well-plate. After 24 h, 100 µl of supernatant was collected, stored at -20ºC, thawed at RT and the virus titres were then determined by $CCID_{50}$ as described (see Chapter 2 section 2.3 for detailed method).

2.8 Blood smear

Blood was collected by tail vein bleed, smeared and air dried on glass slides at RT. The glass slides were stained with Quick Dip (Fronine Laboratory Supplies, Australia).

2.9 Isolation of infectious CHIKV from various mice tissues

Lymph mode, spleen, liver and thigh muscle were excised, weighed and transferred into microcentrifuge tubes containing 1 ml R10 media. The samples were then stored at -80ºC, thawed at RT and homogenised using metal mesh and a syringe plunger. The homogenised samples were transferred into microcentrifuge tubes and centrifuged at 1000 rpm at RT for 1 min in an Eppendorf 5418 microcentrifuge. The supernatants were then transferred into a new microcentrifuge tubes and the virus concentrations were then determined by $CCID_{50}$ as described (see section 2.3 for detailed method).

2.10 Mouse vaccination

CHIKV vaccine was prepared by Medical Innovations Australia Pty. Ltd., Brisbane, Australia. Briefly, CHIKV was cultured in C6/36 cells, inactivated using binary ethylenimine (BEI), concentrated via polyethylene glycol and resuspended in 1X TNE buffer (50 mM Tris–HCl (pH 7.4), 100 mM NaCl and 0.1 mM EDTA). Mice were vaccinated as described previously (Gardner et al., 2010). Briefly, the mice were injected s.c. (at the base of the tail) once with 10 µg of BEI inactivated CHIKV antigen in 50 µl of RPMI 1640 medium.

2.11 Anti-Ly6G antibody treatment

Mice were treated with 0.3mg (in 75 µl RPMI1640) (clone 1A8) (Stemcell technologies, USA) or IgG2a control antibody (clone 2A3) (Stemcell technologies, USA) i.p. at the indicated time points.

2.12 Foot measurement in mice

The width and height of the hind feet were measured using digital vernier callipers (Kincrome, Australia) (Figure 2.1). The percentage of increase in feet area was calculated by:

$$feet\ area = feet\ width\ x\ feet\ height$$

$$\%\ increase\ in\ feet\ area = \left(\frac{Feet\ area\ of\ day\ x - Feet\ area\ of\ day\ 0}{Feet\ area\ of\ day\ 0} \right) x\ 100$$

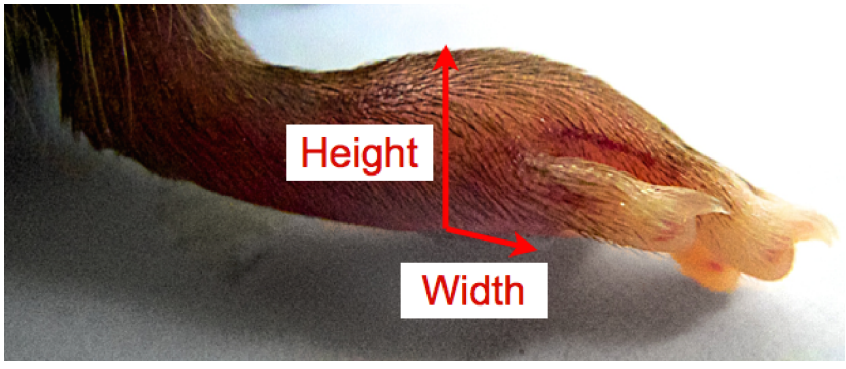

Figure 2.1: Foot measurement in mice.

The height and width of the hind feet were measured using callipers.

2.13 Neutralisation assay

Mouse sera were heat-inactivated at 60ºC for 30 min in a water bath. This incubation destroys complement and kills virus. Heat-inactivated sera were serially diluted three-fold across flat bottom 96-well-plates in RPMI 1640 medium containing L-glutamine (Invitrogen) in a final volume of 50 µl. Virus samples were thawed and diluted in R2 media, to a final concentration of 200 $CCID_{50}$/ml in 50 µl per well. Sera and virus were then incubated in 5% CO_2 atmosphere at 37°C for 1 hr before adding 100 µl of $8x10^3$ Vero cells (in R5 media). After 5 days of incubation, plates were stained with 100 µl of 0.05% crystal violet in 10% formaldehyde-PBS. Serum antibodies prevent the cell from becoming infected by virus. The serum dilution giving 100% protection against cytopathic effect was visualised using crystal violet staining. The presence of crystal violet stained monolayer indicated that serum antibodies protected the cell.

2.14 RNA extraction from virus infected mice's feet

Mice feet were lacerated using surgical blades (Livingstone, Rosebery, Australia). Samples were stored in 1 ml of RNA*later*™ (Ambion, Austin, USA) in a microcentrifuge tube for 24 h at 4°C prior to long-term storage at -70°C. This step ensured maximum penetration of RNA*later*™ into the foot tissue. Total RNA extraction was performed according to manufacturer's instructions. Frozen feet samples were thawed, removed from RNA*later*™, and transferred into 2ml snap-lock tubes (Eppendorf). Two 5 mm, stainless steel beads and 1.5 ml of TriZol Reagent (Invitrogen, NY, USA) were added into each tube. Feet samples were then homogenised using TissueLyser at 25 Hertz for 6 min. The homogenised samples were centrifuged at 12000 rpm at 4ºC for 15 min in a Profuge 14K (United Biosciences, USA). Samples (excluding tissue remnant) were transferred into a fresh microcentrifuge tube, and 200 µl chloroform (Invitrogen) added. The tube was shaken vigorously for 15 sec, and then incubated at RT for 3 min. The mixture was centrifuged at 12,000 rpm at 4°C for 15 min in a Profuge 14K. The resulting RNA containing upper aqueous phase was transferred into new microcentrifuge tube and 450 µl of isopropyl alcohol was added. Samples were incubated at RT for 10 min after gentle inversion. The precipitated RNA was pelleted by centrifugation at 12,000 rpm, 4°C for 15 min. The resulting RNA pellets were washed with 1 ml of 75% ethanol, air dried, resuspended in RNAse-free water (Sigma-Aldrich, USA) and stored at -70°C. RNA purity and concentration were estimated using Nanodrop ND-1000 spectrophotometer (Thermo Scientific, Waltham, USA).

2.15 Synthesis of complementary deoxyribonucleic acid (cDNA) from extracted RNA samples

The first strand cDNA was synthesised in a reaction consisting of 200 ng of random hexamer oligonucleotides (Sigma, Australia), 500 µM deoxynucleoside triphosphates (dNTPs) (Promega Corporation, WI, USA), and 0.25-1.0 µg of the RNA sample made up to 12 µl in H_2O. The samples were incubated in a thermal cycler at 65°C for 5 min, transferred on ice and 4 µL of 5X strand buffer (Invitrogen), 2 µl of 0.1M dithiothreitol (Invitrogen) and 1 µl of H_2O were added. The samples were transferred back to the thermal cycler preheated to 25ºC, incubated for 2 min and 1 µL of Superscript (Invitrogen) was added. The samples incubated at following conditions: 25°C for 10 min, 50°C for 50 min, and 70°C for 15 min.

Negative strand specific cDNA was synthesised by the same procedure (as above) with the exception of the hemaxer oligonucleotides, which was substituted with 10 pg of CHIKV primer with a tag sequence: (5'-GGCAGTATCGTGAATTCGATGCGACACGGAGACGCCAACATT-3') (tag sequence is underlined) (adapted from Plaskon et al. 2009).

2.16 Quantitative real-time PCR (qRT-PCR)

qRT-PCR was performed in reaction consisting of 1 µl of cDNA (see section 2.15), 10 µL of SYBR green Super mix-UDG (Invitrogen), 1 µl bovine sera albumin, 6 µl H_2O, and 1 µl of 10 µM of forward and reverse primer (Table 2.2). PCR cycling and product detection were performed using Rotorgene 6000 (Corbett Research, Mortlake, Australia). The samples incubated at following cycling conditions: one cycle of 50°C for 2 min, one cycle of 95°C for 2 min, 45 cycles of 94°C for 5 sec (DNA denaturation that separates the double-stranded DNA), 60°C for 10 sec (primer annealing) and 72°C for 30 sec (sequence extension and signal acquisition). Data was analysed using Rotor-Gene Real Time Analysis software (Corbett Research, Australia).

Table 2.2: List of primers used for qRT-PCR.

Gene	Sequence (5' to 3')	Reference
Arg-1	Forward: TGGACCTGGCCTTTGTTGA Reverse: GGTTGTCAGGGGAGTGTT	Wongtrakool et al. (2012)
CHIKV nsP1 negative strand	Forward: AATAAATCATAAGGCAGTATCGTGAATTCGATGC Reverse: AATAAATCATAAGTCTGCTCTCTGTCTACATGA	Adapted from Plaskon et al. (2009)

CHIKV-E1 positive strand	Forward: AGCTCCGCGTCCTTTACC Reverse: CAAATTGTCCTGGTCTTCCTG	Designed in house
CXCL2	Forward: GTGAAC TGCGCTGTCAATGC Reverse: CGCCCTTGAGAGTGGCTATG	Feng et al. (2006)
G-CSF forward	Forward: CTCAACTTTCTGCCCAGAGG Reverse: AGCTGGCTTAGGCACTGTGT	Waight et al. (2011)
IL-10 forward	Forward: ACAGGAGAAGGGACGCCAT Reverse: GAAGCCCTACAGACGAGCTCA	Ellett et al. (2010)
IL-1B forward	Forward: TCACAGCAGCACATCAACAAG Reverse: CCAGCAGGTTATCATCATCATCC	Bakker et al. (2008)
ISG-54	Forward: CTCTCTGGAGCAAGCCATTC Reverse: GCCATTGCTTGGTTTTTATG	Designed in-house
KC	Forward: TGTCAGTGCCTGCAGACCAT Reverse: CCTCGCGACCATTCTTGAGT	Feng et al. (2006)
Nur77	Forward: TGATGTTCCCGCCTTTGC Reverse: CAATGCGATTCTGCAGCTCTT	Maxwell et al. (2005)
ROR-γT	Forward: CCGCTGAGAGGGCTTCAC Reverse: TGCAGGAGTAGGCCACATTACA	Carlson et al. (2009)
RPL13a	Forward: GAGGTCGGGTGGAAGTACCA Reverse: GCAT CTTGGCCTTTTCCTT	Mogal and Abdulkadir (2006)
T-bet	Forward: ACCAGAGCGGCAAGTGGG Reverse: TGGACATATAAGCGGTTCCCTG	Carlson et al. (2009)

2.17 DNA gel electrophoresis

PCR products were visualised by electrophoresis at 100 volts for 30 min on a 1.2% (w/v) agarose gel (Biorad, USA) containing 0.02 µg/ml ethidium bromide in 1X Tris acetate EDTA (TAE) Buffer (40mM Tris, 20mM sodium acetate, 1mM EDTA, pH8.2). The gel was visualised using ultraviolet transilluminator.

2.18 Cytokine and chemokine detection by cytometric bead array assay

Cytometric bead array (BD Biosciences, San Jose, USA) assay was performed according to the manufacturer's instructions. Briefly, in a single well of 96-well V-bottom plate, 10 µL of sera was incubated with 1.5 µL of individual bead (coated with capture antibodies that detect desired cytokine e.g. MCP-1) along with an equal volume PE-conjugate in the dark, at RT for 2 hours. The samples were then washed once with 100 µL wash buffer (BD Biosciences, San Jose, USA) per well, centrifuged at 1000 rpm for 3 min and supernatant removed. The samples washed with 100 µl formalin (for CHIKV inactivation), supernatant removed and resuspended in 120 µL of wash buffer per well. Samples were then analysed by BD FACSArray bioanalyzer (BD Biosciences, USA). The data was analysed by FCAP Array™ v2 Software (BD Biosciences, USA).

2.19 Interferon alpha (IFN-α) detection by Mouse IFN-alpha FlowCytomix Simplex Kit

Serum IFN-α was detected using Mouse IFN-alpha FlowCytomix Simplex Kit (eBioscience, USA). The assay was performed according to manufacturer's instructions. Briefly, in a single well of 96-well V-bottom plate, 10 µl of sera was incubated with 5 µl of fluorescence beads coated with monoclonal antibody targeting mouse IFN-α and 10 µl of biotin-conjugate anti-mouse IFN-α monoclonal antibody. The plates were incubated in the dark for 2 hours on a microplate shaker at 500 rpm. The samples were then washed once with 100 µl of assay buffer (eBioscience, USA), centrifuged at 1000 rpm for 5 min, supernatant removed. Beads were washed with 100 µl formalin (for CHIKV inactivation), supernatant removed and the beads were then resuspended in 60 µl of assay buffer per well. Samples were then analysed by BD FACSArray bioanalyzer (BD Biosciences, USA) and data collected was analysed by FCAP Array™ v3.01 Software (BD Biosciences, USA).

2.20 Histology and immunohistochemistry

Histology and immunohistochemistry samples were prepared by HistoTechnology Facility (University of Queensland, Australia). Mouse tissue samples (feet, liver, lymph node, spleen and muscle) were fixed in 10% PBS-buffered formalin. Feet were decalcified in EDTA for 3 weeks.

These tissues were embedded in paraffin wax. Haematoxylin and eosin (H&E) staining was performed using standard methods.

2.20.1 Leder Stain (for neutrophils)

Leder Stain, which detects choloracetate esterase activity, was used to stain neutrophils (Bancroft and Gamble, 2001). Formalin fixed paraffin sections were rehydrated and stained with Naphthol AS-D chloroacetate solution (Sigma-Aldrich, USA) for 30 min at 37ºC, counterstained with Mayer's haematoxylin (Sigma-Aldrich, USA) for 3 min and rinsed with Scott's solution (Sigma-Aldrich, USA) for 30 sec.

2.20.2 Chromotroph 2R staining (for eosinophils)

Chromotroph 2R staining was used to stain eosinophils (Cook, 1974). Formalin fixed paraffin sections were affixed to adhesive slides, rehydrated and stained with Mayer's haematoxylin for 3 minutes and stained with 0.05% chromotrope 2R (W/V) (ProSciTech, Thuringowa, Australia) (dissolved of 0.1% phenol (W/V)) for 30 min. The samples were then dehydrated with ethanol.

2.20.3 F4/80 immuno-stain (for macrophages)

F4/80 immunohistochemistry was used to identify macrophages. Fixed slides were rehydrated in distilled water and incubated in 2.0% hydrogen peroxide in Tris buffered saline (TBS). After 10 min incubation at RT, slides were rinsed with distilled water then undergone antigen heat retrieval at 105ºC using the Biocare Medical decloaking chamber (Biocare, USA). Slides were cooled down for 15 min, washed with TBS and incubated with Biocare Medical Background Sniper (Biocare, USA) for 30 min. The sections were then incubated for 90 min with 0.3% primary antibody (Abcam rat anti-mouse F4/80) in Biocare Medical Da Vinci Green diluent (Biocare, USA). Sections were then washed with TBS, treated with Biocare Medical anti-rat Probe (20 min) (Biocare, USA), developed colour in 3,3 diaminobenzidine (DAB) and counterstained with Mayers' haematoxylin.

2.20.4 Ly6G staining (for neutrophils)

Ly6G staining was used to stain neutrophils. Fixed slides were rehydrated in distilled water and incubated in 2.0% hydrogen peroxide in TBS. After 20 min incubation at RT, slides were rinsed with distilled water. Antigen heat retrieval were performed at 100ºC using the Biocare Medical decloaking chamber. Slides were cooled at RT for 20 min, washed with TBS and incubated with Biocare Medical Background Sniper (Biocare, USA) for 15 min. The sections were incubated for 18 hours with 0.85% primary antibody (Abcam purified rat anti-mouse Ly6G neutrophil #NMP-R14) in Biocare Medical Da Vinci Green diluent. Sections were washed with TBS, incubated with Biocare Medical anti-rat Probe (20 min) followed by Biocare Medical Rat horseradish peroxidase (HRP) polymer (20 min). The colour signal was developed in betazoid DAB (Biocare MACH 1 kit) and counterstained with Mayers' haematoxylin.

2.20.5 ApopTag staining (for apoptotic cells)

ApopTag Kit (Millipore, Australia), which stains the 200 base pair fragmented DNA released during apoptosis, was used to detect apoptotic cells. Fixed slides were rehydrated in distilled water then treated with 150 µl proteinase K (20 µg/ml in 0.05M Tris-HCI, 0.01M $CaCl_2$, pH 8) for 10 min at RT. In a Coplin jar, the slides were washed twice with distilled water and incubated with 3.0% H_2O_2 in PBS for 5 min. The buffer was removed, and the sections were then treated with 18 µl equilibrium solution (from the the ApopTag Kit) for 10 min, 12.5 µl TdT enzyme (from the the ApopTag Kit) for 60 min at 37ºC and a stop wash buffer (from the the ApopTag Kit) for 10 min. The slides were washed with PBS before incubated with 17.5 µl anti-digoxigenin conjugate for 30 min at RT. The colour was developed with DAB and counterstained with haematoxylin.

2.20.6 Safranin O staining (for proteoglycans)

Safranin O staining was used to detect proteoglycan content in cartilage. Fixed slides were rehydrated and stained with Weigert's iron hematoyxlin solution (Sigma, Australia) for 10 min, washed with H_2O for 10 min, stained with fast green solution for 5 min, rinsed with 1% acetic acid solution for 10 sec and stained in 0.1% safranin O solution (BDH, Poole, England) for 5 min. The slides were then dehydrated and mounted using resinous medium.

2.21 Quantification of infiltrating cells in the joint by histology image analysis

Stained whole foot sections were digitally scanned using Scan Scope XT digital slide scanner (Aperio, Vista, CA). Aperio Image Scope analysis software version 11 (Aperio Technologies), Positive Pixel Count algorithm and Color Deconvolution algorithm were used to quantify the infiltrating cells on specific staining. The detailed parameters of these algorithms were listed in Table 2.3.

Table 2.3: Parameters for algorithm detecting specific dye.

Positive Pixel Count version 9.1 and Color Deconvolution version 9.1 were used to quantify specific infiltrating cells following each staining protocol.

1. Positive Pixel Count version 9.1

It detects a pixel at a given hue value (color code), hue width (range of hue value) and saturation.

Staining (cell)	Quantified color	Hue value	Hue width	Saturation
Apotag (apoptotic cells)	Brown (more red)	0.1	0.7	0.04
Ly6G (neutrophils)	Brown (more red)	0.1	0.6	0.04
F4/80 (macrophages)	Brown (more yellow)	0.15	0.6	0.04

2. Color Deconvolution version 9.1

It separates up to three-overlapped color and quantifies one color. Color OD of each color was determined by detecting an area containing single color.

Staining	Quantified color	Color 1 OD (R; G; B) (quantified channel)	Color 2 OD (R; G; B)	Color 3 OD (R; G; B)
Chromotroph 2R (eosinophils)	Pink	0.44; 0.73; 0.55	0.67; 0.66; 0.32	0;0;0
Leder (neutrophils)	Red	0.05; 0.66; 0.74	0.20; 0.56; 0.76	0;0;0

2.22 T cell proliferation assay

Mice spleens were teased through the mesh and transferred to a 10 ml centrifuge tube containing 5 ml of R10 media. Erythrocytes were lysed by mixing the cells with 3 ml of ACS lysing buffer for 30 sec at RT. After 2 min, cell suspensions were added with 7 ml of R10 media, centrifuged down at 1000 rpm for 5 min and plated at $2.5x10^6$ cells/ml in R10 media on a U-bottom 96-well-plate. Splenocytes were stimulated with 10 µg/ml of BEI CHIKV antigen (section 2.10). Phytohemagglutinin (Sigma-Aldrich, USA) (2.5 µg/ml) was used as a positive control. The cells were incubated at 37ºC and 5% CO_2 atmosphere. After 72 hours of incubation, each well was treated with 0.5 µCi of [^{3}H]-thymidine for another 16 hours. The cells were harvested the next day onto MicroBeta Filtermat-96 A using the FilterMate™ Cell Harvester (PerkinElmer). Radioactivity was measured using the MicroBeta Liquid Scintillation Counter (PerkinElmer).

2.23 Anti-CHIKV enzyme-linked immunosorbent assay (ELISA)

BEI CHIKV antigen (1.2 µg/ml) in 0.05M pH 9.6 carbonate coating buffer (100 µl) (SigmaAldrich, USA) was added to Maxisorp Nunc-Immuno plates (Nunc™, Denmark). After overnight incubation at 4ºC, the supernatant were gently discarded. The antigen-coated plates were washed three times with PBST (PBS containing 0.01% (v/v) Tween 20). The plates were blocked with 200 µl/well of 5% skim milk in PBST for 1 hr at RT. Mouse sera were 3-fold serially diluted in PBST with 1% FBS. The serially diluted sera were then transferred on to the antigen coated and blocked plate and incubated for 90 min at RT. Plates were then washed 3 times with PBST. Rat anti-mouse IgG2a/IgG1-biotin (BD Pharmingen, USA)(100 µl) was added to each well and incubated for 90 min at RT. The plates were then washed 3 times with PBST. Streptavidin-HRP was diluted to 1/10000 in PBST and added into each well. The plates were incubated in dark for 1 hr at RT. The plates were washed 3 times with PBST. The colour was developed with 100 µl of ABTS:H_2O_2 in the dark at RT for 5-15 min until green colour fully developed. The developed colour was quantified by measuring the optical density at 405 nanometer (nm) wavelength using a VersaMax™ microplate reader (Molecular Devices, CA, USA).

2.24 ELISA for detecting anti-nuclear antibody (ANA)

ANAs were detected using Mouse ANA Total Ig ELISA kit (Alpha Diagnostic, USA) following manufacturer's instructions.

2.25 Microarray experiments and analyses

RNA samples for microarray experiments extracted as described (see section 2.14). The prepared RNA samples were then processed by Ramaciotti Centre (Sydney, Australia) for microarray experiments using Mouse Gene 1.0ST arrays (Affymetrix). With the assistance of Dr. Nakaya Helder, differentially expressed genes (DEGs) were identified as described (Nakaya et al., 2012). Briefly, robust multiarray average algorithm, which includes global background adjustment and quantile normalisation, was used to normalise all probe sets. Probe sets with no annotations were removed. Principal Component Analysis was performed on the remaining probe sets. DEGs were then identified with the help of a described statistical framework (Ling et al., 2010). DEGs were obtained for day 7 post-infection relative to day 0, separately for WT and $CCR2^{-/-}$ mice, using pooled RNA samples from feet of 4-6 mice for each time point and mouse strain. Genes with low expression levels in the microarray analysis (log_2 expression < 7) for both days 0 and 7 were removed. Ingenuity Pathway Analysis (IPA) (Ingenuity System, USA), Ingenuity's Canonical Pathway Analysis, and Ingenuity's Upstream Regulator Analysis were used to analyse gene networks and functional relationship.

2.26 Statistical analyses

Statistical analysis was performed using IBM SPSS Statistics (version 19). The choice of statistical analysis was dependent on whether the data was normally distributed. The data was considered normally distributed when the difference in the variances was <4, skewness was > -2, and kurtosis was < 2). The Student's t-test was used to compare the mean for normally distributed data. Where the data was not normally distributed and difference in variances was < 4, the Mann Whitney U test was used, and if the difference in variances was > 4, the Kolmogorov-Smirnov test was used. The Student's t-test, Mann Whitney U test and Kolmogorov-Smirnov test are limited for comparison of the mean of two groups. Analysis of variance (ANOVA) tests or repeat measures ANOVA tests were not suitable as these are parametric tests and all data sets contained at least one, usually multiple comparisons, that were not normally distributed.

Chapter 3: CCR2 deficiency promotes exacerbated chronic erosive neutrophil-dominated chikungunya virus arthritis

3.1 Introduction

CCR2 is the receptor for a number of C-C motif chemokines including Chemokine (C-C motif) ligand 2 (CCL2), which is also known as monocyte chemotactic protein-1 (MCP-1). CCL2 recruits monocytes, basophils and T cells to sites of inflammation and has been implicated as an important mediator in a range of inflammatory diseases including *inter alia* RA, multiple sclerosis, atherosclerosis, asthma, neuropathic pain (Subasinghe et al., 2013), obesity, diabetes (Panee, 2012) and cancer (Zollo et al., 2012). A range of therapeutic agents that target CCR2 or CCL2 are being developed (Subasinghe et al., 2013, Panee, 2012, Zollo et al., 2012), although initial trial results for CCR2 blockade in RA patients have been disappointing (Lebre et al., 2011). Nevertheless, CCR2/CCL2 inhibition may ultimately find utility in the treatment of a range of conditions (Subasinghe et al., 2013, Panee, 2012, Zollo et al., 2012). Elevated CCL2 and monocyte/macrophage infiltrates are also prominent features in several viral arthritides, and are well described for alphaviral arthropathies (Suhrbier and Mahalingam, 2009), including CHIKV disease in mice, monkeys and humans (Gardner et al., 2010, Labadie et al., 2010, Suhrbier et al., 2012, Hoarau et al., 2010). Treatments with anti-CCL2 antibody or bindarit, a new drug purported to target CCL2 production, were shown to be effective at ameliorating rheumatic disease in CHIKV and RRV mouse models (Rulli et al., 2011). As CCL2 generally appears to have no direct anti-viral activity (Suhrbier and Mahalingam, 2009, Guabiraba et al., 2010, Lin et al., 2011, Rulli et al., 2011), targeting this chemokine and/or its receptor would appear attractive for treatment of viral arthritides.

The inflammation biology of CCR2/CCL2 has emerged to be complicated. Collagen-induced arthritis in $CCR2^{-/-}$ mice is more severe with increased macrophage and neutrophil infiltrates (Quinones et al., 2004, Rampersad et al., 2011), whereas in other arthritis models, inhibition of CCL2 ameliorated disease (Gong et al., 1997, Shahrara et al., 2008). CCR2 deficiency was associated with reduced monocyte/macrophage infiltration in some settings (Boring et al., 1997, Popivanova et al., 2009, Sawanobori et al., 2008), but not others (Fujii et al., 2012, Quinones et al., 2004). More neutrophil infiltrates were seen in $CCR2^{-/-}$ mice in certain settings (Fujii et al.,

2012, Quinones et al., 2004, Montgomery et al., 2007), unchanged in some (Dunay et al., 2010), less in others (Souto et al., 2011). For dengue and influenza infections in $CCR2^{-/-}$ mice, the viral load was unchanged, and the pathology was attenuated (Guabiraba et al., 2010, Lin et al., 2011). In contrast, cytomegalovirus and West Nile virus infections in these mice resulted in increased viral loads and pathology (Hokeness et al., 2005, Lim et al., 2011).

Given the recent outbreak of CHIKV and the interest in using CCR2/CCL2 blockers for alphaviral arthritides and other diseases, this study sought to determine the effect of CCR2 deficiency in CHIKV arthritis using a recently established mouse model, which mimics many aspects of human disease (Gardner et al., 2010). Herein, we showed that arthritic disease was substantially increased and prolonged in $CCR2^{-/-}$ mice, with no changes in viral load or RNA persistence and only marginal changes in anti-viral immunity. CHIKV infected $CCR2^{-/-}$ mice also showed clear evidence of cartilage damage, a feature not normally associated with CHIKV arthritis. Although recruitment of CCR2+ monocyte/macrophages can contribute to inflammation, they can also be critical for preventing excessive pathology and resolving inflammation.

3.2 Results

3.2.1 CCR2$^{-/-}$ mice had more severe foot swelling than WT mice

Consistent with previous report (Gardner et al., 2010), after CHIKV inoculation into adult wild-type (WT) mice, a clearly discernible foot swelling is observed (Figure 3.1), which peaks on day 6/7 and largely resolves by day 10-14 (Figure 3.1A). The same CHIKV inoculation into CCR2$^{-/-}$ mice resulted in a nearly 2 times higher mean peak foot swelling than that seen in WT mice (Figure 3.1A, day 6), with differences clearly observable by eye (Figure 3.1B). The swelling in CCR2$^{-/-}$ mice also resolved much more slowly, returning to values not significantly different from day zero after day 40 days, whereas in WT mice this occurred after day 14 (Figure 3.1A). Foot swelling in CCR2$^{-/-}$ mice was significantly higher than WT mice for all time points from day 3 to 32 (Figure 3.1A). These observations indicate that the absence of CCR2 gene resulted in a more severe viral arthritis, indicating a protective role for the CCR2 gene in this viral arthritis.

3.2.2 WT and CCR2$^{-/-}$ mice had a similar level of CHIKV viraemia and CHIKV RNA persistence in feet

To investigate the possible cause of the more severe foot swelling seen in CCR2$^{-/-}$ mice, replication of CHIKV was analysed in WT and CCR2$^{-/-}$ mice. No consistent and/or significant differences in viraemia (Figure 3.2A) or tissue virus titres (Figure 3.2B) were seen between WT and CCR2$^{-/-}$ mice, illustrating that CCR2 deficiency did not have a major effect on CHIKV replication.

Chronic alphaviral rheumatic disease is believed to be due to the persistence of virus in joint tissues, with virus shown primarily to persist in macrophages (Labadie et al., 2010). As the longevity of disease is clearly increased in CCR2$^{-/-}$ mice (Figure 3.1A), the levels of viral RNA in these mice were analysed over time. Real time qRT-PCR using CHIKV E1 primers showed no consistent or significant differences in the levels of CHIKV RNA in the feet of CCR2$^{-/-}$ and WT over time (Figure 3.3). The data in Figure 3.2 and Figure 3.3 collectively suggest that the increased clinical disease seen in CCR2$^{-/-}$ mice (Figure 3.1), was not due to increased viral replication or persistence in these mice.

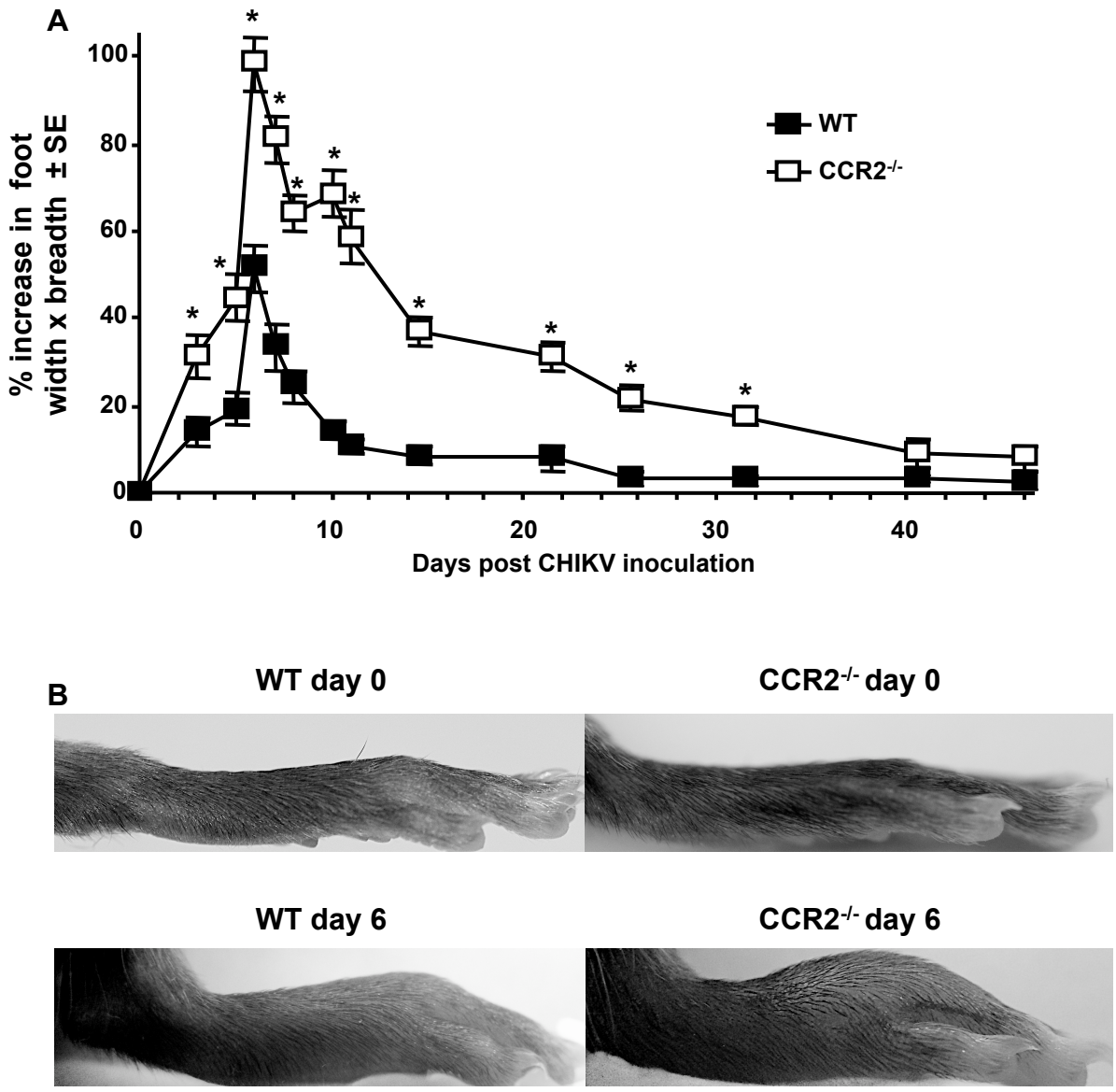

Figure 3.1: Foot swelling in CHIKV infected WT and CCR2$^{-/-}$ mice.

6-8-week old mice were infected with 10^4 $CCID_{50}$ CHIKV into the dorso-lateral metatarsal region of the foot. Feet were measured at the time points indicated. Foot swelling is expressed as a mean percentage increase (compared to uninfected mice feet). **(A)** The mean percentage increase in foot swelling over time for WT mice (n = 16 feet, 8 mice) and CCR2$^{-/-}$ mice (n = 14 feet, 7 mice) (A single experiment, representative of 3 repeat experiments is shown). Asterisks indicate significant differences ($p < 0.01$) by the *t* test or Kolmogorov-Smirnov test; the choice of test at each time point was dependent on skewness, kurtosis, and variance of the data being compared (see section 2.26). (Repeat-measures ANOVA tests were not appropriate as data distribution was mostly non-parametric). **(B)** Images of WT and CCR2$^{-/-}$ feet on day 0 and day 6 (peak arthritis). (n = 16 feet, 8 mice, mean ± SE is presented; data are derived from 2 independent experiments).

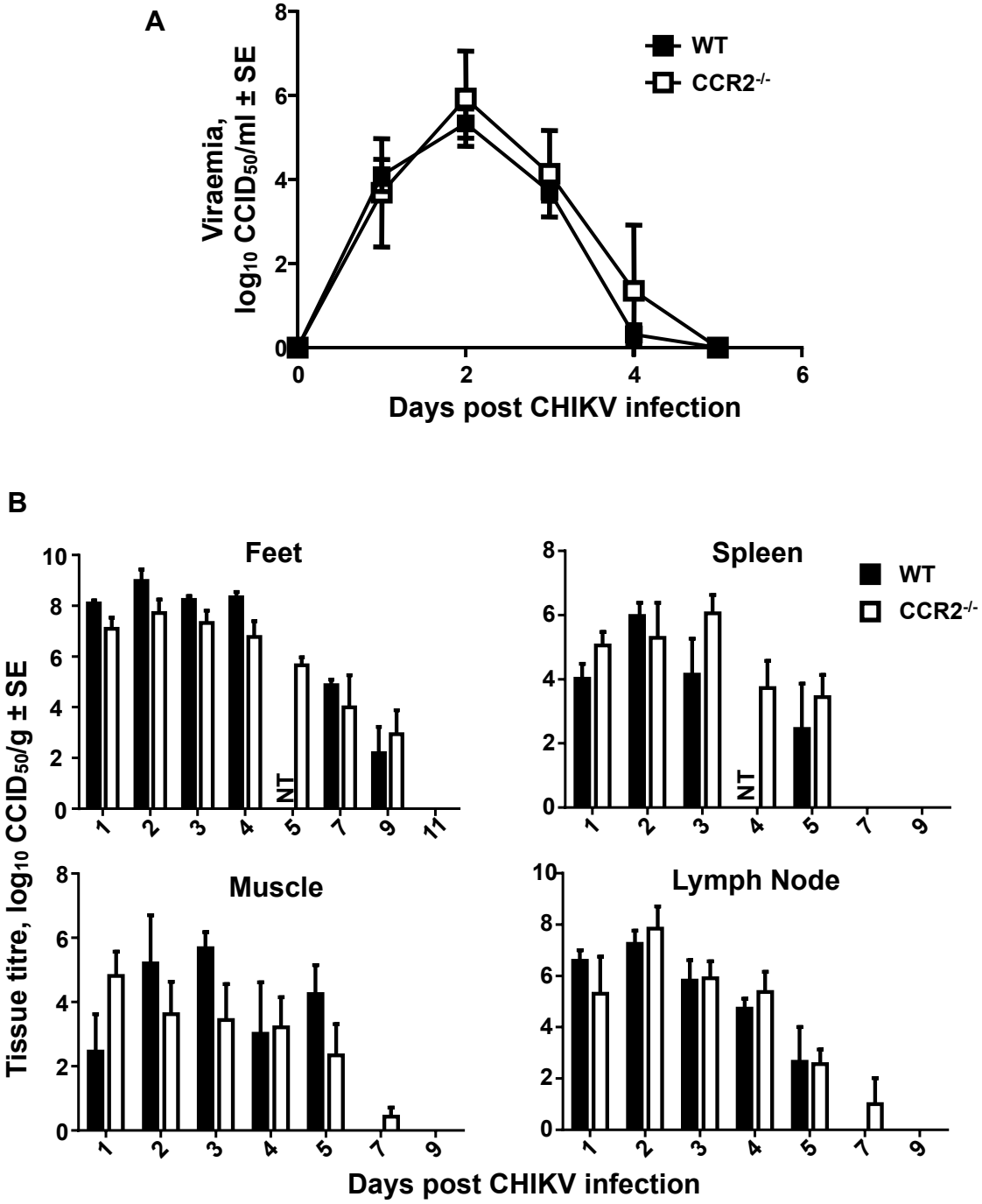

Figure 3.2: Virus replication in WT and CCR2$^{-/-}$ mice.

6-8-week old mice were infected with 10^4 $CCID_{50}$ CHIKV into the dorso-lateral metatarsal region of the foot. At the indicated time points, sera or tissue samples were collected and virus levels measured using a $CCID_{50}$ assay. **(A)** Peripheral blood viraemia. (n = 7 mice for CCR2$^{-/-}$, n = 8-14 WT mice, mean ± SE is presented; data are derived of 2 independent experiments for CCR2$^{-/-}$ mice, and 3 independent experiments for WT mice). **(B)** Virus titres in the indicated tissues (n = 3-6 per time point, mean ± SE is presented) (NT – not tested).

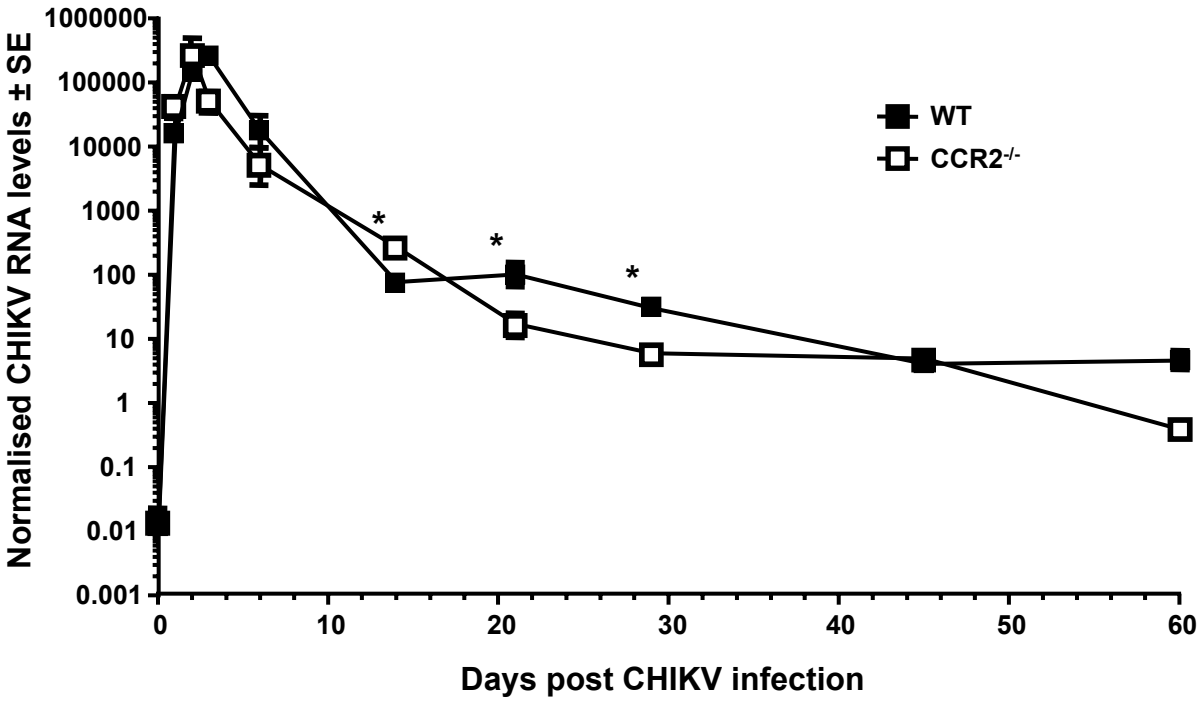

Figure 3.3: qRT-PCR analyses of CHIKV RNA in CHIKV infected WT and CCR2$^{-/-}$ mice.

6-8-week old mice were infected with 10^4 $CCID_{50}$ CHIKV into the dorso-lateral metatarsal region of the foot. At the indicated time points, feet were excised and analysed by qRT-PCR and primers specific for E1 (a major CHIKV structural protein); data was normalised to RPL13A mRNA levels. (n = 3-6 feet from different mice per time point, mean ± SE is presented; data is derived from 2 independent experiments). *$p < 0.05$ by Mann-Whitney U test.

3.2.3 Histology and immunohistochemistry of the cellular infiltrates in the arthritic feet of WT and CCR2$^{-/-}$ mice

Since the virus replication and persistence are similar in WT and CCR2$^{-/-}$ mice while the foot swelling was more severe in CCR2$^{-/-}$ mice, the infiltrating cells in the joint were analysed. Histological examination of arthritic feet in WT mice showed a predominance of mononuclear cell infiltrates on day 6 (the day of peak arthritis) as described previously (Gardner et al., 2010). This could be clearly seen by H&E staining of muscle (compare Figure 3.4A with B and C). Staining of foot sections with F4/80 antibody (a monoclonal antibody recognising mouse monocyte/macrophages), also showed a large number of infiltrating F4/80+ cells (Figure 3.4D) as reported previously (Gardner et al., 2010). Leder staining (Figure 3.4E) showed that neutrophils were largely absent from infiltrates in day 6 feet of WT mice (Figure 3.4E). ApoTag staining revealed some apoptosis, primarily in cells with monocytic and fibroblastic morphology (Figure 3.4F). Chromotrope2R staining showed that eosinophils were largely absent (Figure 3.4G).

The cellular infiltrates in the feet of CCR2$^{-/-}$ mice were quite distinct from those seen in WT mice. H&E staining showed a predominance of neutrophils (compare Figure 3.4H with I and J), (many with hyper-segmented nuclei), with few F4/80+ cells detected in the infiltrates (Figure 3.4K). Prodigious neutrophil infiltrates were also clearly seen by Leder staining (Figure 3.4L). ApoTag staining was more widespread, with frequent staining of cytoplasmic debris (Figure 3.4M, left), suggestive of secondary necrosis. ApoTag staining was often also present in cells with polymorphonuclear morphology (Figure 3.4M, right). The latter suggests inflammatory neutrophils undergoing apoptosis, a well described phenomena in inflammation biology (Ariel and Serhan, 2012). Chromotrope2R staining also revealed a large number of eosinophils were present in the arthritic infiltrates in CCR2$^{-/-}$ feet on day 21 post-infection (Figure 3.4N).

This page intentionally left blank.

Figure 3.4: Histology and immunohistochemistry of rheumatic lesions in CHIKV infected WT and CCR2$^{-/-}$ mice.

A-G, WT mice. **H-N**, CCR2$^{-/-}$ mice. **(A)** and **(H)**, H&E staining of muscle from uninfected mice. **(B)** and **(I)**, H&E staining of muscle day 6 post infection. **(C)** and **(J)**, high magnification of H&E staining of muscle day 6 post-infection. **(D)** and **(K)**, F4/80 antibody (monocyte/macrophage) staining of connective tissue day 6 post-infection. **(E)** and **(L)**, Leder staining (neutrophils) of connective tissue day 6 post-infection. **(F)** and **(M)**, ApoTag staining (apoptotic cells) day 6 post-infection (F, two images, M, two images). **(G)** and **(N)**, Chromotrope 2R staining (eosinophils) of connective tissue day 21 post-infection.

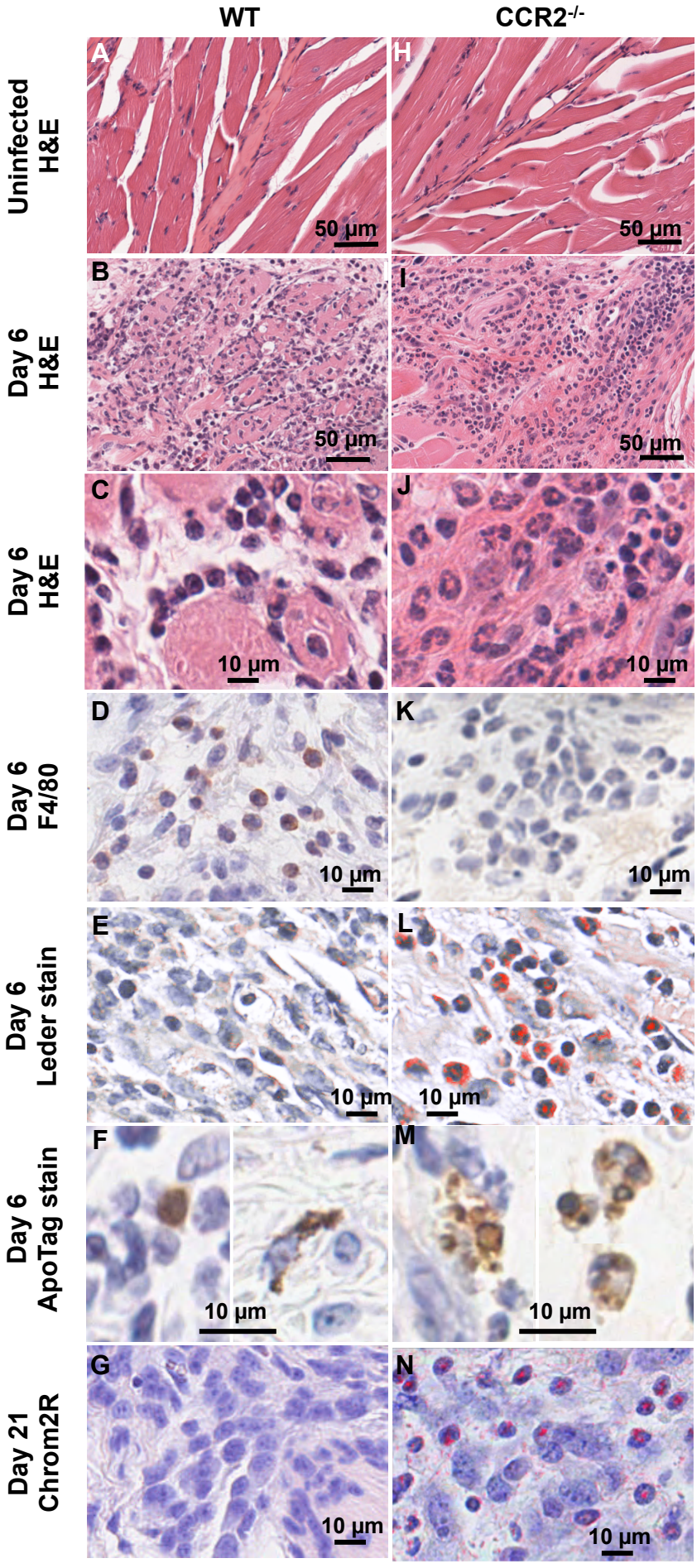
WT
CCR2-/-
Uninfected H&E
Day 6 H&E
Day 6 H&E
Day 6 F4/80
Day 6 Leder stain
Day 6 ApoTag stain
Day 21 Chrom2R
A
B
C
D
E
F
G
H
I
J
K
L
M
N
50 µm
10 µm

3.2.4 Quantitation of histology and immunohistochemistry of the cellular infiltrates in the arthritic feet of WT and CCR2$^{-/-}$ mice.

To quantitate the features described above, slides were digitally scanned (Aperio) and analysed using the Positive Pixel Count algorithm. F4/80 staining increased substantially in WT feet on day 6 post-infection (as reported previously (Gardner et al., 2010)) and was significantly higher than F4/80 staining in CCR2$^{-/-}$ feet at this time (Figure 3.5A). F4/80 staining did not increase significantly in CCR2$^{-/-}$ feet on day 6, but did increase significantly on days 21 and 29 (Figure 3.5A). However, these latter increases were likely associated with infiltrating eosinophils, which also stain with F4/80 antibody (Figure 3.6). Leder staining showed a dramatic increase in CCR2$^{-/-}$ feet on day 6 post-infection and was still significantly elevated on day 14 (Figure 3.5B), consistent with the increase in neutrophils seen by H&E staining. In WT mice, Leder staining was slightly elevated day 6, but was substantially lower than in CCR2$^{-/-}$ feet on days 6 and 14 (Figure 3.5B). Immunohistochemistry using the neutrophil-specific anti-Ly6G antibody confirmed the stark and significant contrast in neutrophil infiltrate between WT and CCR2$^{-/-}$ feet on day 6 (Figure 3.7A, B and C). ApoTag staining of apoptotic cells was also significantly higher in CCR2$^{-/-}$ feet on day 6, and was also significantly elevated on day 14, whereas, in WT mice, there was no significant difference between any of the time points shown (Nakaya et al., 2012) (Figure 3.5C). Chromotrope 2R staining (eosinophils) was slightly elevated on days 6 and 14 in WT mice, but was substantially elevated in CCR2$^{-/-}$ mice on day 21 and 29 (Figure 3.5D).

These data illustrate that the prodigious monocyte/macrophage infiltrate seen in WT mice at this time (Gardner et al., 2010) is likely dependent on CCR2 expression, with its ligand CCL2 strongly induced during CHIKV arthritis (Gardner et al., 2010, Labadie et al., 2010). In addition, the increased and prolonged arthritic disease seen in CCR2$^{-/-}$ mice was associated with a severe neutrophil infiltrate followed by an eosinophil infiltrate, with more apoptotic cells also seen during peak disease.

This page intentionally left blank.

Figure 3.5: Histology quantitation.

(A) Image analysis (strong brown) of F4/80 staining of whole foot sections from WT and $CCR2^{-/-}$ mice at the indicated times post-infection. Dotted line indicates the upper limit of non-specific staining in control slides. (n = 3-5 feet from different per time point and mouse strain, mean ± SE is presented; p values by Kolmogorov-Smirnov test). **(B)** Image analysis (strong red) of Leder staining of whole foot sections of WT and $CCR2^{-/-}$ mice at the indicated times post-infection. (n as above; p values by Kolmogorov-Smirnov, Mann Whitney U and t tests). **(C)** Image analysis (strong brown) of ApoTag staining of whole foot sections of WT and $CCR2^{-/-}$ mice at the indicated times post-infection. (n as above; p values by Kolmogorov-Smirnov tests). **(D)** Image analysis (strong red) of Chromotrope 2R staining of whole foot sections of WT and $CCR2^{-/-}$ mice at the indicated times post-infection. (n as above: p values by Kolmogorov-Smirnov and Mann Whitney U tests)

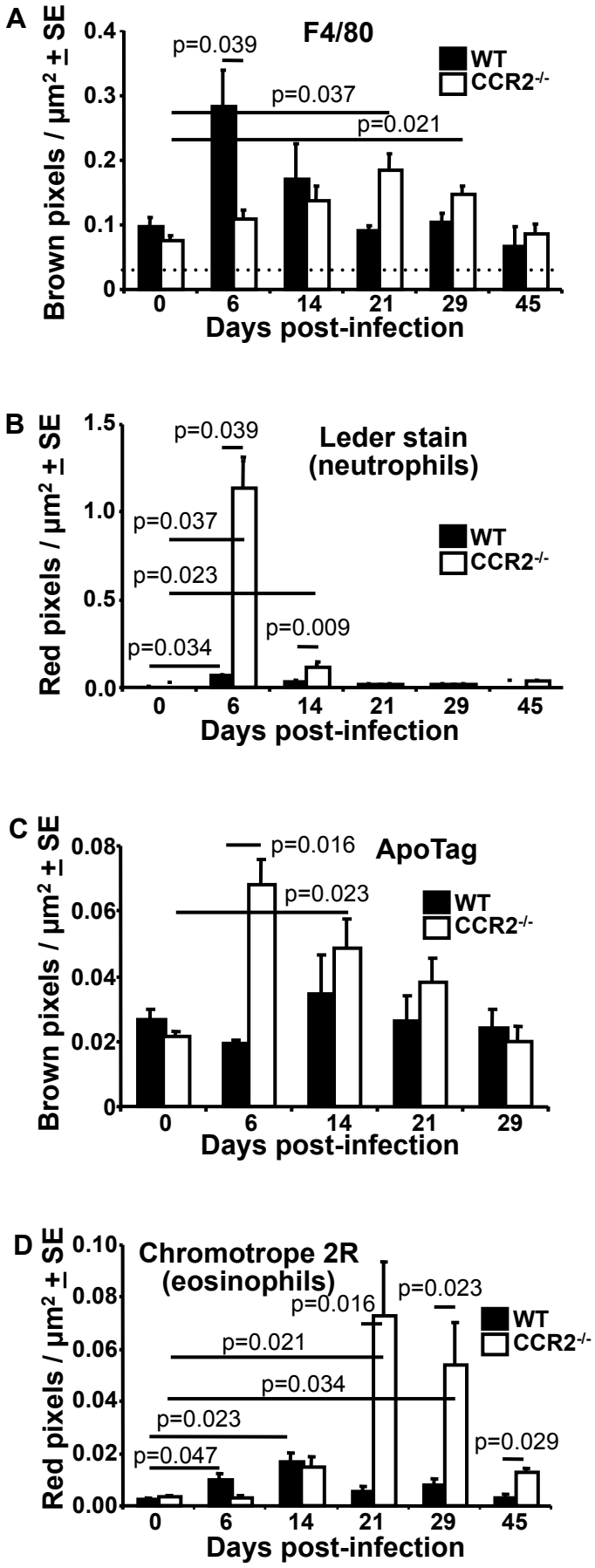
A
F4/80
Brown pixels / µm² ± SE
0.4
0.3
0.2
0.1
0
p=0.039
p=0.037
p=0.021
WT
CCR2-/-
0
6
14
21
29
45
Days post-infection
B
Leder stain
(neutrophils)
Red pixels / µm² ± SE
1.5
1.0
0.5
0.0
p=0.039
p=0.037
p=0.023
p=0.034
p=0.009
WT
CCR2-/-
0
6
14
21
29
45
Days post-infection
C
ApoTag
Brown pixels / µm² ± SE
0.08
0.06
0.04
0.02
0
p=0.016
p=0.023
WT
CCR2-/-
0
6
14
21
29
Days post-infection
D
Chromotrope 2R
(eosinophils)
Red pixels / µm² ± SE
0.10
0.08
0.06
0.04
0.02
0.00
p=0.016
p=0.023
p=0.021
p=0.034
p=0.023
p=0.047
p=0.029
WT
CCR2-/-
0
6
14
21
29
45
Days post-infection

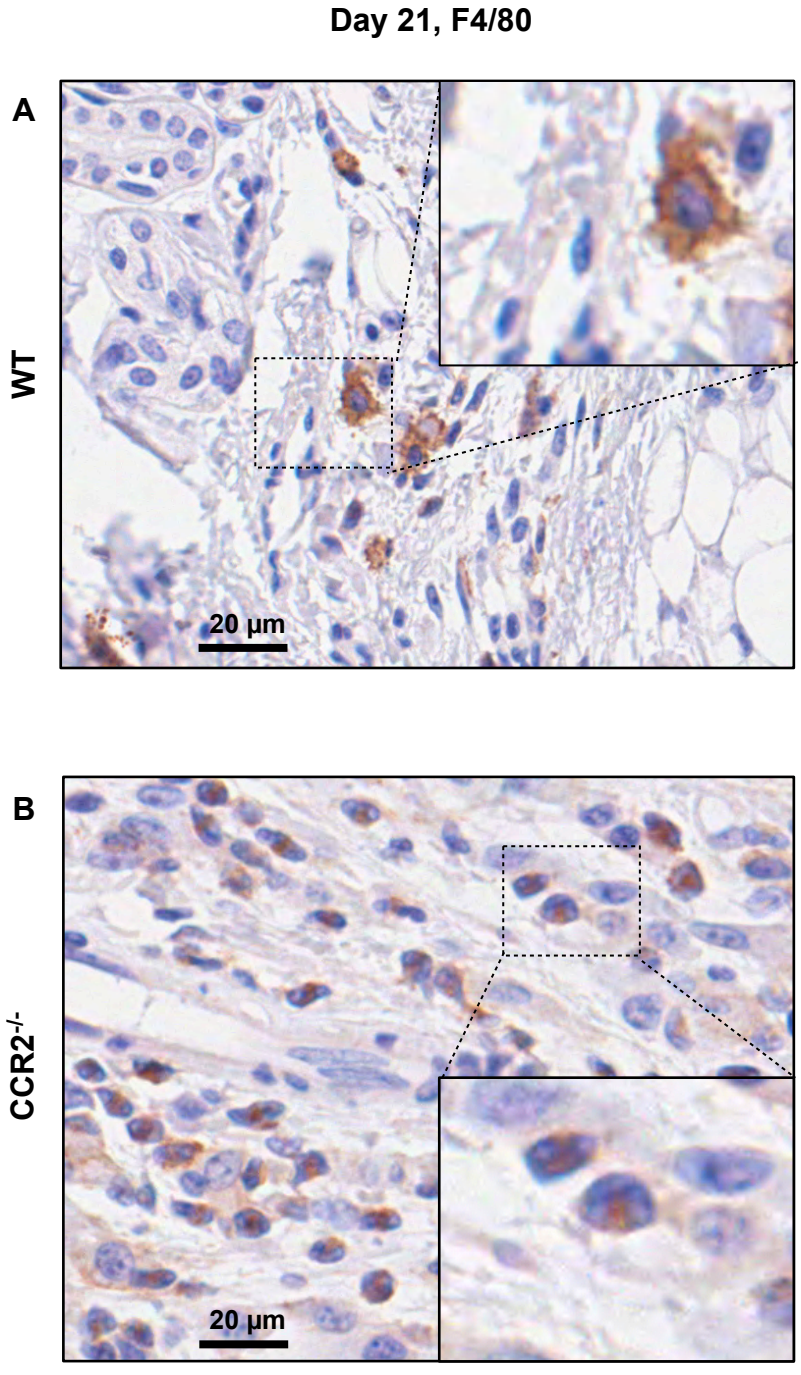

Figure 3.6: F4/80 staining of cells in foot sections from WT and CCR2$^{-/-}$ mice day 21 post CHIKV infection.

(A) In WT mice F4/80 staining was predominantly associated with mononuclear cells (e.g. macrophages), with mononuclear infiltrate largely resolved by day 21 (Figure 3.5A). **(B)** In feet of CCR2$^{-/-}$ mice the increase F4/80 staining seen at this time (Figure 3.5A) was associated with polymorphonuclear cells (likely eosinophils - see Figure 3.5D). Murine eosinophils are known to stain with F4/80 antibody (McGarry and Stewart, 1991, Gouon-Evans et al., 2000).

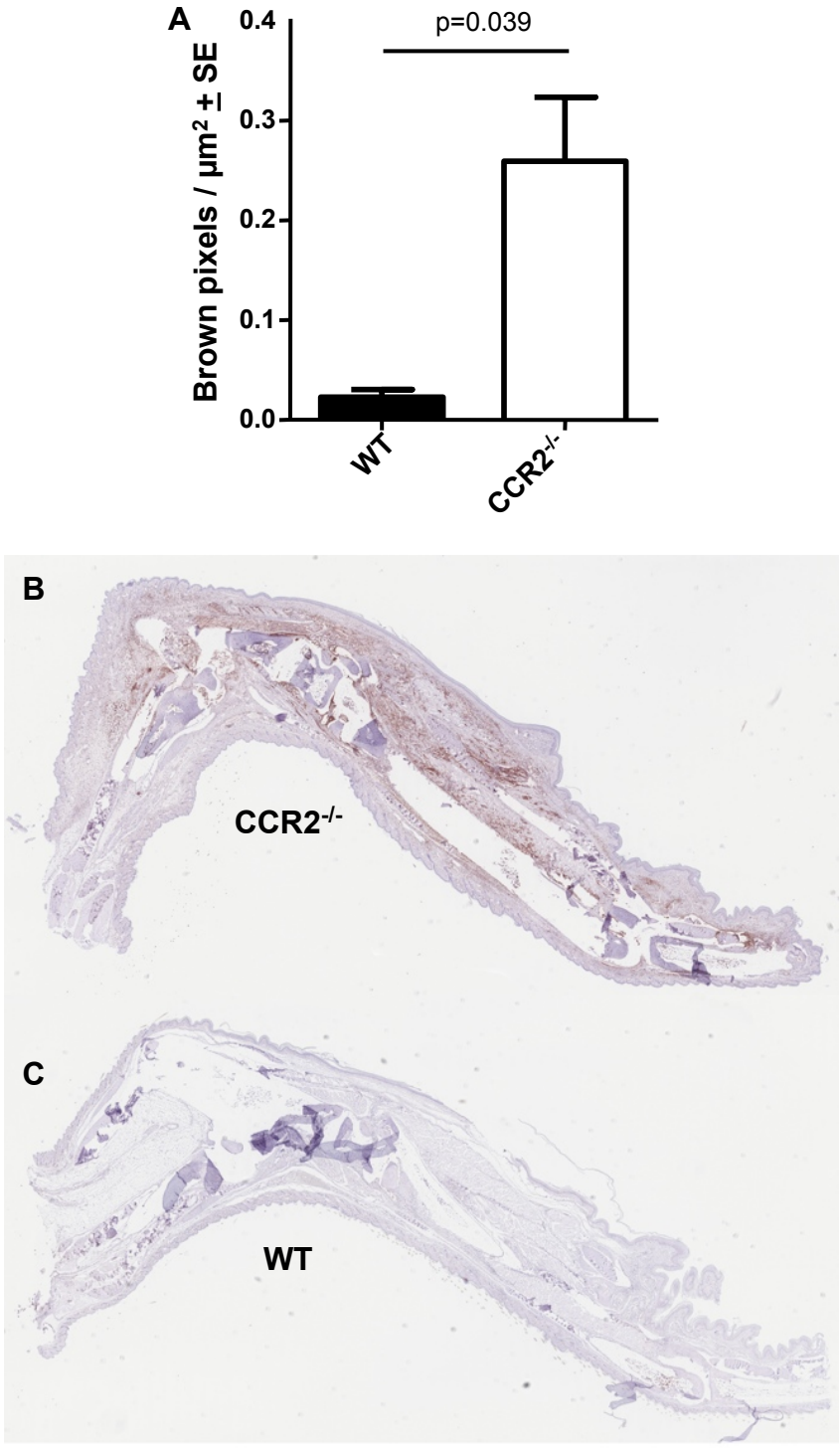

Figure 3.7: Anti-Ly6G staining of feet from CCR2$^{-/-}$ and WT mice.

Immunohistochemistry using anti-Ly6G neutrophil specific antibody. **(A)** Image analysis (strong brown) of anti-Ly6G staining of whole foot sections from WT and CCR2$^{-/-}$ mice at day 6 post-infection (n = 4 mice, mean ± SE is presented; p value by Kolmogorov-Smirnov test). **(B)** Example of a whole foot section from CCR2$^{-/-}$ mouse stained with anti-Ly6G. **(C)** Example of whole foot section from WT mouse stained with anti-Ly6G.

3.2.5 Antibody-based depletion of neutrophils did not ameliorate foot swelling in CCR2$^{-/-}$ mice

Since neutrophils were associated with the more pronounced arthritis in CCR2$^{-/-}$ mice, the role of neutrophils in this model was investigated. Anti-neutrophil antibody was injected into CCR2$^{-/-}$ mice and resulted in the reduction of neutrophils (Figure 3.8B). However, this antibody-based depletion of neutrophils did not ameliorate foot swelling in CCR2$^{-/-}$ mice (Figure 3.8A), and instead resulted in widespread haemorrhage and edema (Figure 3.8C) (reminiscent of the pathology seen in mice with diminished IFN-α/β responses (Rudd et al., 2012)), complicating any analysis of the arthritogenic role of neutrophils using this approach

3.2.6 Cartilage damage in CHIKV infected CCR2$^{-/-}$ mice.

In contrast with most autoimmune arthritides, alphaviral arthritides (and most viral arthritides (Suhrbier and Mahalingam, 2009)) are generally not associated with joint damage (Suhrbier et al., 2012). Joint damage was also not seen in CHIKV-infected WT mice in the current study (in 6/6 feet examined) (Figure 3.9A) (or in CHIKV-infected monkeys (Labadie et al., 2010)). However, H&E staining of joints from CHIKV-infected CCR2$^{-/-}$ mice day 45 post-infection often showed (in 6/6 feet examined) loss of chondrocytes with empty lacunae in multiple foot joints (Figure 3.9B, arrows). Clear signs of cartilage damage at the articular surfaces (never seen in WT mice) were also occasionally observed in CCR2$^{-/-}$ mice (2 joint in 6 feet) (Figure 3.9B, arrowhead). Loss of cartilage collagen (as revealed by Safranin O staining) was not observed in WT mice (Figure 3.9C), but was clearly seen in at least 1, occasionally 2, joints per foot in CCR2$^{-/-}$ mice (6 feet examined) (Figure 3.9D, blue areas indicated by arrows). CCR2 deficiency thus increased the severity of CHIKV arthritis, with cartilage damage clearly apparent.

3.2.7 ANA levels in CCR2$^{-/-}$ and WT mice

ANA are antibodies that are reactive against autologous cell nucleus. Joint damage is a feature of rheumatoid arthritis (Hu et al., 2013) and CHIKV infected CCR2$^{-/-}$ mice showed clear signs of joint damage (Figure 3.9B and D). Since high level of ANA in humans and in mice have been associated with autoimmune disorders includes rheumatoid arthritis (De Rycke et al., 2005), the ANA titres in the CCR2$^{-/-}$ mice were analysed. No detectable ANA was observed in the sera of

either WT or CCR2$^{-/-}$ mice post CHIKV infection (Figure 3.10). This observation suggests that CCR2$^{-/-}$ mice did not develop autoimmunity.

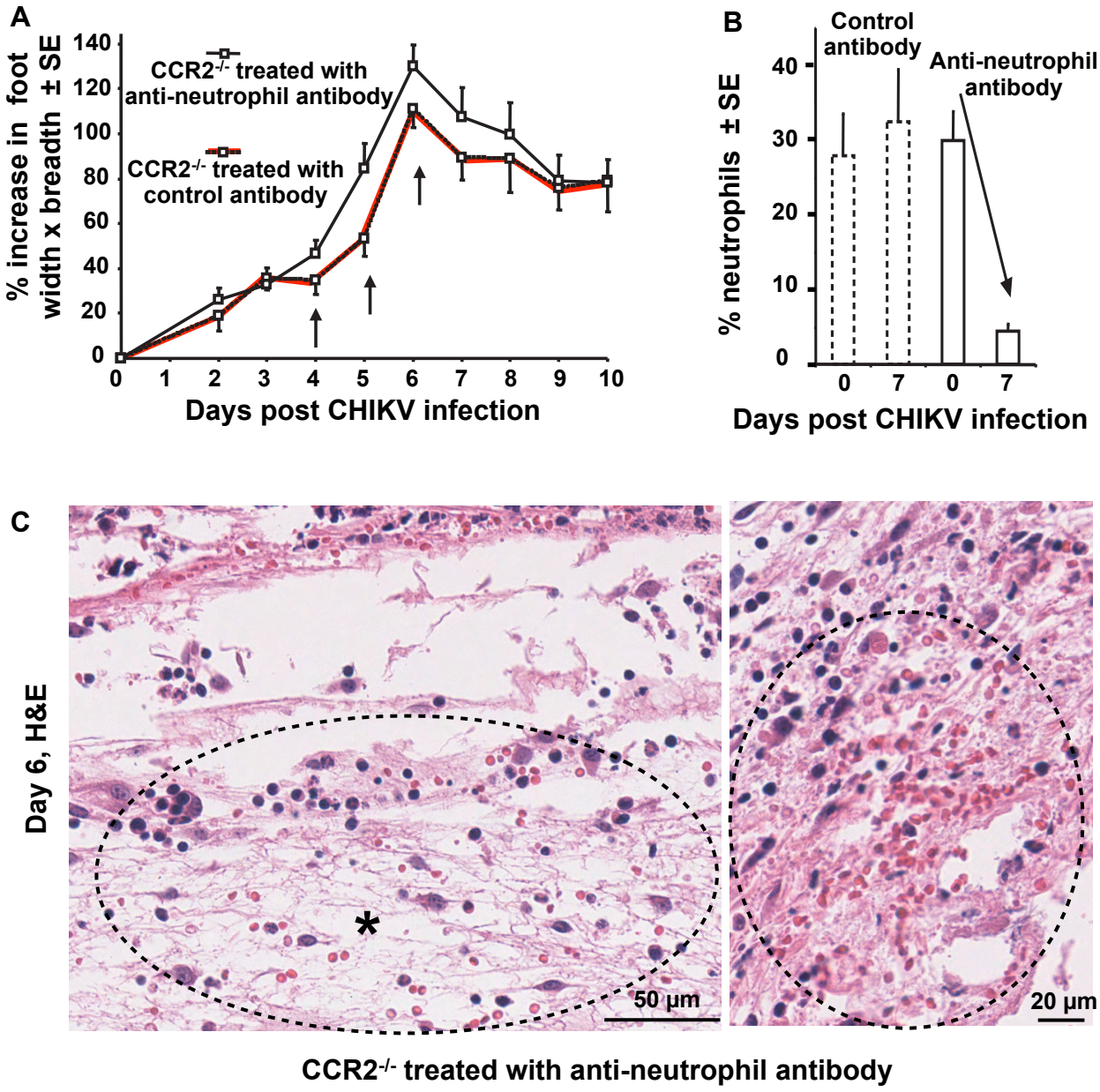

Figure 3.8: Foot swelling after neutrophil depletion in CCR2$^{-/-}$ mice.

Depletion of neutrophils in CCR2$^{-/-}$ mice did not reduce foot swelling. (**A**) Mice were treated with anti-Ly6G antibody or IgG2a control antibody i.p. on days 4, 5 and 6 (arrows). Foot measurements were taken at the indicated time points after CHIKV infection. (n = 5 mice, mean ± SE is presented). (**B**) Blood neutrophils were determined by blood smears and are presented as a percentage of total white blood cells as described previously (Challacombe et al., 2006). (n as above). (**C**) Widespread of haemorrhage (dotted line circle) and edema (*) were observed in tissue of anti-neutrophil antibody treated CCR2$^{-/-}$ mice 6 days post infection.

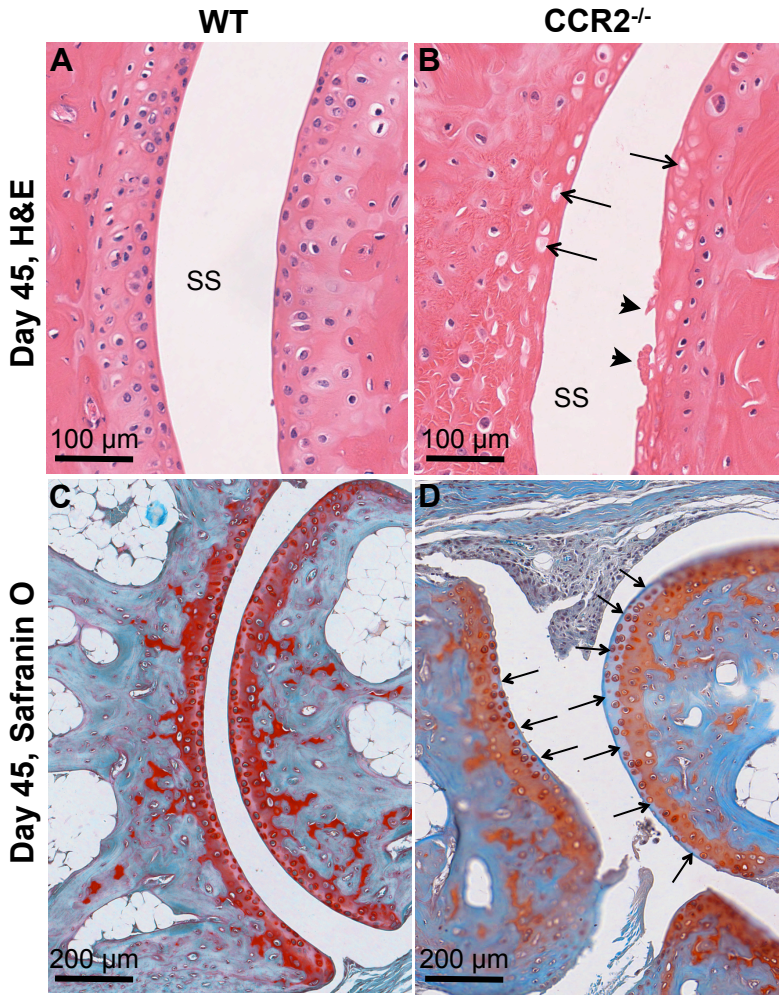

Figure 3.9: Cartilage damage in CCR2$^{-/-}$ feet.

(A) H & E staining of joint from WT mouse day 45 post-infection (SS – synovial space). **(B)** H&E staining of joint from CCR2$^{-/-}$ mouse day 45 post-infection. Arrows indicate empty chondrocytic lacunae within the hyaline cartilage. Arrowheads show cartilage damage at the articular surface. **(C)** Safranin O staining (cartilage) of joint from WT mouse day 45 post-infection. **(D)** Safranin O staining (cartilage) of joint from CCR2$^{-/-}$ mouse day 45 post-infection. Arrows show loss of red collagen staining (replaced by blue staining) at the articular surfaces.

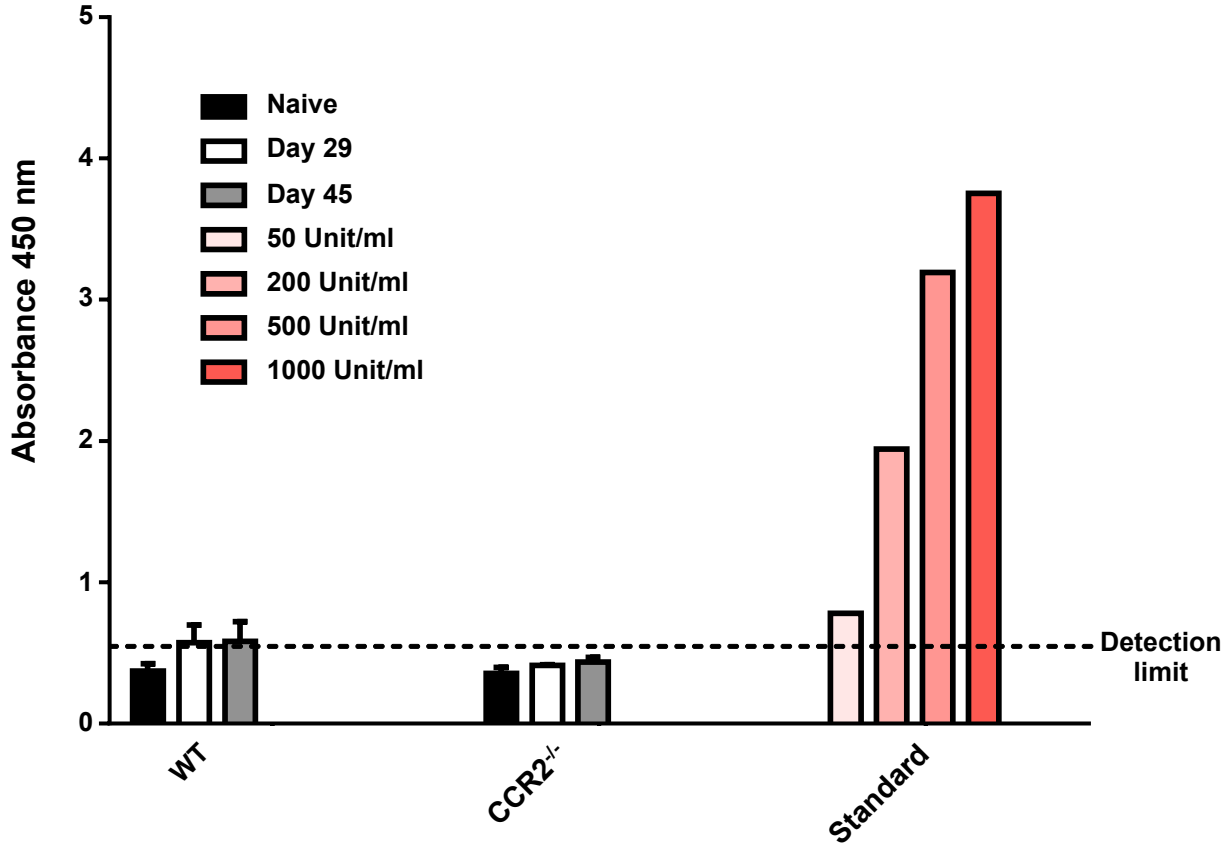

Figure 3.10: ELISA for detection of mouse ANA.

Naïve, day 29 and 45 post-CHIKV infection mice's sera were tested for ANA - an indicator of autoimmune disease. (n = 3-4 mice per group, mean ± SE is presented).

Data for Figure 3.10 was prepared with assistance of Thuy Le.

3.2.8 Anti-viral Th1/Th2/Th17 responses in CHIKV-infected WT and CCR2$^{-/-}$ mice.

CHIKV infections induce a strongly Th1-biased immune response (Gardner et al., 2010, Labadie et al., 2010), with CCR2$^{-/-}$ mice reported having impaired Th1 responses (Boring et al., 1997, Sato et al., 2000, Iijima et al., 2011). However, analysis of the anti-CHIKV IgG2c (Th1) and IgG1 (Th2) titres (Wang et al., 2011a, Schroder et al., 2010), illustrated that the dominant IgG2c responses were not significantly different in CCR2$^{-/-}$ mice (Figure 3.11A, IgG2c). Anti-CHIKV-specific IgG1 levels were, however, significantly elevated in CCR2$^{-/-}$ mice (Figure 3.11A, IgG1), perhaps consistent with the increased eosinophilia seen in these mice (Figure 3.5D). Serum IFN-γ levels (Figure 3.11C) and neutralising antibody levels (Figure 3.11D) were not significantly different between WT and CCR2$^{-/-}$ mice.

qRT-PCR analysis of T-bet, a key transcription factor for Th1 cells (Lipscomb et al., 2009), showed a clear increase in WT mice on day 6 (peak arthritis) (Figure 3.11B, T-bet). However, T-bet mRNA induction and levels were not significantly different (from WT mice) in CCR2$^{-/-}$ mice (Figure 3.11B, T-bet), supporting the view that anti-CHIKV Th1 responses were not significantly impaired in CCR2$^{-/-}$ mice.

Expansion of Th17 cells were reported to be responsible for the increase in neutrophil infiltration and exacerbated arthritic disease seen in collagen-induced arthritis in CCR2$^{-/-}$ mice (Rampersad et al., 2011). However, no significant increases in RORγT mRNA were observed in either mouse strain on day 6 post-infection (Figure 3.11B, RORγT). RORγT is a key transcription factor for Th17 cells (Ruan et al., 2011).

Figure 3.11: Immune responses in WT and CCR2$^{-/-}$ mice post CHIKV infection.

(A) Anti-CHIKV IgG2c and IgG1 titres 7 weeks post-infection as determined by ELISA. (n = 4 mice per group, mean ± SE is presented; p value by Mann Whitney U test). **(B)** qRT-PCR analysis of T-bet (Th1 transcription factor) and RORγT (Th17 transcription factor) at the indicated times post-infection. (n = 4-6 feet and mice per group, mean ± SE is presented; p values by Mann Whitney U test). **(C)** Serum IFN-γ analysed by cytometric bead array (n = 6-8 mice per group, mean ± SE is presented). **(D)** Serum neutralisation titres post CHIKV infection (n = 3-7 mice per group, mean ± SE is presented).

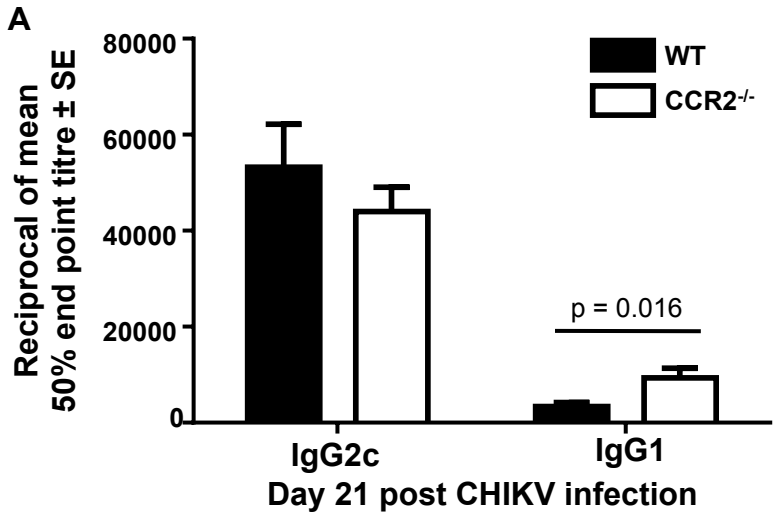
A
Reciprocal of mean 50% end point titre ± SE
80000
60000
40000
20000
0
WT
CCR2-/-
p = 0.016
IgG2c
IgG1
Day 21 post CHIKV infection

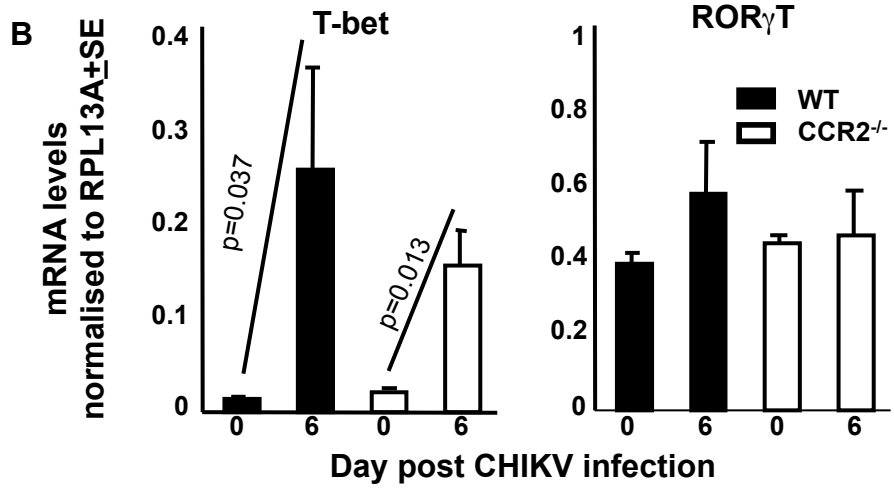
B
mRNA levels normalised to RPL13A±SE
T-bet
RORγT
0.4
0.3
0.2
0.1
0
1
0.8
0.6
0.4
0.2
p=0.037
p=0.013
WT
CCR2-/-
0
6
0
6
Day post CHIKV infection

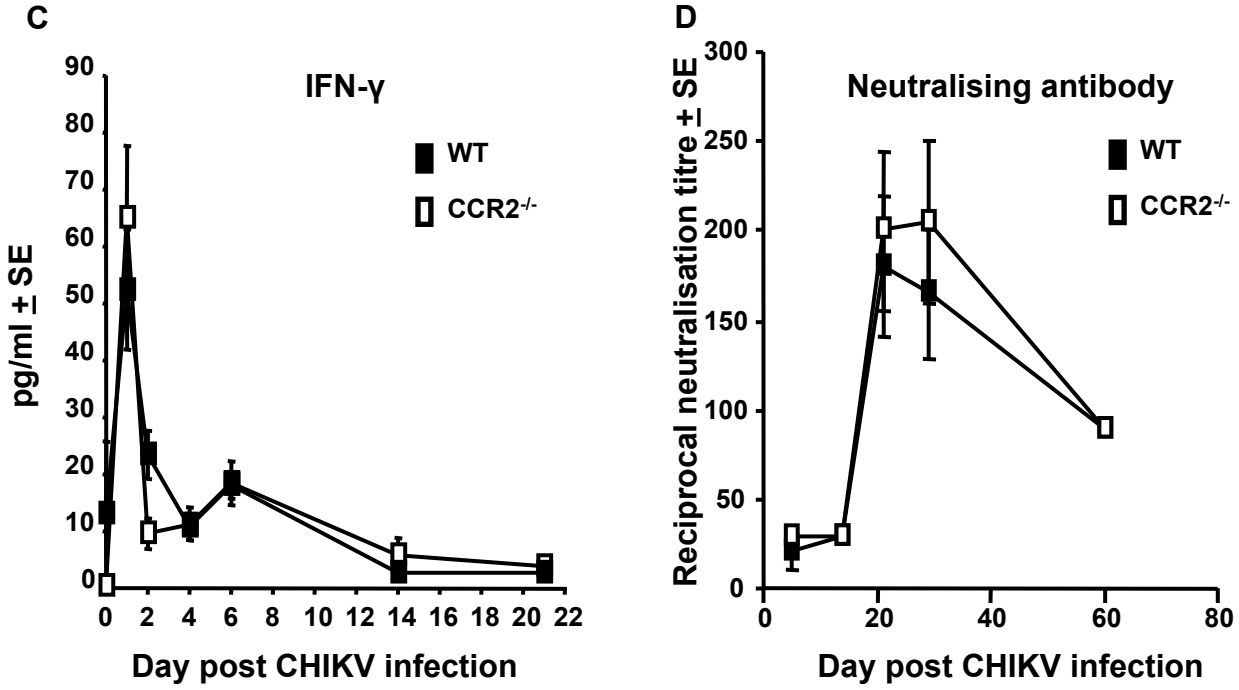
C
IFN-γ
pg/ml ± SE
90
80
70
60
50
40
30
20
10
0
WT
CCR2-/-
0 2 4 6 8 10 12 14 16 18 20 22
Day post CHIKV infection
D
Neutralising antibody
Reciprocal neutralisation titre ± SE
300
250
200
150
100
50
0
WT
CCR2-/-
0 20 40 60 80
Day post CHIKV infection

3.2.9 Changes in inflammatory mediators in the arthritic feet and sera of CCR2$^{-/-}$ mice

Increased neutrophil infiltrates in CCR2$^{-/-}$ mice have been associated with elevated levels of (i) neutrophil-attracting chemokines CXCL1 (keratinocyte chemoattractant) and/or CXCL2 (also known as macrophage inflammatory protein 2-alpha) (Fujii et al., 2012, Quinones et al., 2004, Montgomery et al., 2007), and/or (ii) granulocyte colony-stimulating factor (G-CSF) (Sawanobori et al., 2008), a key growth factor for neutrophil development and recruitment involved in inflammatory arthritis (Eyles et al., 2008). IL-1β can also promote neutrophil recruitment (Sadik et al., 2012), and IL-10 can inhibit neutrophil recruitment (Ajuebor et al., 1999). qRT-PCR analyses showed that significantly more CXCL1, CXCL2, G-CSF and IL-1β, and less IL-10, was present in the arthritic feet of CCR2$^{-/-}$ mice (Figure 3.12A), suggesting multiple mediators were involved in the switch from the predominantly monocyte/macrophage to neutrophil infiltrates. Serum IL-10 was also elevated earlier in the course of infection in WT mice (Figure 3.12B). qRT-PCR analysis also showed that Arg-1 expression (a marker of M2 macrophages), although up-regulated in WT feet as expected (Stoermer et al., 2012), was not up-regulated in CCR2$^{-/-}$ feet (Figure 3.12, Arg-1). M2 macrophages are associated with resolution of inflammation (Ariel and Serhan, 2012).

3.2.10 CHIKV infection in IL-10$^{-/-}$ mice

Induction of IL-10 in feet (Figure 3.12A, day 6, IL-10) and sera (Figure 3.12B, day 1 and 2) was significantly higher in WT mice compared to CCR2$^{-/-}$ mice. This observation is consistent with the view that IL-10 can inhibit neutrophil recruitment (Ajuebor et al., 1999), with WT mice showed a lower level of neutrophil infiltration (Figure 3.5B). To study the role of IL-10 in CHIKV infection, IL-10$^{-/-}$ mice were infected with CHIKV. IL-10$^{-/-}$ mice had significantly higher foot swelling at day 5 and 6 compared to WT mice (Figure 3.13A), despite lower viraemia at day 1 (Figure 3.13B). Immunohistochemistry using the neutrophil-specific anti-Ly6G antibody showed that IL-10$^{-/-}$ mice had higher (but not significantly different) levels of infiltrating neutrophils (Figure 3.13C).

This page intentionally left blank.

Figure 3.12: qRT-PCR of selected genes in feet and IL-10 in sera of WT and CCR2$^{-/-}$ post CHIKV infection.

(A) qRT-PCR analysis of the indicated species at the indicated times post-infection. (n = 3-5 mice per group, mean ± SE is presented; p values by Kolmogorov-Smirnov and t tests). **(B)** Serum IL-10 analysed by cytometric bead array. (n = 6-8 mice per group, mean ± SE is presented; p value by Kolmogorov-Smirnov test).

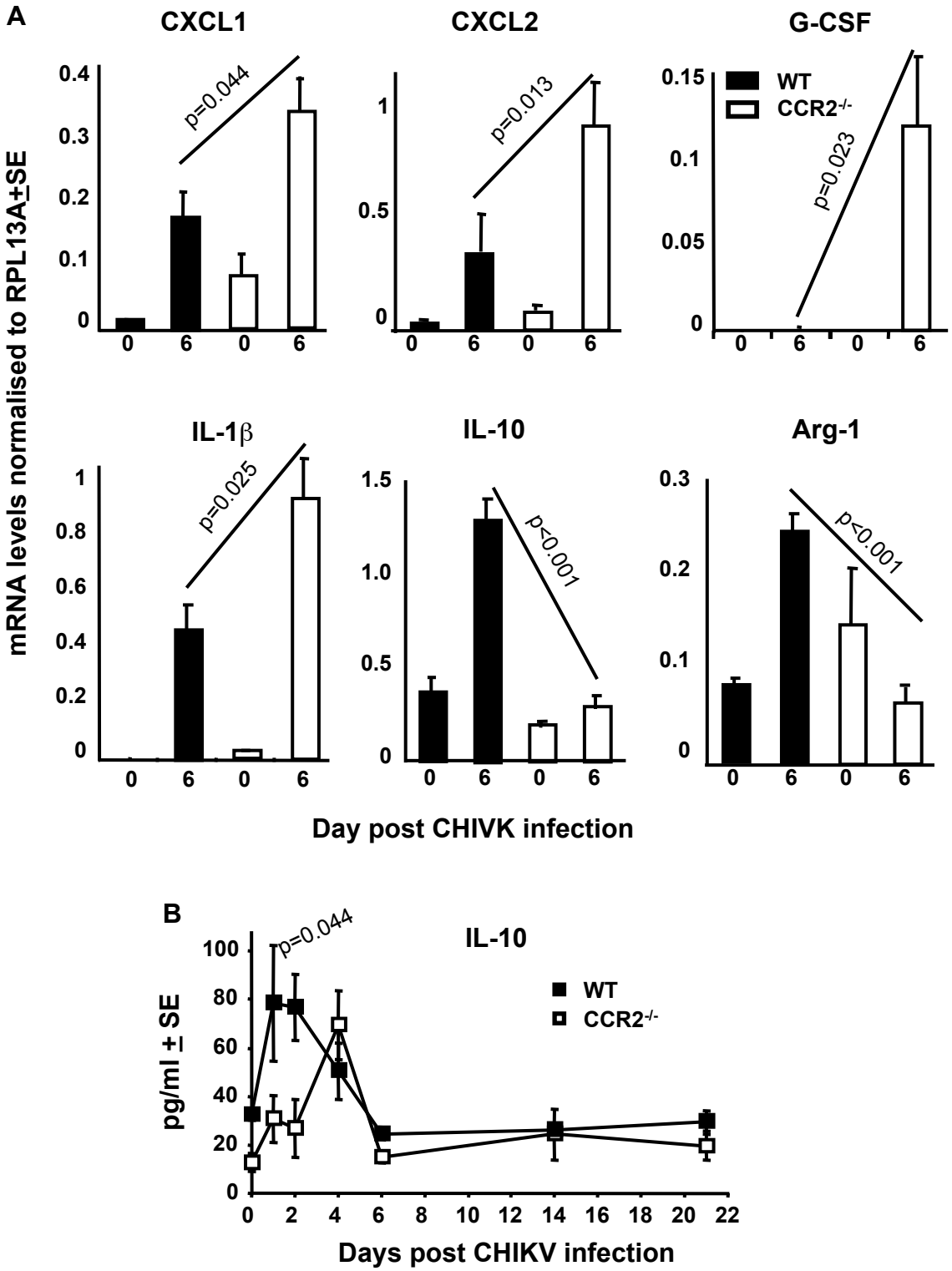
A
CXCL1
CXCL2
G-CSF
IL-1β
IL-10
Arg-1
p=0.044
p=0.013
p=0.023
p=0.025
p<0.001
p<0.001
WT
CCR2-/-
mRNA levels normalised to RPL13A±SE
Day post CHIVK infection
B
IL-10
p=0.044
WT
CCR2-/-
pg/ml ± SE
Days post CHIKV infection

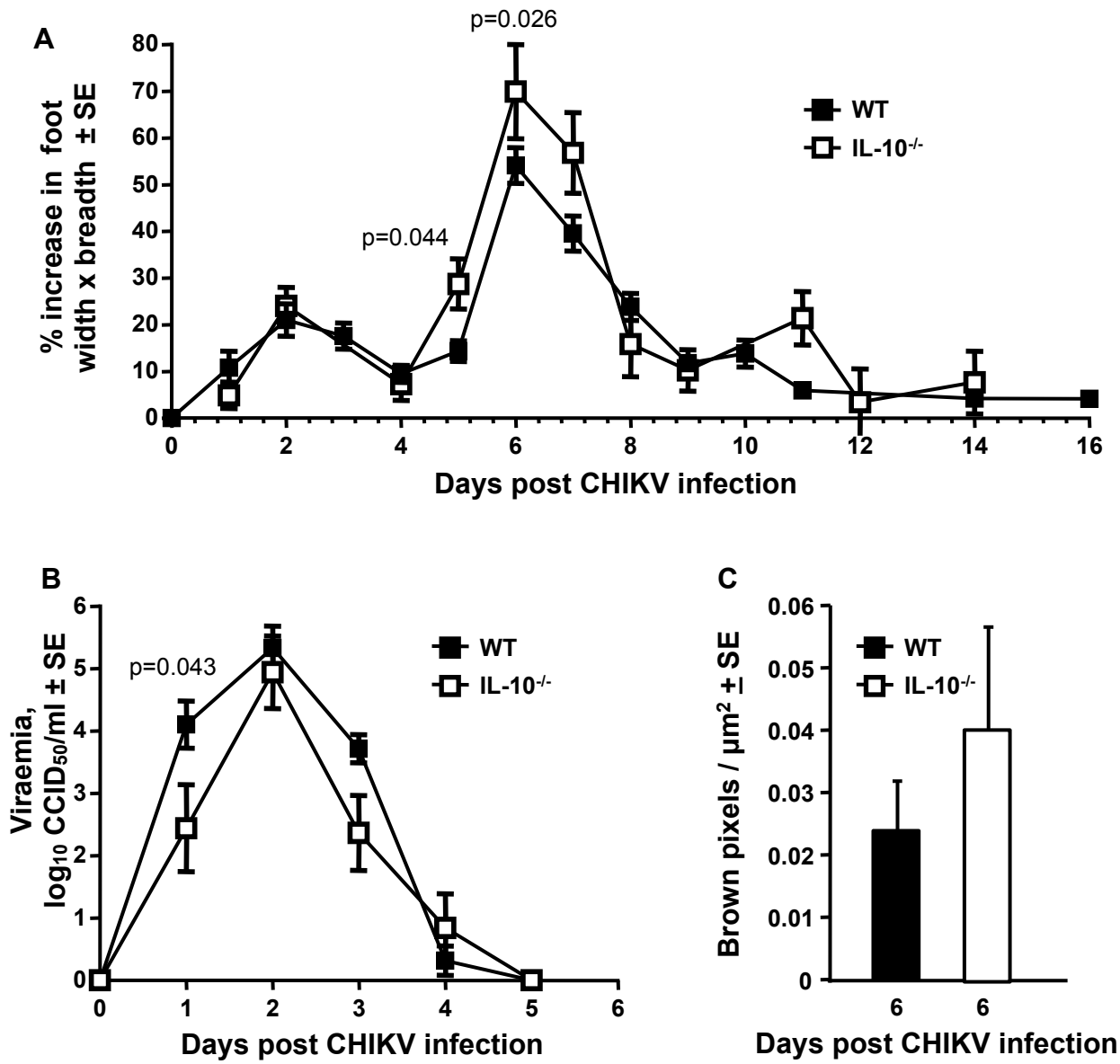

Figure 3.13: Foot swelling, viraemia and neutrophil staining in CHIKV infected IL-10$^{-/-}$ mice.

Increased foot swelling and decreased viraemia in IL-10$^{-/-}$ mice. **(A)** The mean percentage increase in foot swelling over time for WT (n = 16 feet, 8 mice) and IL-10$^{-/-}$ mice (n = 10 feet, 5 mice) (mean ± SE is presented). (p values by Mann-Whitney U test). **(B)** Viraemia. (n = as above, mean ± SE is presented; p value by Mann-Whitney U test). **(C)** Immunohistochemical staining using neutrophil-specific anti-Ly6G antibody (n = 4 feet and mice per mouse strain) quantitated as in Figure 3.7A (not significantly different).

3.2.11 Global gene expression changes induced by CHIKV infection.

Microarray analysis was undertaken to determine what genes were up- and down-regulated in the arthritic feet of CHIKV-infected WT and CCR2$^{-/-}$ mice. The genes up- or down-regulated on day 7 post-infection (one day after peak arthritis to capture genes associated with resolution initiation) relative to day 0 were determined for both mouse strains. A total of 2406 genes were up- or down-regulated following CHIKV infection in WT and/or CCR2$^{-/-}$ mice. When the fold up- or down-regulation of these differentially expressed genes (DEGs) was compared between WT and/or CCR2$^{-/-}$ mice, 81% showed less than 2 fold difference, illustrating that most genes were similarly regulated in feet day 7 post-infection in the two mouse strains. However, consistent with the histological analyses, monocyte/macrophage-associated genes and pathways were more upregulatedin WT feet (Figure 3.14, green), and neutrophil-associated genes and pathways were more upregulated in CCR2$^{-/-}$ feet (Figure 3.14A, blue). Consistent with the higher induction of IL-10 (by qRT-PCR) in the WT mice (Figure 3.12A, IL-10), M2 and resolving macrophage associated genes were more upregulated in WT mice (Figure 3.14A).

To gain a better understanding of the differences in infection-associated gene regulation between CCR2$^{-/-}$ and WT mice, the differences in fold changes in gene expression between the two strains for all 2406 DEGs was expressed as a ratio. For 181 genes (7.5% of all DEGs) the "the fold change in CCR2$^{-/-}$ feet" divided by "the fold change in WT feet" was >1.5 (Figure 3.15A). For 920 genes (38% of all DEGs) "the fold change in WT feet" divided by "the fold change in CCR2$^{-/-}$ feet" was >1.5 (Figure 3.15D). The former 181 genes thus represent genes that were more induced in CCR2$^{-/-}$ mice than in WT mice, and the latter 920 genes represent genes that were less induced in CCR2$^{-/-}$ mice than in WT mice. IPA analysis of the 181 genes more induced in CCR2$^{-/-}$ mice, revealed canonical pathways associated with granulocyte, IL-17A in autoimmunity, RA and inflammation (Figure 3.15B). Although autoimmune pathways were identified (consistent with the worse pathology), CCR2$^{-/-}$ mice did not develop ANAs (Figure 3.10). IPA analysis of the 920 genes less induced in CCR2$^{-/-}$ feet revealed canonical pathways associated with monocyte/macrophage, pattern recognition, autoimmunity, B and T cell (mostly Th cell), NK cell, muscle and inflammation pathways (Figure 3.15C). Many of these pathways are consistent with the aforementioned changes in infiltrates and inflammation. The identification of muscle pathways likely reflects increased muscle damage (Nakaya et al., 2012) in CCR2$^{-/-}$ feet (Figure 3.15C). The identification of NK, T and B cell pathways in this gene set (Figure 3.15C) also suggests reduced recruitment of these cells (Gardner et al., 2010) into the infected feet in CCR2$^{-/-}$ mice; T cells can also express CCR2 (Bruhl et al., 2004).

Figure 3.14: Monocyte/macrophage, M2/resolving macrophages and neutrophils profiles in the feet of CHIKV infected WT and CCR2$^{-/-}$ mice.

(A) Microarray expression data (fold change) of up-regulated genes associated with monocyte/macrophage (green), M2/resolving macrophages (brown) and neutrophils (blue). Fold changes for DEGs from CCR2$^{-/-}$ d0 vs d7, and WT d0 vs d7 are shown with their q significance values (red values - not significant; values of $q<0.05$ were considered significance; statistics by IPA). **(B)** Up-regulated pathways associated with monocytes/macrophages (green) and neutrophils (blue) on day 7 post infection in WT and CCR2$^{-/-}$ mice. -log(<1.3) represents $p<0.05$.

Data for Figure 3.14 was prepared with assistance of Helder Nakaya and Andreas Suhrbier.

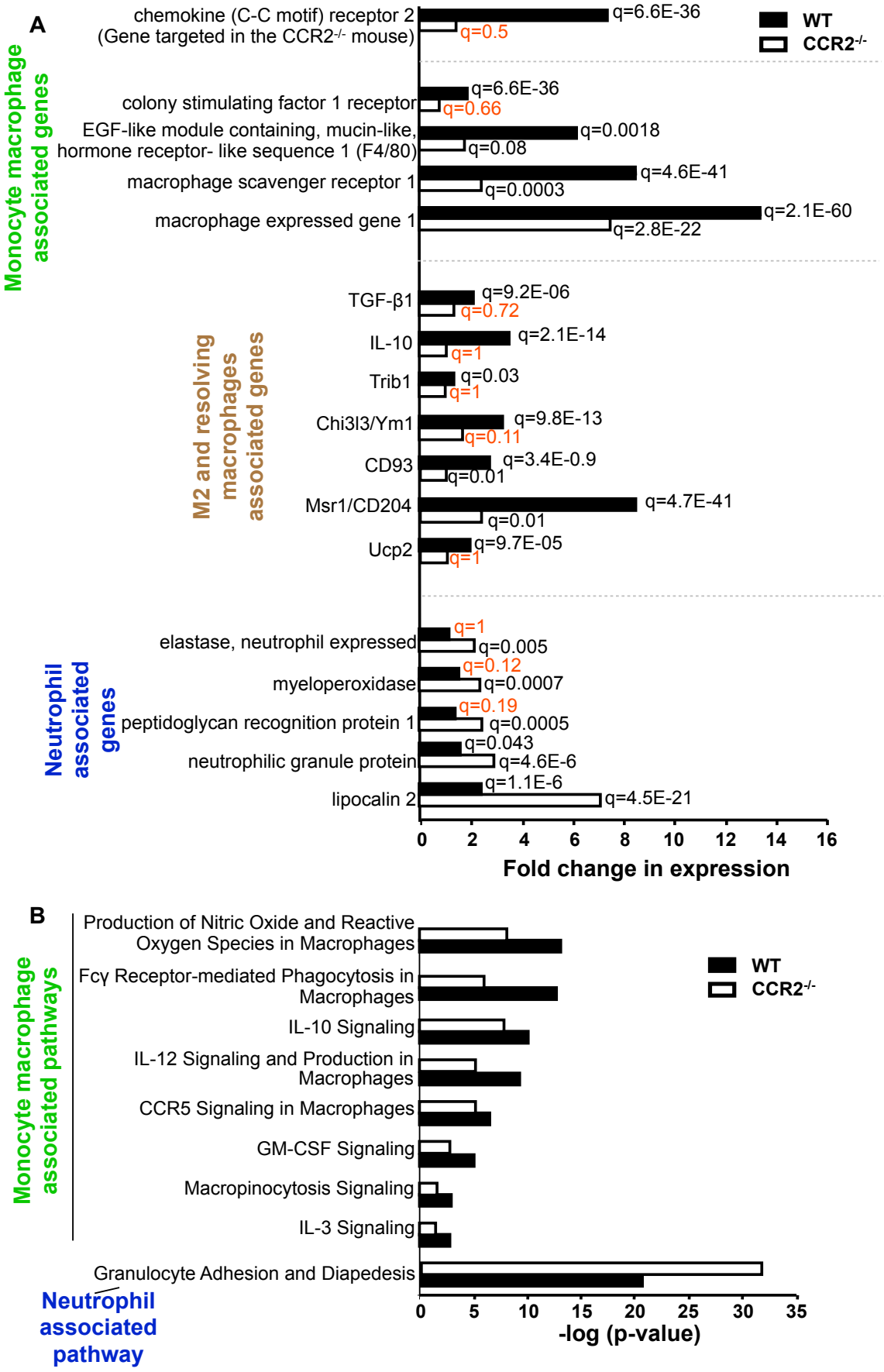
A
Monocyte macrophage associated genes
chemokine (C-C motif) receptor 2 (Gene targeted in the CCR2-/- mouse)
q=6.6E-36
q=0.5
colony stimulating factor 1 receptor
q=6.6E-36
q=0.66
EGF-like module containing, mucin-like, hormone receptor- like sequence 1 (F4/80)
q=0.0018
q=0.08
macrophage scavenger receptor 1
q=4.6E-41
q=0.0003
macrophage expressed gene 1
q=2.1E-60
q=2.8E-22
M2 and resolving macrophages associated genes
TGF-β1
q=9.2E-06
q=0.72
IL-10
q=2.1E-14
q=1
Trib1
q=0.03
q=1
Chi3l3/Ym1
q=9.8E-13
q=0.11
CD93
q=3.4E-0.9
q=0.01
Msr1/CD204
q=4.7E-41
q=0.01
Ucp2
q=9.7E-05
q=1
Neutrophil associated genes
elastase, neutrophil expressed
q=1
q=0.005
myeloperoxidase
q=0.12
q=0.0007
peptidoglycan recognition protein 1
q=0.19
q=0.0005
neutrophilic granule protein
q=0.043
q=4.6E-6
lipocalin 2
q=1.1E-6
q=4.5E-21
WT
CCR2-/-
0 2 4 6 8 10 12 14 16
Fold change in expression
B
Monocyte macrophage associated pathways
Production of Nitric Oxide and Reactive Oxygen Species in Macrophages
Fcγ Receptor-mediated Phagocytosis in Macrophages
IL-10 Signaling
IL-12 Signaling and Production in Macrophages
CCR5 Signaling in Macrophages
GM-CSF Signaling
Macropinocytosis Signaling
IL-3 Signaling
Granulocyte Adhesion and Diapedesis
Neutrophil associated pathway
WT
CCR2-/-
0 5 10 15 20 25 30 35
-log (p-value)

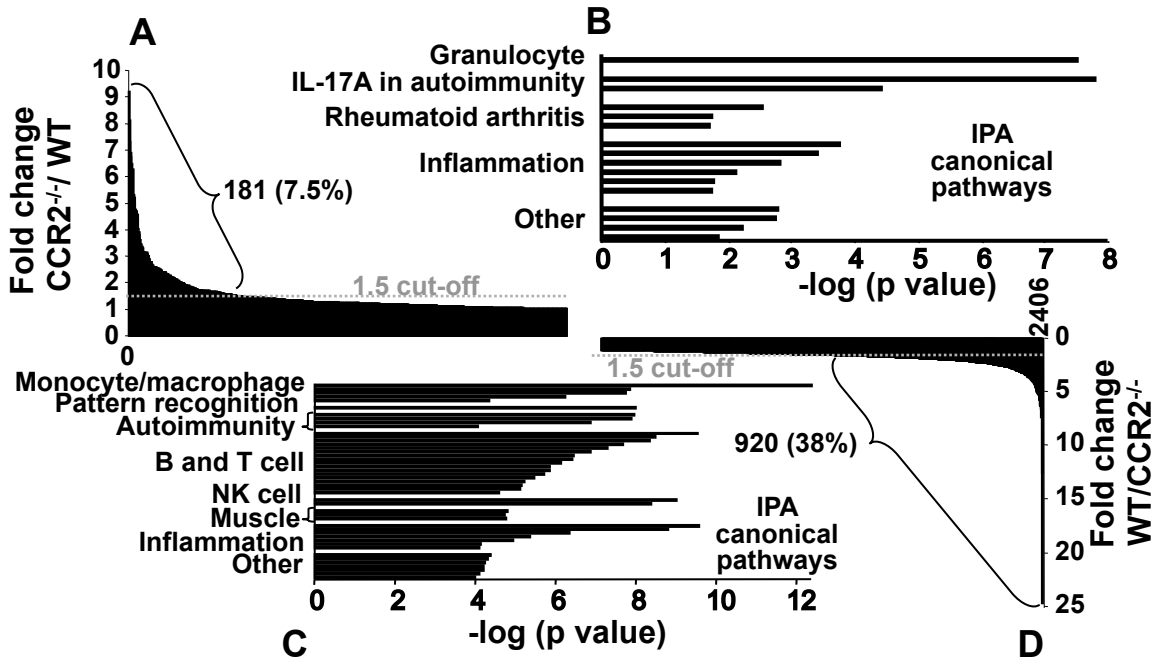

Figure 3.15: Microarray analysis of arthritic feet from WT and CCR2$^{-/-}$ mice.

Genes differentially expressed on day 7 post infection (compared to day 0) for WT and CCR2$^{-/-}$ feet were determined by microarray analysis. 2406 differentially expressed genes were up or down-regulated in WT and/or CCR2$^{-/-}$ feet. **(A)** For 181 of these genes "fold change in CCR2$^{-/-}$ mice"/"fold change in WT mice" was >1.5 fold; (for 603 DEGs this ratio was >1). **(B)** IPA canonical pathway analyses of the 181 genes more induced in CCR2$^{-/-}$ feet are shown, with pathways grouped into themes. Pathways details are shown in Appendix I. **(C)** As in (B) but with the 920 genes less induced in CCR2$^{-/-}$ feet. **(D)** For 920 of these genes the "fold change in WT mice"/"fold change in CCR2$^{-/-}$ mice" was >1.5 fold (bottom right); (for 1794 genes this ratio was >1, for 9 the ratio was =1). Pathways details are shown in Appendix II. -log(<1.3) represents $p < 0.05$.

Data for Figure 3.15 was prepared with assistance by Helder Nakaya and Andreas Suhrbier.

3.3 Discussion

This chapter describes the first analysis of a viral arthritis in CCR2$^{-/-}$ mice and illustrates that deficiency in this gene results in a more severe, prolonged and erosive arthritis. The prodigious monocyte/macrophage infiltrate seen in WT mice was almost entirely replaced by a neutrophil infiltrate in CCR2$^{-/-}$ mice, with this switch associated with dysregulation of a range of inflammatory and anti-inflammatory pathways. Recruitment of CCR2+ monocytes during CHIKV arthritis, although likely contributing to acute inflammatory disease (Suhrbier et al., 2012, Suhrbier and Mahalingam, 2009), thus also protects against even worse neutrophil-mediated pathology.

CXCL1, CXCL2, G-CSF, and IL-1β were increased in the arthritic feet of CCR2$^{-/-}$ mice, whereas IL-10 was decreased, suggesting multiple mediators were involved in promoting neutrophil recruitment (Fujii et al., 2012, Quinones et al., 2004, Montgomery et al., 2007, Sawanobori et al., 2008, Eyles et al., 2008, Sadik et al., 2012, Ajuebor et al., 1999). The reduction in IL-10 and lack of Arg-1 induction, also suggests a paucity of (CCR2+ derived) M2 and resolving macrophages and their anti-inflammatory activities in CCR2$^{-/-}$ mice. This contention is supported by array data that shows less up-regulation of a number of M2 and resolving macrophage markers in CCR2$^{-/-}$ feet (e.g. TGF-β, Ym1, Msr1) (Figure 3.14A, brown). M2 macrophages have high efferocytosis activity, with efferocytosis a key driver of inflammation resolution (Ariel and Serhan, 2012). The increase in ApoTag staining in CCR2$^{-/-}$ mice also suggests that efferocytosis is compromised in these mice, with CCL2 having previously been shown to promote efferocytosis (Tanaka et al., 2010). Evidence for secondary necrosis is also present in CCR2$^{-/-}$ feet (Figure 3.4M, left), and usually occurs when efferocytosis is compromised. Secondary necrosis itself promotes inflammation by releasing a number of soluble inflammatory mediators (Miyake and Yamasaki, 2012).

The eosinophil infiltration that follows the neutrophil infiltration in CCR2$^{-/-}$ mice may be promoted by the tissue damage induced by the neutrophils and/or secondary necrosis, and may help down-regulate the inflammatory response in these animals (Lotfi et al., 2009). Eosinophilic arthritis has been reported previously, and is usually associated with a benign course of disease (Vazquez-Trinanes et al., 2013).

Treatment of WT mice with clodronate (one day prior to CHIKV infection) to deplete monocyte/macrophages was previously shown to reduce foot swelling, but extended the viraemia, after CHIKV infection (Gardner et al., 2010); data that would seem at odds with the observations presented herein. However, the recent recognition that CD4 T cells and IFN-γ play important roles in driving arthritis in this CHIKV mouse model (Nakaya et al., 2012), and the ability of clodronate

treatment to suppress Th1 responses (Brewer et al., 1994), might suggest the observation above (Gardner et al., 2010) has more to do with reduced Th1 responses than reduced monocyte/macrophage infiltration (Cote et al., 2013). (Th1 responses were not significantly affected in CHIKV infected CCR2$^{-/-}$ mice). Clodronate treatment was also recently shown to affect germinal centers (Nikbakht et al., 2013), with compromised antibody responses perhaps explaining the extended viraemia seen after clodronate treatment (Gardner et al., 2010).

Exactly how CCR2+ monocytes recruited during CHIKV infection, and/or the macrophages that develop from them, might prevent excessive neutrophil infiltration and pathology in WT mice remains unclear. IL-10 may be involved (Ajuebor et al., 1999), but is unlikely to be the only player as neutrophil infiltration was not substantially or significantly increased in IL-10$^{-/-}$ mice (Figure 3.13C). Anti-inflammatory macrophages can also suppress neutrophil recruitment by *inter alia* secreting (i) a series of proresolving lipid mediators (Serhan, 2010) and/or (ii) proteases that cleave neutrophil-attracting chemokines (Ortega-Gomez et al., 2013). Regulatory T cells (Tregs) may be involved as (i) depletion of CCR2+ Tregs has been shown to exacerbate collagen-induced arthritis (Bruhl et al., 2004), (ii) anti-inflammatory macrophages can promote Treg expansion via TGF-β and IL-10 (Ortega-Gomez et al., 2013, London et al., 2013), (iii) T cells are important in driving CHIKV arthritis (Nakaya et al., 2012), and (iv) Th cell pathways were decreased in CCR2$^{-/-}$ mice (Figure 3.15C), with the microarray analysis unable to differentiate between Th and Treg cells. The increased IgG1 responses in CCR2$^{-/-}$ mice also support the view that T cell activities were altered in CHIKV-infected CCR2$^{-/-}$ mice. Further work is needed before the mechanisms and cells involved and their relative importance are fully elucidated, with other cell types (e.g. myeloid-derived suppressor cells (Ortega-Gomez et al., 2013)) potentially also involved. What does emerge from these studies is that in CHIKV arthritis (and perhaps other viral arthritides (Suhrbier and Mahalingam, 2009)), inflammation-recruited CCR2+ monocyte/macrophages appear to be important for limiting neutrophil recruitment into the infected and inflamed joint tissues. This contrasts with observations in other arthritis models where these cells promote neutrophil recruitment (Wang et al., 2012a).

The increase in IL-17 pathway activation in CHIKV infected CCR2$^{-/-}$ feet did not appear to be due to increased levels of Th17 cells (as was reported for in collagen-induced arthritis (Rampersad et al., 2011)). Recently, immune complexes present during acute arthritis were shown to induce IL-17 production by neutrophils (Katayama et al., 2013). Given antibody responses are raised against CHIKV (Figure 3.11A), immune complexes are likely to be present in CCR2$^{-/-}$ mice and may thus be responsible for triggering IL-17 production by the infiltrating neutrophils.

The widespread dysregulation of inflammatory processes observed in CHIKV infected $CCR2^{-/-}$ mice suggests considerable care might be warranted when using therapeutic agents that target CCR2/CCL2 for treating alphaviral arthritides (Rulli et al., 2011) (and perhaps other arthritides (Fujii et al., 2012)). Patients who are being treated with CCR2/CCL2-targeting agents (for other conditions) may also be at risk of exacerbated arthritic disease following an alphaviral infection.

Chapter 4: The contribution of B, T, NK cells and IFN-γ in the control of viraemia and mediation of arthritis during CHIKV infection

4.1 Introduction

Infection of adult humans with arthritogenic alphaviruses results in a 5-7 day viraemia and symptomatic infection is nearly always associated with rheumatic disease, primarily polyarthralgia and/or polyarthritis, which can be chronic and debilitating (Suhrbier et al., 2012). Antibodies are well known to provide protection against infections with alphaviruses (Burdeinick-Kerr et al., 2007, Brooke et al., 2010) including CHIKV (Eckels et al., 1970), with several studies demonstrating the antiviral efficacy of other antibody-based interventions (Fric et al., 2013, Selvarajah et al., 2013, Pal et al., 2013). However, the contribution of B cells to alphaviral arthritic disease is less clear, with some studies indicating that B cells have no role in RRV disease (Morrison et al., 2007, Morrison et al., 2006), while another study showed that B cell deficiency leads to more severe arthritic disease in CHIKV-infected mice (Lum et al., 2013).

The role of T cells in controlling alphaviral infection remains controversial. Some studies suggest that T cells play no protective role in controlling viraemia during, for example, CHIKV (Chu et al., 2013), RRV (Morrison et al., 2007, Morrison et al., 2006) and ONNV (Seymour et al., 2013) infections. In contrast, other studies have suggested a protective role for T cells in control of RRV (Linn et al., 1998), SINV (Binder and Griffin, 2001, Burdeinick-Kerr et al., 2007) and VEEV infections (Brooke et al., 2010).

Cytokines are well known to contribute to viral control and the pathology of alphaviral infection. IFN-α/β has been shown to be critical for protection against infection, disease and mortality caused by CHIKV and other alphaviruses, with IFN-α/β induced rapidly, but transiently, early in response to viral infection (Rudd et al., 2012, Schilte et al., 2010, Ryman et al., 2007, Labadie et al., 2010). IFN-γ has been shown to be involved in control of SINV (Binder and Griffin, 2001, Burdeinick-Kerr et al., 2007) and VEEV infections (Brooke et al., 2010). TNF has also been shown to have anti-alphaviral properties (Zaid et al., 2011), but has also been implicated in the pathology of CHIKV (Rudd et al., 2012).

Herein an adult mouse model of CHIKV infection and arthritis was used, where this mouse model mimics many aspects of human CHIKV disease (Gardner et al., 2010). Mice deficient in B cells (μMT mice), B and T cells (Rag-$1^{-/-}$ mice), B, T and NK cells (Rag2/Il2$rg^{-/-}$ mice), CD4+ T cells (MHC-$II^{\Delta/\Delta}$ mice) and IFN-γ (IFN-$\gamma^{-/-}$ mice) were infected with CHIKV, and viraemia and disease were monitored. B cells appear to be critical for control of CHIKV viraemia (consistent with a previous report by Lum et al. (2013)), with all B cell deficient mice showing a persistent steady-state viraemia. B cells may have an indirect role in promoting CHIKV arthritis. T cells were found to have a minor but significant role in controlling viraemia. Importantly, CD4+ T cells (possibly via the action of IFN-γ) were shown to be a major driver of CHIKV arthritis. This is in contrast to previous reports that suggested that T cells play no role in alphaviral arthritis (Morrison et al., 2007, Morrison et al., 2006).

4.2 Results

4.2.1 Viraemia in WT and B cell deficient mice (μMT, Rag-1$^{-/-}$ and Rag2/Il2rg$^{-/-}$ mice) infected with CHIKV

To determine which immune cells are critical for the control of CHIKV viraemia, WT, μMT (B cell deficient), Rag-1$^{-/-}$ (B and T cell deficient) and Rag2/Il2rg$^{-/-}$ (B, T and NK cell deficient) mice were infected with CHIKV via s.c. injection into each foot (Gardner et al., 2010).

At the indicated time points, viraemia was measured using $CCID_{50}$ assay. Viraemia in the B cell deficient mouse strains (μMT, Rag-1$^{-/-}$ and Rag2/Il2rg$^{-/-}$) peaked on days 2-3 post infection, stayed significantly higher than WT mice on days 3, 4 and 5, and then settled to relatively steady-state levels (Figure 4.1, μMT, Rag-1$^{-/-}$ and Rag2/Il2rg$^{-/-}$). This minor-fluctuating infection pattern is also seen in macrophage cell line that persistently infected with RRV (Linn et al., 1998, Way et al., 2002). In contrast, viraemia in WT mice was cleared by day 5 (Figure 4.1, WT). This elevated and persistent viraemia in B-cell deficient mice suggests that B cells are critical for the clearance of CHIKV viraemia.

The steady-state viraemias observed in B cell deficient mice are reminiscent of peripheral blood set point viraemias described for human immunodeficiency virus (HIV), in which the set point levels are deemed to be a reflection of functional anti-viral immunity (Prentice and Tang, 2012). Using a similar approach, the set point viraemias in CHIKV infected mice were determined by taking the mean of all viraemia measurements taken ≥ 10 days post infection (Figure 4.1, red values ± SD). Rag2/Il2rg$^{-/-}$ and Rag-1$^{-/-}$ mice, which both lack B and T cells, had a viraemia that was significantly higher (≈2 logs) than μMT mice that lack B cells (Figure 4.1, see p values). These results suggest that T cells contribute to the control of CHIKV viraemia. NK cells do not appear to play a significant role in the control of CHIKV viraemia, as Rag-1$^{-/-}$ mice (B and T cell deficient) had a similar set point viraemia as Rag2/Il2rg$^{-/-}$ mice (B, T and NK cell deficient) (Figure 4.1).

Figure 4.1: Viraemia in CHIKV infected WT mice and B cell deficient mouse strains (μMT, Rag-1$^{-/-}$ and Rag2/Il2rg$^{-/-}$ mice).

WT, μMT (deficient in B cells), Rag-1$^{-/-}$ (deficient in B and T cells) and Rag2/Il2rg$^{-/-}$ mice (deficient in B, T and NK cells) were infected with CHIKV. Viraemia was measured at the indicated time points. Set point viraemia (in red) is the mean of all viraemia measurements taken ≥ 10 days post infection (n = 3-10 mice per time point, mean ± SE is presented; data are derived from 2-3 independent experiments). **$p < 0.01$ and *$p < 0.05$ (compared to WT mice) by Mann-Whitney U test.

Data for Rag2/Il2rg$^{-/-}$ mice was prepared with assistance of Penny Rudd and Joy Gardner.

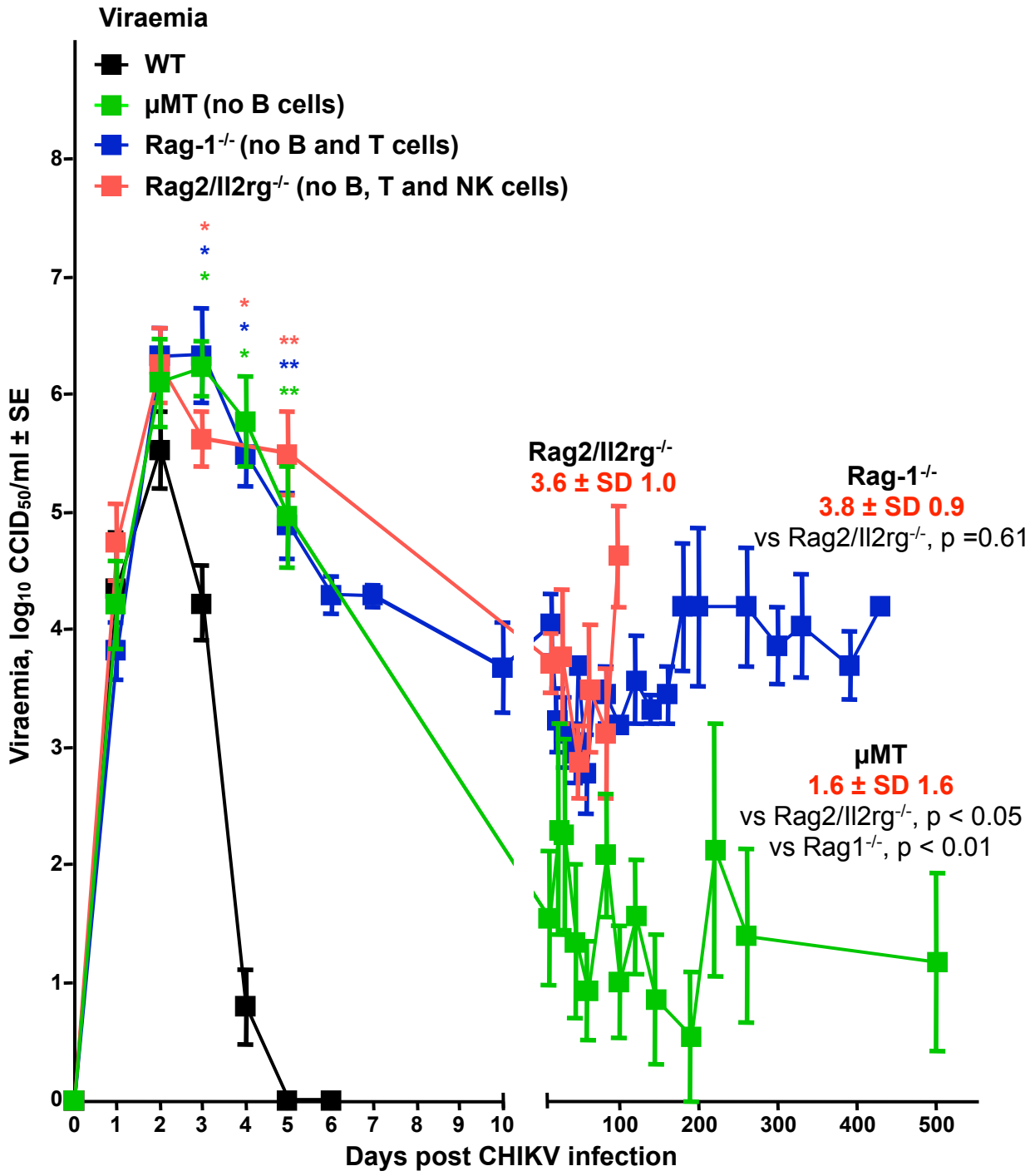
Viraemia
WT
µMT (no B cells)
Rag-1-/- (no B and T cells)
Rag2/Il2rg-/- (no B, T and NK cells)
Viraemia, log10 CCID50/ml ± SE
Days post CHIKV infection
Rag2/Il2rg-/-
3.6 ± SD 1.0
Rag-1-/-
3.8 ± SD 0.9
vs Rag2/Il2rg-/-, p =0.61
µMT
1.6 ± SD 1.6
vs Rag2/Il2rg-/-, p < 0.05
vs Rag1-/-, p < 0.01

4.2.2 Vaccination of μMT mice

The results in section 4.2.1 demonstrate that CHIKV infected μMT mice (B cell deficient) had a lower set point viraemia than the Rag-$1^{-/-}$ mice (B and T cell deficient). This observation suggests that the μMT mice generate CHIKV specific T cells that contribute to the control of CHIKV viraemia. CD8+ cytotoxic T lymphocytes (hereafter referred as CD8+ T cells), have been shown not to influence viraemia in a Ross River virus mouse model (Linn et al., 1998) and not to influence viraemia and disease in a CHIKV mouse model (Teo et al., 2012b), suggesting CD4+ T cells are likely involved. To test whether μMT mice are able to produce protective CHIKV specific T cells, μMT mice were vaccinated with an inactivated (non-adjuvanted) CHIKV whole-virus vaccine, which provides complete protection against CHIKV viraemia and foot swelling in WT mice (Gardner et al., 2010) (see section 2.9 for methods). Vaccinated μMT mice (21 days post vaccination) were found to generate T cell responses to the CHIKV vaccine that were comparable to those seen in WT mice (Figure 4.2A), as measured by T cell proliferation assays using inactivated virus as antigen (see section 2.22 for methods). An enzyme-linked ImmunoSpot assay was attempted, but failed to detect any significant increase of CD8+ T cell activity in vaccinated mice compared to non-vaccinated mice (data not shown). This result is not surprising as unadjuvanted, killed, whole-virus vaccines are generally poor at inducing CD8+ T cell responses (Foged et al., 2012). These data suggest that μMT and WT mice primarily produced CHIKV-specific CD4+ T cells post vaccination.

To examine the efficacy of these vaccine-induced CHIKV-specific T cells in controlling CHIKV viraemia, vaccinated and non-vaccinated μMT mice were challenged with CHIKV. The vaccinated μMT mice had a ≈1 and ≈1.5 log lower viraemia on days 3 and 4 post infection, respectively, when compared with mock-vaccinated μMT mice (Figure 4.2B, *). This effect was lost at later time points (Figure 4.2B), by which time the control μMT mice would presumably have generated their own CHIKV-specific T cells. This experiment supports the view that T cells contribute to viraemia control.

This page intentionally left blank.

Figure 4.2: Viraemia and T cell proliferation assay in vaccinated WT and µMT mice.

µMT and WT mice were vaccinated with inactivated CHIKV antigen. **(A)** Splenocytes derived from mock-vaccinated WT, vaccinated WT, mock-vaccinated 0µMT and vaccinated µMT mice were subjected to a T cell proliferation assay. Counts per minute correlates with the proliferation of CHIKV specific T cells. (n = 5 mice per group; p values by Mann-Whitney U test). **(B)** Vaccinated and mock-vaccinated µMT mice were challenged with CHIKV. Viraemia was measured at the indicated time points. (n = 7-10 mice per group; data is derived from 2 independent experiments). *$p < 0.01$ by Mann-Whitney U test.

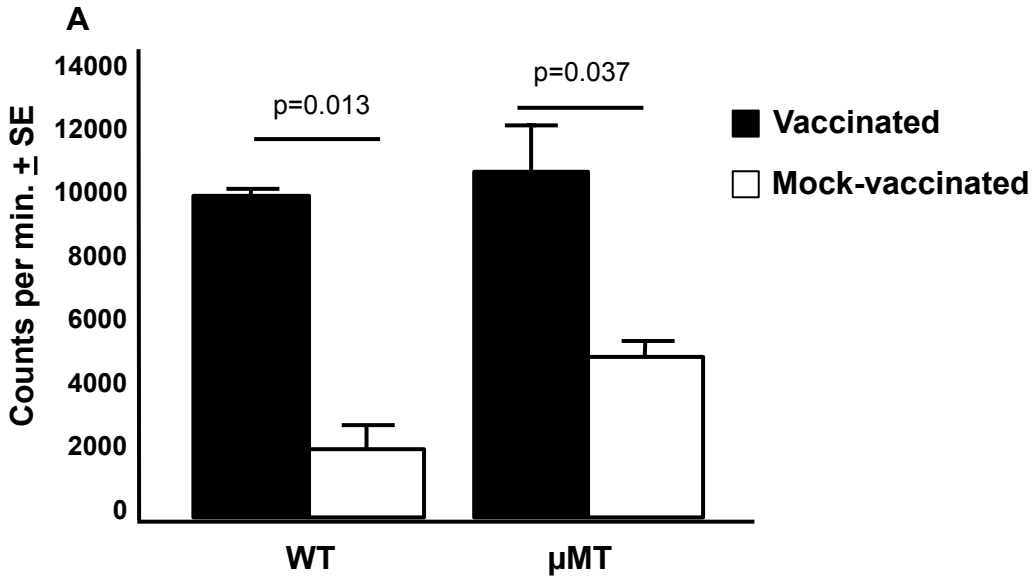
A
14000
12000
10000
8000
6000
4000
2000
0
Counts per min. ± SE
p=0.013
p=0.037
Vaccinated
Mock-vaccinated
WT
µMT

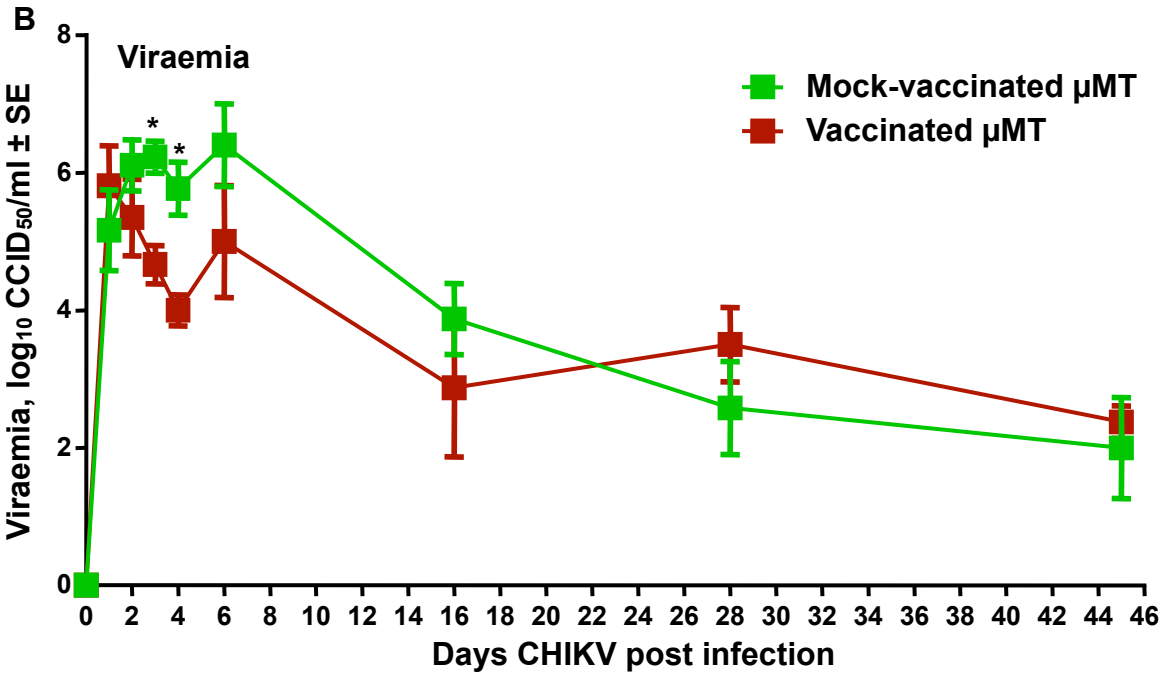
B
Viraemia
Mock-vaccinated µMT
Vaccinated µMT
Viraemia, log10 CCID50/ml ± SE
8
6
4
2
0
*
*
0 2 4 6 8 10 12 14 16 18 20 22 24 26 28 30 32 34 36 38 40 42 44 46
Days CHIKV post infection

4.2.3 Treatment of Rag-1$^{-/-}$ and μMT mice with anti-CHIKV antibodies

Adoptive transfer of antibodies has been suggested as a prophylactic and therapeutic intervention for CHIKV (Fric et al., 2013, Selvarajah et al., 2013, Pal et al., 2013). Persistently infected Rag-1$^{-/-}$ and μMT mice, which lack antibody producing B cells, were treated with 200 μl of hyperimmune sera containing high levels of CHIKV neutralising antibodies (1 in 1250 neutralisation titre). Viraemia in the treated mice became undetectable for 10 and 30 days in Rag-1$^{-/-}$ and μMT mice (Figure 4.3), respectively, but then reappeared to levels seen prior to antibody administration (Figure 4.3). Therefore, passive transfer of antibody was unable permanently to clear the virus from these persistently viraemic mice.

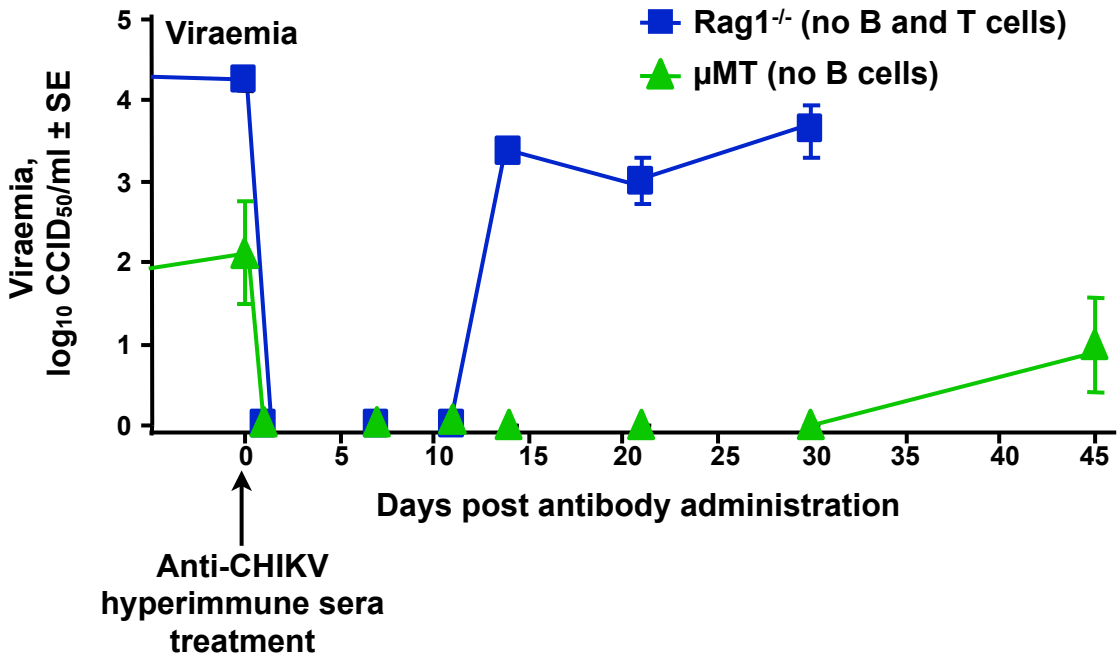

Figure 4.3: Viraemia in persistently infected Rag-1$^{-/-}$ and µMT mice treated with anti-CHIKV hyperimmune sera.

Rag-1$^{-/-}$ mice (deficient in B and T cells) and µMT mice (deficient in B cells), with an established persistent viraemia, were treated with hyperimmune sera containing high levels of CHIKV neutralising antibodies. At the indicated time points, viraemia was measured (n = 4 mice per time point).

4.2.4 CHIKV arthritis in μMT mice

To investigate the role of B cells in the development of arthritis, μMT and WT mice were infected with CHIKV and foot swelling was measured over time (Figure 4.4A and B). Foot swelling was significantly higher in μMT mice than WT mice on days 4, 5, 7, 8, 9, 10 and 11 (Figure 4.4B) consistent with a previous report using a different CHIKV isolate (Lum et al., 2013). However, there was no significant difference in peak foot swelling (day 6) between μMT and WT mice.

The infected joint tissues were also examined by histology (Figure 4.5). Peak swelling of WT and μMT mice (Figure 4.4B, day 6) showed a clear infiltrate of mononuclear cells (Figure 4.5A and B). The density of infiltrating cells during peak arthritis was quantified using the Aperio Positive Pixel Count algorithm, which determined the amount of blue nuclear stain per μm^2. The density of infiltrating mononuclear cells did not differ between WT and μMT mice (Figure 4.5F), illustrating that the increased foot swelling (in μMT mice) was due to the increased levels of arthritis.

4.2.5 CHIKV arthritis in Rag-1$^{-/-}$ mice

To investigate the role of T cells in CHIKV arthritis, Rag-1$^{-/-}$ mice (deficient in B and T cells) were infected with CHIKV. Rag-1$^{-/-}$ mice displayed two distinct peaks in foot swelling, one on day 3 (that was significantly higher than that seen in WT mice) and one on day 6 (Figure 4.4C). Foot swelling in Rag-1$^{-/-}$ mice on day 6 was comparable to that seen in WT mice (Figure 4.4C).

Histological analysis revealed that Rag-1$^{-/-}$ mouse feet had a significantly lower density of infiltrating cells on both day 3 and 6 (Figure 4.5F, Rag-1$^{-/-}$) as quantified by Aperio Positive Pixel Count analysis, when compared to that seen in WT mice (Figure 4.5F, WT). These results illustrated that foot swelling in Rag-1$^{-/-}$ mice was not due to the influx of inflammatory cells but rather was largely attributable to oedema (Figure 4.5C and D, * indicates of oedema). The higher density of inflammatory infiltrates in WT (and μMT mice) when compared with Rag-1$^{-/-}$ mice, further supports the view that T cells are required for the development of CHIKV arthritis.

This page intentionally left blank.

Figure 4.4: Foot swelling in CHIKV infected WT, µMT and Rag-1$^{-/-}$ mice.

WT, µMT (deficient in B cells) and Rag-1$^{-/-}$ mice (deficient in B and T cells) were infected with CHIKV and monitored for foot swelling. **(A)** Images of uninfected WT mice feet (-ve CHIKV) and infected WT mice feet (+ve CHIKV) on day 6 post infection (peak swelling). **(B)** Foot swelling, expressed as percent increase (compared to pre-infection measurements), in infected WT and µMT mice. (n = 10-16 feet, 5-8 mice per time point; data are derived from 3 independent experiments for WT mice and 2 independent experiments for µMT mice). *$p < 0.01$ by Mann-Whitney U test. **(C)** Foot swelling in WT and Rag-1$^{-/-}$. (n = 10-16 feet, 5-8 mice per group; data are derived from 3 independent experiments for WT mice and 2 independent experiments for Rag-1$^{-/-}$ mice). **$p < 0.01$ by Mann-Whitney U test.

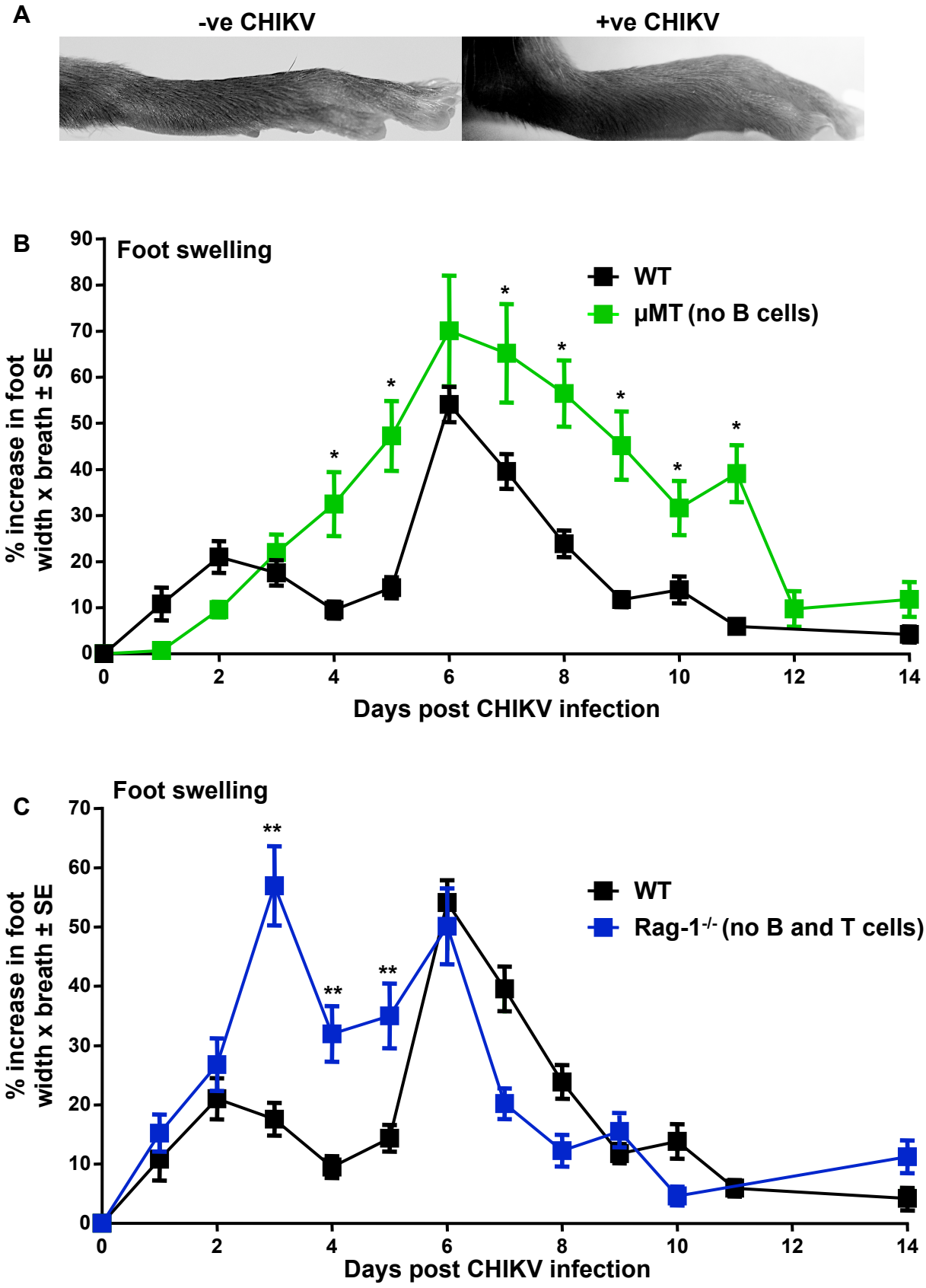
A
-ve CHIKV
+ve CHIKV
B
Foot swelling
WT
µMT (no B cells)
% increase in foot width x breath ± SE
Days post CHIKV infection
C
Foot swelling
WT
Rag-1-/- (no B and T cells)
% increase in foot width x breath ± SE
Days post CHIKV infection

Figure 4.5: Histological analysis and quantification of feet from CHIKV infected WT, μMT, Rag-1$^{-/-}$ and MHC-II$^{\Delta/\Delta}$ mice.

WT, μMT (deficient in B cells), Rag-1$^{-/-}$ (deficient in B and T cells) and MHC-II$^{\Delta/\Delta}$ (deficient in CD4+ T cells) mice were infected with CHIKV s.c. into the feet. At the indicated time points, the infected mice were sacrificed, the feet removed and examined by histology. **(A), (B), (C), (D)** and **(E)** H&E staining of skeletal muscle in CHIKV infected mice feet; * indicates oedema. **(F)** Aperio Positive Pixel Count quantification of digitally scanned H&E stained whole foot sections. Area of nuclear staining (blue) per unit area is used as a measure of the density of infiltrating cells. (n = 4 feet, 4 mice per group). P values by Mann-Whitney U (WT day 6 vs MHC-II$^{\Delta/\Delta}$ day 6) and Kolmogorov Smirnov tests (WT day 6 vs Rag-1$^{-/-}$ day 6).

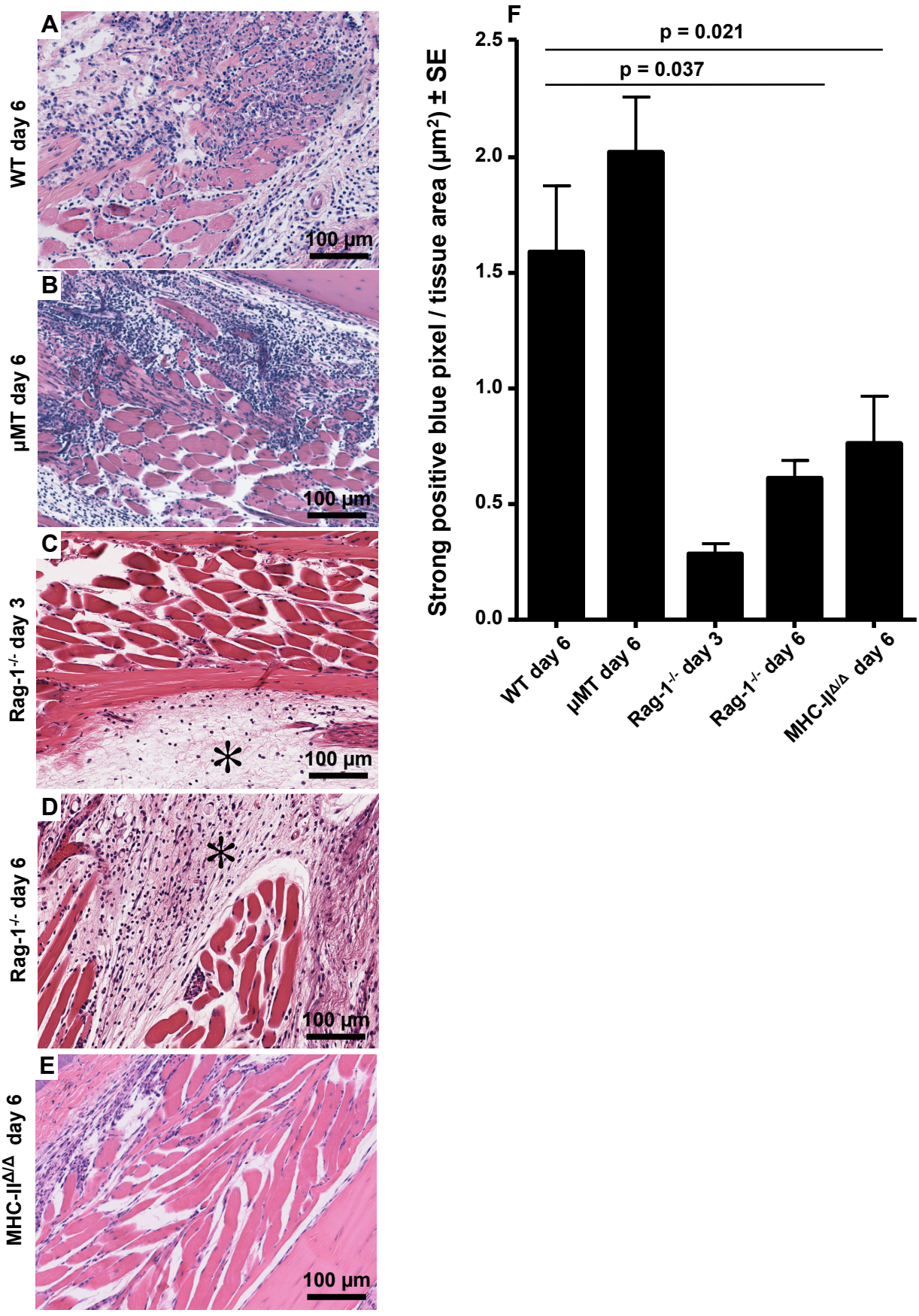
A
WT day 6
100 µm
B
µMT day 6
100 µm
C
Rag-1-/- day 3
100 µm
D
Rag-1-/- day 6
100 µm
E
MHC-IIΔ/Δ day 6
100 µm
F
p = 0.021
p = 0.037
Strong positive blue pixel / tissue area (µm2) ± SE
2.5
2.0
1.5
1.0
0.5
0.0
WT day 6
µMT day 6
Rag-1-/- day 3
Rag-1-/- day 6
MHC-IIΔ/Δ day 6

4.2.6 Investigation of the role of CD4+ T cells in CHIKV viraemia and arthritis using MHC-II $^{\Delta/\Delta}$ mice

Previous results (sections 4.2.1, 4.2.2, and 4.2.4) suggested that T cells may play a role in the control of CHIKV viraemia and the development of CHIKV arthritis. CD4+ T cells are also important drivers of rheumatoid arthritis (Yamada et al., 2011, Snir et al., 2011). To determine whether CD4+ T cells are involved in CHIKV viraemia control and arthritis, MHC-II$^{\Delta/\Delta}$ mice that are deficient in CD4+ T cells were infected with CHIKV. Compared with WT mice, the MHC-II$^{\Delta/\Delta}$ mice had a slight delay in viraemia clearance that approached significance on day 4 (Figure 4.6A), again supporting the view that CD4+ T cells play a significant but secondary role in controlling CHIKV viraemia.

To elucidate the role of CD4+ T cells in CHIKV arthritis, foot swelling in CD4+ T cell deficient MHC-II$^{\Delta/\Delta}$ mice was compared with WT mice following CHIKV infection. MHC-II$^{\Delta/\Delta}$ mice had significantly lower foot swelling compared to WT mice on day 6, 7 and 8 post infection (Figure 4.6B, *), and H&E staining revealed that the feet of MHC-II$^{\Delta/\Delta}$ mice had lower densities of infiltrating cells compared to WT mice during peak arthritis (day 6 post infection) (Figure 4.5A and E; Figure 4.5F, WT and MHC-II$^{\Delta/\Delta}$). These data suggest that CD4+ T cells play an important role in the development of CHIKV arthritis.

4.2.7 Vaccination of μMT mice – foot swelling

μMT mice produced CHIKV-specific CD4+ T cells following vaccination (section 4.2.2). Since result in section 4.2.6 suggested that CD4+ T cells may play a pathogenic role in acute CHIKV arthritis, foot swelling in vaccinated μMT mice was compared with non-vaccinated μMT mice following CHIKV infection. Vaccinated μMT mice had a significantly higher foot swelling on day 2, 3 and 4 compared to mock-vaccinated μMT mice when challenged with CHIKV (Figure 4.7, *). This observation suggests that the pre-existing CHIKV-specific CD4+ T cells present in the vaccinated mice were responsible for the early foot swelling seen in vaccinated mice. Taken together, these data suggest that CD4+ T cells act to reduce CHIKV viraemia but exacerbate CHIKV arthritis.

This page intentionally left blank.

Figure 4.6: Viraemia and foot swelling in CHIKV infected WT and MHC-II$^{\Delta/\Delta}$ mice.

WT and MHC-II $^{\Delta/\Delta}$ mice (CD4+ deficient) were infected with CHIKV. **(A)** Viraemia in WT and MHC-II$^{\Delta/\Delta}$ mice post CHIKV infection. (n = 6-10 mice per group, mean ± SE is presented; data are derived from 3 independent experiments for WT mice and 2 independent experiments for MHC-II$^{\Delta/\Delta}$ mice. P value by t-test. **(B)** Foot swelling in WT and MHC-II$^{\Delta/\Delta}$ mice post CHIKV infection. (n = as above, with both feet; data are derived as above). *$p < 0.05$ by Mann-Whitney U test.

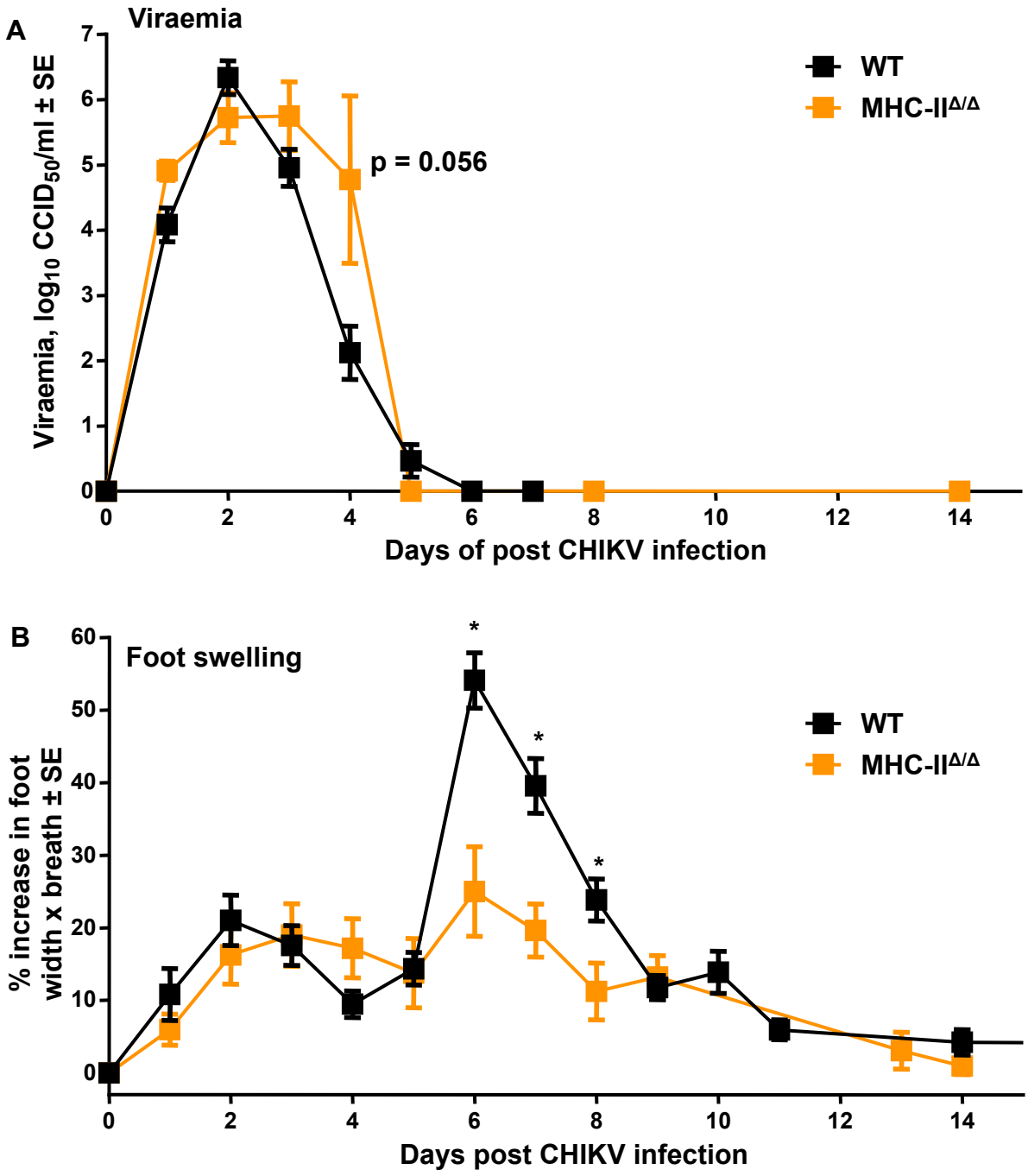
A
Viraemia
Viraemia, log10 CCID50/ml ± SE
p = 0.056
WT
MHC-IIΔ/Δ
Days of post CHIKV infection
B
Foot swelling
% increase in foot width x breath ± SE
*
*
*
WT
MHC-IIΔ/Δ
Days post CHIKV infection

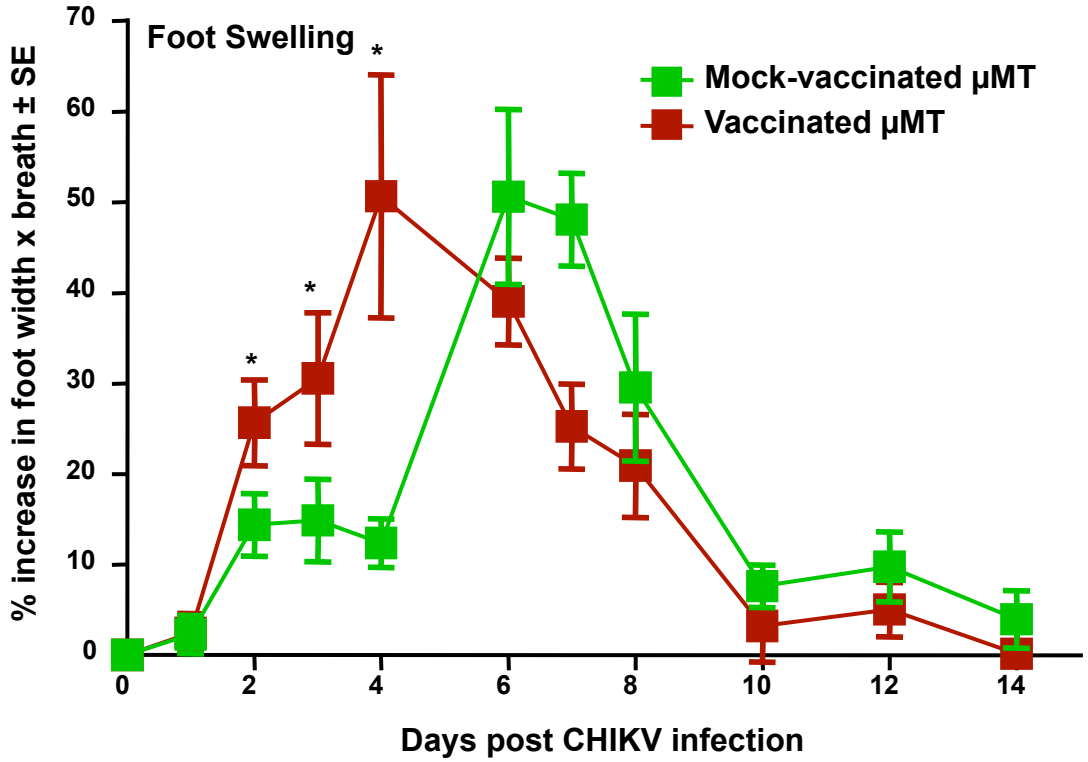

Figure 4.7: Foot swelling in vaccinated µMT mice and mock-vaccinated µMT mice following CHIKV infection.

µMT mice were vaccinated with inactivated CHIKV antigen or mock. After 3 weeks, mice were infected with CHIKV s.c. in the feet. Foot swelling was measured at the indicated time points and values are expressed as percent increase in foot width x breadth (compared to day 0) (n = 10 feet, 5 mice per time point; data are derived from 2 independent experiments). *p < 0.05 by Mann-Whitney U test.

4.2.8 MHC-II$^{\Delta/\Delta}$ mice produce IgG2c antibodies independent of CD4+ T cells

MHC-II$^{\Delta/\Delta}$ mice are deficient in CD4+ T cells, which are known to facilitate B cell IgG class switching (Swain et al., 2012). However, MHC-II$^{\Delta/\Delta}$ mice were able to control viraemia effectively (Figure 4.6A) and did not display persistent viraemia as seen in B cell deficient mice (Figure 4.1). Analysis of the antibody responses in these mice showed that following CHIKV infection, MHC-II$^{\Delta/\Delta}$ mice generated no anti-viral IgG1 responses (Figure 4.8A), but they did produce anti-viral IgG2c responses, albeit at about 100 fold lower titres compared to WT mice (Figure 4.8B). This reduced, yet significant, virus-specific IgG2c is likely responsible for the control of CHIKV seen in these mice. These observations indicate that MHC-II$^{\Delta/\Delta}$ mice control viraemia via CD4+ T cell-independent production of IgG2c.

4.2.9 CHIKV arthritis and viraemia in IFN-γ$^{-/-}$ mice

Activated CD4+ T cells can produce high levels of IFN-γ (Foulds et al., 2006). During CHIKV infection, serum IFN-γ is consistently up regulated in human patients, monkeys and mice (Gardner et al., 2010, Labadie et al., 2010, Hoarau et al., 2010). To examine whether IFN-γ contributes to CHIKV arthritis, IFN-γ$^{-/-}$ mice were challenged with CHIKV. Following infection, CHIKV-infected IFN-γ$^{-/-}$ mice showed a significantly lower foot swelling on days 2-3 and 6-8 when compared with WT mice (Figure 4.9A; $p<0.01$). Viraemia in IFN-γ$^{-/-}$ mice was not significantly different from WT mice (Figure 4.9B, see p values), indicating that the reduced foot swelling in IFN-γ$^{-/-}$ mice was not due to any major reduction in viraemia. These data suggest that IFN-γ is involved in promoting CHIKV arthritis. The likely source of IFN-γ may be CD4+ T cells.

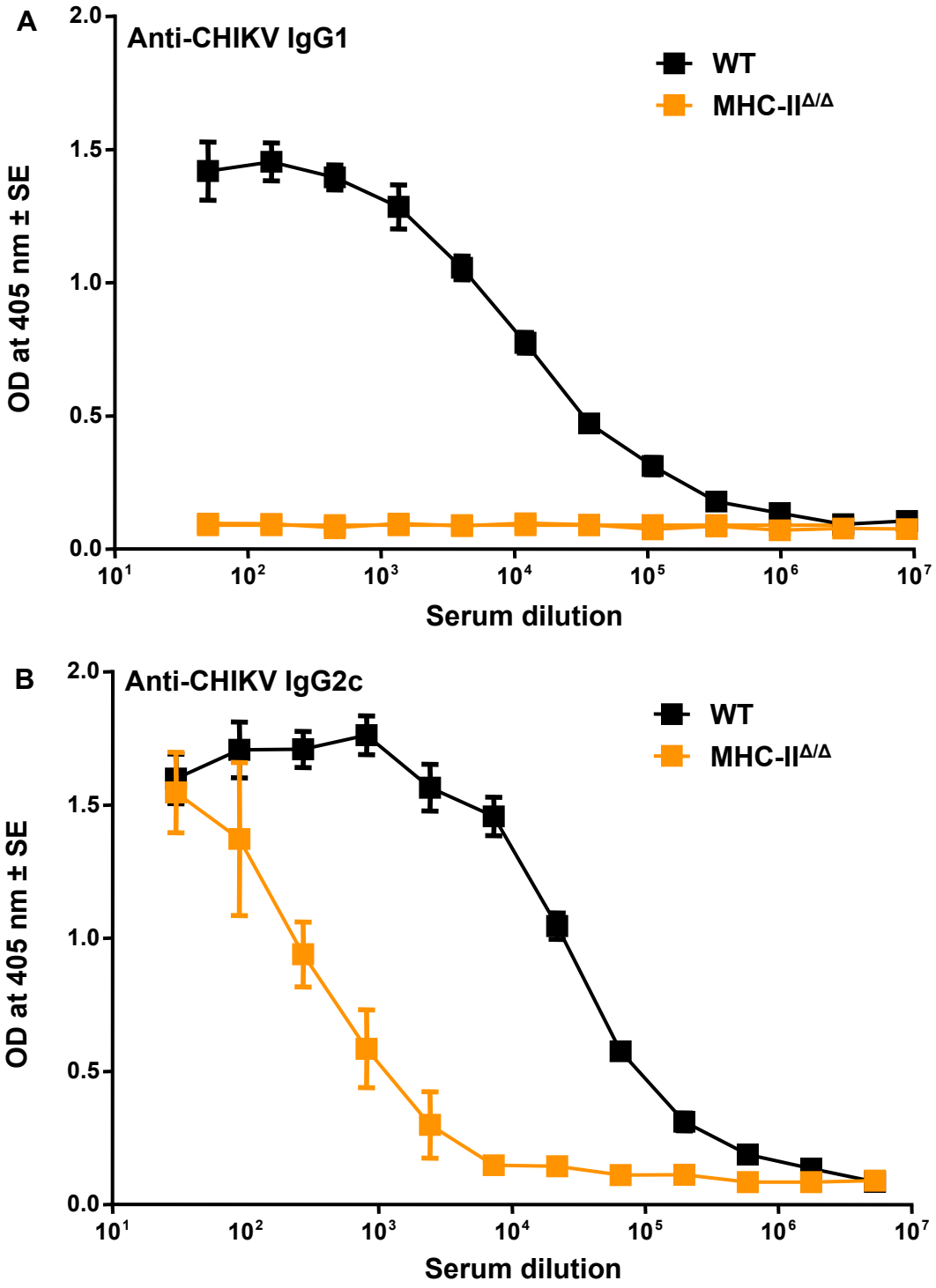

Figure 4.8: The presence of anti-CHIKV antibody in CHIKV infected WT and MHC-II$^{\Delta/\Delta}$ mice.

WT and MHC-II$^{\Delta/\Delta}$ mice were infected with CHIKV. Sera from WT and MHC-II$^{\Delta/\Delta}$ mice were collected on day 21 post-CHIKV infection and assayed for anti-CHIKV antibodies by standard ELISA. **(A)** Anti-CHIKV IgG1. (n = 4 mice per group). **(B)** Anti-CHIKG IgG2c. (n = 4 mice per group).

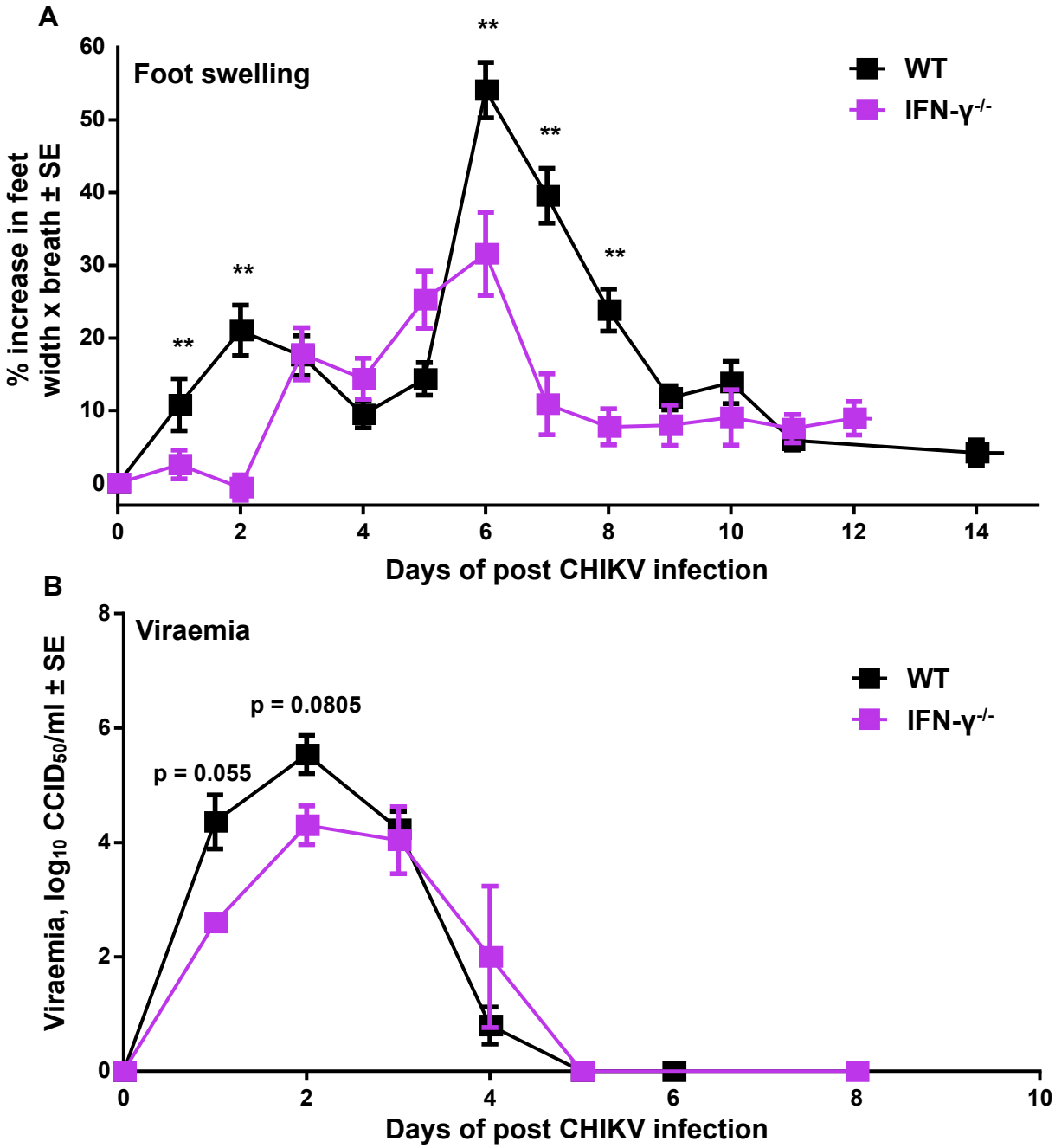

Figure 4.9: Viraemia and foot swelling in WT and IFN-γ$^{-/-}$ mice during CHIKV infection.

WT and IFN-γ$^{-/-}$ mice were infected with CHIKV. **(A)** Foot swelling in WT and IFN-γ$^{-/-}$ mice post CHIKV infection. (n = 10-16 feet, 5-8 mice per group; data are derived from 3 independent experiments for WT mice and 2 independent experiments for IFN-γ$^{-/-}$ mice). **p < 0.01 by Mann-Whitney test. **(B)** Viraemia in WT and IFN-γ$^{-/-}$ mice post CHIKV infection. (n = 5-10 mice per time point). P values by Kolmogorov Smirnov test.

4.2.10 Histological analysis of persistently infected Rag-1$^{-/-}$ mice

Previous data (Eckels et al., 1970, Metz et al., 2013a, Lum et al., 2013) (Figure 4.1) suggest that B cells are critical for control of CHIKV viraemia and CD4+ T cells are implicated in the development of CHIKV arthritis (Figure 4.6B). Rag-1$^{-/-}$ mice, which lack both B and T cells, had relatively high viraemia (Figure 4.1, compare day 1-5), but a lower density of infiltrating cells in the feet compared to WT mice (Figure 4.5A, C and D; Figure 4.5F, Rag1$^{-/-}$). After CHIKV infection, Rag-1$^{-/-}$ mice developed a persistent viraemia (Figure 4.1). This persistent viraemia resulted in surprisingly little overt pathology with mice appearing and behaving normally post infection for up to day 500 (data not shown).

To determine whether persistent CHIKV infection results in any pathology in mice, the liver, lungs, brain, spleen, lymph nodes, muscle, skin, and feet of persistently viraemic (430 days post infection) and uninfected Rag-1$^{-/-}$ mice were examined by histology. H&E analysis revealed that the spleen, kidney and liver of chronically infected Rag-1$^{-/-}$ mice had minor but discernible pathology (Figure 4.10B, D and F) compared to non-infected Rag-1$^{-/-}$ mice (Figure 4.10A, C and E). The spleens of chronically infected Rag-1$^{-/-}$ mice displayed marked increases in polymorphonuclear leukocytes (Figure 4.10B), features that are consistent with chronic infection (Borojevic et al., 1983, Murray et al., 1998, Furze and Selkirk, 2005). In the kidney and liver of persistently viraemic Rag-1$^{-/-}$ mice, an increased cell density was observed (for kidney, compare Figure 4.10C with D, black arrowheads; for liver, compare Figure 4.10E with F, black arrowheads), which is also indicative of chronic inflammation (Emamghorashi et al., 2011). Liver tissue from infected Rag-1$^{-/-}$ mice clearly displayed an increased number of apoptotic cells compared to uninfected Rag-1$^{-/-}$ mice (Figure 4.10F, white arrows), again indicating the presence of chronic inflammation (Ishak, 2000). Together, these histological observations indicate that the persistent viraemia observed in Rag-1$^{-/-}$ mice generates a pathology consistent with mild but chronic inflammation.

This page intentionally left blank.

Figure 4.10: Histological analysis of persistently viraemic Rag-1$^{-/-}$ mice.

Rag-1$^{-/-}$ mice were infected with CHIKV. On day 430 post infection, two viraemic Rag-1$^{-/-}$ mice were sacrificed. **A, C, E,** uninfected Rag-1$^{-/-}$ mice. **B, D, F,** Rag-1$^{-/-}$ mice day 430 post infection. **(A)** and **(B)**, H&E staining of spleen. **(C)** and **(D)**, H&E staining of kidney. Black arrowheads indicate increased cell density. **(E)** and **(F)**, H&E staining of liver. Black arrowheads indicate increased cell density; white arrows indicate apoptotic cells.

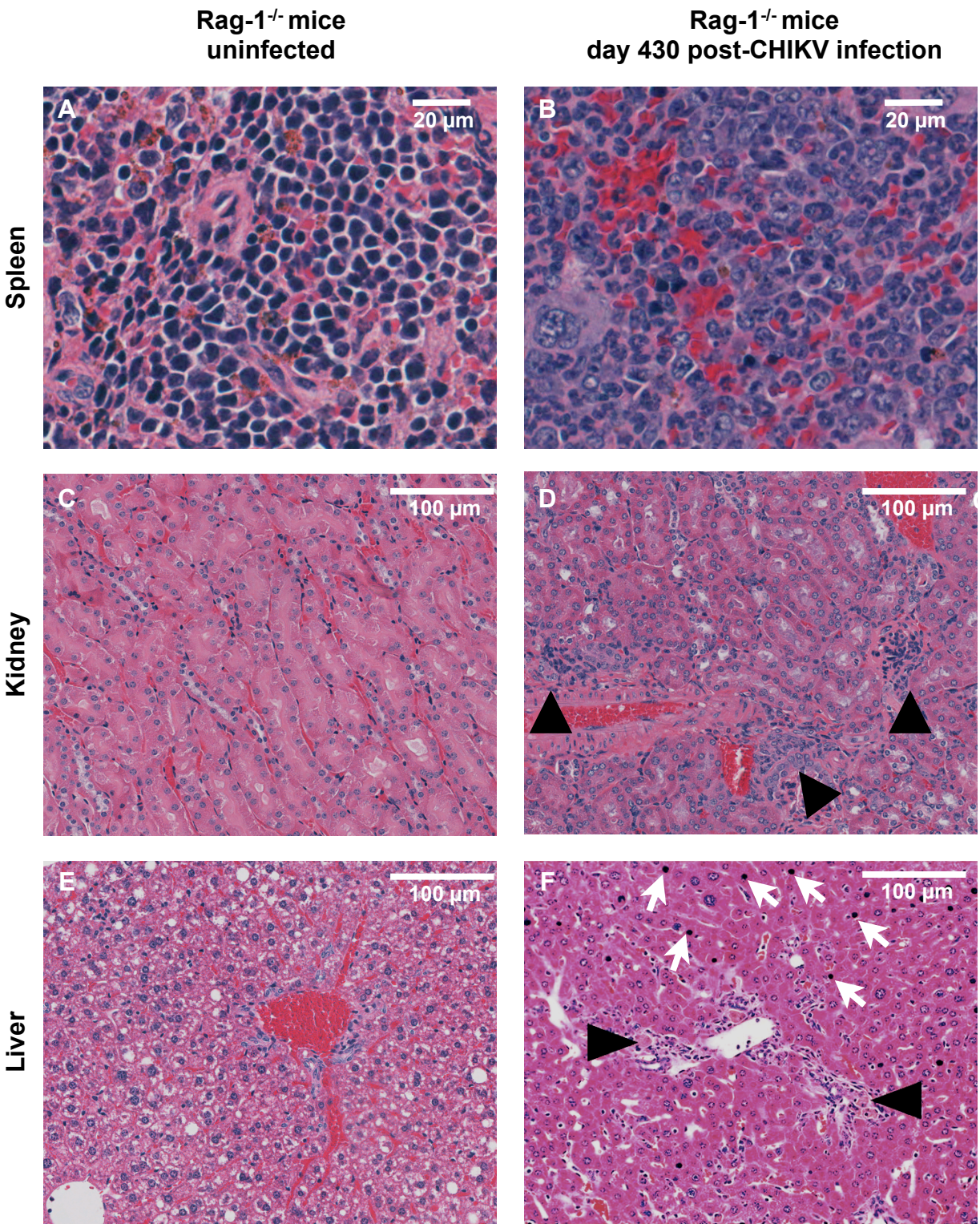
Rag-1-/- mice
uninfected
Rag-1-/- mice
day 430 post-CHIKV infection
Spleen
Kidney
Liver
A
20 µm
B
20 µm
C
100 µm
D
100 µm
E
100 µm
F
100 µm

4.2.11 Cytokine profile in the sera of persistently infected Rag-1$^{-/-}$ mice

Histological analysis of chronically infected Rag-1$^{-/-}$ mice provided evidence of an ongoing local inflammatory response (section 4.2.10). To further investigate the presence of ongoing systemic inflammation, serum cytokine levels were measured in uninfected Rag-1$^{-/-}$ mice and persistently viraemic Rag-1$^{-/-}$ mice, by using cytometric bead array and IFN-alpha FlowCytomix assay. IFN-γ, TNF and IL-6 levels peaked on day 1-3, and then dropped, but remained persistently up-regulated (Figure 4.11), with IFN-γ and TNF previously shown to have anti-alphaviral activities (Ryman et al., 2007, Zaid et al., 2011). The initial induction of these pro-inflammatory cytokines in Rag-1$^{-/-}$ mice was similar to the induction of these cytokines in WT mice during acute infection (Gardner et al., 2010). However, in WT mice the levels of these cytokines returned to pre-infection levels after 14 days (Gardner et al., 2010).

IFN-α levels, which were up-regulated during acute infection in Rag-1$^{-/-}$ mice (Figure 4.11, day 1-3), did not remain elevated, despite ongoing viraemia in these mice (Figure 4.1, Rag-1$^{-/-}$). Production of IFN-α/β is well characterised and known to be tightly controlled and usually transient (Bonjardim et al., 2009, Komuro et al., 2008). This pattern of IFN-α/β production appeared to be largely retained in Rag-1$^{-/-}$ mice after CHIKV infection despite ongoing viraemia. These data suggest that IFN-γ, TNF and IL-6, but not IFN-α, were associated with viraemia control in persistently infected Rag-1$^{-/-}$ mice.

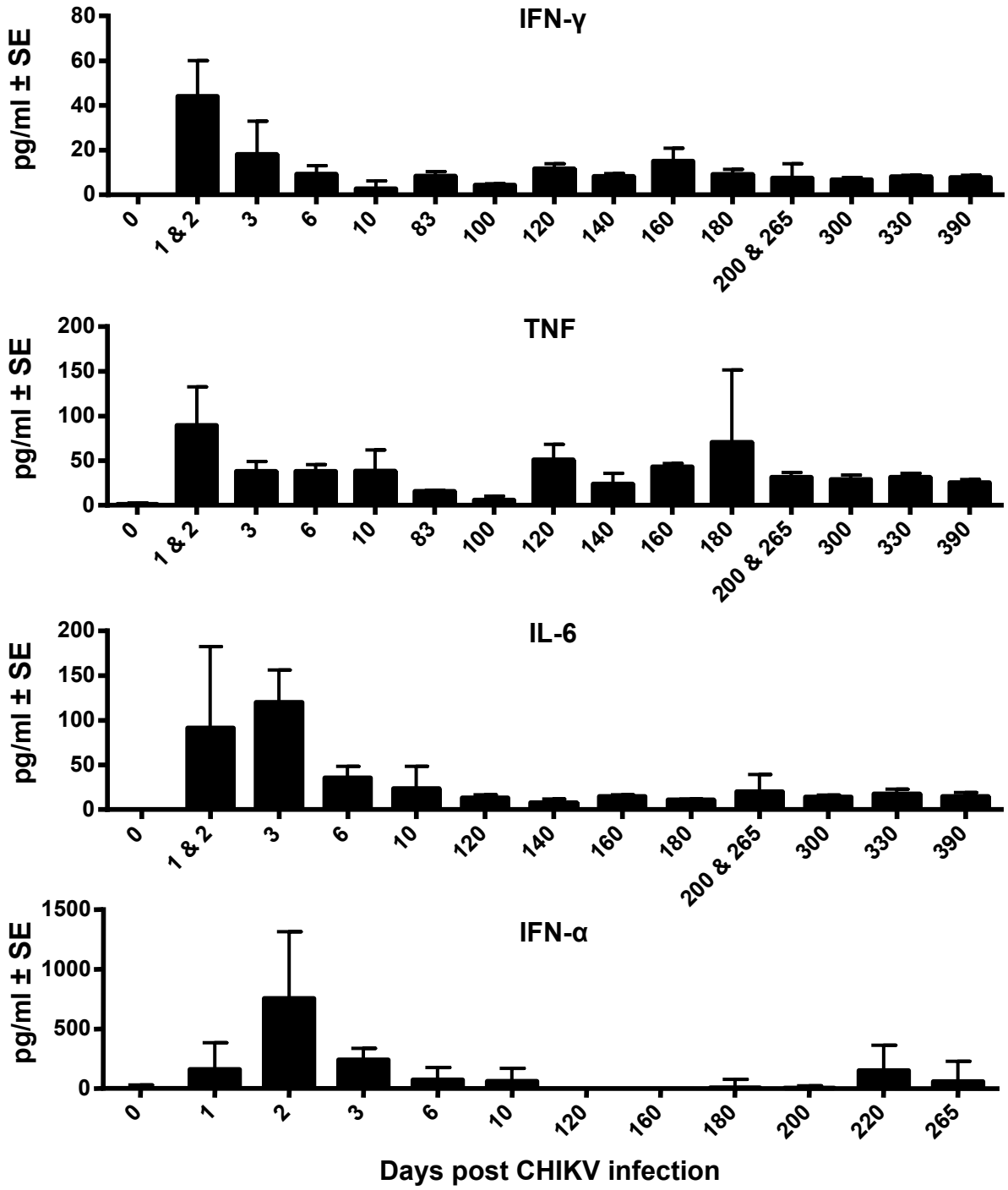

Figure 4.11: Serum cytokine levels in persistently viraemic Rag-1$^{-/-}$ mice.

Rag-1$^{-/-}$ mice were infected with CHIKV s.c. in the feet. Sera were collected at the indicated time points and analysed for IFN-γ, TNF, IL-6 and IFN-α levels using cytometric bead array (IFN-γ, TNF, IL-6) and Mouse IFN-alpha FlowCytomix assay (IFN-α). (n = 2-4 mice per time point).

4.2.12 Persistent virus recovered from Rag1$^{-/-}$ mice

The ability of alphaviruses to acquire mutations and better evade the antiviral effects of IFNα/β have been reported (Lidbury et al., 2011, Stoermer Burrack et al., 2014) with CHIKV and other alphaviruses having evolved strategies to counter the host's type I and II interferon responses (Ryman and Klimstra, 2008, Fros et al., 2010). Virus isolated from Rag-1$^{-/-}$ mice on 100 and 429 days post-infection behaved no differently from parental virus (with respect to viraemia and foot swelling) when isolated from blood, expanded in C6/36 cells, and used to infect WT mice (data not shown). CHIKV thus appears unable (via mutations) to evade further the innate factors that maintain the viraemia at the set-point level in Rag1$^{-/-}$ mice. One might speculate that TNF (Zaid et al., 2011) (rather than IFN-γ (Fros et al., 2010)) plays a dominant role in viraemia suppression in these mice (Figure 4.11), and that the evolution of entirely new protein domains that can counter the anti-viral effects of TNF is unrealistic in the limited time frame.

Despite the low fidelity of RNA replication (Coffey et al., 2011), sequencing of virus isolated day 100 from Rag-1$^{-/-}$ mice (and expanded in C6/36 cells) showed only a limited number of mutations (see Appendix VI), perhaps suggesting constraints on error accumulation (Crotty et al, 2001). (Alternatively, other viral species did arise in Rag-1$^{-/-}$ mice, but expanded poorly in C6/36 cells).

4.3 Discussion

This chapter investigated the role of B cells, T cells, NK cells and IFN-γ in controlling CHIKV viraemia and mediating arthritis using a mouse model of CHIKV disease. WT mice and mice deficient in B cells (μMT mice), B and T cells (Rag-$1^{-/-}$ mice), B, T and NK cells (Rag2/Il2$rg^{-/-}$ mice), CD4+ T cells (MHC-$II^{\Delta/\Delta}$ mice) and IFN-γ (IFN-$\gamma^{-/-}$ mice) were infected with CHIKV. The viraemia and arthritis seen in these CHIKV infected mouse strains are summarised in Table 4.1, along with the implications of the results.

Table 4.1: Viraemia and arthritis in WT and knock-out mice infected with CHIKV.

The conclusions were derived by comparing the viraemia and arthritis of knock-out mice with WT mice.

Mice	Deficiency	Viraemia	Arthritis	Conclusions
WT	None	Resolved day 5 p.i.	Peak at day 6	-
μMT	B cells	Persistent (Figure 4.1)	• Similar to WT mice (Figure 4.4B)	• B cells are critical for viraemia clearance
Rag-$1^{-/-}$	B and T cells	Persistent and higher than μMT mice (Figure 4.1)	• Higher than WT mice on day 3-5 (Figure 4.4C) • With oedema (Figure 4.5C,D)	• B cells are critical for viraemia clearance • T cells are associated with CHIKV arthritis and played a minor role viraemia control
Rag2/Il2$rg^{-/-}$	B, T and NK cells	Persistent and higher than μMT mice; similar to Rag-$1^{-/-}$ mice (Figure 4.1)	• Lower than WT (& μMT) mice^ • Similar to Rag-$1^{-/-}$ mice^ • No oedema^	• B cells are critical for viraemia clearance • NK cells are less critical in controlling CHIKV viraemia • NK cells do not mediate CHIKV arthritis
MHC-$II^{\Delta/\Delta}$	CD4+ T cells	Resolved day 5 p.i. (Figure 4.6A)	Lower than WT (Figure 4.5E,F & Figure 4.6B)	• CD4+ T cells promote CHIKV arthritis
IFN-$\gamma^{-/-}$	IFN-γ	Resolved day 5 p.i. (Figure 4.9B)	Lower than WT (Figure 4.9A)	• IFN-γ promotes CHIKV arthritis

*p.i. = post infection; ^ = data not shown (by others from Suhrbier Group).

4.3.1 Role of T cells in viraemia control

CHIKV infection triggers a strong T cell response in humans and mice (Hoarau et al., 2010, Wauquier et al., 2011, Gardner et al., 2010), suggesting the involvement of T cells in the immune control of CHIKV. The data presented in this chapter demonstrated that T cells play a role (although secondary to antibodies) in the control of CHIKV viraemia. The evidences presented herein are (i) Rag-$1^{-/-}$ mice had a higher set point viraemia compared to μMT mice (Figure 4.1), and Rag-$1^{-/-}$ mice also had a viraemia relapse 20 days earlier than μMT mice after both strains of mice were treated with an equal amount of adoptively transferred anti-CHIKV antibody (Figure 4.3). (ii) Vaccination of μMT mice induced a T cell response (Figure 4.2A) that was sufficient to reduce viraemia on day 3 and 4 post infection (Figure 4.2B, *). As unadjuvanted, killed, whole-virus vaccines are generally poor at inducing CD8+ T cells (Foged et al., 2012) and CD4+ T cell recall responses usually peak at around day 4 (Wuthrich et al., 2005), this observation provides further evidence for an antibody-independent role of CD4+ T cells in CHIKV viraemia suppression. (iii) CHIKV infected MHC-$II^{\Delta/\Delta}$ displayed a delay in viraemia control when compared to WT mice (Figure 4.6A). Taken together, the evidence presented in this chapter indicates that T cells play a minor but significant role in controlling CHIKV viraemia.

4.3.2 Role of T cells in arthritis

Previous reports indicated that T cells are not implicated in RRV-induced (another alphavirus) arthritis (Morrison et al., 2007, Morrison et al., 2006). However, investigation of CHIKV associated arthritis in this chapter clearly implicates T cells, specifically CD4+ T cells, in the development of CHIKV-induced arthritis. A lower density of infiltrating cells was observed in Rag-$1^{-/-}$ and MHC-$II^{\Delta/\Delta}$ mice following infection (Figure 4.5C, D and E), and there was an early exacerbation of foot swelling observed in vaccinated μMT mice following infection (Figure 4.7, *). The microarray analyses conducted by Nakaya et al. (2012) also showed evidence for strong T cell signals during peak CHIKV arthritis. Similarly, the pathogenic role of T cells demonstrated herein are also consistent with the findings of another study that used $CD4^{-/-}$ mice to demonstrate an arthritic role of CD4+ T cells in CHIKV disease (Teo et al., 2012b).

4.3.3 Role of B cells in viraemia control

B cells are well known in clearing the viraemia of alphaviruses including CHIKV and SINV (Lum et al., 2013, Teo et al., 2012b, Burdeinick-Kerr et al., 2007, Hawman et al., 2013, Brooke et al., 2010). The results presented in this chapter also suggest that clearance of CHIKV viraemia was critically dependent on B cells, as mice deficient in B cells failed to clear CHIKV viraemia (Figure 4.1). Altogether, the findings by others and data presented herein clearly support the view that B cells are essential for viraemia clearance.

The clearance of viraemia in MHC-II$^{\Delta/\Delta}$ mice (Figure 4.6A) was likely due to the generation of anti-CHIKV IgG2c antibody responses (Figure 4.8B). This finding is in agreement with a study of CHIKV infection in CD4$^{-/-}$ mice that also produced anti-CHIKV antibody that effectively cleared the virus (Lum et al., 2013). CD4+ T cells are well known to facilitate the B cell isotype switching that results in IgG2c production (Mitchison, 2004). However, CD4+ T cell-independent production of IgG2c has been reported (Lee et al., 2005, Swanson et al., 2010), where class switching is induced by IFN-α/β (Swanson et al., 2010). CHIKV infection triggers a high level of IFN-α/β in humans and mice (Rudd et al., 2012, Hoarau et al., 2010), suggesting that IFN-α/β might have contributed to the CD4+ T cell independent production of IgG2c observed in MHC-II$^{\Delta/\Delta}$ mice following CHIKV infection.

4.3.4 Viraemia levels are not correlated to arthritis severity

Data in this chapter indicate that a higher level of viraemia does not necessarily result in a more severe level of arthritis. The higher viraemia observed in Rag-1$^{-/-}$ and Rag2/Il2rg$^{-/-}$ mice did not lead to a more severe arthritis (compare Figure 4.1 and Figure 4.4C for Rag-1$^{-/-}$ mice; data not shown for Rag2/Il2rg$^{-/-}$ mice). Similarly, the more severe arthritis seen in vaccinated μMT mice (Figure 4.7; *) was not associated with a higher viraemia in the same period (Figure 4.2B). Additionally, μMT, Rag-1$^{-/-}$ and Rag2/Il2rg$^{-/-}$ mice did not exhibit any ongoing arthritic disease (data not shown), despite the presence of persistent viraemia. Therefore, viraemia is required but not sufficient for inducing arthritic disease in CHIKV infected mice.

4.3.5 Role of IFN-γ in viraemia control and arthritis

Given that IFN-γ may protect against CHIKV infection (Figure 4.11, IFN-γ), one might expect that IFN-$\gamma^{-/-}$ mice would experience a more severe infection (i.e. higher viraemia); however, IFN-$\gamma^{-/-}$ mice did not show any significant increase in viraemia when compared with WT mice (Figure 4.9B). It is possible that the contribution of IFN-γ may be minimal during acute infections when IFN-α/β levels are also high (Rudd et al., 2012). Furthermore, CHIKV infected IFN-$\gamma^{-/-}$ mice have been previously shown to be capable of producing anti-CHIKV antibodies, which would also contribute to the control of viraemia in these mice (Lum et al., 2013).

IFN-γ producing CD4+ T cells are implicated in RA (Snir et al., 2011, Yamada et al., 2011); IFN-γ levels are elevated in synovial fluid of RRV-infected patients (Lidbury et al., 2008), and serum IFN-γ is up-regulated in CHIKV infected patients (Wauquier et al., 2011, Hoarau et al., 2010), monkeys (Labadie et al., 2010) and mice (Gardner et al., 2010). The data presented herein shows that IFN-γ is implicated in CHIKV arthritis, with IFN-$\gamma^{-/-}$ mice displaying a lower foot swelling compared to WT mice (Figure 4.9A). This observation contradicts the finding of another study that suggested that IFN-γ had no role in CHIKV arthritis (Teo et al., 2012b). This discrepancy might be attributable to the different isolates of CHIKV used (LR2006-OPY1 used in this study vs SGP11), as different isolates of CHIKV have previously been shown to induce a differing severity of arthritis (Gardner et al., 2010).

4.3.6 TNF and IFN-γ (not IFN-α) were associated with persistently viraemic Rag-$1^{-/-}$ mice

On-going up regulation of IFN-γ and TNF in Rag-$1^{-/-}$ mice suggested that these cytokines might be associated with the control of persistent CHIKV viraemia (Figure 4.11). These data are consistent with the anti-alphaviral role of IFN-γ and TNF (Zaid et al., 2011, Ryman et al., 2007) and the dysregulation of IFN-γ and TNF in macrophages persistently infected with RRV *in vitro* (Way et al., 2002). IFN-γ also up-regulates protein kinase R (PKR), which is known to inhibit viral protein synthesis (Schroder et al., 2004). PKR also facilitates the maturation of functional TNF (Schroder et al., 2004).

4.3.7 Conclusion

In summary, this study described a likely role for CD4+ T cells in mediating the onset of CHIKV arthritis (possibly via the production of IFN-γ) and a critical role for B cells in clearing CHIKV viraemia (via antibody production). While adoptively transferred antibodies were seen to clear viraemia in B cell deficient mice, viral clearance occurred for only a brief period (Figure 4.3). This observation suggests that CHIKV might persist in the tissues until the transferred antibodies have lost their bioactivity, resulting in relapses. The persistence of CHIKV in the tissues of CHIKV infected mice is the subject of the next chapter.

Chapter 5: Long-term persistence of CHIKV RNA in WT mice is associated with signs of chronic inflammation

5.1 Introduction

While acute symptoms of CHIKV disease (characterised by polyarthritis/polyarthralgia, fever, rash and/or myalgia) generally resolve within 1-2 weeks, chronic arthritic disease can persist for months and sometimes over a year (Suhrbier et al., 2012). Recent studies indicate that a high percentage of CHIKV infected patients (ranging from 4.7-75.4%), especially the elderly (Chaaitanya et al., 2011, Sissoko et al., 2009, Gerardin et al., 2013), experience long-term (3-36 months) unresolved arthritic symptoms (see Table 1.2). These symptoms include arthralgia, myalgia, joint stiffness and rheumatic musculoskeletal pain (see Table 1.2). Consistent with the chronic symptoms, these patients were found to have elevated levels of (i) anti-CHIKV IgG antibodies (Kelvin et al., 2011, Gerardin et al., 2013) and (ii) proinflammatory cytokines IL-6 and IL-12 in serum (Chow et al., 2011, Chopra et al., 2012).

Given that most alphaviral viraemias usually last no longer than 7-10 days, how alphaviral infections lead to these chronic symptoms is unclear. Viral persistence in tissues has long been thought to contribute to symptoms, since viral antigen and/or viral RNA of RRV and CHIKV have been detected in the joints of affected patients (Soden et al., 2000, Hoarau et al., 2010). Hoarau et al. (2010) showed that CHIKV RNA and antigen could be detected in the synovial macrophages of a patient that experienced chronic rheumatic manifestations at the 18-months post onset of disease. This was consistent with a CHIKV study in primates showing the persistence of CHIKV RNA in splenic macrophages up to 97-days post infection (Labadie et al., 2010). The mechanisms of CHIKV persistence were not investigated in these studies; however, it has been proposed that CHIKV-induced apoptosis and phagocytosis could facilitate CHIKV persistence in macrophages (Krejbich-Trotot et al., 2011, Joubert et al., 2012, Suhrbier and La Linn, 2004). In addition, CHIKV could be transmitted to neighbouring cell via tight junction, where this mode of transmission could also facilitate CHIKV persistence (Lee et al., 2011). To gain more insights into long-term persistence of CHIKV RNA and its role in driving chronic arthritic disease, the mouse model of CHIKV infection and disease was investigated. The data obtained from this model clearly showed that both CHIKV RNA, including negative-strand RNA, can persist in the feet up to day 100 post infection, despite the presence of neutralising antibody. Interferon stimulated gene 54 (ISG-54), a factor that is up-regulated in response to viral infection and double stranded RNA

(dsRNA), was found to be persistently up-regulated in these feet, suggesting ongoing viral RNA replication. Microarray analysis of persistently infected feet (day 30 post infection) and subsequent Ingenuity'S Upstream Regulator Analysis revealed a profile very similar to that seen in a chronically infected human (Hoarau et al., 2010). This data also clearly revealed the presence of an ongoing local inflammatory response that is dominated by type I IFN responses, as well as by responses associated with apoptosis, autophagy, M2 macrophages, cytokines (IL-6, IL-12 and IFN-γ) and T cells.

5.2 Results

5.2.1 Isolation of infectious CHIKV from feet

Chronic CHIKV arthritis might be triggered by the persistence of CHIKV in the affected tissues. To examine viral persistence in the feet, WT mice were infected with CHIKV. Feet were excised and subjected to three different methods to attempt recovery of infectious virus (Table 5.1, see section 2.6 for detailed procedures). Using either the mortar-pestle or homogeniser method, infectious CHIKV could be isolated from the feet of infected mice up to day 9 post infection, but not day 14 post infection (Table 5.1). Using the collagenase digestion method, infectious CHIKV was successfully isolated from the feet up to day 14 post infection, but not day 21 post infection (Table 5.1). Infectious CHIKV can thus be recovered from feet of mice infected with CHIKV for at least 14 days post infection, even when viraemia was cleared at 4-5 days post infection (Figure 4.1, WT).

Table 5.1: Isolation of infectious CHIKV from the infected feet using 3 different methods.

*For detailed method, see section 2.6. n.t. = not tested

Methods*	Virus detection (no. positive / no. tests)			
	Day 1-6	Day 9	Day 14	Day 21
1. Mortar and pestle	6/6	3/3	0/2	0/2
2. Homogeniser	n.t.	3/3	0/2	n.t.
3. Collagenase digestion	n.t.	3/3	2/2	0/2

5.2.2 Quantification of CHIKV RNA levels in the feet of CHIKV-infected mice

Infectious CHIKV was found to persist in the feet up to 14 days post infection, indicating that CHIKV continues to replicate in the feet well after the viraemia has been cleared (typically day 4-5). To further examine whether CHIKV RNA can persist and replicate in the feet of infected mice beyond the viraemic period, CHIKV RNA levels were analysed by qRT-PCR. Total RNA from infected feet was extracted, and CHIKV RNA levels were quantified by qRT-PCR using primers targeting the E1 structural protein of CHIKV. Negative strand-specific qRT-PCR was used to quantify nsP1 portion of negative strand CHIKV RNA using a modification of the tagged-primer system described previously (Plaskon et al., 2009). Briefly, the process used tagged-primer to generate cDNA incorporated with tag, a unique 20 nucleotides sequence that improve accuracy and specificity of subsequent quantification by qRT-PCR (Plaskon et al., 2009). Another tagged-primer was then used in qRT-PCR to ensure that only tag-incorporated cDNA was amplified and quantified. During alphavirus infections, negative strand RNA is synthesised from positive strand RNA and provides a template for positive strand RNA synthesis, with negative strand RNA comprising 2-5% of total RNA (Wang et al., 1991, Sawicki and Sawicki, 1980). The presence of negative strand CHIKV RNA is thus indicative of active CHIKV RNA replication. Significant levels of both total RNA (Figure 5.1A) and negative stranded RNA (Figure 5.1B) were detected up to 100 days post infection, suggesting ongoing RNA replication. This observation is consistent with earlier reports showing that RRV can persistently infect macrophages *in vitro* for at least 148 days post infection (Way et al., 2002, Linn et al., 1996). The qRT-PCR shown in Figure 5.1A yielded a PCR product, shown by gel electrophoresis (Figure 5.2), that matches the predicted size of 168 base pair. Together, these data suggest that actively replicating CHIKV can persist in the infected foot tissues long after the viraemic period.

Figure 5.1: Quantification of CHIKV RNA in CHIKV infected feet and spleens.

Mice were infected with CHIKV. At the indicated time points, total RNA was extracted from infected spleens and/or feet. **(A)** Total RNA was reverse transcribed into cDNA then qRT-PCR was used to quantify total CHIKV RNA using primers specific for the E1 structural protein of CHIKV. Data was normalised using mRNA levels of housekeeping gene, RPL13A. Y axis values are relative only. *$p < 0.05$ (compared to uninfected mice) by Mann-Whitney U test. **(B)** Negative strand-specific cDNA was generated then qRT-PCR was used to quantify negative strand RNA using primers specific for nsP1 portion of negative strand CHIKV RNA. Method for B is distinct from the method for A. ($n = 3$-7 feet from different mice per time point, mean ± SE is presented; data are derived from 2 independent experiments). **$p < 0.01$ and *$p < 0.05$ (compared to uninfected mice) by Mann-Whitney U test.

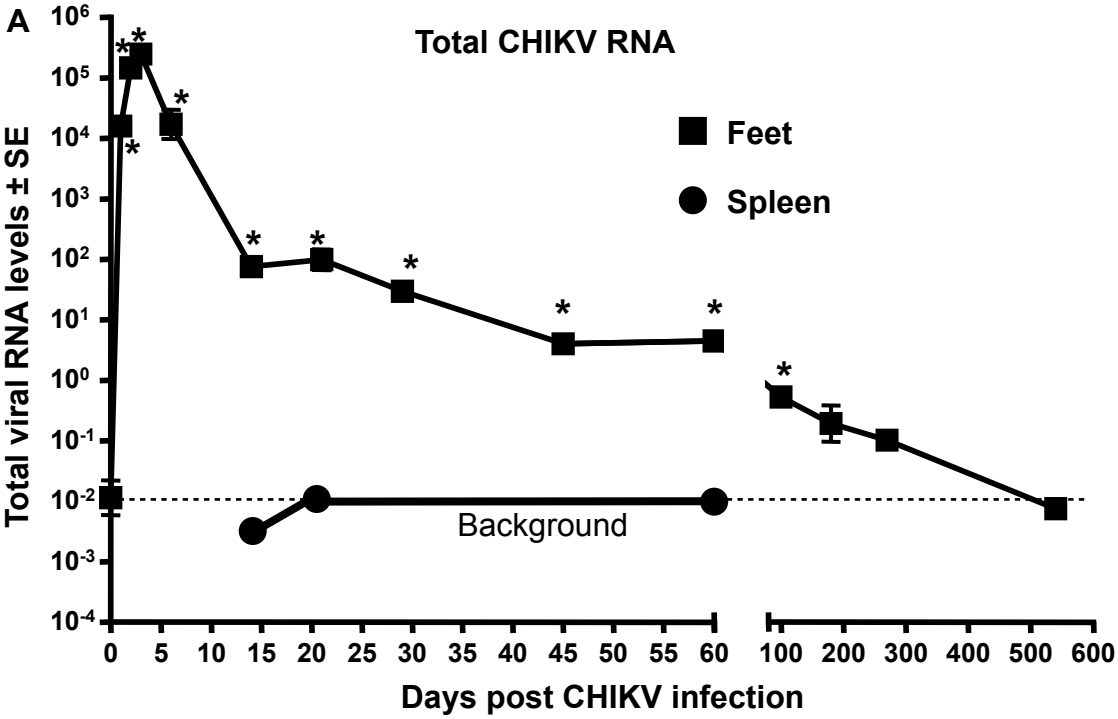
A
Total CHIKV RNA
Feet
Spleen
Total viral RNA levels ± SE
Background
Days post CHIKV infection

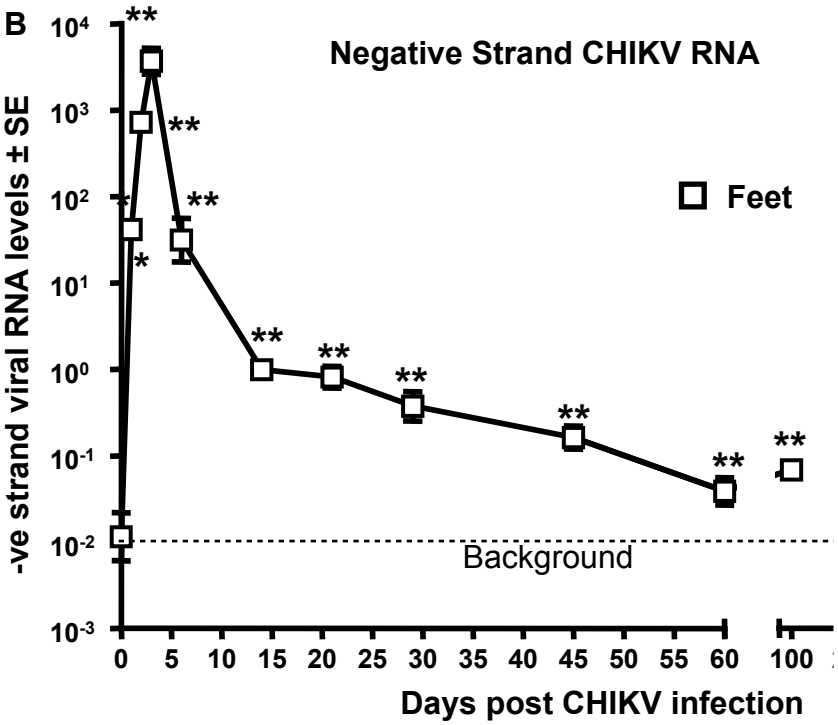
B
Negative Strand CHIKV RNA
Feet
-ve strand viral RNA levels ± SE
Background
Days post CHIKV infection

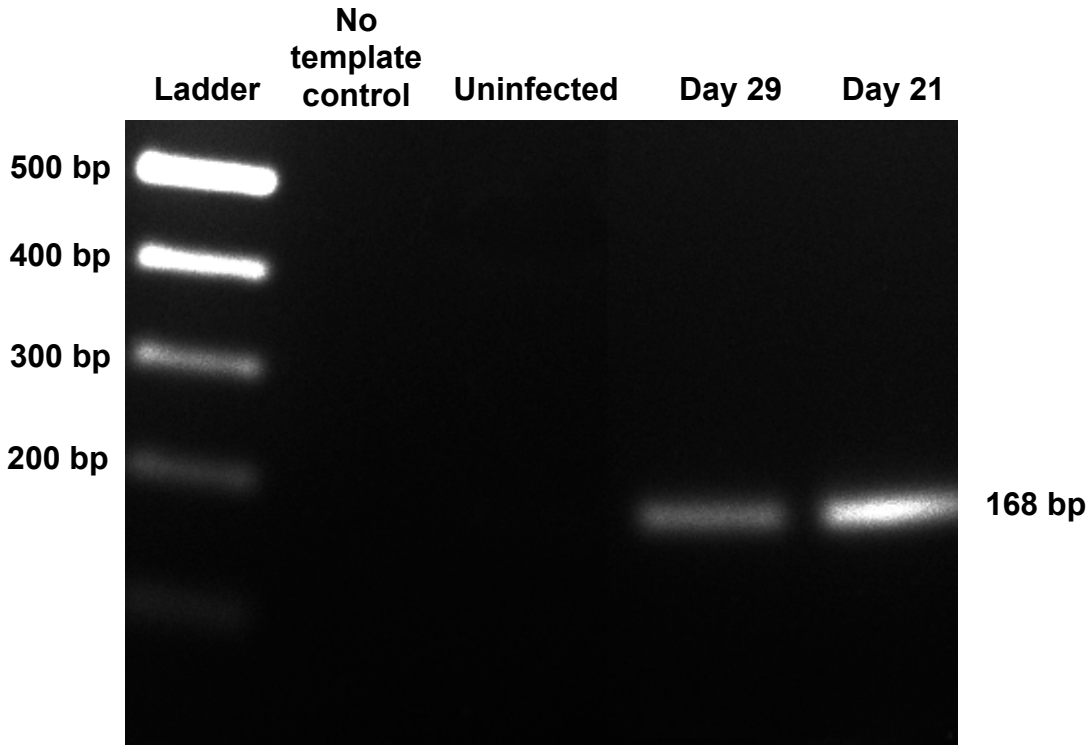

Figure 5.2: Gel electrophoresis image of the RNA E1 qRT-PCR product.

Total RNA was extracted from infected feet, reverse transcribed into cDNA then analysed by qRT-PCR using primers targeting the E1 structural protein of CHIKV E1 protein. The qRT-PCR products were run on a 2% agarose gel and visualised by ethidium bromide staining. The no template control (no cDNA) and cDNA from uninfected feet did not produce any bands, indicating an absence of CHIKV RNA. Samples from infected feet on day 29 and 21 post infection produced bands that matched the predicted size (168 base pair in length), suggesting the signals detected by qRT-PCR are CHIKV specific.

5.2.3 Curve fit of the decline in CHIKV RNA levels in feet

To gain insights into the decline of CHIKV RNA levels, a curve fit of the reduction of CHIKV RNA levels over time was sought (Figure 5.3A) based on data shown in Figure 5.1A and B. The curve fits of both total and negative strand CHIKV RNA after the end of the viraemic period emerged to represent simple exponential decays approximating to y=e-0.06/0.07x (Figure 5.3A), suggesting that both total and negative strand CHIKV RNA levels decline at a similar rate (see below, *). The rate of decline in RNA levels suggest a decay with a constant half-life of 10-11 days.

$$* \; y=e^{-0.065x}$$

- "*y*" is CHIKV RNA level
- "*x*" is the days of post infection

5.2.4 Relative ratio of the levels of total CHIKV RNA to negative strand CHIKV RNA

To gain further insights into the decline of CHIKV RNA levels, relative ratios of total RNA to negative strand CHIKV RNA were calculated (Figure 5.3B). The ratios were higher during the initial viraemic period (days 1-2), with ratios settling to a relative constant level thereafter (Figure 5.3B). The decline of this ratio may reflect a reduction of sub-genomic RNA levels (see Figure 1.3E2) following the initial viraemic period, with sub-genomic RNAs are known to be the dominant RNA species during alphavirus replication (Perri et al., 2000).

Figure 5.3: Curve fit of reduction in RNA levels over time and ratio of total CHIKV RNA to negative strand CHIKV RNA.

Viral RNA data shown in Figure 5.1A and B at different times post-infection were used for preparation of **(A)** the curve fit of reduction in total and negative RNA levels over time starting after the end of the viraemic period **(B)** the ratio of total CHIKV RNA to negative strand CHIKV RNA at different times post-infection. SE was derived from the variance in the values obtained for total CHIKV RNA. The Y-axis represents relative units only and does not represent a specific quantity of viral RNA, as methods for quantitation of total CHIKV RNA and –RNA are distinct. (n = 3-7 feet from different mice per time point, mean ± SE is presented; data are derived from 2 independent experiments)

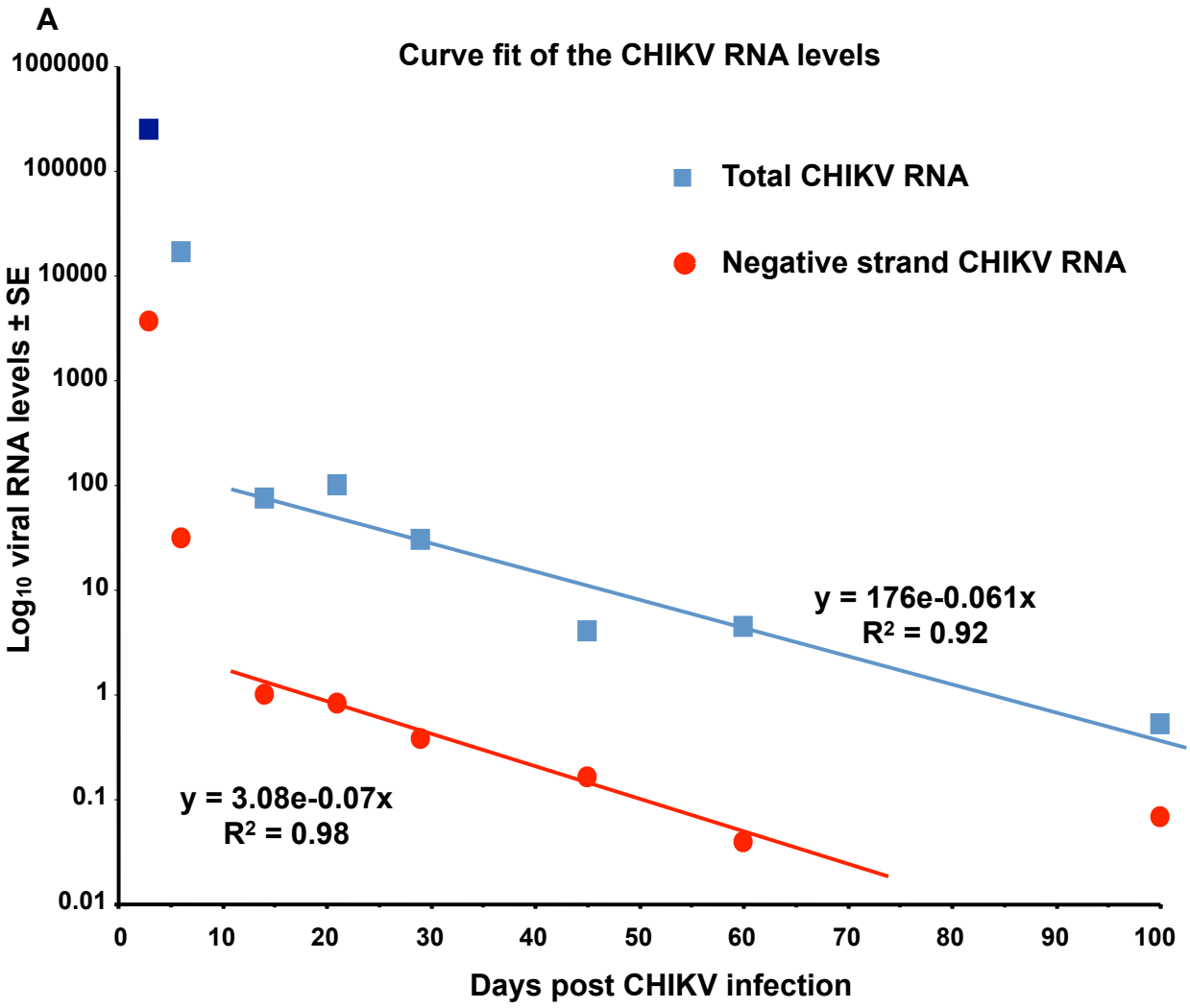
A
Curve fit of the CHIKV RNA levels
Total CHIKV RNA
Negative strand CHIKV RNA
y = 176e-0.061x
R² = 0.92
y = 3.08e-0.07x
R² = 0.98
Log10 viral RNA levels ± SE
1000000
100000
10000
1000
100
10
1
0.1
0.01
0
10
20
30
40
50
60
70
80
90
100
Days post CHIKV infection

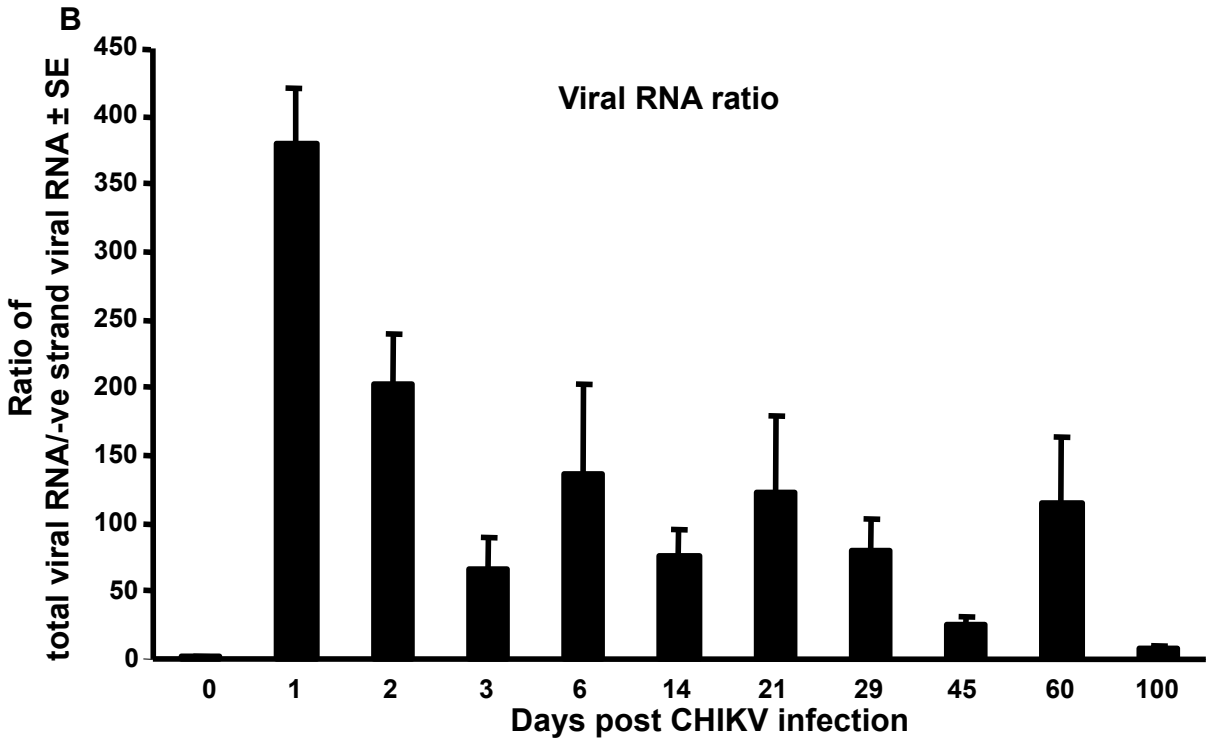
B
Viral RNA ratio
Ratio of
total viral RNA/-ve strand viral RNA ± SE
450
400
350
300
250
200
150
100
50
0
0
1
2
3
6
14
21
29
45
60
100
Days post CHIKV infection

5.2.5 Quantification of CHIKV RNA levels in the spleen of CHIKV-infected mice

Previous study shows that CHIKV RNAs persist in the spleens of macaques up to day 97 post infection (Labadie et al., 2010). To determine if CHIKV RNAs also persist in the spleens of mice, total CHIKV RNA levels in the spleens were analysed by qRT-PCR as in section 5.2.2. In contrast with the findings in macaques (Labadie et al., 2010, Messaoudi et al., 2013), qRT-PCR analysis of total RNA levels in the spleen showed that levels of persistent viral total RNA dropped to levels below detection by day 14 (Figure 5.1A). This observation indicates that the site of CHIKV persistence is different between macaques and mice.

5.2.6 Neutralising antibody response post CHIKV infection

Data in chapter 4 showed that antibodies are critical for the clearance of CHIKV viraemia. However, data in this chapter indicate that infected feet contain actively replicating CHIKV up to day 100 post infection. This persistence of CHIKV prompted us to examine the time course of antibody levels in infected mice. Mice were infected with CHIKV and serum neutralising antibody titres were measured over time. A neutralising antibody response could be detected as early as day 4 post infection (Figure 5.4). The neutralising antibody titre peaked around day 20-30 post infection, and then dropped but remained evident until at least day 150 post infection (Figure 5.4). These data suggest that CHIKV persists, despite rapid up-regulation, attainment of high levels and long-term maintenance of neutralising antibody responses.

5.2.7 Quantification of ISG-54 expression in CHIKV infected feet

CHIKV infection induces robust IFN-α/β responses, with a number of IFN-α/β-stimulated genes induced (Nakaya et al., 2012) including ISG-54 (Thon-Hon et al., 2012). To determine whether the observed persistent viral RNA in the feet was associated with ongoing stimulation of interferon responses, qRT-PCR was used to determine ISG-54 mRNA levels over time post infection with CHIKV. Significant levels of ISG-54 mRNA were detected in feet for up to 100 days post infection of mice (Figure 5.5), indicating ongoing stimulation of interferon responses. These data further support the view that persistent CHIKV RNA is replicating thereby stimulating anti-viral and inflammatory responses (Ohl and Tenbrock, 2011).

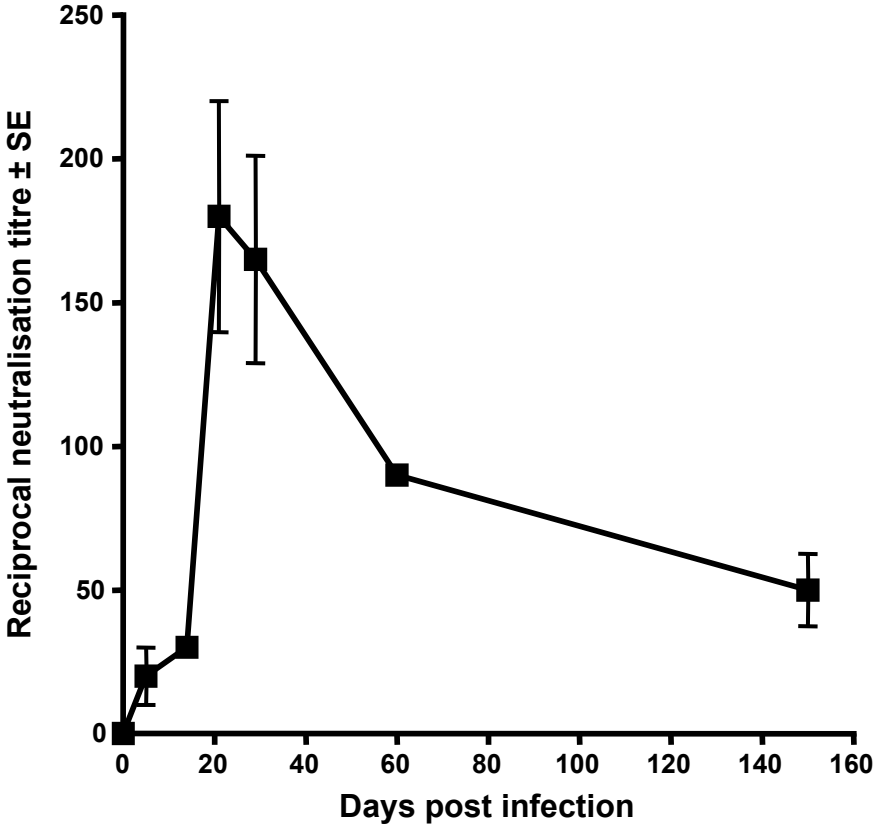

Figure 5.4: Neutralising antibody titres in CHIKV infected mice over time.

Mice were infected with CHIKV and at the indicated time points sera were collected and tested for neutralising antibody titres (n = 3-6 per time point, mean ± SE is shown; data are derived from 2 independent experiments).

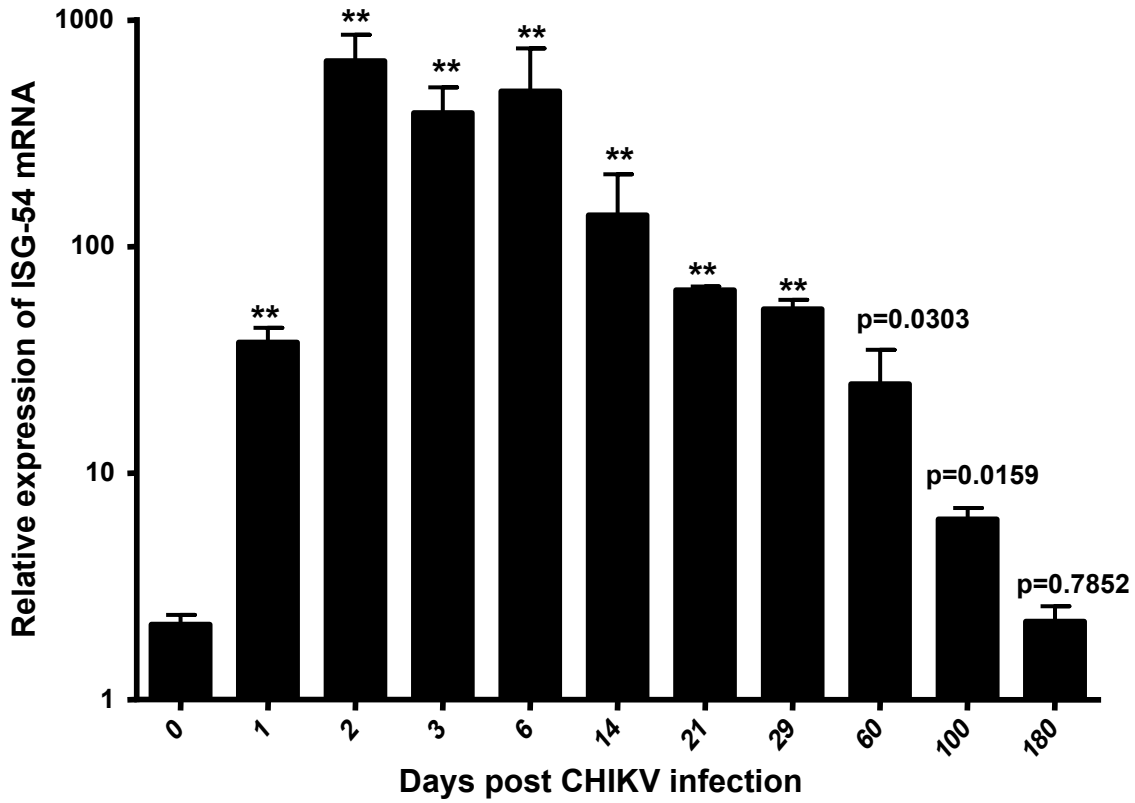

Figure 5.5: ISG-54 mRNA levels in feet of CHIKV-infected mice over time.

Mice were infected with CHIKV, and at the indicated time points, total RNA was extracted from infected feet, reverse transcribed into cDNA then quantified for ISG-54 RNA by qRT-PCR using primers specific to murine ISG-54. ISG-54 mRNA levels were normalised to RPL13A mRNA levels (n = 3-7 mice per time point, mean ± SE is presented; data are derived from 2-3 independent experiments). ** = $p < 0.01$ (compared to uninfected mice). All statistics by Mann-Whitney U test.

5.2.8 Comparison of global gene expression between CHIKV-infected feet on day 0 and day 30 post infection

Using microarray analysis, a previous study revealed that pathways related to T cell, autoimmunity, antigen presentation, NK cell, innate sensing, monocytes/macrophage, apoptosis, B cell, cytokines/chemokines and complement were up-regulated in the feet of CHIKV infected mice during peak arthritis (day 6-7 post infection) (Nakaya et al., 2012). The same study also revealed that CHIKV arthritis shares many inflammatory pathways with RA (Nakaya et al., 2012). Given that CHIKV RNA (Figure 5.1) and signs of inflammation (Figure 5.5) persisted for extended periods post infection, a similar microarray analysis was undertaken to analyse global gene expression changes in persistently infected feet on day 30 post infection. With bioinformatics assistance of Dr Helder Nakaya, microarray analysis was conducted as described (Nakaya et al, 2012) by Ramaciotti Centre (Sydney, Australia) comparing feet from day 0 and day 30. Probe sets with no annotations were removed, only expressed genes with a mean $\log_2$ expression ≥ 6 across all samples were included, and t-tests were performed between day 0 and day 30 samples for 4,805 filtered genes. Genes where $p < 0.05$ were included. No false discovery rate corrections were undertaken. Fold changes ranged from 1.05-1.55. A total of 547 DEGs were identified, of these 192 genes were up-regulated, and 355 genes were down-regulated on day 30 following CHIKV infection.

5.2.8.1 Ingenuity's Canonical Pathway Analysis of up-regulated genes

To gain a better understanding of the pathways stimulated by the persistence of CHIKV RNA in feet, the up-regulated genes were analysed using IPA. Canonical pathways analysis of the 192 up-regulated genes induced on day 30 post infection, revealed activation of pathways associated with T cells, autoimmunity, antigen presentation, NK cells, innate sensing, monocytes/macrophages, apoptosis and cytokines (Figure 5.6). These up-regulated pathways were broadly similar to the pathways described for day 7 post infection (Nakaya et al., 2012), suggesting that many of the inflammatory pathways are retained on day 30 post infection. However, there were some apparent differences. B cell and complement-associated pathways were present on day 7, but were not identified on day 30. However, it should be noted that the low fold change (1.05-1.55) and the low number of up-regulated genes (192) limit the conclusions that can be reached by such comparisons.

The continued activation of IFN-α/β signalling pathways on day 30 post infection (Figure 5.6, innate sensing and cytokines) is consistent with the view that persistent replicating CHIKV dsRNA continues to stimulate IFN-α/β responses (section 5.2.7). The up-regulation of genes in monocyte/macrophage pathways is consistent with the view that macrophages remain involved in chronic disease (Suhrbier et al., 2012), consistent with the observation that macrophages are the main cellular reservoirs of persistent RRV and CHIKV RNA (Soden et al., 2000, Labadie et al., 2010). The up-regulation of T cell pathways suggests ongoing involvement of T cells in chronic CHIKV arthritis, with their key role in acute arthritis described in Chapter 4 (Figure 4.6B). Taken together, the pathways shown to be activated on day 30 post infection suggest that persistence of CHIKV may contribute to an ongoing CHIKV-induced arthritic disease.

5.2.8.2 Ingenuity's Canonical Pathway Analysis of down-regulated genes

To gain a better understanding of the pathways inhibited by the persistence of CHIKV RNA in feet, the down-regulated genes were analysed using IPA. Canonical pathways analysis of the 355 down-regulated genes induced on day 30 post infection, revealed inhibition of signalling pathways associated with mammalian target of rapamycin, regulation of eukaryotic initiation factor 4, p70S6 kinase, eukaryotic initiation factor 2 and aryl hydrocarbon receptor with molecules largely associated with protein translation (only pathways with $p < 0.05$ and at least 3 molecules assigned were selected) (pathway details are shown in Appendix IV). Alphavirus infections are well known for inducing shutdown of host cell translation processes (Jose et al., 2009). Therefore, inhibition of protein translation-associated pathways would suggest ongoing CHIKV infections.

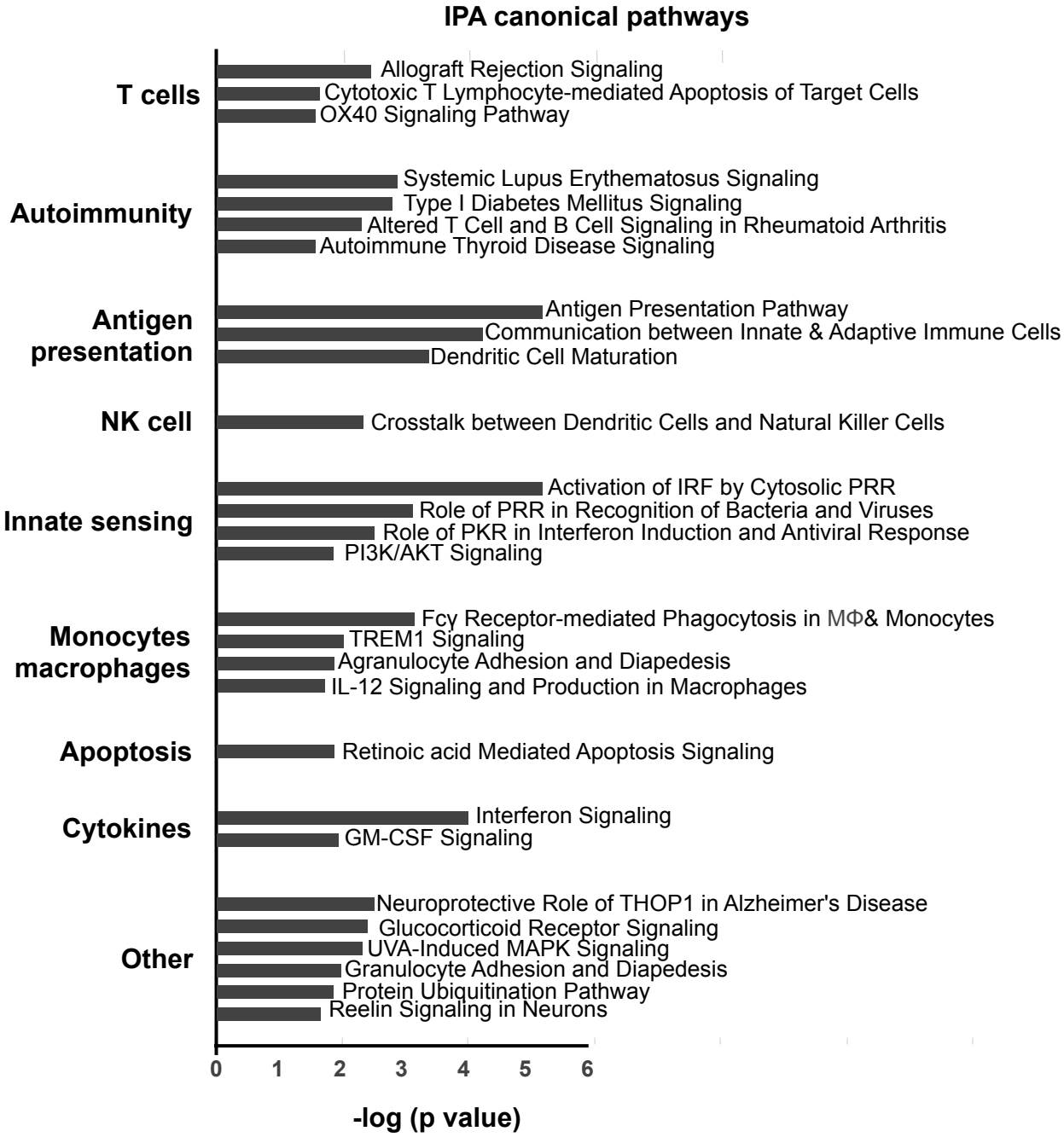

Figure 5.6: IPA of canonical pathways active in CHIKV-infected feet on day 30 post infection.

Ingenuity's Canonical Pathway Analysis of the 192 genes differentially expressed in feet of mice at day 30 post infection, with pathways grouped into themes. A higher -log (p value) denotes a more significant overlap between the analysed DEGs and genes in the IPA knowledge database. -log (<1.3) represents $p < 0.05$. Pathways shown here have a -log (>1.5) and have at least three molecules assigned to the pathway. Pathway details are shown in Appendix III.

Data for Figure 5.6 was prepared with assistance from Helder Nakaya.

5.2.8.3 Ingenuity's Upstream Regulator Analysis of up-regulated genes

The same 192 up regulated genes analysed above were analysed using Ingenuity's Upstream Regulator Analysis (Figure 5.7). This analysis identified multiple upstream regulators involved in type I IFN responses, with other upstream regulators associated with apoptosis, autophagy, M2 macrophages, cytokines and T cells also identified (Figure 5.7). Identification of type I IFN pathways as dominant upstream regulators is consistent with the increase of interferon signalling pathways identified by canonical pathway analysis (Figure 5.6; innate sensing) and the up-regulation of ISG-54 mRNA in the feet on day 30 post infection (Figure 5.5). Importantly, IFN-α was also detected in the synovial tissues of a patient with chronic CHIKV arthritis (Hoarau et al., 2010).

The upstream regulator analysis also identified DDX58 (also known as retinoic acid-inducible gene 1 (RIG-I)) (Figure 5.7, see *), an observation consistent with a previous study suggesting DDX58 might be a cytoplasmic sensor for CHIKV RNA that triggers IFN-α/β production (Schilte et al., 2010) via interferon promoter stimulator-1 (IPS-1) (Rudd et al., 2012). Tripartite motif-containing 24 (TRIM24) and microRNA 21 (mir-21) were identified as upstream regulators but were assigned negative activation Z-scores. These two molecules have a negative regulatory role in type I IFN responses (Chen et al., 2013, Tisserand et al., 2011), and their predicted negative activations are again consistent with the observed up-regulation of IFN-α/β responses.

The upstream regulator analysis also identified Activation of Poly(ADP-ribose) polymerase-1 (PARP-1) (Figure 5.7, apoptosis), an enzyme that is associated with apoptosis. This observation is consistent with previous reports demonstrating that alphavirus infection, including CHIKV infection, is associated with induction of PARP-1 (Nargi-Aizenman et al., 2002, Krejbich-Trotot et al., 2011). Importantly, PARP-1 was also detected in the synovial tissues of a patient with chronic CHIKV arthritis (Hoarau et al., 2010).

The analysis assigned immunity-related GTPase M (IRGM) with a negative activation Z score (Figure 5.7, autophagy). IRGM is a protein that interferes with autophagy during infection with RNA viruses, including viruses from the *togaviradae* family (Gregoire et al., 2011). Autophagy plays a protective role in CHIKV infection, with inhibition of autophagy genes enhancing CHIKV replication *in vitro* (Joubert et al., 2012). Thus, negative activation of IRGM would suggest an increase in autophagy and suppression of CHIKV replication.

Signal transducer and activator of transcription 3 (STAT3) is another factor that was identified as an upstream regulator (Figure 5.7, M2 macrophages). STAT3 is a critical transcription factor for M2 macrophage differentiation (Tang et al., 2013, Wang et al., 2012b). Recently, M2 macrophage differentiation was shown to be associated with CHIKV persistence (Stoermer et al., 2012). The identification of STAT3 would suggest activation of M2 macrophages and suggests the persistence of CHIKV RNA (shown in Figure 5.1) promotes M2 differentiation.

The identification of IL-6 as an upstream regulator suggests an ongoing arthritic pathology (Figure 5.7, other cytokines), as previous reports have shown that serum IL-6 was up-regulated in patients with chronic arthritic symptoms (Chow et al., 2011, Chopra et al., 2012), with elevated IL-6 also expressed in the synovial tissues of a patient with chronic CHIKV arthritis (Hoarau et al., 2010). Moreover, IL-6 is a key cytokine implicated in RA (Shoda and Yamamoto, 2007) and several other viral arthritides (Suhrbier and Mahalingam, 2009).

Similarly, IL-12 that was identified here (Figure 5.7, other cytokines) also found to be elevated in the sera of patients experiencing chronic CHIKV arthritis (Hoarau et al., 2010). IL-12 is a key driver of Th1 response. Therefore, the up-regulation of IL-12 is consistent with the up-regulation of IFN-γ, a key Th1 cytokine (Figure 5.7, other cytokines). Up-regulation of IFN-γ is also consistent with previous clinical studies showing that IFN-γ was detected in the sera and synovial tissue of patients that experienced chronic CHIKV and RRV arthritis, respectively (Schilte et al., 2013, Soden et al., 2000); perhaps, this observation is also in agreement with the pathogenic role of IFN-γ in acute arthritis (Figure 4.9A).

5.2.8.4 Ingenuity's Upstream Regulator Analysis of down-regulated genes

Ingenuity's Upstream Regulator Analysis of the 355 down-regulated genes on day 30 post infection, identified only one significant upstream regulator (selection criteria: $p < 10^{10}$) that is glutathione *S*-transferases P1. The glutathione *S*-transferases P1 has previously been shown to prevent inflammation by inhibiting the production of inflammatory factors TNF-α, IL-1β, MCP-1 and nitric oxide (Luo et al., 2009). Thus, suppression of glutathione *S*-transferases P1 would suggest an ongoing promotion of inflammation in the feet.

Figure 5.7: Ingenuity's Upstream Regulator Analysis of differentially expressed genes identified in CHIKV-infected feet on day 30 post infection.

Ingenuity's Upstream Regulator Analysis of the 192 genes up-regulated genes identified in feet of mice at day 30 post infection. A positive z-score indicates that the identified pathway normally up regulates specific genes found in the 192 gene set. A negative z-score indicates that the identified pathway normally down regulates specific genes in the 192 gene set. Upstream regulators details are shown in Appendix V.

Data for Figure 5.7 was prepared with assistance from Helder Nakaya.

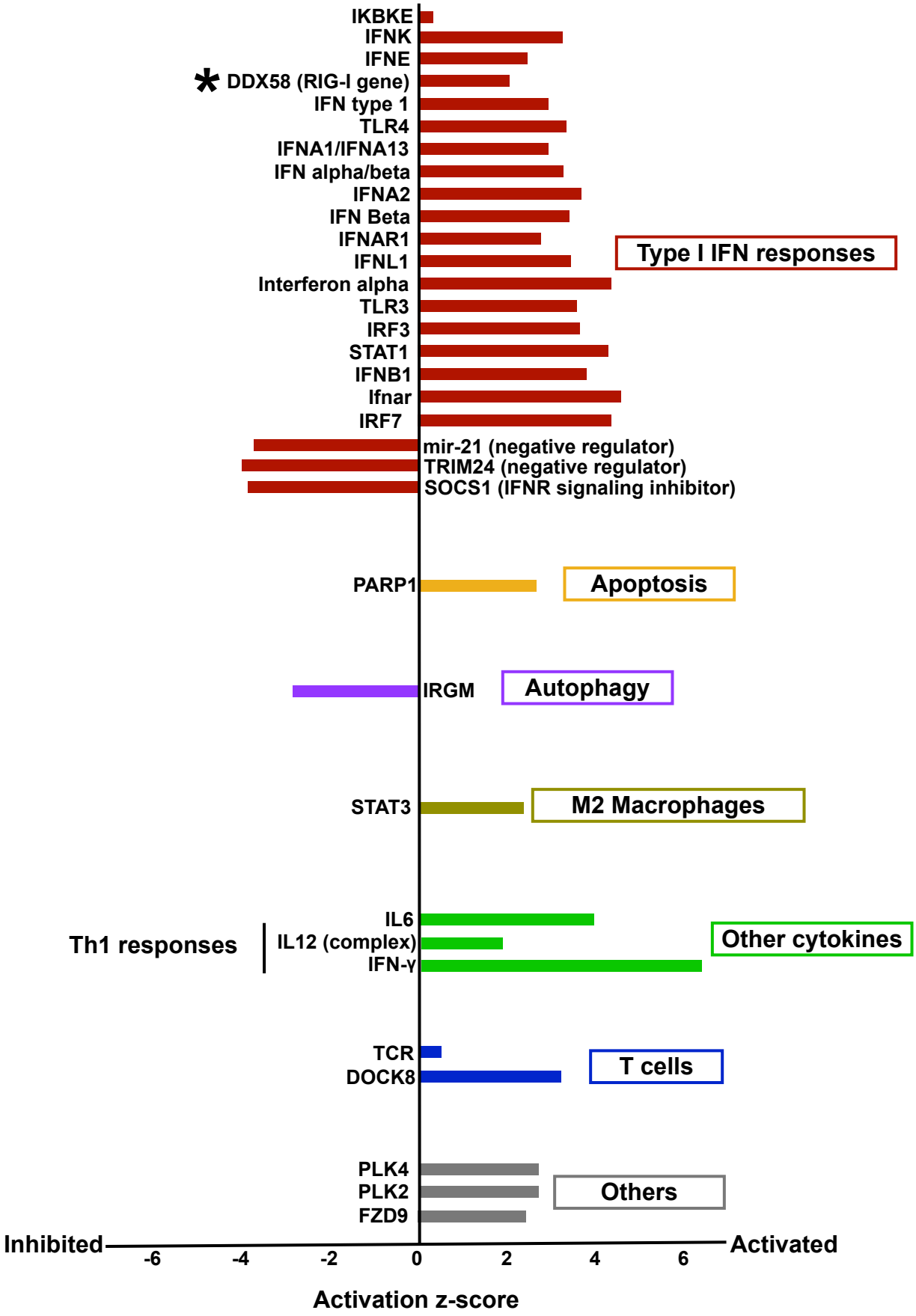
IKBKE
IFNK
IFNE
* DDX58 (RIG-I gene)
IFN type 1
TLR4
IFNA1/IFNA13
IFN alpha/beta
IFNA2
IFN Beta
IFNAR1
IFNL1
Interferon alpha
TLR3
IRF3
STAT1
IFNB1
Ifnar
IRF7
Type I IFN responses
mir-21 (negative regulator)
TRIM24 (negative regulator)
SOCS1 (IFNR signaling inhibitor)
PARP1
Apoptosis
IRGM
Autophagy
STAT3
M2 Macrophages
Th1 responses
IL6
IL12 (complex)
IFN-γ
Other cytokines
TCR
DOCK8
T cells
PLK4
PLK2
FZD9
Others
Inhibited
Activated
-6
-4
-2
0
2
4
6
Activation z-score

5.3 Discussion

Many CHIKV patients experience chronic arthritic symptoms (Suhrbier et al., 2012). The results in Chapter 5 provide evidence that chronic inflammation is triggered by persistence of CHIKV RNA. Firstly, CHIKV RNA and negative strand RNA (indicative of RNA replication) were shown to persist in the feet of infected mice (Figure 5.1) well after the viraemic period and despite the presence of neutralising antibodies (Figure 5.4). Secondly, the persistent CHIKV RNA in the feet of infected mice was associated with signs of ongoing stimulation of type I IFN responses, with ISG-54 persistently up-regulated (Figure 5.5). Finally, microarray gene expression analysis of chronically infected feet illustrated pronounced type I IFN responses (Figure 5.6, innate sensing and Figure 5.7, type I IFN responses). Taken together these data suggest that CHIKV RNA continues to replicate in foot tissues of mice for extended periods, with the replicating dsRNA continuing to induce type I IFN responses. These data are consistent with human (Hoarau et al., 2010) and primate studies (Labadie et al., 2010), which show that viral RNA and protein persist, despite robust immune responses. The mouse studies here now extend these data and suggest that the persistent RNA may be replicating, even after live virus can no longer be recovered from feet (Table 5.1).

5.3.1 Evidence of ongoing CHIKV replication *in vivo*

CHIKV RNA replication begins with synthesis of negative strand RNA from positive strand genomic RNA (Figure 1.4F1). The negative strand RNA serves as a template for the generation of new positive strand RNA, which includes both genomic and subgenomic viral RNAs (Figure 1.4F2 and F3). Both the former and latter processes generate viral dsRNA intermediates, which are known to trigger type I IFN responses (Bowie and Unterholzner, 2008). In this study, significant levels of CHIKV RNA (and negative strand RNA) were present in the feet up to 100 days post infection (Figure 5.1), with up-regulation of type I IFN responses (Figure 5.7, type I IFN responses) and ISG-54 (Figure 5.5). These data suggest that ongoing viral RNA replication continues to induce type I IFN responses (Plaskon et al., 2009, Sawicki and Sawicki, 1980).

5.3.2 Decline in viral RNA

The curves fits of CHIKV RNA decline indicate that the decline after the viraemic period follows a simple exponential decay with a half life of 10-11 days (Figure 5.3A). Future studies may

utilise these curves as a basis for comparing the decay rate of CHIKV RNA under diferent conditions. For example, if an anti-CHIKV treatment leads to a higher magnitude of decline, the treatment might be considered aneffective treatment as it would take a shorter time to reduce a given amount of CHIKV RNA.

Given the high error rates usually associated with the replication of RNA viruses (Crotty et al., 2001) and the loss of infectious virus and the subsequent steady decline in viral RNA levels, one might speculate that CHIKV RNA first becomes too mutated to generate replication competent virus (Crotty et al., 2001) and eventually becomes too mutated to maintain CHIKV RNA replication (Figure 5.1). These progressive failures in generating replication competent virus may account for the lack of live virus recovery from the mouse feet at chronic stage (Table 5.1). The high neutralising antibodies appear at chronic stage (Figure 5.4) could also hinder the live virus recovery from the mice tissue. In contrast to mice, live virus could be recovered from the macaque spleens, lymph nodes and livers at chronic stage (Labadie et al., 2010). This difference suggests that the CHIKV infection in mice is distinct from CHIKV infection in monkey. However, it is important to note that, despite numerous attempts, there was no successive live virus recovery from synovial biopsies of chronic CHIKV and RRV patients (Soden et al., 2000, Hoarau et al., 2010).

5.3.3 Immune responses that control CHIKV persistence

The obvious up-regulation of type I IFN responses clearly indicate that type I IFN play a substantial antiviral role in controlling CHIKV persistence (sections 5.2.7, 5.2.8.1 and 5.2.8.3). T cell responses also appear to be crucial in controlling CHIKV persistence: (i) up-regulation of IL-12 and IFN-γ suggests ongoing Th1 responses (Figure 5.7, other cytokines); (ii) up-regulation of T cell receptor and dedicator of cytokinesis 8 (DOCK8) would suggest ongoing CD8+ T cell responses (Randall et al., 2011) that are perhaps important for clearance of persistent viral CHIKV RNA. One might speculate that the persistence of anti-CHIKV antibodies seen in patients (Kelvin et al., 2011, Gerardin et al., 2013) and mice (Figure 5.4) might facilitate the persistence of CHIKV via antibody-dependent enhancement (ADE) of infection (Suhrbier and Linn, 2004) a process whereby virus infectivity is increased due to the uptake of antibody-virus complex into cells via Fc gamma receptors (FcRγ). Although previous study showed that ADE increased the infectivity of RRV in monocytes and macrophages (Linn et al., 1996, Mahalingam and Lidbury, 2002), CHIKV viraemia was unaffected in mice deficient for the FcRγ (deficient in FcRγRI and FcRγRIII) (Poo et al., submitted).

5.3.4 CHIKV-induced chronic inflammation in mice versus humans

The microarray analysis showed that many of the pathways up-regulated during peak arthritis (day 6/7) (Nakaya et al., 2012) were retained in persistently infected feet (day 30 post infection) (Figure 5.6). This may suggest that many of the drivers of acute inflammation are maintained during chronic disease. Importantly, the upstream regulator analysis identified pathways (Figure 5.7; specifically type I IFN, PARP-1, IL-6 and IFN-γ) that activated in our mouse model have also been shown to be activated in chronic human alphavirus infections (Hoarau et al., 2010, Soden et al., 2000). Hoarau et al. (2010) also demonstrated that T cells persisted in the synovial tissue of a patient that experienced chronic CHIKV arthritis. Recently, Hoarau et al. (2013) showed peripheral blood mononucleated cell derived T cells isolated from convalescent CHIKV patients were able to produce IFN-γ after challenged with CHIKV peptides *ex vivo*. Both T cell related observations from chronic CHIKV patients are in line with the T cell and IFN-γ signatures identified here in mice (Figure 5.6 and Figure 5.7).

5.3.5 Conclusion

In conclusion, this mouse model of CHIKV infection and disease recapitulates not only acute disease (Gardner et al., 2010) but also chronic CHIKV arthritic disease, with key pathways identified in mice also found in chronic disease in humans. The findings obtained using this model also support the notion that persistence of replicating CHIKV RNA contributes to chronic arthritic symptoms. To ameliorate the chronic arthritic disease cause by CHIKV infection, future studies might focus on factors that can clear persistent CHIKV RNA in the tissues or ameliorate the inflammatory responses without compromising the host's control of persistent viral RNA.

Chapter 6: Summary

The unprecedented size of the recent and ongoing CHIKV outbreak has highlighted the necessity for improved interventions. As this thesis goes to press, ≈3,700 cases of CHIKV disease have been reported in the Caribbean (Robles, 2014). A good understanding of CHIKV immunobiology is necessary for the development of such interventions. Although the understanding of CHIKV disease has advanced considerably in recent years, the role of several immune factors in CHIKV disease remained poorly defined. The findings in this thesis contribute to an improved understanding of the role of several immune factors in CHIKV disease.

6.1 Summary of Chapter 3: CCR2 deficiency promotes exacerbated chronic erosive neutrophil-dominated chikungunya virus arthritis

6.1.1 Major findings

The main findings of this chapter are:

1) The predominantly monocyte/macrophage infiltrate seen in wild-type mice was replaced by a pronounced neutrophil infiltrate in $CCR2^{-/-}$ mice, which resulted in an enhanced and prolonged arthritis and was associated with cartilage damage.

2) Changes in the expression of multiple inflammatory mediators accounted for this switch in the arthritic infiltrates, with the loss of M2 macrophages and associated anti-inflammatory activities (e.g. efferocytosis, see Figure 6.1) also likely to be involved in the prolonged inflammatory response.

3) Although infiltrating CCR2+ monocytes/macrophages contribute to inflammation, they also appear to be important for resolving inflammation and preventing excessive pathology (manifesting as more severe and prolonged arthritis and cartilage damage).

6.1.2 Major implications

Implications for treatment

These results argue that therapeutic targeting of inflammatory monocytes/macrophages may not be without risk. For instance, considerable care might be warranted when targeting

chemokines like CCL2 using anti-CCL2 antibody or bindarit for the treatment of alphaviral arthritides (Rulli et al., 2009, Rulli et al., 2011). Patients being treated with anti CCL2/CCR2 drugs may also be at risk of adverse pathology following an alphaviral infection.

A role for monocytes or macrophages for inhibiting neutrophil recruitment during CHIKV arthritis

During infection, CCL2 recruits CCR2+ monocytes to the site of infection (Figure 6.1). The recruited monocytes then develop into classically activated M1 macrophages that promote inflammation, trigger anti-viral defence and contribute to arthritic inflammation (Figure 6.1) (Suhrbier and Mahalingam, 2009). Macrophages can then also polarise into M2 and/or resolving macrophages populations, which are usually required for effective inflammation resolution (Figure 6.1).

Unresolved is how recruitment of CCR2+ monocytes inhibits infiltration of neutrophils, either the CCR2+ monocytes themselves and/or macrophages derived from them are likely to be involved (Figure 6.1; see question marks). Anti-inflammatory macrophages may prevent neutrophil infiltration by secreting proresolving lipid mediators (Serhan, 2010) and/or proteases that anti-inflammatory macrophages (Ortega-Gomez et al., 2013). IL-10, which anti-inflammatory macrophages secrete, may be marginally involved, with foot swelling and neutrophil infiltration only slightly elevated (the latter not significantly) in CHIKV infected IL-$10^{-/-}$ mice (Figure 3.13A and C). The IL-10 can also promote the expansion of CCR2+ T-regulatory cells, which play a protective role in collagen-induced arthritis (Ortega-Gomez et al., 2013).

Implications for the cell type harbouring persistent CHIKV RNA

CHIKV is reported to persist in macrophages found in spleen (monkeys) (Labadie et al., 2010, Messaoudi et al., 2013) and synovial fluid in humans (Hoarau et al., 2010). RRV is also reported to be able to establish persistent infection in cell cultures of murine macrophage cell line (RAW 264.7) (Linn et al., 1998, Way et al., 2002) and human synovial cells (with macropahge-like feature) (Journeaux et al., 1987). Prolific infiltration of CCR2+ macrophages in joints was observed in WT mice, but not in $CCR2^{-/-}$ mice. Despite the difference in the levels of macrophage infiltration, WT and $CCR2^{-/-}$ mice had similar levels of persistent CHIKV RNA, suggesting that CHIKV RNA is unlikely to persist in recruited macrophages derived from CCR2+ monocytes. Conceivably, CHIKV RNA persistence is restricted to resident tissue macrophages. Such

macrophages tend to have an M2 phenotype (Davies et al., 2013), with a recent study suggesting that CHIKV persists in M2 macrophages (Stoermer et al., 2012) (Figure 6.1). The overall reduction in M2 macrophage markers seen in the array (Figure 3.14, brown) likely largely relates to CCR2+ monocyte-derived macrophages, with the tissue-resident macrophages not specifically analysed.

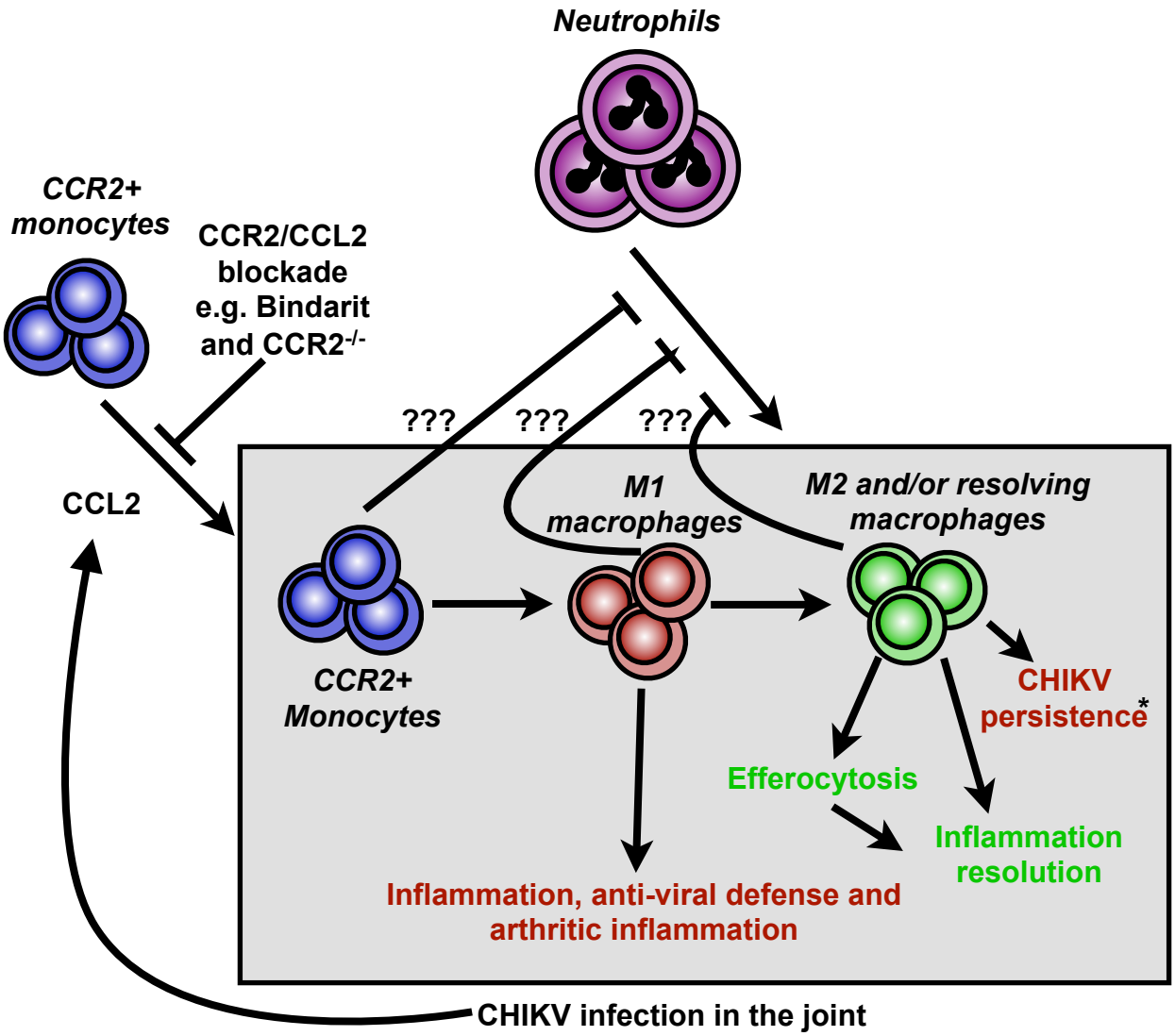

Figure 6.1: Relationship of monocytes/macrophages and neutrophils in CHIKV arthritis.

CHIKV infection in the joints triggers the induction of CCL2 that leads to the recruitment of CCR2+ monocytes from the circulating blood into CHIKV infected joints. The recruited CCR2+ monocytes then develop into classically activated M1 macrophages that promote inflammation, trigger anti-viral defence and arthritic inflammation. Macrophages can also differentiate into a M2 and/or resolving macrophages populations. These macrophages are usually required for effective

inflammation resolution but are also implicated in harbouring persistent CHIKV RNA (Stoermer et al., 2012). It remains unclear that how monocytes and/or macrophages derived from them could suppress the infiltration of neutrophils. * Stoermer et al. (2012)

6.1.3 Future directions

1) Treating WT mice with CCR2 inhibitors

CCR2 deficiency exacerbates CHIKV arthritis in mice. To determine whether this means that treatment with CCR2 inhibitors would also exacerbate disease, WT mice might be treated with CCR2 inhibitors. There are several commercial available CCR2 inhibitors, namely RS504393 (Berkhout et al., 2003, Pevida et al., 2012), INCB3344 (Brodmerkel et al., 2005, Chan et al., 2012) and MK-0812 (Min et al., 2010, Butora et al., 2007, Wisniewski et al., 2010). MK-0812 has been used to treat patients with rheumatoid arthritis, although initial trial results were disappointing (Lebre et al., 2011). Therefore, future experiment should use MK-0812 to treat WT mice as this treatment will not only provide insights on CCR2 inhibition in CHIKV arthritis but also assist the understandings of CCR2 drugs in treating arthritic disease.

2) Adoptively transfer of CCR2+ monocytes to CCR2$^{-/-}$ mice

Recruitment of CCR2+ monocytes appears to be crucial in preventing the infiltration of neutrophils that then promote severe CHIKV arthritis (Figure 6.1). How these cells achieve this remains unclear. To gain further insights WT CCR2+ monocytes might be adoptively transferred into CCR2$^{-/-}$ mice to see whether this would inhibit neutrophil infiltration. It may also be useful to titrate the number of adoptively transferred CCR2+ monocytes, to determine how many cells are required to inhibit neutrophil infiltration. Once established, CCR2+ monocytes from various other knockout mice (e.g. IL-10$^{-/-}$ and IL-1β$^{-/-}$) might be tested to see whether the effect was lost.

3) Targeting resident tissue macrophages

CHIKV can persist in macrophages (Hoarau et al., 2010, Labadie et al., 2010), with a recent study proposing that M2 macrophages promote CHIKV persistence (Figure 6.1) (Stoermer et al., 2012). Thus targeting macrophages, specifically M2 macrophages, during the chronic stage of infection and disease may be useful in preventing CHIKV persistence and thus chronic disease. Preliminary studies in our group demonstrate that depleting macrophages population during the

chronic stage can change the levels of persistent viral RNA in feet. When mice day 30 post-infection were treated with 15 μg macrophage-depleting anti-F4/80 antibody s.c., a ≈ 5 fold reduction of qRT-PCR detectable viral RNA as measured 4 days post-treatment (data not shown).

6.2 Summary of Chapter 4: The contribution of B, T and NK cells and IFN-γ in the control of viraemia and mediation of arthritis during CHIKV infection

6.2.1 Major findings

The main findings of this chapter are:

1) CD4+ T cells play an important role in mediating CHIKV arthritis.

2) T cells play a significant role, albeit minor, in controlling viraemia.

3) IFN-γ plays an important role in mediating CHIKV arthritis.

6.2.2 Major implication

Implications for the understandings of CHIKV arthritis

Previous studies indicated T cells are not implicated in triggering alphaviral arthritis (Morrison et al., 2007, Morrison et al., 2006). However, the results herein clearly suggest that CD4+ T cells are implicated in CHIKV arthritis. This contention is also supported by (i) the strong T cells signals detected during peak arthritis (Nakaya et al., 2012) and (ii) findings by another group demonstrating the involvement of CD4+ T cells in CHIKV arthritis (Teo et al., 2012b). Results herein also suggest that IFN-γ (likely produced by CD4+ T cells) is involved in promoting CHIKV arthritis, with IFN-γ previously found to be elevated in synovium fluid of acute RRV patients (Lidbury et al., 2008) and synovial tissue of chronic RRV patients (Soden et al., 2000). Anti-IFN-γ also ameliorated disease in a mouse model of RRV disease (Lidbury et al., 2008), suggesting that therapeutic targeting of this cytokine might be considered. Viraemia was not increased in IFN-$\gamma^{-/-}$ mice, suggesting the anti-viral activities of IFN-γ are not critical for CHIKV control (see below).

6.2.3 Future directions

1) To investigate the role of IFN-γ in arthritis caused by different isolates of CHIKV

In contrast to the findings in this thesis, Teo et al. (2012b) reported that IFN-γ had no significant role in CHIKV arthritis. This discrepancy might be attributable to the different isolates of CHIKV used. To further investigate this issue, IFN-$\gamma^{-/-}$ mice (and control WT mice on the same background) might be infected with various CHIKV isolates (including LR2006-OPY1 and SGP11) and the disease severity directly compared.

2) Assessing the effectiveness of anti-IFN-γ antibodies in treating CHIKV arthritis

IFN-γ deficiency reduced acute arthritis and did not lead to increased viraemia in CHIKV infected mice (Figure 4.9A and B). In addition, microarray analysis reveals that IFN-γ signature is still active in persistently infected feet during the chronic stage of disease (Figure 5.7, other cytokines). Therefore, treatment that inhibits IFN-γ may be a viable therapeutic option to ameliorate CHIKV arthritis, as suggested previously for RRV (Lidbury et al., 2008). Since IFN-γ affects acute arthritis and associates with chronic arthritis, anti-IFN-γ treatment will be administered during acute (days 2-6), chronic (days 10-30) and overall period (days 2-30) to test the effectiveness of anti-IFN-γ antibodies in treating CHIKV arthritis at different stages of the disease. Disease severity (arthritis and viraemia), viral persistence (CHIKV RNA levels) and anti-CHIKV antibody levels (antiviral antibody titres and IgG isotypes) in these mice might be monitored, to determine what other potentially detrimental effects such treatment may have.

6.3 Summary of Chapter 5: Long-term persistence of CHIKV RNA in WT mice is associated with signs of chronic inflammation

6.3.1 Major findings

The main findings of this chapter are:

1) CHIKV RNA, including negative strand viral RNA, persisted for up to 100 days post-infection in joint tissues, long after the end of the viraemic period (day 4-5).

2) Infectious CHIKV can be recovered from feet of mice for at least 14 days post-infection, even when viraemia was cleared at 4-5 days post infection.

3) Although antibodies were essential for clearance of the CHIKV viraemia, antibodies appeared unable to prevent persistence of CHIKV and CHIKV RNA in tissue. The persistent CHIKV RNA in the feet may account for the persistent arthritis because:
(i) IFN pathways and ISG (e.g. ISG-54) were persistently up- regulated, suggesting on-going inflammation, with these responses perhaps involved in controlling CHIKV persistence; and (ii) many of the pathways induced during the acute phase were maintained in the chronic phase.

4) PARP-1, an enzyme that is associated with apoptosis, was identified as an up-stream regulator during the chronic stage of CHIKV infection. This result is consistent with findings on apoptosis-facilitated CHIKV persistence, which show that the up-regulation of PARP-1 in chronic CHIKV patients (Hoarau et al., 2010) and CHIKV infected cells (Krejbich-Trotot et al., 2011).

5) The mouse model of CHIKV infection and disease, which was used in this study, recapitulates not only acute disease but also chronic CHIKV arthritic disease, with key pathways identified in mice also found in chronic disease in humans (Hoarau et al., 2010).

6.3.2 Major implications

Implications for the utilisation of mouse model to study chronic CHIKV infection

This study reveals the remarkable similarity between chronic CHIKV infection in humans and mice, with both sharing similar inflammatory signatures and both showing persistence of CHIKV RNA. These observations indicate that this mouse model is useful for studies that seek to better understand chronic CHIKV disease. The model may thus also find utility for testing interventions that aim to ameliorate chronic CHIKV arthritic disease.

6.3.3 Future directions

1) To better characterise the inflammatory signatures and identify potential viral genomes associated with chronic CHIKV arthritis

Although results herein indicate that CHIKV infection leads to the persistence of CHIKV and chronic inflammation, the factors that are associated with, and regulate, CHIKV persistence and

chronic inflammation are not comprehensively understood. A better understanding of these factors will facilitate the development of better treatments for chronic CHIKV. Further evaluation may use RNA-sequencing to study the total RNA population in mice feet with persistent CHIKV RNA. This approach should identify more DEGs than the microarray study, as background subtraction issues are less of an issue with this technology. Background subtraction issues tend to compromise the ability to find significantly differentially regulated genes in microarray studies when fold changes are low. This approach will not only help identifying more comprehensively the factors that are associated with CHIKV persistence and inflammation, but may also give insights into the viral genome changes associated with persistence. The insights arising from such mouse studies might also guide further analyses of patient samples (e.g. synovial samples).

2) CD8+ T cells role in controlling CHIKV persistence

Studies suggest that CD8+ T cells do not appear to play a role in controlling acute viraemia (Linn et al., 1998, Chu et al., 2013, Teo et al., 2012b), but these studies did not examine whether CD8+ T cells could play a role in controlling CHIKV persistence *in vivo*. Further studies might focus on evaluating the role T cells, specifically CD8+ T cells, in controlling CHIKV persistence in the tissue. This evaluation can be achieved by infecting mice with deficient in CD8+ T cells (e.g. B6.129S2-*Cd8a*^{tm1Mak}/J) and other components of CD8+ T cells like perforin (e.g. C57BL/6-*Prf1*^{tm1Sdz}/J) and granzyme B (B6;129S2-*Gzmb*^{tm1Ley}/J). These studies would provide insights on whether cytolytic activities are involved in clearing persistent CHIKV RNA. If CD8+ T cells are shown to be crucial, future therapeutics may look into ways for enhancing CD8+ T cells, for example, by inhibiting programmed cell death protein 1 that are highly expressed in CD8+ T cells that have been exhausted during chronic viral infection (Barber et al., 2006).

3) Evaluating the effect of anti-IL-6 therapeutics on CHIKV arthritis

Targeting IL-6 may be worth exploring as a therapeutic intervention given that IL-6 was (i) implicated in RA (Shoda and Yamamoto, 2007), (ii) up-regulated in CHIKV patients with chronic arthritic symptoms (Chow et al., 2011, Chopra et al., 2012, Hoarau et al., 2010), and (iii) was identified as an upstream regulator during chronic infection of CHIKV infection in mice (Figure 5.7; other cytokines). Interventions targeting IL-6, such as siltuximab/sirukumab and tocilizumab (IL-6 and IL-6 receptor targeting agents, respectively), have been clinically proven to ameliorate a

range of inflammatory autoimmune diseases, including RA, juvenile idiopathic arthritis and Castleman's disease (Tanaka et al., 2014, Yoshida and Tanaka, 2014).

References

Aaskov, J. G., Dalglish, D. A., Harper, J. J., Douglas, J. F., Donaldson, M. D. & Hertzog, P. J. 1987. Natural killer cells in viral arthritis. *Clin Exp Immunol,* 68**,** 23-32.

Aaskov, J. G., Fraser, J. R. & Dalglish, D. A. 1981. Specific and non-specific immunological changes in epidemic polyarthritis patients. *Aust J Exp Biol Med Sci,* 59**,** 599-608.

Ahern, D. J. & Brennan, F. M. 2011. The role of Natural Killer cells in the pathogenesis of rheumatoid arthritis: major contributors or essential homeostatic modulators? *Immunol Lett,* 136**,** 115-21.

Ajuebor, M. N., Das, A. M., Virag, L., Flower, R. J., Szabo, C. & Perretti, M. 1999. Role of resident peritoneal macrophages and mast cells in chemokine production and neutrophil migration in acute inflammation: evidence for an inhibitory loop involving endogenous IL-10. *J Immunol,* 162**,** 1685-91.

Akahata, W., Yang, Z.-Y., Andersen, H., Sun, S., Holdaway, H. A., Kong, W.-P., Lewis, M. G., Higgs, S., Rossmann, M. G., Rao, S. & Nabel, G. J. 2010. A virus-like particle vaccine for epidemic Chikungunya virus protects nonhuman primates against infection. *Nature Medicine,* 16**,** 334-338.

Apandi, Y., Nazni, W. A., Azleen, Z. a. N., Vythilingam, I., Noorazian, M. Y., Azahari, A. H., Zainah, S. & Lee, H. L. 2009. The first isolation of chikungunya virus from non-human primates in Malaysia. *Journal of General and Molecular Virology* 1**,** 35-39.

Arankalle, V. A., Shrivastava, S., Cherian, S., Gunjikar, R. S., Walimbe, A. M., Jadhav, S. M., Sudeep, A. B. & Mishra, A. C. 2007. Genetic divergence of Chikungunya viruses in India (1963-2006) with special reference to the 2005-2006 explosive epidemic. *J Gen Virol,* 88**,** 1967-76.

Ariel, A. & Serhan, C. N. 2012. New Lives Given by Cell Death: Macrophage Differentiation Following Their Encounter with Apoptotic Leukocytes during the Resolution of Inflammation. *Front Immunol,* 3**,** 4.

Azami, N. A., Salleh, S. A., Shah, S. A., Neoh, H. M., Othman, Z., Zakaria, S. Z. & Jamal, R. 2013. Emergence of chikungunya seropositivity in healthy Malaysian adults residing in outbreak-free locations: chikungunya seroprevalence results from the Malaysian Cohort. *BMC Infect Dis,* 13**,** 67.

Bakker, E. N., Matlung, H. L., Bonta, P., De Vries, C. J., Van Rooijen, N. & Vanbavel, E. 2008. Blood flow-dependent arterial remodelling is facilitated by inflammation but directed by vascular tone. *Cardiovasc Res,* 78**,** 341-8.

Bancroft, J. D. & Gamble, M. 2001. *Theory and practice of histological techniques,* Edinburgh ; New York, Churchill Livingstone.

Barber, D. L., Wherry, E. J., Masopust, D., Zhu, B., Allison, J. P., Sharpe, A. H., Freeman, G. J. & Ahmed, R. 2006. Restoring function in exhausted CD8 T cells during chronic viral infection. *Nature,* 439**,** 682-7.

Benedict, M. Q., Levine, R. S., Hawley, W. A. & Lounibos, L. P. 2007. Spread of the tiger: global risk of invasion by the mosquito Aedes albopictus. *Vector borne and zoonotic diseases,* 7**,** 76-85.

Berkhout, T. A., Blaney, F. E., Bridges, A. M., Cooper, D. G., Forbes, I. T., Gribble, A. D., Groot, P. H., Hardy, A., Ife, R. J., Kaur, R., Moores, K. E., Shillito, H., Willetts, J. & Witherington, J. 2003. CCR2: characterization of the antagonist binding site from a combined receptor modeling/mutagenesis approach. *J Med Chem,* 46**,** 4070-86.

Binder, G. K. & Griffin, D. E. 2001. Interferon-gamma-mediated site-specific clearance of alphavirus from CNS neurons. *Science,* 293**,** 303-6.

Binn, L. N., Harrison, V. R. & Randall, R. 1967. Patterns of viremia and antibody observed in rhesus monkeys inoculated with chikungunya and other serologically related group A arboviruses. *The American journal of tropical medicine and hygiene,* 16**,** 782-5.

Bodenmann, P. & Genton, B. 2006. Chikungunya: an epidemic in real time. *Lancet,* 368**,** 258.

Bonjardim, C. A., Ferreira, P. C. & Kroon, E. G. 2009. Interferons: signaling, antiviral and viral evasion. *Immunol Lett,* 122**,** 1-11.

Borgherini, G., Poubeau, P., Jossaume, A., Gouix, A., Cotte, L., Michault, A., Arvin-Berod, C. & Paganin, F. 2008. Persistent arthralgia associated with chikungunya virus: a study of 88 adult patients on reunion island. *Clin Infect Dis,* 47**,** 469-75.

Boring, L., Gosling, J., Chensue, S. W., Kunkel, S. L., Farese, R. V., Jr., Broxmeyer, H. E. & Charo, I. F. 1997. Impaired monocyte migration and reduced type 1 (Th1) cytokine responses in C-C chemokine receptor 2 knockout mice. *J Clin Invest,* 100**,** 2552-61.

Borojevic, R., Santos-Da-Silva, C. & Carvalho, E. A. 1983. Chronic schistosomiasis mansoni: splenic myelopoiesis and inhibition of neutrophil granulocytopoiesis mediated by the sera of patients. *J Infect Dis,* 148**,** 422-6.

Bouquillard, E. & Combe, B. 2009. A report of 21 cases of rheumatoid arthritis following Chikungunya fever. A mean follow-up of two years. *Joint Bone Spine,* 76**,** 654-7.

Bowie, A. G. & Unterholzner, L. 2008. Viral evasion and subversion of pattern-recognition receptor signalling. *Nature Reviews Immunology,* 8**,** 911-922.

Brandler, S., Ruffie, C., Combredet, C., Brault, J. B., Najburg, V., Prevost, M. C., Habel, A., Tauber, E., Despres, P. & Tangy, F. 2013. A recombinant measles vaccine expressing chikungunya virus-like particles is strongly immunogenic and protects mice from lethal challenge with chikungunya virus. *Vaccine,* 31**,** 3718-25.

Brewer, J. M., Richmond, J. & Alexander, J. 1994. The demonstration of an essential role for macrophages in the in vivo generation of IgG2a antibodies. *Clin Exp Immunol,* 97**,** 164-71.

Brighton, S. W., Prozesky, O. W. & De La Harpe, A. L. 1983. Chikungunya virus infection. A retrospective study of 107 cases. *S Afr Med J,* 63**,** 313-5.

Brodmerkel, C. M., Huber, R., Covington, M., Diamond, S., Hall, L., Collins, R., Leffet, L., Gallagher, K., Feldman, P., Collier, P., Stow, M., Gu, X., Baribaud, F., Shin, N., Thomas, B., Burn, T., Hollis, G., Yeleswaram, S., Solomon, K., Friedman, S., Wang, A., Xue, C. B., Newton, R. C., Scherle, P. & Vaddi, K. 2005. Discovery and pharmacological characterization of a novel rodent-active CCR2 antagonist, INCB3344. *J Immunol,* 175**,** 5370-8.

Brooke, C. B., Deming, D. J., Whitmore, A. C., White, L. J. & Johnston, R. E. 2010. T cells facilitate recovery from Venezuelan equine encephalitis virus-induced encephalomyelitis in the absence of antibody. *J Virol,* 84**,** 4556-68.

Bruhl, H., Cihak, J., Schneider, M. A., Plachy, J., Rupp, T., Wenzel, I., Shakarami, M., Milz, S., Ellwart, J. W., Stangassinger, M., Schlondorff, D. & Mack, M. 2004. Dual role of CCR2 during initiation and progression of collagen-induced arthritis: evidence for regulatory activity of CCR2+ T cells. *J Immunol,* 172**,** 890-8.

Buonaguro, L., Tagliamonte, M., Visciano, M. L., Tornesello, M. L. & Buonaguro, F. M. 2013. Developments in virus-like particle-based vaccines for HIV. *Expert Rev Vaccines,* 12**,** 119-27.

Burdeinick-Kerr, R., Wind, J. & Griffin, D. E. 2007. Synergistic roles of antibody and interferon in noncytolytic clearance of Sindbis virus from different regions of the central nervous system. *J Virol,* 81**,** 5628-36.

Burt, F. J., Rolph, M. S., Rulli, N. E., Mahalingam, S. & Heise, M. T. 2012. Chikungunya: a re-emerging virus. *Lancet,* 379**,** 662-71.

Butora, G., Jiao, R., Parsons, W. H., Vicario, P. P., Jin, H., Ayala, J. M., Cascieri, M. A. & Yang, L. 2007. 3-Amino-1-alkyl-cyclopentane carboxamides as small molecule antagonists of the human and murine CC chemokine receptor 2. *Bioorg Med Chem Lett,* 17**,** 3636-41.

Carey, D. E. 1971. Chikungunya and dengue: a case of mistaken identity? *Journal of the history of medicine and allied sciences,* 26**,** 243-62.

Carlson, M. J., West, M. L., Coghill, J. M., Panoskaltsis-Mortari, A., Blazar, B. R. & Serody, J. S. 2009. In vitro-differentiated TH17 cells mediate lethal acute graft-versus-host disease with severe cutaneous and pulmonary pathologic manifestations. *Blood,* 113**,** 1365-74.

Caspar, D. L. & Klug, A. 1962. Physical principles in the construction of regular viruses. *Cold Spring Harb Symp Quant Biol,* 27**,** 1-24.

Chaaitanya, I. K., Muruganandam, N., Sundaram, S. G., Kawalekar, O., Sugunan, A. P., Manimunda, S. P., Ghosal, S. R., Muthumani, K. & Vijayachari, P. 2011. Role of

proinflammatory cytokines and chemokines in chronic arthropathy in CHIKV infection. *Viral Immunol,* 24**,** 265-71.

Challacombe, J. M., Suhrbier, A., Parsons, P. G., Jones, B., Hampson, P., Kavanagh, D., Rainger, G. E., Morris, M., Lord, J. M., Le, T. T., Hoang-Le, D. & Ogbourne, S. M. 2006. Neutrophils are a key component of the antitumor efficacy of topical chemotherapy with ingenol-3-angelate. *J Immunol,* 177**,** 8123-32.

Chan, C. T., Moore, J. P., Budzyn, K., Guida, E., Diep, H., Vinh, A., Jones, E. S., Widdop, R. E., Armitage, J. A., Sakkal, S., Ricardo, S. D., Sobey, C. G. & Drummond, G. R. 2012. Reversal of vascular macrophage accumulation and hypertension by a CCR2 antagonist in deoxycorticosterone/salt-treated mice. *Hypertension,* 60**,** 1207-12.

Charrel, R. N., De Lamballerie, X. & Raoult, D. 2007. Chikungunya outbreaks--the globalization of vectorborne diseases. *N Engl J Med,* 356**,** 769-71.

Chattopadhyay, A., Wang, E., Seymour, R., Weaver, S. C. & Rose, J. K. 2013. A chimeric vesiculo/alphavirus is an effective alphavirus vaccine. *J Virol,* 87**,** 395-402.

Chen, Y., Chen, J., Wang, H., Shi, J., Wu, K., Liu, S., Liu, Y. & Wu, J. 2013. HCV-induced miR-21 contributes to evasion of host immune system by targeting MyD88 and IRAK1. *PLoS Pathog,* 9**,** e1003248.

Chopra, A., Anuradha, V., Ghorpade, R. & Saluja, M. 2012. Acute Chikungunya and persistent musculoskeletal pain following the 2006 Indian epidemic: a 2-year prospective rural community study. *Epidemiol Infect,* 140**,** 842-50.

Chopra, A., Saluja, M. & Venugopalan, A. 2014. Chloroquine effectiveness and inflammatory cytokine response in early persistent post chikungunya musculoskeletal pain and arthritis. *Arthritis Rheum,* 66**,** 319-326.

Chow, A., Her, Z., Ong, E. K., Chen, J. M., Dimatatac, F., Kwek, D. J., Barkham, T., Yang, H., Renia, L., Leo, Y. S. & Ng, L. F. 2011. Persistent arthralgia induced by Chikungunya virus infection is associated with interleukin-6 and granulocyte macrophage colony-stimulating factor. *J Infect Dis,* 203**,** 149-57.

Chu, H., Das, S. C., Fuchs, J. F., Suresh, M., Weaver, S. C., Stinchcomb, D. T., Partidos, C. D. & Osorio, J. E. 2013. Deciphering the protective role of adaptive immunity to CHIKV/IRES a novel candidate vaccine against Chikungunya in the A129 mouse model. *Vaccine,* 31**,** 3353-60.

Chusri, S., Siripaitoon, P., Hirunpat, S. & Silpapojakul, K. 2011. Case reports of neuro-Chikungunya in southern Thailand. *Am J Trop Med Hyg,* 85**,** 386-9.

Coffey, L. L., Beeharry, Y., Borderia, A. V., Blanc, H. & Vignuzzi, M. 2011. Arbovirus high fidelity variant loses fitness in mosquitoes and mice. *Proc Natl Acad Sci U S A,* 108**,** 16038-43.

Cook, H. C. 1974. *Manual of histological demonstration techniques. H. C. Cook*, Butterworths.

Cote, C. H., Bouchard, P., Van Rooijen, N., Marsolais, D. & Duchesne, E. 2013. Monocyte depletion increases local proliferation of macrophage subsets after skeletal muscle injury. *BMC Musculoskelet Disord,* 14**,** 359.

Couderc, T., Chrétien, F., Schilte, C., Disson, O., Brigitte, M., Guivel-Benhassine, F., Touret, Y., Barau, G., Cayet, N., Schuffenecker, I., Despres, P., Arenzana-Seisdedos, F., Michault, A., Albert, M. L. & Lecuit, M. 2008. A Mouse Model for Chikungunya: Young Age and Inefficient Type-I Interferon Signaling Are Risk Factors for Severe Disease. *PLoS Pathogens,* 4**,** e29.

Couderc, T., Khandoudi, N., Grandadam, M., Visse, C., Gangneux, N., Bagot, S., Prost, J. F. & Lecuit, M. 2009. Prophylaxis and therapy for Chikungunya virus infection. *J Infect Dis,* 200**,** 516-23.

Couturier, E., Guillemin, F., Mura, M., Leon, L., Virion, J. M., Letort, M. J., De Valk, H., Simon, F. & Vaillant, V. 2012. Impaired quality of life after chikungunya virus infection: a 2-year follow-up study. *Rheumatology (Oxford),* 51**,** 1315-22.

Crotty, S., Cameron, C. E. & Andino, R. 2001. RNA virus error catastrophe: direct molecular test by using ribavirin. *Proc Natl Acad Sci U S A,* 98**,** 6895-900.

Dalton, D. K., Pitts-Meek, S., Keshav, S., Figari, I. S., Bradley, A. & Stewart, T. A. 1993. Multiple defects of immune cell function in mice with disrupted interferon-gamma genes. *Science,* 259**,** 1739-42.

Das, T., Jaffar-Bandjee, M. C., Hoarau, J. J., Krejbich Trotot, P., Denizot, M., Lee-Pat-Yuen, G., Sahoo, R., Guiraud, P., Ramful, D., Robin, S., Alessandri, J. L., Gauzere, B. A. & Gasque, P. 2010. Chikungunya fever: CNS infection and pathologies of a re-emerging arbovirus. *Progress in neurobiology,* 91**,** 121-9.

Davies, L. C., Jenkins, S. J., Allen, J. E. & Taylor, P. R. 2013. Tissue-resident macrophages. *Nat Immunol,* 14**,** 986-95.

De Andrade, D. C., Jean, S., Clavelou, P., Dallel, R. & Bouhassira, D. 2010. Chronic pain associated with the Chikungunya Fever: long lasting burden of an acute illness. *BMC Infect Dis,* 10**,** 31.

De Rycke, L., Baeten, D., Kruithof, E., Van Den Bosch, F., Veys, E. M. & De Keyser, F. 2005. The effect of TNFalpha blockade on the antinuclear antibody profile in patients with chronic arthritis: biological and clinical implications. *Lupus,* 14**,** 931-7.

Delatte, H., Paupy, C., Dehecq, J. S., Thiria, J., Failloux, A. B. & Fontenille, D. 2008. [Aedes albopictus, vector of chikungunya and dengue viruses in Reunion Island: biology and control]. *Parasite,* 15**,** 3-13.

Delogu, I. & De Lamballerie, X. 2011. Chikungunya disease and chloroquine treatment. *J Med Virol,* 83**,** 1058-9.

Dorshkind, K., Montecino-Rodriguez, E. & Signer, R. A. 2009. The ageing immune system: is it ever too old to become young again? *Nat Rev Immunol,* 9**,** 57-62.

Dunay, I. R., Fuchs, A. & Sibley, L. D. 2010. Inflammatory monocytes but not neutrophils are necessary to control infection with Toxoplasma gondii in mice. *Infect Immun,* 78**,** 1564-70.

Eckels, K. H., Harrison, V. R. & Hetrick, F. M. 1970. Chikungunya virus vaccine prepared by Tween-ether extraction. *Applied microbiology,* 19**,** 321-5.

Economopoulou, A., Dominguez, M., Helynck, B., Sissoko, D., Wichmann, O., Quenel, P., Germonneau, P. & Quatresous, I. 2009. Atypical Chikungunya virus infections: clinical manifestations, mortality and risk factors for severe disease during the 2005-2006 outbreak on Reunion. *Epidemiology and infection,* 137**,** 534-41.

Edelman, R., Tacket, C. O., Wasserman, S. S., Bodison, S. A., Perry, J. G. & Mangiafico, J. A. 2000. Phase II safety and immunogenicity study of live chikungunya virus vaccine TSI-GSD-218. *The American journal of tropical medicine and hygiene,* 62**,** 681-5.

Ellett, J. D., Atkinson, C., Evans, Z. P., Amani, Z., Balish, E., Schmidt, M. G., Van Rooijen, N., Schnellmann, R. G. & Chavin, K. D. 2010. Murine Kupffer cells are protective in total hepatic ischemia/reperfusion injury with bowel congestion through IL-10. *J Immunol,* 184**,** 5849-58.

Enserink, M. 2008. Entomology. A mosquito goes global. *Science,* 320**,** 864-6.

Eyles, J. L., Hickey, M. J., Norman, M. U., Croker, B. A., Roberts, A. W., Drake, S. F., James, W. G., Metcalf, D., Campbell, I. K. & Wicks, I. P. 2008. A key role for G-CSF-induced neutrophil production and trafficking during inflammatory arthritis. *Blood,* 112**,** 5193-201.

Fayzulin, R. & Frolov, I. 2004. Changes of the secondary structure of the 5' end of the Sindbis virus genome inhibit virus growth in mosquito cells and lead to accumulation of adaptive mutations. *Journal of virology,* 78**,** 4953-64.

Feng, C. G., Kaviratne, M., Rothfuchs, A. G., Cheever, A., Hieny, S., Young, H. A., Wynn, T. A. & Sher, A. 2006. NK cell-derived IFN-gamma differentially regulates innate resistance and neutrophil response in T cell-deficient hosts infected with Mycobacterium tuberculosis. *J Immunol,* 177**,** 7086-93.

Foged, C., Hansen, J. & Agger, E. M. 2012. License to kill: Formulation requirements for optimal priming of CD8(+) CTL responses with particulate vaccine delivery systems. *Eur J Pharm Sci,* 45**,** 482-91.

Foulds, K. E., Wu, C. Y. & Seder, R. A. 2006. Th1 memory: implications for vaccine development. *Immunol Rev,* 211**,** 58-66.

Fric, J., Bertin-Maghit, S., Wang, C. I., Nardin, A. & Warter, L. 2013. Use of human monoclonal antibodies to treat Chikungunya virus infection. *J Infect Dis,* 207**,** 319-22.

Frolov, I., Hardy, R. & Rice, C. M. 2001. Cis-acting RNA elements at the 5' end of Sindbis virus genome RNA regulate minus- and plus-strand RNA synthesis. *RNA,* 7**,** 1638-51.

Fros, J. J., Liu, W. J., Prow, N. A., Geertsema, C., Ligtenberg, M., Vanlandingham, D. L., Schnettler, E., Vlak, J. M., Suhrbier, A., Khromykh, A. A. & Pijlman, G. P. 2010. Chikungunya virus nonstructural protein 2 inhibits type I/II interferon-stimulated JAK-STAT signaling. *J Virol,* 84**,** 10877-87.

Fujii, H., Baba, T., Yamagishi, M., Kawano, M. & Mukaida, M. 2012. The role of a chemokine receptor, CCR2, in suppressing the development of arthritis in IL-1 receptor antagonist-deficient mice. *Inflammation and Regeneration,* 32**,** 124-131.

Furze, R. C. & Selkirk, M. E. 2005. Comparative dynamics and phenotype of the murine immune response to Trichinella spiralis and Trichinella pseudospiralis. *Parasite Immunol,* 27**,** 181-8.

Ganu, M. A. & Ganu, A. S. 2011. Post-chikungunya chronic arthritis--our experience with DMARDs over two year follow up. *J Assoc Physicians India,* 59**,** 83-6.

Garcia-Arriaza, J., Cepeda, V., Hallengard, D., Sorzano, C. O., Kummerer, B. M., Liljestrom, P. & Esteban, M. 2014. A Novel Poxvirus-based Vaccine (MVA-CHIKV) is Highly Immunogenic and Protects Mice against Chikungunya Infection. *J Virol*.

Gardner, C. L., Burke, C. W., Higgs, S. T., Klimstra, W. B. & Ryman, K. D. 2012. Interferon-alpha/beta deficiency greatly exacerbates arthritogenic disease in mice infected with wild-type chikungunya virus but not with the cell culture-adapted live-attenuated 181/25 vaccine candidate. *Virology,* 425**,** 103-12.

Gardner, J., Anraku, I., Le, T. T., Larcher, T., Major, L., Roques, P., Schroder, W. A., Higgs, S. & Suhrbier, A. 2010. Chikungunya virus arthritis in adult wild-type mice. *J Virol,* 84**,** 8021-32.

Garoff, H., Huylebroeck, D., Robinson, A., Tillman, U. & Liljestrom, P. 1990. The signal sequence of the p62 protein of Semliki Forest virus is involved in initiation but not in completing chain translocation. *The Journal of cell biology,* 111**,** 867-76.

George, J. & Raju, R. 2000. Alphavirus RNA genome repair and evolution: molecular characterization of infectious sindbis virus isolates lacking a known conserved motif at the 3' end of the genome. *Journal of virology,* 74**,** 9776-85.

Gerardin, P., Barau, G., Michault, A., Bintner, M., Randrianaivo, H., Choker, G., Lenglet, Y., Touret, Y., Bouveret, A., Grivard, P., Le Roux, K., Blanc, S., Schuffenecker, I., Couderc, T., Arenzana-Seisdedos, F., Lecuit, M. & Robillard, P. Y. 2008. Multidisciplinary prospective study of mother-to-child chikungunya virus infections on the island of La Reunion. *PLoS medicine,* 5**,** e60.

Gerardin, P., Fianu, A., Michault, A., Mussard, C., Boussaid, K., Rollot, O., Grivard, P., Kassab, S., Bouquillard, E., Borgherini, G., Gauzere, B. A., Malvy, D., Breart, G. & Favier, F. 2013. Predictors of Chikungunya rheumatism: a prognostic survey ancillary to the TELECHIK cohort study. *Arthritis Res Ther,* 15**,** R9.

Gerosa, F., Baldani-Guerra, B., Nisii, C., Marchesini, V., Carra, G. & Trinchieri, G. 2002. Reciprocal activating interaction between natural killer cells and dendritic cells. *J Exp Med,* 195**,** 327-33.

Gifford, G. E. & Heller, E. 1963. Effect of Actinomycin D on Interferon Production by 'Active' and 'Inactive' Chikungunya Virus in Chick Cells. *Nature,* 200**,** 50-1.

Gong, J. H., Ratkay, L. G., Waterfield, J. D. & Clark-Lewis, I. 1997. An antagonist of monocyte chemoattractant protein 1 (MCP-1) inhibits arthritis in the MRL-lpr mouse model. *J Exp Med,* 186**,** 131-7.

Gouon-Evans, V., Rothenberg, M. E. & Pollard, J. W. 2000. Postnatal mammary gland development requires macrophages and eosinophils. *Development,* 127**,** 2269-82.

Gregoire, I. P., Richetta, C., Meyniel-Schicklin, L., Borel, S., Pradezynski, F., Diaz, O., Deloire, A., Azocar, O., Baguet, J., Le Breton, M., Mangeot, P. E., Navratil, V., Joubert, P. E., Flacher, M., Vidalain, P. O., Andre, P., Lotteau, V., Biard-Piechaczyk, M., Rabourdin-Combe, C. & Faure, M. 2011. IRGM is a common target of RNA viruses that subvert the autophagy network. *PLoS Pathog,* 7**,** e1002422.

Guabiraba, R., Marques, R. E., Besnard, A. G., Fagundes, C. T., Souza, D. G., Ryffel, B. & Teixeira, M. M. 2010. Role of the chemokine receptors CCR1, CCR2 and CCR4 in the pathogenesis of experimental dengue infection in mice. *PLoS One,* 5**,** e15680.

Guo, J., Hui, D. J., Merrick, W. C. & Sen, G. C. 2000. A new pathway of translational regulation mediated by eukaryotic initiation factor 3. *EMBO J,* 19**,** 6891-9.

Hardy, R. W. & Rice, C. M. 2005. Requirements at the 3' end of the sindbis virus genome for efficient synthesis of minus-strand RNA. *Journal of virology,* 79**,** 4630-9.

Harrison, V. R., Eckels, K. H., Bartelloni, P. J. & Hampton, C. 1971. Production and evaluation of a formalin-killed Chikungunya vaccine. *Journal of immunology,* 107**,** 643-7.

Hawman, D. W., Stoermer, K. A., Montgomery, S. A., Pal, P., Oko, L., Diamond, M. S. & Morrison, T. E. 2013. Chronic joint disease caused by persistent chikungunya virus infection is controlled by the adaptive immune response. *J Virol,* 87**,** 13878-88.

Her, Z., Malleret, B., Chan, M., Ong, E. K. S., Wong, S. C., Kwek, D. J. C., Tolou, H., Lin, R. T. P., Tambyah, P. A., Renia, L. & Ng, L. F. P. 2010. Active Infection of Human Blood Monocytes by Chikungunya Virus Triggers an Innate Immune Response. *The Journal of Immunology,* 184**,** 5903-5913.

Hoarau, J. J., Gay, F., Pelle, O., Samri, A., Jaffar-Bandjee, M. C., Gasque, P. & Autran, B. 2013. Identical Strength of the T Cell Responses against E2, nsP1 and Capsid CHIKV Proteins in Recovered and Chronic Patients after the Epidemics of 2005-2006 in La Reunion Island. *PLoS One,* 8**,** e84695.

Hoarau, J. J., Jaffar-Bandjee, M. C., Krejbich-Trotot, P., Das, T., Li-Pat-Yuen, G., Dassa, B., Denizot, M., Guichard, E., Ribera, A., Henni, T., Tallet, F., Moiton, M. P., Gauzere, B. A.,

Bruniquet, S., Jaffar Bandjee, Z., Morbidelli, P., Martigny, G., Jolivet, M., Gay, F., Grandadam, M., Tolou, H., Vieillard, V., Debre, P., Autran, B. & Gasque, P. 2010. Persistent Chronic Inflammation and Infection by Chikungunya Arthritogenic Alphavirus in Spite of a Robust Host Immune Response. *The Journal of Immunology,* 184**,** 5914-5927.

Hokeness, K. L., Kuziel, W. A., Biron, C. A. & Salazar-Mather, T. P. 2005. Monocyte chemoattractant protein-1 and CCR2 interactions are required for IFN-alpha/beta-induced inflammatory responses and antiviral defense in liver. *J Immunol,* 174**,** 1549-56.

Holzer, G. W., Coulibaly, S., Aichinger, G., Savidis-Dacho, H., Mayrhofer, J., Brunner, S., Schmid, K., Kistner, O., Aaskov, J. G., Falkner, F. G., Ehrlich, H., Barrett, P. N. & Kreil, T. R. 2011. Evaluation of an inactivated Ross River virus vaccine in active and passive mouse immunization models and establishment of a correlate of protection. *Vaccine,* 29**,** 4132-41.

Horwood, P., Bande, G., Dagina, R., Guillaumot, L., Aaskov, J. & Pavlin, B. 2013. The threat of chikungunya in Oceania. *Western Pac Surveill Response J,* 4**,** 8-10.

Hu, Y., Cheng, W., Cai, W., Yue, Y., Li, J. & Zhang, P. 2013. Advances in research on animal models of rheumatoid arthritis. *Clin Rheumatol,* 32**,** 161-5.

Iijima, N., Mattei, L. M. & Iwasaki, A. 2011. Recruited inflammatory monocytes stimulate antiviral Th1 immunity in infected tissue. *Proc Natl Acad Sci U S A,* 108**,** 284-9.

Isaacs, A. & Lindenmann, J. 1957. Virus interference. I. The interferon. *Proc R Soc Lond B Biol Sci,* 147**,** 258-67.

Ishak, K. G. 2000. Pathologic features of chronic hepatitis. A review and update. *Am J Clin Pathol,* 113**,** 40-55.

Jaffar-Bandjee, M. C., Das, T., Hoarau, J. J., Trotot, P. K., Denizot, M., Ribera, A., Roques, P. & Gasque, P. 2009. Chikungunya virus takes centre stage in virally induced arthritis: possible cellular and molecular mechanisms to pathogenesis. *Microbes and Infection***,** 1-13.

Jaffar-Bandjee, M. C., Ramful, D., Gauzere, B. A., Hoarau, J. J., Krejbich-Trotot, P., Robin, S., Ribera, A., Selambarom, J. & Gasque, P. 2010. Emergence and clinical insights into the pathology of Chikungunya virus infection. *Expert Review of Anti-infective Therapy,* 8**,** 987-996.

Jose, J., Snyder, J. E. & Kuhn, R. J. 2009. A structural and functional perspective of alphavirus replication and assembly. *Future Microbiol,* 4**,** 837-56.

Joubert, P. E., Werneke, S. W., De La Calle, C., Guivel-Benhassine, F., Giodini, A., Peduto, L., Levine, B., Schwartz, O., Lenschow, D. J. & Albert, M. L. 2012. Chikungunya virus-induced autophagy delays caspase-dependent cell death. *J Exp Med,* 209**,** 1029-47.

Juliano, S. A., O'meara, G. F., Morrill, J. R. & Cutwa, M. M. 2002. Desiccation and thermal tolerance of eggs and the coexistence of competing mosquitoes. *Oecologia,* 130**,** 458-469.

Kam, Y. W., Lum, F. M., Teo, T. H., Lee, W. W., Simarmata, D., Harjanto, S., Chua, C. L., Chan, Y. F., Wee, J. K., Chow, A., Lin, R. T., Leo, Y. S., Le Grand, R., Sam, I. C., Tong, J. C., Roques, P., Wiesmuller, K. H., Renia, L., Rotzschke, O. & Ng, L. F. 2012. Early neutralizing IgG response to Chikungunya virus in infected patients targets a dominant linear epitope on the E2 glycoprotein. *EMBO Mol Med,* 4**,** 330-43.

Katayama, M., Ohmura, K., Yukawa, N., Terao, C., Hashimoto, M., Yoshifuji, H., Kawabata, D., Fujii, T., Iwakura, Y. & Mimori, T. 2013. Neutrophils are essential as a source of IL-17 in the effector phase of arthritis. *PLoS One,* 8**,** e62231.

Keller, M. A. & Stiehm, E. R. 2000. Passive immunity in prevention and treatment of infectious diseases. *Clin Microbiol Rev,* 13**,** 602-14.

Kelvin, A. A., Banner, D., Silvi, G., Moro, M. L., Spataro, N., Gaibani, P., Cavrini, F., Pierro, A., Rossini, G., Cameron, M. J., Bermejo-Martin, J. F., Paquette, S. G., Xu, L., Danesh, A., Farooqui, A., Borghetto, I., Kelvin, D. J., Sambri, V. & Rubino, S. 2011. Inflammatory cytokine expression is associated with chikungunya virus resolution and symptom severity. *PLoS Negl Trop Dis,* 5**,** e1279.

Khan, A. H., Morita, K., Parquet Md Mdel, C., Hasebe, F., Mathenge, E. G. & Igarashi, A. 2002. Complete nucleotide sequence of chikungunya virus and evidence for an internal polyadenylation site. *The Journal of general virology,* 83**,** 3075-84.

Kielian, M. & Jungerwirth, S. 1990. Mechanisms of enveloped virus entry into cells. *Molecular biology & medicine,* 7**,** 17-31.

Kielian, M. & Rey, F. A. 2006. Virus membrane-fusion proteins: more than one way to make a hairpin. *Nature reviews. Microbiology,* 4**,** 67-76.

Kimura, T. & Griffin, D. E. 2000. The role of CD8(+) T cells and major histocompatibility complex class I expression in the central nervous system of mice infected with neurovirulent Sindbis virus. *J Virol,* 74**,** 6117-25.

Kistner, O., Barrett, N., Brühmann, A., Reiter, M., Mundt, W., Savidis-Dacho, H., Schober-Bendixen, S., Dorner, F. & Aaskov, J. 2007. The preclinical testing of a formaldehyde inactivated Ross River virus vaccine designed for use in humans. *Vaccine,* 25**,** 4845-4852.

Kitamura, D. & Rajewsky, K. 1992. Targeted disruption of mu chain membrane exon causes loss of heavy-chain allelic exclusion. *Nature,* 356**,** 154-6.

Komuro, A., Bamming, D. & Horvath, C. M. 2008. Negative regulation of cytoplasmic RNA-mediated antiviral signaling. *Cytokine,* 43**,** 350-8.

Krejbich-Trotot, P., Denizot, M., Hoarau, J. J., Jaffar-Bandjee, M. C., Das, T. & Gasque, P. 2011. Chikungunya virus mobilizes the apoptotic machinery to invade host cell defenses. *FASEB J,* 25**,** 314-25.

Kuhn, R., Lohler, J., Rennick, D., Rajewsky, K. & Muller, W. 1993. Interleukin-10-deficient mice develop chronic enterocolitis. *Cell,* 75**,** 263-74.

Kuhn, R. J. 2007. Togaviridae: THe Viruses and Their Replication *In:* FIELDS, B. N., KNIPE, D. M. & HOWLEY, P. M. (eds.) *Fields' virology.* 5th ed. Philadelphia: Wolters kluwer/Lippincott Williams & Wilkins.

Kuhn, R. J., Niesters, H. G., Hong, Z. & Strauss, J. H. 1991. Infectious RNA transcripts from Ross River virus cDNA clones and the construction and characterization of defined chimeras with Sindbis virus. *Virology,* 182**,** 430-41.

Kularatne, S. A., Weerasinghe, S. C., Gihan, C., Wickramasinghe, S., Dharmarathne, S., Abeyrathna, A. & Jayalath, T. 2012. Epidemiology, clinical manifestations, and long-term outcomes of a major outbreak of chikungunya in a hamlet in sri lanka, in 2007: a longitudinal cohort study. *J Trop Med,* 2012**,** 639178.

Kumar, M., Sudeep, A. B. & Arankalle, V. A. 2012. Evaluation of recombinant E2 protein-based and whole-virus inactivated candidate vaccines against chikungunya virus. *Vaccine,* 30**,** 6142-9.

Kumar, N. P., Joseph, R., Kamaraj, T. & Jambulingam, P. 2008. A226V mutation in virus during the 2007 chikungunya outbreak in Kerala, India. *Journal of General Virology,* 89**,** 1945-1948.

Labadie, K., Larcher, T., Joubert, C., Mannioui, A., Delache, B., Brochard, P., Guigand, L., Dubreil, L., Lebon, P., Verrier, B., De Lamballerie, X., Suhrbier, A., Cherel, Y., Le Grand, R. & Roques, P. 2010. Chikungunya disease in nonhuman primates involves long-term viral persistence in macrophages. *J Clin Invest,* 120**,** 894-906.

Lanier, L. L. 2008. Evolutionary struggles between NK cells and viruses. *Nat Rev Immunol,* 8**,** 259-68.

Larrieu, S., Pouderoux, N., Pistone, T., Filleul, L., Receveur, M. C., Sissoko, D., Ezzedine, K. & Malvy, D. 2010. Factors associated with persistence of arthralgia among Chikungunya virus-infected travellers: report of 42 French cases. *J Clin Virol,* 47**,** 85-8.

Lebre, M. C., Vergunst, C. E., Choi, I. Y., Aarrass, S., Oliveira, A. S., Wyant, T., Horuk, R., Reedquist, K. A. & Tak, P. P. 2011. Why CCR2 and CCR5 blockade failed and why CCR1 blockade might still be effective in the treatment of rheumatoid arthritis. *PLoS One,* 6**,** e21772.

Lebrun, G., Chadda, K., Reboux, A. H., Martinet, O. & Gauzere, B. A. 2009. Guillain-Barre syndrome after chikungunya infection. *Emerging infectious diseases,* 15**,** 495-6.

Ledgerwood, J. E. 2013. *Chikungunya Virus Vaccine Trial in Healthy Adults* [Online]. Available: http://clinicaltrials.gov/ct2/show/NCT01489358?term=VLP+CHIKV&rank=1 [Accessed 26 March 2013.

Lee, B. O., Rangel-Moreno, J., Moyron-Quiroz, J. E., Hartson, L., Makris, M., Sprague, F., Lund, F. E. & Randall, T. D. 2005. CD4 T cell-independent antibody response promotes resolution of primary influenza infection and helps to prevent reinfection. *J Immunol,* 175**,** 5827-38.

Lee, C. Y., Kam, Y. W., Fric, J., Malleret, B., Koh, E. G., Prakash, C., Huang, W., Lee, W. W., Lin, C., Lin, R. T., Renia, L., Wang, C. I., Ng, L. F. & Warter, L. 2011. Chikungunya virus neutralization antigens and direct cell-to-cell transmission are revealed by human antibody-escape mutants. *PLoS Pathog,* 7**,** e1002390.

Lemant, J., Boisson, V., Winer, A., Thibault, L., Andre, H., Tixier, F., Lemercier, M., Antok, E., Cresta, M. P., Grivard, P., Besnard, M., Rollot, O., Favier, F., Huerre, M., Campinos, J. L. & Michault, A. 2008. Serious acute chikungunya virus infection requiring intensive care during the Reunion Island outbreak in 2005-2006. *Critical care medicine,* 36**,** 2536-41.

Levitt, N. H., Ramsburg, H. H., Hasty, S. E., Repik, P. M., Cole, F. E., Jr. & Lupton, H. W. 1986. Development of an attenuated strain of chikungunya virus for use in vaccine production. *Vaccine,* 4**,** 157-62.

Lidbury, B. A., Simeonovic, C., Maxwell, G. E., Marshall, I. D. & Hapel, A. J. 2000. Macrophage-induced muscle pathology results in morbidity and mortality for Ross River virus-infected mice. *J Infect Dis,* 181**,** 27-34.

Lidbury, B. A., Rulli, N. E., Suhrbier, A., Smith, P. N., Mccoll, S. R., Cunningham, A. L., Tarkowski, A., Van Rooijen, N., Fraser, R. J. & Mahalingam, S. 2008. Macrophage-derived proinflammatory factors contribute to the development of arthritis and myositis after infection with an arthrogenic alphavirus. *J Infect Dis,* 197**,** 1585-93.

Lidbury, B. A., Rulli, N. E., Musso, C. M., Cossetto, S. B., Zaid, A., Suhrbier, A., Rothenfluh, H. S., Rolph, M. S. & Mahalingam, S. 2011. Identification and characterization of a ross river virus variant that grows persistently in macrophages, shows altered disease kinetics in a mouse model, and exhibits resistance to type I interferon. *J Virol,* 85**,** 5651-63.

Lim, J. K., Obara, C. J., Rivollier, A., Pletnev, A. G., Kelsall, B. L. & Murphy, P. M. 2011. Chemokine receptor Ccr2 is critical for monocyte accumulation and survival in West Nile virus encephalitis. *J Immunol,* 186**,** 471-8.

Lin, K. L., Sweeney, S., Kang, B. D., Ramsburg, E. & Gunn, M. D. 2011. CCR2-antagonist prophylaxis reduces pulmonary immune pathology and markedly improves survival during influenza infection. *J Immunol,* 186**,** 508-15.

Ling, Z. Q., Wang, Y., Mukaisho, K., Hattori, T., Tatsuta, T., Ge, M. H., Jin, L., Mao, W. M. & Sugihara, H. 2010. Novel statistical framework to identify differentially expressed genes allowing transcriptomic background differences. *Bioinformatics,* 26**,** 1431-6.

Linn, M. L., Aaskov, J. G. & Suhrbier, A. 1996. Antibody-dependent enhancement and persistence in macrophages of an arbovirus associated with arthritis. *J Gen Virol,* 77 (Pt 3)**,** 407-11.

Linn, M. L., Mateo, L., Gardner, J. & Suhrbier, A. 1998. Alphavirus-specific cytotoxic T lymphocytes recognize a cross-reactive epitope from the capsid protein and can eliminate virus from persistently infected macrophages. *J Virol,* 72**,** 5146-53.

Lipscomb, M. W., Chen, L., Taylor, J. L., Goldbach, C., Watkins, S. C., Kalinski, P., Butterfield, L. H., Wesa, A. K. & Storkus, W. J. 2009. Ectopic T-bet expression licenses dendritic cells for IL-12-independent priming of type 1 T cells in vitro. *J Immunol,* 183**,** 7250-8.

Lobigs, M. & Garoff, H. 1990. Fusion function of the Semliki Forest virus spike is activated by proteolytic cleavage of the envelope glycoprotein precursor p62. *Journal of virology,* 64**,** 1233-40.

Lodoen, M. B. & Lanier, L. L. 2005. Viral modulation of NK cell immunity. *Nat Rev Microbiol,* 3**,** 59-69.

London, A., Benhar, I., Mattapallil, M. J., Mack, M., Caspi, R. R. & Schwartz, M. 2013. Functional macrophage heterogeneity in a mouse model of autoimmune central nervous system pathology. *J Immunol,* 190**,** 3570-8.

Lopez, S., Yao, J. S., Kuhn, R. J., Strauss, E. G. & Strauss, J. H. 1994. Nucleocapsid-glycoprotein interactions required for assembly of alphaviruses. *Journal of virology,* 68**,** 1316-23.

Lotfi, R., Herzog, G. I., Demarco, R. A., Beer-Stolz, D., Lee, J. J., Rubartelli, A., Schrezenmeier, H. & Lotze, M. T. 2009. Eosinophils oxidize damage-associated molecular pattern molecules derived from stressed cells. *J Immunol,* 183**,** 5023-31.

Lulla, A., Lulla, V. & Merits, A. 2012. Macromolecular assembly-driven processing of the 2/3 cleavage site in the alphavirus replicase polyprotein. *J Virol,* 86**,** 553-65.

Lum, F. M., Teo, T. H., Lee, W. W., Kam, Y. W., Renia, L. & Ng, L. F. 2013. An essential role of antibodies in the control of Chikungunya virus infection. *J Immunol,* 190**,** 6295-302.

Lundstrom, K. 2014. Alphavirus-based vaccines. *Viruses,* 6**,** 2392-415.

Luo, L., Wang, Y., Feng, Q., Zhang, H., Xue, B., Shen, J., Ye, Y., Han, X., Ma, H., Xu, J., Chen, D. & Yin, Z. 2009. Recombinant protein glutathione S-transferases P1 attenuates inflammation in mice. *Mol Immunol,* 46**,** 848-57.

Madsen, L., Labrecque, N., Engberg, J., Dierich, A., Svejgaard, A., Benoist, C., Mathis, D. & Fugger, L. 1999. Mice lacking all conventional MHC class II genes. *Proc Natl Acad Sci U S A,* 96**,** 10338-43.

Mahalingam, S. & Lidbury, B. A. 2002. Suppression of lipopolysaccharide-induced antiviral transcription factor (STAT-1 and NF-kappa B) complexes by antibody-dependent enhancement of macrophage infection by Ross River virus. *Proc Natl Acad Sci U S A,* 99**,** 13819-24.

Mallilankaraman, K., Shedlock, D. J., Bao, H., Kawalekar, O. U., Fagone, P., Ramanathan, A. A., Ferraro, B., Stabenow, J., Vijayachari, P., Sundaram, S. G., Muruganandam, N., Sarangan, G., Srikanth, P., Khan, A. S., Lewis, M. G., Kim, J. J., Sardesai, N. Y., Muthumani, K. & Weiner, D. B. 2011. A DNA Vaccine against Chikungunya Virus Is Protective in Mice and Induces Neutralizing Antibodies in Mice and Nonhuman Primates. *PLoS Neglected Tropical Diseases,* 5**,** e928.

Manimunda, S. P., Mavalankar, D., Bandyopadhyay, T. & Sugunan, A. P. 2011. Chikungunya epidemic-related mortality. *Epidemiol Infect,* 139**,** 1410-2.

Marchette, N. J., Rudnick, A., Garcia, R. & Macvean, D. W. 1978. Alphaviruses in Peninusular Malaysia: I. Virus isolations and animal serology. *The Southeast Asian journal of tropical medicine and public health,* 9**,** 317-29.

Martinez, F. O., Helming, L. & Gordon, S. 2009. Alternative activation of macrophages: an immunologic functional perspective. *Annu Rev Immunol,* 27**,** 451-83.

Mathew, A. J., Goyal, V., George, E., Thekkemuriyil, D. V., Jayakumar, B., Chopra, A. & Trivandrum, C. S. G. 2011. Rheumatic-musculoskeletal pain and disorders in a naive group of individuals 15 months following a Chikungunya viral epidemic in south India: a population based observational study. *Int J Clin Pract,* 65**,** 1306-12.

Mavalankar, D., Shastri, P., Bandyopadhyay, T., Parmar, J. & Ramani, K. V. 2008. Increased mortality rate associated with chikungunya epidemic, Ahmedabad, India. *Emerg Infect Dis,* 14**,** 412-5.

Maxwell, M. A., Cleasby, M. E., Harding, A., Stark, A., Cooney, G. J. & Muscat, G. E. 2005. Nur77 regulates lipolysis in skeletal muscle cells. Evidence for cross-talk between the beta-adrenergic and an orphan nuclear hormone receptor pathway. *J Biol Chem,* 280**,** 12573-84.

Mcgarry, M. P. & Stewart, C. C. 1991. Murine eosinophil granulocytes bind the murine macrophage-monocyte specific monoclonal antibody F4/80. *J Leukoc Biol,* 50**,** 471-8.

Mcintosh, B. M., Paterson, H. E., Donaldson, J. M. & De Sousa, J. 1963. Chikungunya virus: viral susceptibility and transmission studies with some vertebrates and mosquitoes. *S. Afr. J. M ed. Sci.,* 28**,** 45-52.

Mcintosh, B. M., Paterson, H. E., Mcgillivray, G. & Desousa, J. 1964. Further Studies on the Chikungunya Outbreak in Southern Rhodesia in 1962. I. Mosquitoes, Wild Primates and Birds in Relation to the Epidemic. *Annals of tropical medicine and parasitology,* 58**,** 45-51.

Messaoudi, I., Vomaske, J., Totonchy, T., Kreklywich, C. N., Haberthur, K., Springgay, L., Brien, J. D., Diamond, M. S., Defilippis, V. R. & Streblow, D. N. 2013. Chikungunya virus infection results in higher and persistent viral replication in aged rhesus macaques due to defects in anti-viral immunity. *PLoS Negl Trop Dis,* 7**,** e2343.

Metz, S. W., Gardner, J., Geertsema, C., Le, T. T., Goh, L., Vlak, J. M., Suhrbier, A. & Pijlman, G. P. 2013a. Effective chikungunya virus-like particle vaccine produced in insect cells. *PLoS Negl Trop Dis,* 7**,** e2124.

Metz, S. W., Martina, B. E., Van Den Doel, P., Geertsema, C., Osterhaus, A. D., Vlak, J. M. & Pijlman, G. P. 2013b. Chikungunya virus-like particles are more immunogenic in a lethal AG129 mouse model compared to glycoprotein E1 or E2 subunits. *Vaccine,* 31**,** 6092-6.

Min, S.-H., Wang, Y., Gonsiorek, W., Anilkumar, G., Kozlowski, J., Lundell, D., Fine, J. S. & Grant, E. P. 2010. Pharmacological targeting reveals distinct roles for CXCR2/CXCR1 and

CCR2 in a mouse model of arthritis. *Biochemical and Biophysical Research Communications,* 391**,** 1080-1086.

Mitchison, N. A. 2004. T-cell-B-cell cooperation. *Nat Rev Immunol,* 4**,** 308-12.

Miyake, Y. & Yamasaki, S. 2012. Sensing necrotic cells. *Adv Exp Med Biol,* 738**,** 144-52.

Mogal, A. & Abdulkadir, S. A. 2006. Effects of Histone Deacetylase Inhibitor (HDACi); Trichostatin-A (TSA) on the expression of housekeeping genes. *Mol Cell Probes,* 20**,** 81-6.

Mombaerts, P., Iacomini, J., Johnson, R. S., Herrup, K., Tonegawa, S. & Papaioannou, V. E. 1992. RAG-1-deficient mice have no mature B and T lymphocytes. *Cell,* 68**,** 869-77.

Montgomery, R. R., Booth, C. J., Wang, X., Blaho, V. A., Malawista, S. E. & Brown, C. R. 2007. Recruitment of macrophages and polymorphonuclear leukocytes in L:yme carditis. *Infect Immun,* 75**,** 613-20.

Moro, M. L., Grilli, E., Corvetta, A., Silvi, G., Angelini, R., Mascella, F., Miserocchi, F., Sambo, P., Finarelli, A. C., Sambri, V., Gagliotti, C., Massimiliani, E., Mattivi, A., Pierro, A. M., Macini, P. & Study Group "Infezioni Da Chikungunya In, E.-R. 2012. Long-term chikungunya infection clinical manifestations after an outbreak in Italy: a prognostic cohort study. *J Infect,* 65**,** 165-72.

Morrison, T. E., Fraser, R. J., Smith, P. N., Mahalingam, S. & Heise, M. T. 2007. Complement contributes to inflammatory tissue destruction in a mouse model of Ross River virus-induced disease. *J Virol,* 81**,** 5132-43.

Morrison, T. E., Oko, L., Montgomery, S. A., Whitmore, A. C., Lotstein, A. R., Gunn, B. M., Elmore, S. A. & Heise, M. T. 2011. A Mouse Model of Chikungunya Virus–Induced Musculoskeletal Inflammatory Disease. *AJPA,* 178**,** 32-40.

Morrison, T. E., Whitmore, A. C., Shabman, R. S., Lidbury, B. A., Mahalingam, S. & Heise, M. T. 2006. Characterization of Ross River virus tropism and virus-induced inflammation in a mouse model of viral arthritis and myositis. *J Virol,* 80**,** 737-49.

Mosser, D. M. & Edwards, J. P. 2008. Exploring the full spectrum of macrophage activation. *Nature Publishing Group,* 8**,** 958-969.

Murray, P. J. & Wynn, T. A. 2011. Protective and pathogenic functions of macrophage subsets. *Nature Reviews Immunology,* 11**,** 723-737.

Murray, P. J., Young, R. A. & Daley, G. Q. 1998. Hematopoietic remodeling in interferon-gamma-deficient mice infected with mycobacteria. *Blood,* 91**,** 2914-24.

Muthumani, K., Lankaraman, K. M., Laddy, D. J., Sundaram, S. G., Chung, C. W., Sako, E., Wu, L., Khan, A., Sardesai, N., Kim, J. J., Vijayachari, P. & Weiner, D. B. 2008. Immunogenicity of novel consensus-based DNA vaccines against Chikungunya virus. *Vaccine,* 26**,** 5128-5134.

Nakaya, H. I., Gardner, J., Poo, Y. S., Major, L., Pulendran, B. & Suhrbier, A. 2012. Gene profiling of chikungunya virus arthritis reveals significant overlap with rheumatoid arthritis. *Arthritis Rheum,* 64**,** 3553-3563.

Nakgoi, K., Nitatpattana, N., Wajjwalku, W., Pongsopawijit, P., Kaewchot, S., Yoksan, S., Siripolwat, V., Souris, M. & Gonzalez, J. P. 2013. Dengue, Japanese encephalitis and Chikungunya virus antibody prevalence among captive monkey (Macaca nemestrina) colonies of Northern Thailand. *Am J Primatol*.

Nargi-Aizenman, J. L., Simbulan-Rosenthal, C. M., Kelly, T. A., Smulson, M. E. & Griffin, D. E. 2002. Rapid activation of poly(ADP-ribose) polymerase contributes to Sindbis virus and staurosporine-induced apoptotic cell death. *Virology,* 293**,** 164-71.

Ng, L. F. P., Chow, A., Sun, Y.-J., Kwek, D. J. C., Lim, P.-L., Dimatatac, F., Ng, L. C., Ooi, E.-E., Choo, K.-H., Her, Z., Kourilsky, P. & Leo, Y.-S. 2009. IL-1β, IL-6, and RANTES as Biomarkers of Chikungunya Severity. *PLoS ONE,* 4**,** e4261.

Nikbakht, N., Shen, S. & Manser, T. 2013. Cutting edge: Macrophages are required for localization of antigen-activated B cells to the follicular perimeter and the subsequent germinal center response. *J Immunol,* 190**,** 4923-7.

Ohl, K. & Tenbrock, K. 2011. Inflammatory cytokines in systemic lupus erythematosus. *J Biomed Biotechnol,* 2011**,** 432595.

Ortega-Gomez, A., Perretti, M. & Soehnlein, O. 2013. Resolution of inflammation: an integrated view. *EMBO Mol Med,* 5**,** 661-74.

Ou, J. H., Rice, C. M., Dalgarno, L., Strauss, E. G. & Strauss, J. H. 1982. Sequence studies of several alphavirus genomic RNAs in the region containing the start of the subgenomic RNA. *Proc Natl Acad Sci U S A,* 79**,** 5235-9.

Ou, J. H., Strauss, E. G. & Strauss, J. H. 1981. Comparative studies of the 3'-terminal sequences of several alpha virus RNAs. *Virology,* 109**,** 281-9.

Ou, J. H., Strauss, E. G. & Strauss, J. H. 1983. The 5'-terminal sequences of the genomic RNAs of several alphaviruses. *Journal of molecular biology,* 168**,** 1-15.

Ozden, S., Huerre, M., Riviere, J. P., Coffey, L. L., Afonso, P. V., Mouly, V., De Monredon, J., Roger, J. C., El Amrani, M., Yvin, J. L., Jaffar, M. C., Frenkiel, M. P., Sourisseau, M., Schwartz, O., Butler-Browne, G., Despres, P., Gessain, A. & Ceccaldi, P. E. 2007. Human muscle satellite cells as targets of Chikungunya virus infection. *PLoS One,* 2**,** e527.

Padmakumar, B., Jayan, J. B., Menon, R. M. R., Krishnankutty, B., Payippallil, R. & Nisha, R. S. 2009. Comparative evaluation of four therapeutic regimes in chikungunya arthritis: a prospective randomized parallel-group study. *Indian Journal of Rheumatology,* 4**,** 94-101.

Pal, P., Dowd, K. A., Brien, J. D., Edeling, M. A., Gorlatov, S., Johnson, S., Lee, I., Akahata, W., Nabel, G. J., Richter, M. K., Smit, J. M., Fremont, D. H., Pierson, T. C., Heise, M. T. &

Diamond, M. S. 2013. Development of a highly protective combination monoclonal antibody therapy against Chikungunya virus. *PLoS Pathog,* 9**,** e1003312.

Palha, N., Guivel-Benhassine, F., Briolat, V., Lutfalla, G., Sourisseau, M., Ellett, F., Wang, C. H., Lieschke, G. J., Herbomel, P., Schwartz, O. & Levraud, J. P. 2013. Real-time whole-body visualization of Chikungunya Virus infection and host interferon response in zebrafish. *PLoS Pathog,* 9**,** e1003619.

Panee, J. 2012. Monocyte Chemoattractant Protein 1 (MCP-1) in obesity and diabetes. *Cytokine,* 60**,** 1-12.

Partidos, C. D., Paykel, J., Weger, J., Borland, E. M., Powers, A. M., Seymour, R., Weaver, S. C., Stinchcomb, D. T. & Osorio, J. E. 2012. Cross-protective immunity against o'nyong-nyong virus afforded by a novel recombinant chikungunya vaccine. *Vaccine,* 30**,** 4638-43.

Pastorino, B., Muyembe-Tamfum, J. J., Bessaud, M., Tock, F., Tolou, H., Durand, J. P. & Peyrefitte, C. N. 2004. Epidemic resurgence of Chikungunya virus in democratic Republic of the Congo: identification of a new central African strain. *J Med Virol,* 74**,** 277-82.

Paul, S. D. & Singh, K. R. 1968. Experimental infection of Macaca radiata with Chikungunya virus and transmission of virus by mosquitoes. *The Indian journal of medical research,* 56**,** 802-11.

Peck, R., Brown, A. & Wust, C. J. 1979. In vitro heterologous cytotoxicity by T effector cells from mice immunized with Sindbis virus. *J Immunol,* 123**,** 1763-6.

Perri, S., Driver, D. A., Gardner, J. P., Sherrill, S., Belli, B. A., Dubensky, T. W., Jr. & Polo, J. M. 2000. Replicon vectors derived from Sindbis virus and Semliki forest virus that establish persistent replication in host cells. *J Virol,* 74**,** 9802-7.

Petitdemange, C., Becquart, P., Wauquier, N., Beziat, V., Debre, P., Leroy, E. M. & Vieillard, V. 2011. Unconventional repertoire profile is imprinted during acute chikungunya infection for natural killer cells polarization toward cytotoxicity. *PLoS Pathog,* 7**,** e1002268.

Pevida, M., Gonzalez-Rodriguez, S., Lastra, A., Hidalgo, A., Menendez, L. & Baamonde, A. 2012. CCL2 released at tumoral level contributes to the hyperalgesia evoked by intratibial inoculation of NCTC 2472 but not B16-F10 cells in mice. *Naunyn Schmiedebergs Arch Pharmacol,* 385**,** 1053-61.

Pfeffer, M., Kinney, R. M. & Kaaden, O. R. 1998. The alphavirus 3'-nontranslated region: size heterogeneity and arrangement of repeated sequence elements. *Virology,* 240**,** 100-8.

Pialoux, G., Gauzere, B. A., Jaureguiberry, S. & Strobel, M. 2007. Chikungunya, an epidemic arbovirosis. *Lancet Infect Dis,* 7**,** 319-27.

Pialoux, G., Gauzere, B. A. & Strobel, M. 2006. [Chikungunya virus infection: review through an epidemic]. *Med Mal Infect,* 36**,** 253-63.

Pierre, V., Filleul, L., Solet, J. L., Renault, P., Sissoko, D. & Lassalle, C. 2006. [Chikungunya epidemic on Reunion Island, 2005-2006]. *Presse medicale,* 35**,** 1188-9; author reply 1189.

Plante, K., Wang, E., Partidos, C. D., Weger, J., Gorchakov, R., Tsetsarkin, K., Borland, E. M., Powers, A. M., Seymour, R., Stinchcomb, D. T., Osorio, J. E., Frolov, I. & Weaver, S. C. 2011. Novel Chikungunya Vaccine Candidate with an IRES-Based Attenuation and Host Range Alteration Mechanism. *PLoS Pathogens,* 7**,** e1002142.

Plaskon, N. E., Adelman, Z. N. & Myles, K. M. 2009. Accurate strand-specific quantification of viral RNA. *PLoS One,* 4**,** e7468.

Poo, Y.S**.**, Rudd, PA, Gardner, J., Wilson, J., Larcher, T., Colle, M.A., Le, T.T., Nakaya, H.I., Warrilow, D., Allcock, R., Bielefeldt-Ohmannm, H., Lopez, A., Suhrbier, A. (submitted) Immune factors involved in acute and chronic chikungunya virus infection.

Popivanova, B. K., Kostadinova, F. I., Furuichi, K., Shamekh, M. M., Kondo, T., Wada, T., Egashira, K. & Mukaida, N. 2009. Blockade of a chemokine, CCL2, reduces chronic colitis-associated carcinogenesis in mice. *Cancer Res,* 69**,** 7884-92.

Powers, A. M., Brault, A. C., Shirako, Y., Strauss, E. G., Kang, W., Strauss, J. H. & Weaver, S. C. 2001. Evolutionary relationships and systematics of the alphaviruses. *Journal of virology,* 75**,** 10118-31.

Powers, A. M. & Logue, C. H. 2007. Changing patterns of chikungunya virus: re-emergence of a zoonotic arbovirus. *The Journal of general virology,* 88**,** 2363-77.

Prentice, H. A. & Tang, J. 2012. HIV-1 dynamics: a reappraisal of host and viral factors, as well as methodological issues. *Viruses,* 4**,** 2080-96.

Prow, T. W., Chen, X., Prow, N. A., Fernando, G. J., Tan, C. S., Raphael, A. P., Chang, D., Ruutu, M. P., Jenkins, D. W., Pyke, A., Crichton, M. L., Raphaelli, K., Goh, L. Y., Frazer, I. H., Roberts, M. S., Gardner, J., Khromykh, A. A., Suhrbier, A., Hall, R. A. & Kendall, M. A. 2010. Nanopatch-targeted skin vaccination against West Nile Virus and Chikungunya virus in mice. *Small,* 6**,** 1776-84.

Pushko, P., Parker, M., Ludwig, G. V., Davis, N. L., Johnston, R. E. & Smith, J. F. 1997. Replicon-helper systems from attenuated Venezuelan equine encephalitis virus: expression of heterologous genes in vitro and immunization against heterologous pathogens in vivo. *Virology,* 239**,** 389-401.

Quinones, M. P., Ahuja, S. K., Jimenez, F., Schaefer, J., Garavito, E., Rao, A., Chenaux, G., Reddick, R. L., Kuziel, W. A. & Ahuja, S. S. 2004. Experimental arthritis in CC chemokine receptor 2-null mice closely mimics severe human rheumatoid arthritis. *J Clin Invest,* 113**,** 856-66.

Rampersad, R. R., Tarrant, T. K., Vallanat, C. T., Quintero-Matthews, T., Weeks, M. F., Esserman, D. A., Clark, J., Di Padova, F., Patel, D. D., Fong, A. M. & Liu, P. 2011. Enhanced Th17-cell responses render CCR2-deficient mice more susceptible for autoimmune arthritis. *PLoS One,* 6**,** e25833.

Randall, K. L., Chan, S. S., Ma, C. S., Fung, I., Mei, Y., Yabas, M., Tan, A., Arkwright, P. D., Al Suwairi, W., Lugo Reyes, S. O., Yamazaki-Nakashimada, M. A., Garcia-Cruz Mde, L., Smart, J. M., Picard, C., Okada, S., Jouanguy, E., Casanova, J. L., Lambe, T., Cornall, R. J., Russell, S., Oliaro, J., Tangye, S. G., Bertram, E. M. & Goodnow, C. C. 2011. DOCK8 deficiency impairs CD8 T cell survival and function in humans and mice. *J Exp Med,* 208**,** 2305-20.

Reed, L. J. & Muench, H. 1938. A SIMPLE METHOD OF ESTIMATING FIFTY PER CENT ENDPOINTS. *American Journal of Epidemiology,* 27**,** 493-497.

Renault, P., Solet, J. L., Sissoko, D., Balleydier, E., Larrieu, S., Filleul, L., Lassalle, C., Thiria, J., Rachou, E., De Valk, H., Ilef, D., Ledrans, M., Quatresous, I., Quenel, P. & Pierre, V. 2007. A major epidemic of chikungunya virus infection on Reunion Island, France, 2005-2006. *Am J Trop Med Hyg,* 77**,** 727-31.

Robles, F. 2014. *Virus Advances Through East Caribbean* [Online]. New York Times. Available: http://www.nytimes.com/2014/02/09/world/americas/virus-advances-through-east-caribbean.html?_r=0 [Accessed 18 February 2014 2014].

Ross, R. W. 1956. The Newala epidemic. III. The virus: isolation, pathogenic properties and relationship to the epidemic. *The Journal of hygiene,* 54**,** 177-91.

Roy, C. J., Adams, A. P., Wang, E., Plante, K., Gorchakov, R., Seymour, R. L., Vinet-Oliphant, H. & Weaver, S. C. 2014. Chikungunya Vaccine Candidate is Highly Attenuated and Protects Nonhuman Primates Against Telemetrically-monitored Disease Following a Single Dose. *J Infect Dis*.

Ruan, Q., Kameswaran, V., Zhang, Y., Zheng, S., Sun, J., Wang, J., Devirgiliis, J., Liou, H. C., Beg, A. A. & Chen, Y. H. 2011. The Th17 immune response is controlled by the Rel-RORgamma-RORgamma T transcriptional axis. *J Exp Med,* 208**,** 2321-33.

Rudd, P. A., Wilson, J., Gardner, J., Larcher, T., Babarit, C., Le, T. T., Anraku, I., Kumagai, Y., Loo, Y. M., Gale, M., Akira, S., Khromykh, A. A. & Suhrbier, A. 2012. Interferon Response Factors 3 and 7 Protect against Chikungunya Virus Hemorrhagic Fever and Shock. *Journal of Virology,* 86**,** 9888-9898.

Rulli, N. E., Guglielmotti, A., Mangano, G., Rolph, M. S., Apicella, C., Zaid, A., Suhrbier, A. & Mahalingam, S. 2009. Amelioration of alphavirus-induced arthritis and myositis in a mouse model by treatment with bindarit, an inhibitor of monocyte chemotactic proteins. *Arthritis Rheum,* 60**,** 2513-23.

Rulli, N. E., Rolph, M. S., Srikiatkhachorn, A., Anantapreecha, S., Guglielmotti, A. & Mahalingam, S. 2011. Protection from arthritis and myositis in a mouse model of acute chikungunya virus disease by bindarit, an inhibitor of monocyte chemotactic protein-1 synthesis. *J Infect Dis,* 204**,** 1026-30.Ryman, K. D., Klimstra, W. B., Nguyen, K. B., Biron, C. A. & Johnston, R. E. 2000. Alpha/beta interferon protects adult mice from fatal Sindbis virus infection and is an important determinant of cell and tissue tropism. *J Virol,* 74**,** 3366-78.

Ryman, K. D., Meier, K. C., Gardner, C. L., Adegboyega, P. A. & Klimstra, W. B. 2007. Non-pathogenic Sindbis virus causes hemorrhagic fever in the absence of alpha/beta and gamma interferons. *Virology,* 368**,** 273-85.

Ryman, K. D. & Klimstra, W. B. 2008. Host responses to alphavirus infection. *Immunol Rev,* 225**,** 27-45.

Sadik, C. D., Kim, N. D., Iwakura, Y. & Luster, A. D. 2012. Neutrophils orchestrate their own recruitment in murine arthritis through C5aR and FcgammaR signaling. *Proc Natl Acad Sci U S A,* 109**,** E3177-85.

Sato, N., Ahuja, S. K., Quinones, M., Kostecki, V., Reddick, R. L., Melby, P. C., Kuziel, W. A. & Ahuja, S. S. 2000. CC chemokine receptor (CCR)2 is required for langerhans cell migration and localization of T helper cell type 1 (Th1)-inducing dendritic cells. Absence of CCR2 shifts the Leishmania major-resistant phenotype to a susceptible state dominated by Th2 cytokines, b cell outgrowth, and sustained neutrophilic inflammation. *J Exp Med,* 192**,** 205-18.

Sawanobori, Y., Ueha, S., Kurachi, M., Shimaoka, T., Talmadge, J. E., Abe, J., Shono, Y., Kitabatake, M., Kakimi, K., Mukaida, N. & Matsushima, K. 2008. Chemokine-mediated rapid turnover of myeloid-derived suppressor cells in tumor-bearing mice. *Blood,* 111**,** 5457-66.

Sawicki, D. L. & Sawicki, S. G. 1980. Short-lived minus-strand polymerase for Semliki Forest virus. *J Virol,* 34**,** 108-18.

Schaffner, F., Bellini, R., Petric, D., Scholte, E. J., Zeller, H. & Rakotoarivony, L. M. 2013. Development of guidelines for the surveillance of invasive mosquitoes in Europe. *Parasit Vectors,* 6**,** 209.

Schilte, C., Couderc, T., Chretien, F., Sourisseau, M., Gangneux, N., Guivel-Benhassine, F., Kraxner, A., Tschopp, J., Higgs, S., Michault, A., Arenzana-Seisdedos, F., Colonna, M., Peduto, L., Schwartz, O., Lecuit, M. & Albert, M. L. 2010. Type I IFN controls chikungunya virus via its action on nonhematopoietic cells. *Journal of Experimental Medicine,* 207**,** 429-442.

Schilte, C., Staikowsky, F., Couderc, T., Madec, Y., Carpentier, F., Kassab, S., Albert, M. L., Lecuit, M. & Michault, A. 2013. Chikungunya virus-associated long-term arthralgia: a 36-month prospective longitudinal study. *PLoS Negl Trop Dis,* 7**,** e2137.

Schroder, K., Hertzog, P. J., Ravasi, T. & Hume, D. A. 2004. Interferon-gamma: an overview of signals, mechanisms and functions. *J Leukoc Biol,* 75**,** 163-89.

Schroder, W. A., Le, T. T., Major, L., Street, S., Gardner, J., Lambley, E., Markey, K., Macdonald, K. P., Fish, R. J., Thomas, R. & Suhrbier, A. 2010. A physiological function of inflammation-associated SerpinB2 is regulation of adaptive immunity. *J Immunol,* 184**,** 2663-70.

Schuffenecker, I., Iteman, I., Michault, A., Murri, S., Frangeul, L., Vaney, M. C., Lavenir, R., Pardigon, N., Reynes, J. M., Pettinelli, F., Biscornet, L., Diancourt, L., Michel, S.,

Duquerroy, S., Guigon, G., Frenkiel, M. P., Brehin, A. C., Cubito, N., Despres, P., Kunst, F., Rey, F. A., Zeller, H. & Brisse, S. 2006. Genome microevolution of chikungunya viruses causing the Indian Ocean outbreak. *PLoS medicine,* 3**,** e263.

Schultz-Cherry, S., Dybing, J. K., Davis, N. L., Williamson, C., Suarez, D. L., Johnston, R. & Perdue, M. L. 2000. Influenza virus (A/HK/156/97) hemagglutinin expressed by an alphavirus replicon system protects chickens against lethal infection with Hong Kong-origin H5N1 viruses. *Virology,* 278**,** 55-9.

Schwartz, O. & Albert, M. L. 2010. Biology and pathogenesis of chikungunya virus. *Nat Rev Microbiol,* 8**,** 491-500.

Selvarajah, S., Sexton, N. R., Kahle, K. M., Fong, R. H., Mattia, K. A., Gardner, J., Lu, K., Liss, N. M., Salvador, B., Tucker, D. F., Barnes, T., Mabila, M., Zhou, X., Rossini, G., Rucker, J. B., Sanders, D. A., Suhrbier, A., Sambri, V., Michault, A., Muench, M. O., Doranz, B. J. & Simmons, G. 2013. A neutralizing monoclonal antibody targeting the acid-sensitive region in chikungunya virus E2 protects from disease. *PLoS Negl Trop Dis,* 7**,** e2423.

Serhan, C. N. 2010. Novel lipid mediators and resolution mechanisms in acute inflammation: to resolve or not? *Am J Pathol,* 177**,** 1576-91.

Seymour, R. L., Rossi, S. L., Bergren, N. A., Plante, K. S. & Weaver, S. C. 2013. The role of innate versus adaptive immune responses in a mouse model of O'nyong-nyong virus infection. *Am J Trop Med Hyg,* 88**,** 1170-9.

Shahrara, S., Proudfoot, A. E., Park, C. C., Volin, M. V., Haines, G. K., Woods, J. M., Aikens, C. H., Handel, T. M. & Pope, R. M. 2008. Inhibition of monocyte chemoattractant protein-1 ameliorates rat adjuvant-induced arthritis. *J Immunol,* 180**,** 3447-56.

Shoda, H. & Yamamoto, K. 2007. [Molecular pathogenesis of rheumatoid arthritis--the roles of synovial cells, immune cells, and pro-inflammatory cytokines]. *Nihon Rinsho,* 65**,** 1164-6.

Simizu, B., Yamamoto, K., Hashimoto, K. & Ogata, T. 1984. Structural proteins of Chikungunya virus. *Journal of virology,* 51**,** 254-8.

Singh, S. K. & Unni, S. K. 2011. Chikungunya virus: host pathogen interaction. *Reviews in Medical Virology,* 21**,** 78-88.

Sissoko, D., Malvy, D., Ezzedine, K., Renault, P., Moscetti, F., Ledrans, M. & Pierre, V. 2009. Post-Epidemic Chikungunya Disease on Reunion Island: Course of Rheumatic Manifestations and Associated Factors over a 15-Month Period. *PLoS Neglected Tropical Diseases,* 3**,** e389.

Snir, O., Rieck, M., Gebe, J. A., Yue, B. B., Rawlings, C. A., Nepom, G., Malmstrom, V. & Buckner, J. H. 2011. Identification and functional characterization of T cells reactive to citrullinated vimentin in HLA-DRB1*0401-positive humanized mice and rheumatoid arthritis patients. *Arthritis Rheum,* 63**,** 2873-83.

Soden, M., Vasudevan, H., Roberts, B., Coelen, R., Hamlin, G., Vasudevan, S. & La Brooy, J. 2000. Detection of viral ribonucleic acid and histologic analysis of inflamed synovium in Ross River virus infection. *Arthritis Rheum,* 43**,** 365-9.

Solanki, B. S., Arya, S. C. & Maheshwari, P. 2007. Chikungunya disease with nephritic presentation. *International journal of clinical practice,* 61**,** 1941.

Solignat, M., Gay, B., Higgs, S., Briant, L. & Devaux, C. 2009. Replication cycle of chikungunya: A re-emerging arbovirus. *Virology,* 393**,** 183-197.

Song, J., Willinger, T., Rongvaux, A., Eynon, E. E., Stevens, S., Manz, M. G., Flavell, R. A. & Galan, J. E. 2010. A mouse model for the human pathogen Salmonella typhi. *Cell Host Microbe,* 8**,** 369-76.

Sourisseau, M., Schilte, C., Casartelli, N., Trouillet, C., Guivel-Benhassine, F., Rudnicka, D., Sol-Foulon, N., Le Roux, K., Prevost, M. C., Fsihi, H., Frenkiel, M. P., Blanchet, F., Afonso, P. V., Ceccaldi, P. E., Ozden, S., Gessain, A., Schuffenecker, I., Verhasselt, B., Zamborlini, A., Saib, A., Rey, F. A., Arenzana-Seisdedos, F., Despres, P., Michault, A., Albert, M. L. & Schwartz, O. 2007. Characterization of reemerging chikungunya virus. *PLoS Pathog,* 3**,** e89.

Souto, F. O., Alves-Filho, J. C., Turato, W. M., Auxiliadora-Martins, M., Basile-Filho, A. & Cunha, F. Q. 2011. Essential role of CCR2 in neutrophil tissue infiltration and multiple organ dysfunction in sepsis. *Am J Respir Crit Care Med,* 183**,** 234-42.

Stoermer, K. A., Burrack, A., Oko, L., Montgomery, S. A., Borst, L. B., Gill, R. G. & Morrison, T. E. 2012. Genetic ablation of arginase 1 in macrophages and neutrophils enhances clearance of an arthritogenic alphavirus. *J Immunol,* 189**,** 4047-59.

Stoermer Burrack, K. A., Hawman, D. W., Jupille, H. J., Oko, L., Minor, M., Shives, K. D., Gunn, B. M., Long, K. M. & Morrison, T. E. 2014. Attenuating mutations in nsP1 reveal tissue-specific mechanisms for control of Ross River virus infection. *J Virol,* 88**,** 3719-32.

Strauss, J. H. & Strauss, E. G. 1994. The alphaviruses: gene expression, replication, and evolution. *Microbiological reviews,* 58**,** 491-562.

Subasinghe, N. L., Lanter, J., Markotan, T., Opas, E., Mckenney, S., Crysler, C., Hou, C., O'neill, J., Johnson, D. & Sui, Z. 2013. A novel series of N-(azetidin-3-yl)-2-(heteroarylamino)acetamide CCR2 antagonists. *Bioorg Med Chem Lett,* 23**,** 1063-9.

Suckling, A. J., Jagelman, S. & Webb, H. E. 1978. A comparison of brain lysosomal enzyme activities in four experimental togavirus encephalitides. *J Neurol Sci,* 35**,** 355-64.

Suhrbier, A., Jaffar-Bandjee, M. C. & Gasque, P. 2012. Arthritogenic alphaviruses—an overview. *Nature Publishing Group,* 8**,** 420-429.

Suhrbier, A. & La Linn, M. 2004. Clinical and pathologic aspects of arthritis due to Ross River virus and other alphaviruses. *Curr Opin Rheumatol,* 16**,** 374-9.

Suhrbier, A. & Mahalingam, S. 2009. The immunobiology of viral arthritides. *Pharmacol Ther,* 124**,** 301-8.

Sun, J. C. & Lanier, L. L. 2011. NK cell development, homeostasis and function: parallels with CD8(+) T cells. *Nat Rev Immunol,* 11**,** 645-57.

Swain, S. L., Mckinstry, K. K. & Strutt, T. M. 2012. Expanding roles for CD4(+) T cells in immunity to viruses. *Nat Rev Immunol,* 12**,** 136-48.

Swanson, C. L., Wilson, T. J., Strauch, P., Colonna, M., Pelanda, R. & Torres, R. M. 2010. Type I IFN enhances follicular B cell contribution to the T cell-independent antibody response. *J Exp Med,* 207**,** 1485-500.

Takeuchi, O. & Akira, S. 2009. Innate immunity to virus infection. *Immunol Rev,* 227**,** 75-86.

Tanaka, T., Narazaki, M., Ogata, A. & Kishimoto, T. 2014. A new era for the treatment of inflammatory autoimmune diseases by interleukin-6 blockade strategy. *Semin Immunol*.

Tanaka, T., Terada, M., Ariyoshi, K. & Morimoto, K. 2010. Monocyte chemoattractant protein-1/CC chemokine ligand 2 enhances apoptotic cell removal by macrophages through Rac1 activation. *Biochem Biophys Res Commun,* 399**,** 677-82.

Tang, X., Mo, C., Wang, Y., Wei, D. & Xiao, H. 2013. Anti-tumour strategies aiming to target tumour-associated macrophages. *Immunology,* 138**,** 93-104.

Teng, T. S., Foo, S. S., Simamarta, D., Lum, F. M., Teo, T. H., Lulla, A., Yeo, N. K., Koh, E. G., Chow, A., Leo, Y. S., Merits, A., Chin, K. C. & Ng, L. F. 2012. Viperin restricts chikungunya virus replication and pathology. *J Clin Invest,* 122**,** 4447-60.

Teo, T.-H., Lum, F.-M., Lee, W. W. L. & Ng, L. F. P. 2012a. Mouse models for Chikungunya virus: deciphering immune mechanisms responsible for disease and pathology. *Immunologic Research,* 53**,** 136-147.

Teo, T. H., Lum, F. M., Claser, C., Lulla, V., Lulla, A., Merits, A., Renia, L. & Ng, L. F. P. 2012b. A Pathogenic Role for CD4+ T Cells during Chikungunya Virus Infection in Mice. *The Journal of Immunology,* 190**,** 259-269.

Thon-Hon, V. G., Denizot, M., Li-Pat-Yuen, G., Giry, C., Jaffar-Bandjee, M. C. & Gasque, P. 2012. Deciphering the differential response of two human fibroblast cell lines following Chikungunya virus infection. *Virol J,* 9**,** 213.

Tisserand, J., Khetchoumian, K., Thibault, C., Dembele, D., Chambon, P. & Losson, R. 2011. Tripartite motif 24 (Trim24/Tif1alpha) tumor suppressor protein is a novel negative regulator of interferon (IFN)/signal transducers and activators of transcription (STAT) signaling pathway acting through retinoic acid receptor alpha (Raralpha) inhibition. *J Biol Chem,* 286**,** 33369-79.

Tiwari, M., Parida, M., Santhosh, S. R., Khan, M., Dash, P. K. & Rao, P. V. L. 2009. Assessment of immunogenic potential of Vero adapted formalin inactivated vaccine derived from novel ECSA genotype of Chikungunya virus. *Vaccine,* 27**,** 2513-2522.

Tsetsarkin, K. A., Mcgee, C. E., Volk, S. M., Vanlandingham, D. L., Weaver, S. C. & Higgs, S. 2009. Epistatic Roles of E2 Glycoprotein Mutations in Adaption of Chikungunya Virus to Aedes Albopictus and Ae. Aegypti Mosquitoes. *PLoS ONE,* 4**,** e6835.

Vanlandingham, D. L., Hong, C., Klingler, K., Tsetsarkin, K., Mcelroy, K. L., Powers, A. M., Lehane, M. J. & Higgs, S. 2005. Differential infectivities of o'nyong-nyong and chikungunya virus isolates in Anopheles gambiae and Aedes aegypti mosquitoes. *The American journal of tropical medicine and hygiene,* 72**,** 616-21.

Vazeille, M., Moutailler, S., Coudrier, D., Rousseaux, C., Khun, H., Huerre, M., Thiria, J., Dehecq, J. S., Fontenille, D., Schuffenecker, I., Despres, P. & Failloux, A. B. 2007. Two Chikungunya isolates from the outbreak of La Reunion (Indian Ocean) exhibit different patterns of infection in the mosquito, Aedes albopictus. *PLoS One,* 2**,** e1168.

Vazquez-Trinanes, C., Sopena, B., Gonzalez-Gonzalez, L., Diaz, R., Rivera, A., Freire, M. & Martinez-Vazquez, C. 2013. Synovial fluid eosinophilia: a case series with a long follow-up and literature review. *Rheumatology (Oxford),* 52**,** 346-51.

Volk, S. M., Chen, R., Tsetsarkin, K. A., Adams, A. P., Garcia, T. I., Sall, A. A., Nasar, F., Schuh, A. J., Holmes, E. C., Higgs, S., Maharaj, P. D., Brault, A. C. & Weaver, S. C. 2010. Genome-scale phylogenetic analyses of chikungunya virus reveal independent emergences of recent epidemics and various evolutionary rates. *J Virol,* 84**,** 6497-504.

Voss, J. E., Vaney, M. C., Duquerroy, S., Vonrhein, C., Girard-Blanc, C., Crublet, E., Thompson, A., Bricogne, G. & Rey, F. A. 2010. Glycoprotein organization of Chikungunya virus particles revealed by X-ray crystallography. *Nature,* 468**,** 709-12.

Wahlberg, J. M., Boere, W. A. & Garoff, H. 1989. The heterodimeric association between the membrane proteins of Semliki Forest virus changes its sensitivity to low pH during virus maturation. *Journal of virology,* 63**,** 4991-7.

Wahlberg, J. M., Bron, R., Wilschut, J. & Garoff, H. 1992. Membrane fusion of Semliki Forest virus involves homotrimers of the fusion protein. *Journal of virology,* 66**,** 7309-18.

Waight, J. D., Hu, Q., Miller, A., Liu, S. & Abrams, S. I. 2011. Tumor-derived G-CSF facilitates neoplastic growth through a granulocytic myeloid-derived suppressor cell-dependent mechanism. *PLoS One,* 6**,** e27690.

Wang, Y. F., Sawicki, S. G. & Sawicki, D. L. 1991. Sindbis virus nsP1 functions in negative-strand RNA synthesis. *Journal of virology,* 65**,** 985-8.

Wang, E., Volkova, E., Adams, A. P., Forrester, N., Xiao, S.-Y., Frolov, I. & Weaver, S. C. 2008. Chimeric alphavirus vaccine candidates for chikungunya. *Vaccine,* 26**,** 5030-5039.

Wang, D., Suhrbier, A., Penn-Nicholson, A., Woraratanadharm, J., Gardner, J., Luo, M., Le, T. T., Anraku, I., Sakalian, M., Einfeld, D. & Dong, J. Y. 2011a. A complex adenovirus vaccine against chikungunya virus provides complete protection against viraemia and arthritis. *Vaccine,* 29**,** 2803-9.

Wang, E., Kim, D. Y., Weaver, S. C. & Frolov, I. 2011b. Chimeric Chikungunya Viruses Are Nonpathogenic in Highly Sensitive Mouse Models but Efficiently Induce a Protective Immune Response. *Journal of Virology,* 85**,** 9249-9252.

Wang, B., Zinselmeyer, B. H., Runnels, H. A., Labranche, T. P., Morton, P. A., Kreisel, D., Mack, M., Nickerson-Nutter, C., Allen, P. M. & Miller, M. J. 2012a. In vivo imaging implicates CCR2+ monocytes as regulators of neutrophil recruitment during arthritis. *Cellular Immunology,* 278**,** 103-112.

Wang, X., Crowe, P. J., Goldstein, D. & Yang, J. L. 2012b. STAT3 inhibition, a novel approach to enhancing targeted therapy in human cancers (review). *Int J Oncol,* 41**,** 1181-91.

Wang, J. W. & Roden, R. B. 2013. Virus-like particles for the prevention of human papillomavirus-associated malignancies. *Expert Rev Vaccines,* 12**,** 129-41.

Wauquier, N., Becquart, P., Nkoghe, D., Padilla, C., Ndjoyi-Mbiguino, A. & Leroy, E. M. 2011. The Acute Phase of Chikungunya Virus Infection in Humans Is Associated With Strong Innate Immunity and T CD8 Cell Activation. *Journal of Infectious Diseases,* 204**,** 115-123.

Way, S. J., Lidbury, B. A. & Banyer, J. L. 2002. Persistent Ross River virus infection of murine macrophages: an in vitro model for the study of viral relapse and immune modulation during long-term infection. *Virology,* 301**,** 281-92.

Weaver, S. C., Dalgarno, L., Frey, T. K., Huang, H. V., Kinney, R. M., Roehrig, R. J. T., Shope, R. E. & Strauss, E. G. 2000. Family Togaviridae. *In:* VAN REGENMORTEL, M. H. V. (ed.) *Virus taxonomy : classification and nomenclature of viruses : seventh report of the International Committee on Taxonomy of Viruses.* San Diego: Academic Press.

Weaver, S. C., Osorio, J. E., Livengood, J. A., Chen, R. & Stinchcomb, D. T. 2012. Chikungunya virus and prospects for a vaccine. *Expert Review of Vaccines,* 11**,** 1087-1101.

Werneke, S. W., Schilte, C., Rohatgi, A., Monte, K. J., Michault, A., Arenzana-Seisdedos, F., Vanlandingham, D. L., Higgs, S., Fontanet, A., Albert, M. L. & Lenschow, D. J. 2011. ISG15 is critical in the control of Chikungunya virus infection independent of UbE1L mediated conjugation. *PLoS Pathog,* 7**,** e1002322.

White, A., Berman, S. & Lowenthal, J. P. 1972. Comparative immunogenicities of Chikungunya vaccines propagated in monkey kidney monolayers and chick embryo suspension cultures. *Applied microbiology,* 23**,** 951-2.

White, L. J., Wang, J. G., Davis, N. L. & Johnston, R. E. 2001. Role of alpha/beta interferon in Venezuelan equine encephalitis virus pathogenesis: effect of an attenuating mutation in the 5' untranslated region. *J Virol,* 75**,** 3706-18.

White, L. K., Sali, T., Alvarado, D., Gatti, E., Pierre, P., Streblow, D. & Defilippis, V. R. 2011. Chikungunya virus induces IPS-1-dependent innate immune activation and protein kinase R-independent translational shutoff. *J Virol,* 85**,** 606-20.

Wisniewski, T., Bayne, E., Flanagan, J., Shao, Q., Wnek, R., Matheravidathu, S., Fischer, P., Forrest, M. J., Peterson, L., Song, X., Yang, L., Demartino, J. A. & Struthers, M. 2010. Assessment of chemokine receptor function on monocytes in whole blood: In vitro and ex vivo evaluations of a CCR2 antagonist. *J Immunol Methods,* 352**,** 101-10.

Wongtrakool, C., Grooms, K., Ping, X. D., Rivera, H., Ward, J., Roser-Page, S., Roman, J., Brown, L. A. & Gauthier, T. W. 2012. In utero nicotine exposure promotes M2 activation in neonatal mouse alveolar macrophages. *Pediatr Res,* 72**,** 147-53.

Yamada, H., Nakashima, Y., Okazaki, K., Mawatari, T., Fukushi, J., Oyamada, A., Fujimura, K., Iwamoto, Y. & Yoshikai, Y. 2011. Preferential accumulation of activated Th1 cells not only in rheumatoid arthritis but also in osteoarthritis joints. *J Rheumatol,* 38**,** 1569-75.

Yoshida, Y. & Tanaka, T. 2014. Interleukin 6 and Rheumatoid Arthritis. *Biomed Res Int,* 2014**,** 698313.

Zaid, A., Rulli, N. E., Rolph, M. S., Suhrbier, A. & Mahalingam, S. 2011. Disease exacerbation by etanercept in a mouse model of alphaviral arthritis and myositis. *Arthritis Rheum,* 63**,** 488-91.

Zhang, W., Mukhopadhyay, S., Pletnev, S. V., Baker, T. S., Kuhn, R. J. & Rossmann, M. G. 2002. Placement of the structural proteins in Sindbis virus. *J Virol,* 76**,** 11645-58.

Ziegler, S. A., Lu, L., Da Rosa, A. P., Xiao, S. Y. & Tesh, R. B. 2008. An animal model for studying the pathogenesis of chikungunya virus infection. *The American journal of tropical medicine and hygiene,* 79**,** 133-9.

Zollo, M., Di Dato, V., Spano, D., De Martino, D., Liguori, L., Marino, N., Vastolo, V., Navas, L., Garrone, B., Mangano, G., Biondi, G. & Guglielmotti, A. 2012. Targeting monocyte chemotactic protein-1 synthesis with bindarit induces tumor regression in prostate and breast cancer animal models. *Clin Exp Metastasis*.

Appendices

Appendix I

Table 7.1: Details of the IPA pathways shown in Figure 3.15B.

Ingenuity Canonical Pathways	-log(p-value)	Molecules
Granulocyte		
Granulocyte Adhesion and Diapedesis	7.52	CXCL3,IL36G,MMP3,CXCL13,CXCR2,PPBP,CCL3L1/CCL3L3,CCL20,IL1B,CXCL6,CCL19
Agranulocyte Adhesion and Diapedesisa	7.27	CXCL3,IL36G,MMP3,CXCL13,CXCR2,PPBP,CCL3L1/CCL3L3,CCL20,IL1B,CXCL6,CCL19
IL-17A in autoimmunity		
Role of IL-17A in Psoriasis	7.78	CXCL3,S100A9,CCL20,S100A8,CXCL6
Role of IL-17A in Arthritis	4.41	CXCL3,CCL20,PTGS2,NOS2,CXCL6
Rheumatoid arthritis		
Altered T Cell and B Cell Signaling in Rheumatoid Arthritis	2.55	IL36G,CXCL13,LTB,IL1B
Role of Osteoblasts, Osteoclasts and Chondrocytes in Rheumatoid Arthritis	1.73	IL36G,SFRP2,MMP3,IL1B,Bmpr1b
Role of Macrophages, Fibroblasts and Endothelial Cells in Rheumatoid Arthritis	1.71	IL36G,SFRP2,MMP3,LTB,IL1B,NOS2
Inflammation		
Acute Phase Response Signaling	3.77	IL36G,HP,C1S,RBP2,IL1B,SERPINA3,OSMR
Communication between Innate and Adaptive Immune Cells	3.41	IL36G,HLA-B,CCL3L1/CCL3L3,IL1B,CD8A
Atherosclerosis Signaling	2.83	CCR3,IL36G,MMP3,IL1B,S100A8
Dendritic Cell Maturation	2.13	STAT4,IL36G,HLA-B,LTB,IL1B
Aryl Hydrocarbon Receptor Signaling	1.76	GSTM3,ALDH1A2,NQO1,IL1B
LPS/IL-1 Mediated Inhibition of RXR Function	1.74	IL36G,GSTM3,ALDH1A2,IL1B,SMOX
Other		
LXR/RXR Activation	2.77	IL36G,IL1B,S100A8,PTGS2,NOS2
Retinoate Biosynthesis I	2.73	SDR16C5,ALDH1A2,RBP2
Cholecystokinin/Gastrin-mediated Signaling	2.23	IL36G,IL1B,EPHA4,PTGS2
Xenobiotic Metabolism Signaling	1.85	GSTM3,ALDH1A2,NQO1,IL1B,SMOX,NOS2

Details of the IPA pathways shown in Figure 3.15 for the 181 genes where "the fold change in CCR2mice" divided by "the fold change in WT mice" was >1.5; i.e. pathways associated withgenes more induced in $CCR2^{-/}$ feet. [a]Same genes as in "Granulocyte Adhesion and Diapedesis". Only pathways with (i) a -log(p value) > 1.5 and (ii) 4 or more molecules are shown

Appendix II

Table 7.2: Details of the IPA pathways shown in Figure 3.15C.

Ingenuity Canonical Pathways	-log(p-value)	Molecules
Monocyte/macrophage		
Dendritic Cell Maturation	12.4	PLCB2,LEP,NFKBIE,PIK3R5,HLA-DQA1,HLA-DRB1,HLA-DMB, CD83,HLADQB1,FCGR2B,TREM2,FCGR1A,PIK3CG,COL10A1,TNFRSF1B,FCGR3A,HLA-DMA,TYROBP,IL10,MYD88,HLA-B, IL15,CD40,PLCG2,PIK3R6,FCER1G,CD86,STAT2,PIK3CD, IRF8,TNF
Fcγ Receptor-mediated Phagocytosis in Macrophages and Monocytes	7.87	RAC2,PXN,TLN1,FYB,FCGR1A,INPP5D,PLD4, NCF1,PIK3CG,SYK,LYN,HCK,VAV1,FGR,FCGR3A,ACTA1,LCP2,PRKCB
Production of Nitric Oxide and Reactive Oxygen Species in Macrophages	7.74	PTPN6,PPP1R3C,NFKBIE,PIK3R5,PPP1R3A, APOC2,NCF4, SPI1,IRF1,NCF1,ALB,RHOG,PLCG2,PIK3CG, CYBA,NCF2, PIK3R6,CYBB,PIK3CD,SERPINA1,IRF8,TNFRSF1B,TNF,SIRPA,PRKCB
MSP-RON Signaling Pathway	6.24	CSF2RB,ITGB2,ITGAM,CCL12,PIK3CG,PIK3R6,PIK3R5,PIK3CD,CCR2,TNF,ACTA1
IL-12 Signaling and Production in Macrophages	4.36	IL10,MYD88,PIK3R5,APOC2,SPI1,IRF1,ALB,CD40,TGFB1, PIK3CG,PIK3R6,SERPINA1,PIK3CD,IRF8,TNF,PRKCB
Pattern recognition		
Role of Pattern Recognition Receptors in Recognition of Bacteria and Viruses	8.01	Tlr11,NLRP3,IL10,MYD88,PIK3R5,C1QC,C1QA,C1QB,IRF7,PLCG2,PIK3CG,SYK,TLR1,PIK3R6,PIK3CD,TNF,C3AR1,PRKCB
Autoimmunity		
Altered T Cell and B Cell Signaling in Rheumatoid Arthritis	7.96	HLA-DMA,Tlr11,CD79B,IL10,IL15,HLA-DQA1,HLA-DRB1,HLA-DMB,HLADQB1,CD79A,CD40,TGFB1,TLR1,FCER1G,CD86, Tlr13,TNF
Type I Diabetes Mellitus Signaling	7.88	HLA-DMA,SOCS3,CASP3,MYD88,NFKBIE,HLA-B,HLA-DQA1, APAF1,HLA-DRB1,HLA-DMB,HLA-DQB1,IRF1,PRF1,FCER1G, CD86,BID,TNFRSF1B,HLA-F,TNF
Autoimmune Thyroid Disease Signaling	6.88	HLA-DMA,PRF1,CD40,IL10,HLA-B,HLA-DQA1,FCER1G,HLA-DRB1,CD86,HLA-DMB,HLA-DQB1,HLA-F
Systemic Lupus Erythematosus Signaling	4.07	PTPN6,CD79B,IL10,HLA-B,PIK3R5,FCGR2B,FCGR1A, CD79A,INPP5D,CD40,PIK3CG,CD72,PLCG2,PIK3R6,FCER1G, LYN,CD86,PIK3CD,HLA-F,TNF,FCGR3A
B and T cells		
Role of NFAT in Regulation of the Immune Response	9.55	PLCB2,NFKBIE,PIK3R5,HLA-DQA1,HLA-DRB1,HLA-DMB, HLA-DQB1,FCGR2B,FCGR1A,CD79A,GNB4,PIK3CG, FCGR3A,HLA-DMA,CD79B,ITPR1,GNAI2,BTK,SYK,PLCG2, PIK3R6,FCER1G,LYN,CD86,MEF2C,PIK3CD,LCP2

T Helper Cell Differentiation	8.5	HLA-DMA,IL2RG,IL10,HLA-DQA1,HLA-DRB1,HLA-DMB,HLA-DQB1,CD40,TGFB1,FCER1G,IL10RB,IL10RA, CD86,IL2RA, TNFRSF1B,TNF
FcγRIIB Signaling in B Lymphocytes	8.36	BTK,CD79B,SYK,PIK3CG,PLCG2,LYN,PIK3R6 ,PIK3R5,PIK3CD,DOK1,FCGR2B,CD79A,INPP 5D
iCOS-iCOSL Signaling in T Helper Cells	7.68	HLA-DMA,IL2RG,NFKBIE,CSK,HLA-DQA1,PIK3R5,HLA-DRB1,HLA-DMB,HLA-DQB1,ITPR1,INPP5D,CD40,PIK3CG, PIK3R6,FCER1G,VAV1,IL2RA,PIK3CD,LCP2
Antigen Presentation Pathway	7.3	PSMB9,NLRC5,HLA-DMA,HLA-B,HLA-DQA1,CIITA,HLA-DRB1,HLA-DMB,CD74,HLA-F,TAP1
B Cell Receptor Signaling	6.87	RAC2,PTPN6,CD79B,POU2F2,NFKBIE,CSK,PIK3R5,FCGR2B, CD79A,INPP5D,BTK,SYNJ1,DAPP1,SYK,PIK3CG,PLCG2,PIK3R6,LYN,VAV1,PIK3AP1,PIK3CD,PRKCB
PI3K Signaling in B Lymphocytes	6.45	PLCB2,CD79B,NFKBIE,ITPR1,FCGR2B,INPP5D,CD79A,BTK,DAPP1,CD40,CD180,SYK,PIK3CG,PLCG2,LYN,VAV1,PIK3AP1, PIK3CD,PRKCB
CD28 Signaling in T Helper Cells	6.41	HLA-DMA,PTPN6,NFKBIE,CSK,HLA-DQA1,PIK3R5,HLA-DRB1,HLA-DMB,HLA-DQB1,ITPR1,PIK3CG,SYK,PIK3R6, FCER1G,CD86,VAV1,PIK3CD,LCP2
Graft-versus-Host Disease Signaling	6.14	HLA-DMA,PRF1,HLA-B,HLA-DQA1,FCER1G,HLA-DRB1,CD86, HLA-DMB,HLA-DQB1,HLA-F,TNF
Tec Kinase Signaling	5.86	PIK3R5,ITGA5,BTK,GNAI2,GNB4,RHOG,PLCG2,PIK3CG,LYN, FCER1G,PIK3R6,HCK,VAV1,STAT2,PIK3CD,TNF,FGR,ACTA1, ITGA4,PRKCB
B Cell Development	5.85	HLA-DMA,CD79B,CD40,HLA-DQA1,HLA-DRB1,CD86, HLA-DMB, HLA-DQB1,CD79A
Allograft Rejection Signaling	5.72	HLA-DMA,PRF1,H2-T24,CD40,IL10,HLA-B,FCER1G,HLA-DQA1, CD86,HLA-DRB1,HLA-DMB,HLA-DQB1,HLA-F,TNF
IL-4 Signaling	5.49	HLA-DMA,IL2RG,PTPN6,HLA-DQA1,PIK3R5,HLA-DRB1, HLA-DMB,HLA-DQB1,INPP5D,SYNJ1,PIK3CG,PIK3R6,PIK3CD
CTLA4 Signaling in Cytotoxic T Lymphocytes	5.24	HLA-DMA,PTPN6,HLA-DQA1,PIK3R5,HLA-DRB1,HLA-DMB, HLA-DQB1,PIK3CG,SYK,PIK3R6,FCER1G,CD86,PIK3CD,LCP2
Cytotoxic T Lymphocyte-mediated Apoptosis of Target Cells	5.17	HLA-DMA,PRF1,H2-T24,CASP3,HLA-B,FCER1G,APAF1, HLA-DQA1,BID,HLA-DRB1,HLA-DMB,HLA-DQB1,HLA-F
PKCθ Signaling in T Lymphocytes	5.13	HLA-DMA,RAC2,NFKBIE,HLA-DQA1,PIK3R5,HLA-DRB1,HLA-DMB,HLA-DQB1,PLCG2,PIK3CG,PIK3R6,FCER1G,CD86 , VAV1,PIK3CD,LCP2
Communication between Innate and Adaptive Immune Cells	4.61	Tlr11,CD40,IL10,TLR1,IL15,HLA-B,FCER1G,CD86,Tlr13, HLA-DRB1,CD83,HLA-F,TNF
NK cells		

Natural Killer Cell Signaling	9.02	RAC2,PTPN6,Klra4 (includes others),LAIR1,TYROBP,PIK3R5, SH3BP2,INPP5D,SYNJ1,SYK,KLRC4-KLRK1/KLRK1,PLCG2, PIK3CG,PIK3R6,FCER1G,VAV1,PIK3CD,SH2D1B,LCP2,FCGR3A,PRKCB
Crosstalk between Dendritic Cells and Natural Killer Cells	8.4	IL2RG,TYROBP,CD69,IL15,HLA-B,HLA-DRB1,TLN1,CD83, TREM2,CSF2RB,PRF1,CD40,KLRC4-KLRK1/KLRK1, CD86,TNFRSF1B,HLA-F,TNF,ACTA1
Muscle		
Actin Cytoskeleton Signaling	4.79	RAC2,PXN,MYLPF,CSK,ACTN2,PIK3R5,ITGA5,MYH7,TLN1, IQGAP2,MYH2,PIK3CG,PIK3R6,MYH3,VAV1,PIK3CD,NCKAP1L,TMSB10/TMSB4X,PIP4K2A, ACTA1,MYH1,ITGA4
Calcium Signaling	4.74	RAP2B,TNNT1,CHRNA1,ATP2B1,TNNC2,TNNC1,TNNT2,TRDN,CHRNB1,Tpm1,MYH7,ITPR1,MYH2,MYH3,RYR1,MEF2C,TNNI1,SLC8A1,ACTA1,MYH1
Paxillin Signaling	4.76	ITGB2,PXN,ITGAM,PIK3CG,ACTN2,CSK,PIK3R6,PIK3R5,ITGA5,PIK3CD,TLN1,ITGA7,ACTA1,ITGA4
Inflammation		
TREM1 Signaling	9.57	Tlr11,TYROBP,IL10,MYD88,LAT2,ITGA5,CD83,FCGR2B,CD40, CCL12,CCL7,PLCG2,TLR1,CD86,Tlr13,TNF
Leukocyte Extravasation Signaling	8.81	RAC2,MMP14,PIK3R5,MMP25,PIK3CG,CYBA, CYBB,ACTA1, ITGA4,PXN,CXCR4,ACTN2,ARHGAP4,ITGA5, NCF4,SELPLG, GNAI2,BTK,ITGB2,NCF1,WIPF1,ITGAM,PLCG2,NCF2,PIK3R6, VAV1,PIK3CD,PRKCB
Atherosclerosis Signaling	6.36	ALOX12B,MSR1,CXCR4,APOC2,PLA2G7,F3,TNFRSF14, SELPLG,ITGB2,ALB,CD40,CCL12,TGFB1,COL10A1,SERPINA1, CCR2,TNF,ITGA4
Fc Epsilon RI Signaling	5.38	RAC2,PIK3R5,INPP5D,BTK,SYNJ1,PLCG2,PIK3CG,SYK,LYN, FCER1G,PIK3R6,VAV1,PIK3CD,TNF,LCP2,PRKCB
Integrin Signaling	4.96	RAP2B,RAC2,PXN,ARHGAP26,ACTN2,PIK3R5,ITGA5,TLN1, PARVB,ITGB2,WIPF1,RHOG,ITGAM,PIK3CG, PLCG2,PIK3R6, ZYX,PIK3CD,ITGA7,ACTA1,ITGA4
Role of JAK1 and JAK3 in γc Cytokine Signaling	4.13	SOCS3,IL2RG,FES,PIK3CG,SYK,IL15,PIK3R6, PIK3R5,IL2RA, PIK3CD
NF-κB Activation by Viruses	4.09	ITGB2,CCR5,PIK3CG,NFKBIE,PIK3R6,PIK3R5,ITGA5,PIK3CD, TNFRSF14,ITGA4,PRKCB
Other		
Virus Entry via Endocytic Pathways	4.4	RAC2,HLA-B,PIK3R5,ITGA5,ITGB2,FLNC,PLCG2,PIK3CG, PIK3R6,PIK3CD,ACTA1,PRKCB,ITGA4
Induction of Apoptosis by HIV1	4.32	CASP3,CXCR4,NFKBIE,APAF1,BID,BAX,TNFRSF1B,NAIP,TNF,BAK1
LXR/RXR Activation	4.26	TTR,MSR1,VTN,AHSG,NR1H3,APOC2,ABCG1,ALB,CCL12,CCL7,SERPINA1,PLTP,GC,TNFRSF1B,TNF
Role of Tissue Factor in Cancer	4.21	F10,ARRB2,CASP3,PIK3CG,LYN,HCK,PIK3R6

		,PIK3R5,PLAUR, FGB,PIK3CD,RPS6KA2,F3,FGR
ILK Signaling	4.2	PXN,FBLIM1,CASP3,ACTN2,PIK3R5,MYH7,PARVB,ITGB2, RHOG,MYH2,FLNC,PIK3CG,PIK3R6,MYH3,PIK3CD,TMSB10/TMSB4X,TNF,ACTA1,MYH1
Phospholipase C Signaling	4.1	PLCB2,CD79B,MYLPF,ITGA5,ITPR1,FCGR2B,CD79A,BTK, PLD4,TGM2,GNB4,RHOG,SYK,PLCG2,FCER1G,LYN,MEF2C,ARHGEF2,ADCY7,LCP2,ITGA4,PRKCB

Details of the IPA pathways shown in Figure 3.15 for the 920 gene where "the fold change in WT mice" divided by "the fold change in $CCR2^{-/-}$ mice" was >1.5; i.e. pathways associated with the genes less induced in $CCR2^{-/-}$ feet. Only pathways with a -log(p value) > 4 are shown.

Appendix III

Table 7.3: Details of the IPA pathways shown in Figure 5.6.

Ingenuity Canonical Pathways	-log(p-value)	Molecules
T cells		
Allograft Rejection Signaling	2.35	HLA-G,CD40,H2-K2/H2-Q9,HLA-B
Cytotoxic T Lymphocyte-mediated Apoptosis of Target Cells	1.57	HLA-G,H2-K2/H2-Q9,HLA-B
OX40 Signaling Pathway	1.5	HLA-G,H2-K2/H2-Q9,HLA-B
Autoimmunity		
Type I Diabetes Mellitus Signaling	2.75	HLA-G,HLA-B,HSPD1,STAT1,IRF1
Systemic Lupus Erythematosus Signaling	2.67	HLA-G,PTPRC,PIK3R3,CD40,HLA-B,FCGR1A,FCGR3A
Autoimmune Thyroid Disease Signaling	2.2	HLA-G,CD40,HLA-B
Altered T Cell and B Cell Signaling in Rheumatoid Arthritis	1.5	CD40,TLR1,Tlr13
Antigen presentation		
Antigen Presentation Pathway	4.97	HLA-G,NLRC5,HLA-B,CANX,PSMB8
Communication between Innate and Adaptive Immune Cells	4.05	CXCL10,HLA-G,CD40,HLA-B,TLR1,Tlr13
Dendritic Cell Maturation	3.24	PIK3R3,CD40,HLA-B,STAT1,TREM2,FCGR1A,FCGR3A
NK cell		
Crosstalk between Dendritic Cells and Natural Killer Cells	2.23	HLA-G,CD40,HLA-B,TREM2
Innate sensing		
Activation of IRF by Cytosolic Pattern Recognition Receptors	4.96	IFIH1,CD40,DDX58,ZBP1,STAT1,IFIT2
Role of Pattern Recognition Receptors in Recognition of Bacteria and Viruses	2.98	IFIH1,PIK3R3,DDX58,TLR1,C1QB
Role of PKR in Interferon Induction and Antiviral Response	2.4	STAT1,FCGR1A,IRF1
PI3K/AKT Signaling	1.77	PIK3R3,YWHAH,LIMS1,ITGA4
Monocytes macrophages		
Fcγ Receptor-mediated Phagocytosis in Macrophages and Monocytes	3.01	PIK3R3,HCK,FYB,FCGR1A,FCGR3A
TREM1 Signaling	1.93	CD40,TLR1,Tlr13
Agranulocyte Adhesion and Diapedesis	1.79	CXCL10,CXCL9,CCL13,Ccl8,ITGA4
IL-12 Signaling and Production in Macrophages	1.64	PIK3R3,CD40,STAT1,IRF1
Apoptosis		
Retinoic acid Mediated Apoptosis Signaling	1.78	PARP9,IRF1,PARP14
Cytokines		
Interferon Signaling	3.82	IFIT3,PSMB8,STAT1,IRF1
GM-CSF Signaling	1.85	PIK3R3,HCK,STAT1
Other		
Neuroprotective Role of THOP1 in Alzheimer's Disease	2.4	HLA-G,NFYA,HLA-B
Glucocorticoid Receptor Signaling	2.29	PIK3R3,CCL13,HMGB1,YWHAH,STAT1,HSPA5,FCGR1A
UVA-Induced MAPK Signaling	2.21	PIK3R3,STAT1,PARP9,PARP14
Granulocyte Adhesion and Diapedesis	1.89	CXCL10,CXCL9,CCL13,Ccl8,ITGA4
Protein Ubiquitination Pathway	1.77	USP18,HLA-B,PSMD1,PSMB8,HSPD1,HSPA5
Reelin Signaling in Neurons	1.59	PIK3R3,HCK,ITGA4

Details of the IPA pathways shown in Figure 5.7 for the 192 genes more induced in the feet of day 30 post infected mice. Only pathways with a -log(p value) > 1.5 are shown. Pathways with a -log(p value) > 1.3 (means $p < 0.05$) and at least 3 molecules assigned are shown.

Appendix IV

Table 7.4: Details of the IPA pathways for section 5.2.8.2

Ingenuity Canonical Pathways	-log(p-value)	Molecules
mTOR Signaling	2.09	RPS29,ULK1,RPS27,RHOG,IRS1,RPS8,RPS21
Regulation of eIF4 and p70S6K Signaling	2.06	RPS29,RPS27,EIF4EBP2,IRS1,RPS8,RPS21
EIF2 Signaling	1.64	RPS29,RPS27,RPS8,RPS21,RPL13A,RPL13
Aryl Hydrocarbon Receptor Signaling	1.58	MYC,DCT,RXRB,MGST3,HSPB1

Details of the IPA pathways described in section 5.2.8.2 of day 30 post infected mice. Pathways with a -log(p value) > 1.3 (means $p < 0.05$) and at least 3 molecules assigned are shown.

Appendix V

Table 7.5: Details of the ingenuity upstream regulator analysis of the 192 more induced in the feet of day 30 post infected mice shown in Figure 5.7.

Red = type I IFN responses; green = Th1 responses; blue = T cells responses; orange = apoptosis; purple = autophagy; grey = others. Only p values < 1E10 are shown.

Uspstream Regulator	Activation z-score	Type	p-value of overlap	Target molecules in dataset
IKBKE	0.101	kinase	9.65E-10	Ccl2,CXCL10,HLA-B,IFIH1,IFIT2,IFIT3,Irg1,STAT1
IFNK	3.134	cytokine	1.59E-10	CD40,CXCL10,CXCL9,IFIH1,IRF1,STAT1,ZBP1
IFNE	2.449	cytokine	8.28E-11	CD40,CXCL10,CXCL9,IFIH1,IFIT2,STAT1,USP18,ZBP1
DDX58 (RIG-I gene)	2.039	enzyme	4.01E-11	CXCL10,DDX58,IFI44,IFIH1,IFIT1B,IFIT2,IFIT3,IRF1,STAT1
IFN type 1	2.911	group	2.22E-11	Ccl2,CXCL10,CXCL9,DDX58,IFIH1,IFIT1B,IFIT2,IRF1,STAT1
TLR4	3.324	transmembrane receptor	1.26E-11	Ccl2,CCR5,CD274,CD40,CXCL10,CXCL9,HMGB1,IFIT1B,IFIT2,IFIT3,Iigp1,IRF1,IRGM,PLEK,RGS1,STAT1,TREM2
IFNA1/IFNA13	2.925	cytokine	8.54E-12	CD40,CXCL10,CXCL9,IFIH1,IFIT2,IRF1,STAT1,Tgtp1/Tgtp2,USP18,ZBP1
IFN alpha/beta	3.264	group	5.57E-12	CCR2,CD40,CXCL10,CXCL9,IFIT2,IFIT3,IRF1,IRGM,STAT1,Tgtp1/Tgtp2,TLR1
IFNA2	3.655	cytokine	1.97E-12	CXCL10,CXCL9,DDX58,DDX60,EMR1,HERC6,HLA-B,IFI44,IFIH1,IFIT2,IFIT3,IRF1,PARP9,STAT1,USP18,ZBP1
IFN Beta	3.412	group	6.48E-13	CD274,CD40,CXCL10,DDX58,HLA-B,HLA-G,IFIH1,IFIT1B,IFIT2,IRF1,STAT1,USP18,ZBP1
IFNAR1	2.75	transmembrane receptor	3.57E-13	CD40,CXCL10,CXCL9,HLA-B,IFI44,IFIH1,IFIT1B,IFIT2,IFIT3,Irg1,Oasl2,STAT1,USP18
IFNL1	3.44	cytokine	7.49E-14	CD40,CXCL10,CXCL9,DDX58,DDX60,HERC6,IFI44,IFIH1,IFIT2,IFIT3,STAT1,USP18
Interferon alpha	4.357	group	5.06E-14	CCR5,CD40,CXCL10,CXCL9,DDX58,FCGR1A,HLA-B,HLA-G,IFIH1,IFIT1B,IFIT2,IFIT3,IRF1,ITGA4,PSMB8,STAT1,Tgtp1/Tgtp2,TLR1,USP18,ZBP1
TLR3	3.558	transmembrane receptor	2.44E-14	Ccl2,CD274,CD40,CXCL10,CXCL9,DDX58,GBP4,IFI44,IFIH1,IFIT2,IFIT3,Iigp1,Irg1,Oasl2,PIK3R3,RGS1,STAT1,USP18
IRF3	3.632	transcription regulator	7.44E-16	Ccl2,CXCL10,CXCL9,DDX58,FCGR1A,IFI44,IFIH1,IFIT1B,IFIT2,IFIT3,IRGM,Oasl2,PARP14,STAT1,Trim30a/Trim30d,USP18,ZBP1
STAT1	4.265	transcription regulator	2.42E-17	Ccl2,Ccl8,CD274,CD40,CXCL10,CXCL9,FCGR1A,Gbp6 (includes others),HERC6,IFIT1B,IFIT2,IFIT3,IRF1,Irg1,IRGM,PSMB8,PTN,Rnf213,STAT1,Tgtp1/Tgtp2,USP18
IFNB1	3.754	cytokine	1.39E-23	Ccl2,CCR5,CD274,CD40,CXCL10,CXCL9,DDX58,GBP4,Gbp6 (includes others),GBP7,Gbp8,Gvin1 (includes

				others),IFIH1,IFIT1B,IFIT2,IFIT3,IRF1,Irg1,IRGM,STAT1,Tgtp1/Tgtp2,Tlr13,Trim30a/Trim30d,USP18,VCL,ZBP1
Ifnar	4.518	group	1.39E-27	Ccl2,CD274,CD40,CXCL10,CXCL9,DDX58,HLA-B,HLA-G,IFIH1,IFIT1B,IFIT2,IFIT3,IRF1,IRGM,ITGA4,NLRC5,PSMB8,Rnf213,STAT1,USP18,ZBP1
IRF7	4.345	transcription regulator	5.94E-20	CD40,CXCL10,CXCL9,DDX58,FCGR1A,GBP4,IFI44,IFIH1,IFIT1B,IFIT2,IFIT3,IRF1,IRGM,Oasl2,PARP14,PSMB8,STAT1,Trim30a/Trim30d,USP18,ZBP1
mir-21	-3.769	microRNA	9.95E-18	AOAH,CD180,CD274,CXCL10,CXCL9,FCGR1A,Gbp6 (includes others),GBP7,Gbp8,Gvin1 (includes others),Iigp1,IRF1,IRGM,NLRC5,STAT1,Tgtp1/Tgtp2,TLR1,TREM2
TRIM24	-4.054	transcription regulator	9.42E-20	CXCL10,DDX58,DDX60,GBP4,HERC6,IFI44,IFIH1,IFIT1B,IFIT2,IFIT3,Iigp1,IRF1,IRGM,PSMB8,STAT1,Tgtp1/Tgtp2,USP18
SOCS1	-3.908	other	4.58E-20	Ccl2,CD40,CXCL10,CXCL9,DDX58,Gbp6 (includes others),GBP7,Gvin1 (includes others),IFI44,IFIH1,IFIT1B,IFIT2,IFIT3,Iigp1,IRF1,Irg1,Oasl2,STAT1
PARP1	2.646	enzyme	2.19E-10	Ccl2,CD274,CXCL10,CXCL9,GBP4,Gbp6 (includes others),GBP7,Iigp1,STAT1,Tgtp1/Tgtp2
IRGM	-2.828	other	3.81E-10	CCNB2,CXCL10,CXCL9,IFIT1B,IFIT2,IFIT3,Iigp1,USP18
STAT3	2.317	transcription regulator	2.52E-10	Ccl8,CCR5,CD274,CD40,CXCL10,CXCL9,FCGR1A,GLIPR1,HLA-B,IFI44,IFIH1,IFIT1B,IFIT3,IRF1,Lyz1/Lyz2,PSMB8,PTN,STAT1
IFNG	6.301	cytokine	1.10E-21	BST1,C1QB,Ccl2,Ccl8,CCR2,CCR5,CD274,CD40,CTSS,CXCL10,CXCL9,CYBB,DDX58,DTX3L,FCGR1A,FCGR3A,GBP4,Gbp6 (includes others),GBP7,Gbp8,Gvin1 (includes others),HCK,HERC6,HLA-B,HLA-G,HMGB1,HSPD1,IFI44,IFIH1,IFIT2,IFIT3,Iigp1,IRF1,Irg1,IRGM,NLRC5,PARP9,PLEK,PSMB8,PTN,STAT1,Tgtp1/Tgtp2,TLR1,TREM2,USP18
IL12 (complex)	1.822	complex	5.69E-11	Ccl2,CCR2,CCR5,CXCL10,CXCL9,EMR1,IFIH1,IFIT1B,IFIT2,Iigp1,IRF1,ITGA4,Tgtp1/Tgtp2,Trim30a/Trim30d
IL6	3.886	cytokine	6.68E-10	Ccl2,CCNB2,CCR2,CCR5,CD40,CXCL10,CXCL9,CYBB,EMR1,FCGR1A,HLA-B,HSPA5,IFIT1B,IFIT2,IRF1,LY86,Lyz1/Lyz2,MAD2L1,PSMB8,PTPRC,STAT1,TLR1
DOCK8	3.162	other	3.57E-11	CD40,CXCL10,CXCL9,IFIT1B,IFIT2,IFIT3,Iigp1,IRF1,RGS1,STAT1
TCR	0.467	complex	5.27E-11	CCR2,CCR5,CXCL10,CXCL9,DDX58,GBP4,HSPA5,HSPD1,IFI44,IFIH1,IFIT2,IFIT3,IRF1,PIK3R3,PTPRC,STAT1
FZD9	2.425	G-protein coupled receptor	9.19E-10	Ccl2,CXCL10,IFI44,IFIT1B,Oasl2,STAT1
PLK2	2.646	kinase	2.98E-10	CD40,CXCL10,CXCL9,IFIT2,Iigp1,IRF1,RGS1
PLK4	2.646	kinase	2.19E-10	CD40,CXCL10,CXCL9,IFIT2,Iigp1,IRF1,RGS1

Appendix VI

Table 7.6: Mutations identified in CHIKV recovered from Rag-1$^{-/-}$ mice day 100 post infection.

Parental Reunion Island isolate LR2006 OPY1 (passaged twice in C6/36 cells) used herein (Gardner et al., 2010) and virus isolated from Rag-1$^{-/-}$ mice at day 100 post infection (Rag100) were grown in C6/36 cells, partially purified (0.22 µM filtration, DNase/RNase treated, and 100,000 g 1 h centrifugation), RNA isolated (QIAamp Viral RNA Mini Kit) and reverse transcribed, with the resultant viral cDNA amplified using the Illustra GenomiPhi V2 DNA Amplification Kit (GE Healthcare). The sequence of the viral genome was then determined using semi-conductor sequencing (Ion Torrent PGM) at the Lotterywest State Biomedical Facility Genomics (University of Western Australia). Ion 314 chips were used to generate >200,000 reads of ≈100 bp. The sequence was assembled using Geneious Pro software and aligned with LR2006 OPY1 (Accession: DQ443544.2). Sequence changes are indicated below, changes highlighted in red. Three coding changes were identified.

Nucleotide position	Virus	Nucleotide	Amino Acid
776	LR2006 OPY1	A	K
	Parental	G	E
	Rag100	G	E
1052	LR2006 OPY1	A and G	M/V
	Parental	G	V
	Rag100	G	V
4167	LR2006 OPY1	A and G	D/G
	Parental	A	D
	Rag100	A	D
4302	LR2006 OPY1	A	Y
	Parental	A	Y
	Rag100	**G**	**C (nsP3^{1409})**
5049	LR2006 OPY1	G and T	R/I
	Parental	T	I
	Rag100	T	I
5903	LR2006 OPY1	C	L
	Parental	C	L
	Rag100	T	L
8978	LR2006 OPY1	A	Q
	Parental	A	Q
	Rag100	**G**	**R(E2^{471})**

9203	LR2006 OPY1	A	K
	Parental	A	K
	Rag100	**G and A**	**R and K (E2^{346})**
11073	LR2006 OPY1	A	L
	Parental	A	L
	Rag100	G	L
3' UTR; **11395**, **11421** and **11455**	LR2006 OPY1	C	-
	Parental	C	-
	Rag100	**T**	-

Data was prepared with assistance of Helle Bielefeldt-Ohmann and Penny Rudd.